

# UNCLASSIFIED

AD NUMBER
AD848798
NEW LIMITATION CHANGE
TO Approved for public release, distribution unlimited
FROM Distribution authorized to U.S. Gov't. agencies and their contractors; Administrative/Operational Use; JAN 1969. Other requests shall be referred to Air Force Weapons Lab., Kirtland AFB, NM.
AUTHORITY
AFWL ltr, 1 Mar 1972

THIS PAGE IS UNCLASSIFIED

CB (1)

## ENGINEERING CLASSIFICATION OF IN-SITU ROCK

AD848798



Don U. Deere

Andrew H. Merritt

Richard F. Coon

University of Illinois

Department of Civil Engineering

Urbana, Illinois 61801

Contract AF 29(601)-6850

MAR 1 1969

TECHNICAL REPORT NO. AFWL-TR-67-144

January 1969

AIR FORCE WEAPONS LABORATORY

Air Force Systems Command

Kirtland Air Force Base

New Mexico

This document is subject to special export controls and each transmittal to foreign governments or foreign nationals may be made only with prior approval of AFWL (WLDC) , Kirtland AFB, NM, 87117



ENGINEERING CLASSIFICATION OF IN-SITU ROCK

Don U. Deere

Andrew H. Merritt

Richard F. Coon

University of Illinois  
Department of Civil Engineering  
Urbana, Illinois 61801  
Contract AF 29(601)-6850

TECHNICAL REPORT NO. AFWL-TR-67-144

This document is subject to special export controls and each transmittal to foreign governments or foreign nationals may be made only with prior approval of AFWL (WLDC), Kirtland AFB, NM, 87117. Distribution is limited because of the technology discussed in the report.



FOREWORD

This report was prepared by the Department of Civil Engineering, University of Illinois, Urbana, Illinois, under Contract AF 29(601)-6850. The research was performed under Program Element 61102H, Project 5710, Task Area RSS2144, and was funded by the Defense Atomic Support Agency (DASA).

Inclusive dates of research were 15 June 1965 through 1 November 1967. The report was submitted 14 January 1969 by the Air Force Weapons Laboratory Project Officer, Captain J. R. Salley (WLDC). Captain Joseph J. O'Kobrick was the former Project Officer for the Air Force.

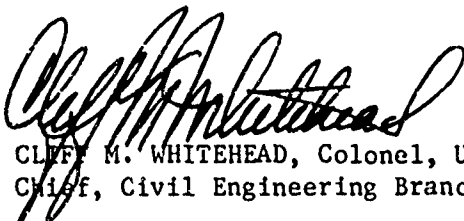
Information in this report is embargoed under the US Export Control Act of 1949, administered by the Department of Commerce. This report may be released by departments or agencies of the US Government to departments or agencies of foreign governments with which the United States has defense treaty commitments, subject to approval of AFWL (WLDC), Kirtland AFB, NM, 87117.

Dr. Don U. Deere, Professor of Civil Engineering and of Geology, was the project supervisor. R. F. Coon, Research Associate in Civil Engineering, was immediately responsible for all phases of the test program and preparation of the written report. A. H. Merritt, Research Assistant in Civil Engineering, worked on all phases of the investigation and prepared Part A of the report. J. H. Coulson, Research Assistant in Civil Engineering, assisted in laboratory testing and data analysis. Birdwell, Inc., Division of Seismograph Service Corporation, performed contracted geophysical testing for this investigation. Acknowledgment is extended to the Corps of Engineers, Walla Walla District; US Bureau of Reclamation, Denver; the California Department of Water Resources; and the US Geological Survey, Nevada Test Site, who granted access to their projects for field testing and provided core samples and engineering data.

This technical report has been reviewed and is approved.



J. R. SALLEY, Captain, USAF  
Project Officer



CLIFF M. WHITEHEAD, Colonel, USAF  
Chief, Civil Engineering Branch



GEORGE C. DARBY, JR., Colonel, USAF  
Chief, Development Division

## ABSTRACT

An engineering classification for in-situ rock is proposed which is based upon the results of field exploration and laboratory testing. The field program included a study of more than fifteen construction projects from which data were obtained from geophysical testing, borehole photography, water pressure testing, and geologic mapping. Laboratory analyses of 530 samples taken from these projects included physical and mineralogical descriptions, unit weights, absorption, strength, modulus of elasticity, and sonic velocities (saturated and dry). The rock types investigated included granite, basalt, gneiss, schist, sandstone, limestone, and siltstone.

Geologic discontinuities such as joints, faults, and weathered rock are of major importance in an engineering evaluation of in-situ rock because of their effect upon the deformability, shear strength, and permeability of the mass. A quantitative description of these features can be made using two methods of indexing rock quality; the RQD and the Velocity Index. The RQD (Rock Quality Designation) is a function of the length of core pieces bounded by joint surfaces and is calculated for each coring run. The Velocity Index is the square of the ratio of in-situ to laboratory sonic velocities. The relationship between these two indices suggests that each is influenced to about the same degree by the amount of jointing in the rock. Therefore, either method can be used in classifying in-situ rock.

The application of the proposed classification to the prediction of in-situ rock properties is shown by comparing rock quality measurements with other engineering data. Comparisons are presented between rock quality and the modulus of deformation determined by plate jack and pressure chamber tests, in-situ permeability determined by water pressure tests, and the overall character of the rock indicated by the rate of construction and support requirements for underground openings.

(Distribution Limitation Statement No. 2)

This page intentionally left blank.

## CONTENTS

### PART A

#### ENGINEERING CLASSIFICATION OF IN-SITU ROCK

<u>Section</u>		<u>Page</u>
1.	INTRODUCTION . . . . .	1
	1. Nature of the Problem . . . . .	1
	2. Scope of the Investigation . . . . .	4
	3. Sites Studied . . . . .	5
2.	CLASSIFICATION SYSTEMS FOR IN-SITU ROCK . . . . .	9
	1. Introduction . . . . .	9
	2. Classification Systems . . . . .	9
	3. Conclusion . . . . .	23
3.	FIELD INVESTIGATION METHODS . . . . .	25
	1. Introduction . . . . .	25
	2. Core Logging . . . . .	25
	3. Geologic Mapping . . . . .	31
	4. Borehole Photography . . . . .	31
	5. Permeability Measurements . . . . .	34
	6. Geophysical Testing . . . . .	41
4.	LABORATORY INVESTIGATIONS . . . . .	59
	1. Introduction . . . . .	59
	2. Sonic Pulse Velocities . . . . .	59
	3. Unconfined Strength and Modulus of Elasticity . . . . .	62
	4. Evaluation of Test Results . . . . .	62
5.	RELATIONSHIP OF ROCK QUALITY AND IN-SITU TEST RESULTS . . . . .	69
	1. Introduction . . . . .	69
	2. Borehole Photography . . . . .	69
	3. Permeability . . . . .	69
	4. 3-D Sonic Logs . . . . .	76
	5. Electrical Resistivity . . . . .	87
	6. Conclusions . . . . .	91
6.	ENGINEERING CLASSIFICATION FOR IN-SITU ROCK . . . . .	92
	1. Introduction . . . . .	92
	2. Indices of Rock Quality . . . . .	92

## CONTENTS (Cont'd)

<u>Section</u>	<u>Page</u>
3. Correlation of Rock Quality Indices . . . . .	95
4. Engineering Classification . . . . .	110
PART B	
CORRELATION OF ENGINEERING BEHAVIOR AND THE ENGINEERING CLASSIFICATION OF IN-SITU ROCK	
7. ENGINEERING PROPERTIES OF IN-SITU ROCK . . . . .	117
1. Introduction . . . . .	117
2. Deformation Characteristics of In-Situ Rock . . . . .	118
3. Permeability of In-Situ Rock . . . . .	118
4. Shear Strength of In-Situ Rock . . . . .	120
8. PLATE JACK TEST . . . . .	121
1. Introduction . . . . .	121
2. Site Preparation . . . . .	121
3. Test Setup . . . . .	122
4. Deformation Measurements . . . . .	129
5. Testing Procedure . . . . .	130
6. Interpretation of Test Results . . . . .	133
7. Special Uses of the Plate Jack Test . . . . .	137
9. PRESSURE CHAMBER TESTS . . . . .	138
1. Introduction . . . . .	138
2. Site Preparation . . . . .	138
3. Test Setup . . . . .	138
4. Deformation Measurements . . . . .	140
5. Testing Procedure . . . . .	141
6. Interpretation of Test Results . . . . .	141
7. Radial Jack Test . . . . .	143
10. BOREHOLE DEFORMATION TESTS . . . . .	146
1. Introduction . . . . .	146
2. The CEBTP Apparatus . . . . .	146
3. The Janod-Mermin Apparatus . . . . .	146
4. The Sounding Dilatometer . . . . .	147

## CONTENTS (Cont'd)

<u>Section</u>	<u>Page</u>
5. Menard Pressure Meter . . . . .	147
6. Summary . . . . .	147
11. OTHER STATIC TESTS . . . . .	149
1. The Cable Method . . . . .	149
2. Tank Test . . . . .	152
12. COMPARISON OF IN-SITU STATIC TESTS . . . . .	153
1. Introduction . . . . .	153
2. Comparison of the Modulus of Deformation and the Modulus of Elasticity . . . . .	153
3. Comparison of Moduli Measured in the Vertical and Horizontal Directions . . . . .	154
4. Comparison of Moduli Obtained Perpendicular and Parallel to Stratification . . . . .	157
5. Comparison of Moduli Obtained Before and After Grouting . . . . .	157
6. Comparison of Moduli Obtained by Borehole Deformation and Plate Jack Tests . . . . .	160
7. Comparison of Moduli Obtained by Pressure Chamber and Plate Jack Tests . . . . .	160
13. THE RELATIONSHIP BETWEEN STATIC AND DYNAMIC MODULUS MEASUREMENTS . . . . .	164
1. Introduction . . . . .	164
2. Comparison of In-Situ Dynamic and Static Moduli . . . . .	165
14. THE RELATIONSHIP BETWEEN IN-SITU STATIC MODULI AND ROCK QUALITY . . . . .	168
1. Introduction . . . . .	168
2. Comparison of RQD and In-Situ Moduli . . . . .	169
3. Comparison of Rock Quality Indices and Modulus Ratio . . . . .	173
4. The Deformation Ratio . . . . .	185
15. MEASUREMENT OF DEFORMATION CAUSED BY ENGINEERING STRUCTURES . . . . .	192
1. Introduction . . . . .	192
2. Deformation Measurements Within the Structure . . . . .	192
3. Deformation Measurements Within the Rock Mass . . . . .	193
4. Comparison of Deformation Moduli from In-Situ Tests and Observations of Structures . . . . .	195

# CONTENTS (Cont'd)

<u>Section</u>	<u>Page</u>
16. CORRELATION OF ROCK QUALITY AND RATE OF CONSTRUCTION OF TUNNELS . . . . .	199
1. Introduction . . . . .	199
2. Case History No. 1 - Shaft in Schist, East Coast . . . . .	200
3. Case History No. 2 - Tunnels No. 1 and No. 2, Tehachapi Project, California . . . . .	205
4. Case History No. 3 - Straight Creek Tunnel Pilot Bore, Colorado . . . . .	205
5. Summary . . . . .	208
17. CORRELATION OF ROCK QUALITY AND SUPPORT REQUIREMENTS FOR UNDERGROUND OPENINGS . . . . .	211
1. Introduction . . . . .	211
2. Case History No. 1 - Tunnels 1 and 2, Pigeon River, North Carolina . . . . .	214
3. Case History No. 2 - Tunnel No. 3, Tehachapi Project, California . . . . .	216
4. Case History No. 3 - Straight Creek Tunnel Pilot Bore, Colorado . . . . .	216
5. Summary of Support Data . . . . .	221
18. CONCLUSIONS AND RECOMMENDATIONS FOR FUTURE RESEARCH . . . . .	224
1. Engineering Classification of In-Situ Rock . . . . .	224
2. Measurement of In-Situ Deformability . . . . .	224
3. Relationship of Classification and In-Situ Deformability . . . . .	227
4. Relationship of Classification and Construction Rate of Tunnels and Shafts . . . . .	228
5. Relationship of Classification and Support Requirements . . . . .	229
6. Relationship of Classification and In-Situ Permeability and Slope Stability . . . . .	229
7. Recommendations for Future Research . . . . .	229
APPENDIX A. IN-SITU STATIC TESTS - SUMMARY OF FIELD AND LABORATORY PROPERTIES . . . . .	231
APPENDIX B. IN-SITU STATIC TESTS - SUMMARY OF MODULUS RATIOS AND ROCK QUALITY INDICES . . . . .	253
BIBLIOGRAPHY . . . . .	262
DISTRIBUTION . . . . .	273

# TABLES

<u>Table</u>		<u>Page</u>
1.1	SUMMARY OF ROCK MECHANICS DATA FROM PROJECTS UNDER INVESTIGATION . . . . .	6
2.1	TERMS DESCRIBING IN-SITU ROCK CONDITIONS . . . . .	10
2.2	DESCRIPTIVE TERMINOLOGY FOR JOINT SPACING AND THICKNESS OF BEDDING UNITS . . . . .	12
2.3	CLASSIFICATION OF IN-SITU ROCK . . . . .	13
2.4	SOUNDNESS CLASSIFICATION OF ROCKS IN-SITU . . . . .	15
2.5	GEOLOGICAL DIAGNOSTICS OF ROCK GRADE . . . . .	15
2.6	CLASSIFICATION OF GNEISSIC ROCKS AT ROSIERES DAM . . . . .	16
2.7	CLASSIFICATION OF ROCK AT LATIYAN DAM . . . . .	16
2.8	CORRELATION OF ROCK QUALITY AND THE RESULTS OF IN-SITU JACKING AND SEISMIC TESTS, LATIYAN DAM . . . . .	17
2.9	MODIFIED CORE RECOVERY AS AN INDEX OF ROCK QUALITY . . . . .	18
2.10	ROCK QUALITY BASED ON GEOLOGIC CHARACTERISTICS OBSERVED IN THE STRAIGHT CREEK TUNNEL PILOT BORE . . . . .	20
2.11	STRUCTURAL CLASSIFICATION OF ROCK . . . . .	22
4.1	PERCENT ABSORPTION FOR SEVERAL SATURATION CYCLES . . . . .	60
6.1	DESCRIPTION OF IN-SITU ROCK QUALITY . . . . .	114
6.2	ENGINEERING CLASSIFICATION FOR IN-SITU ROCK . . . . .	115
8.1	COMPARISON OF MODULI MEASURED BY RIGID AND FLEXIBLE PLATE JACK TESTS . . . . .	137
15.1	COMPARISON OF PREDICTED AND ACTUAL MOVEMENTS IN UNDERGROUND OPENINGS . . . . .	198
17.1	SUMMARY OF WIDTH OF TUNNEL OPENING, SUPPORT REQUIREMENTS, AND ROCK QUALITY INDICES . . . . .	222
18.1	CORRELATION OF ENGINEERING BEHAVIOR AND THE ENGINEERING CLASSIFICATION FOR IN-SITU ROCK . . . . .	225



## ILLUSTRATIONS

<u>Figure</u>		<u>Page</u>
2.1	REPRESENTATION OF STRENGTH OF A ROCK MASS . . . . .	11
2.2	CORRELATION OF ROCK QUALITY AS DETERMINED BY VELOCITY RATIO AND RQD . . . . .	19
2.3	ROCK QUALITY PLOTTED AGAINST ELECTRICAL RESISTIVITY AND SEISMIC VELOCITY . . . . .	21
2.4	CORRELATION OF ROCK QUALITY DESIGNATION AND CORE INDEX NUMBER . . . . .	24
3.1	TECHNIQUES FOR DETERMINING ROCK QUALITY FROM DRILL CORE . . .	28
3.2	RELATIONSHIP BETWEEN ROCK QUALITY DESIGNATION AND CORE INDEX NUMBER - GRANITE GNEISS AND BASALT . . . . .	29
3.3	RELATIONSHIP BETWEEN ROCK QUALITY DESIGNATION AND CORE INDEX NUMBER - GNEISS, DACITE, AND RHYOLITE . . . . .	30
3.4	WATER PRESSURE TEST - DETAILS IN BOREHOLE . . . . .	35
3.5	RELATIONSHIP BETWEEN ASSUMED OVERBURDEN PRESSURE AND INJECTION PRESSURE AT FAILURE . . . . .	37
3.6	WATER PRESSURE TESTING - LEAKAGE VS. PRESSURE . . . . .	38
3.7	TWO-DIMENSIONAL CONFIGURATION OF 3-D SONDE - BOREHOLE GEOMETRY	43
3.8	VARIABLE DENSITY LOGGING SYSTEM . . . . .	44
3.9	MAXIMUM HOLE DIAMETER MEASURABLE BY CALIPER TOOL FOR DIFFERENT SIZE JOINTS . . . . .	46
3.10	RELATIONSHIP BETWEEN FIELD (GAMMA-GAMMA) AND LABORATORY DENSITIES . . . . .	48
3.11	REFRACTION SEISMIC SURVEY . . . . .	52
3.12	UP-HOLE AND CROSS-HOLE SEISMIC SURVEYS . . . . .	54
3.13	SCHEMATIC ELECTRODE CONFIGURATION FOR RESISTIVITY CURVES . . .	57
4.1	SCHEMATIC INTERCONNECTION DIAGRAM FOR SONIC PULSE VELOCITY MEASURING EQUIPMENT . . . . .	61
4.2	STRESS-STRAIN BEHAVIOR AND SONIC PULSE VELOCITY FOR ROCK IN UNIAXIAL COMPRESSION - DWORSHAK 1 . . . . .	64
4.3	STRESS-STRAIN BEHAVIOR AND SONIC PULSE VELOCITY FOR ROCK IN UNIAXIAL COMPRESSION - DWORSHAK 2 . . . . .	65
4.4	STRESS-STRAIN BEHAVIOR AND SONIC PULSE VELOCITY FOR ROCK IN UNIAXIAL COMPRESSION - YELLOWTAIL 1 . . . . .	66
4.5	STRESS-STRAIN BEHAVIOR AND SONIC PULSE VELOCITY FOR ROCK IN UNIAXIAL COMPRESSION - YELLOWTAIL 2 . . . . .	67

# ILLUSTRATIONS (Cont'd)

<u>Figure</u>		<u>Page</u>
5.1	RELATIONSHIP BETWEEN NUMBER OF JOINTS IDENTIFIED BY BOREHOLE PHOTOGRAPHY AND THOSE IDENTIFIED IN THE CORE . . .	70
5.2	RELATIONSHIP BETWEEN ROCK QUALITY DESIGNATION AND PERMEABILITY - DWORSHAK DAM . . . . .	71
5.3	RELATIONSHIP BETWEEN ROCK QUALITY DESIGNATION AND PERMEABILITY - TWO FORKS DAMSITE . . . . .	72
5.4	RELATIONSHIP BETWEEN ROCK QUALITY DESIGNATION AND PERMEABILITY - HACKENSACK GAS STORAGE FACILITY . . . . .	73
5.5	RELATIONSHIP BETWEEN ROCK QUALITY DESIGNATION AND PERMEABILITY - WASHINGTON SUBWAY . . . . .	74
5.6	RELATIONSHIP BETWEEN ROCK QUALITY DESIGNATION AND PERMEABILITY - WORLD TRADE CENTER SITE . . . . .	75
5.7	3-D SONIC VELOCITY LOG - REFLECTION PATTERN CAUSED BY HIGH ANGLE FRACTURES AT SOME DISTANCE FROM THE BOREHOLE, DWORSHAK DAM . . . . .	78
5.8	3-D SONIC VELOCITY LOG - PHASING PATTERN CAUSED BY HIGH ANGLE JOINTS INTERSECTING THE BOREHOLE, YELLOWTAIL DAM . . .	79
5.9	3-D SONIC VELOCITY LOG - REFLECTION PATTERN CAUSED BY LOW ANGLE JOINTS INTERSECTING THE BOREHOLE, TWO FORKS DAM . .	80
5.10	SCHEMATIC DIAGRAM OF "W" PATTERN CAUSED BY ENERGY REFLECTION FROM A DENSITY INTERFACE . . . . .	81
5.11	3-D SONIC VELOCITY LOG - SIGNAL ATTENUATION CAUSED BY SOLUTION CAVITIES IN LIMESTONE, YELLOWTAIL DAM . . . . .	83
5.12	3-D SONIC VELOCITY LOG - INCREASED TRAVEL TIME AND SIGNAL ATTENUATION CAUSED BY FAULTING AND JOINTING, BORING F, TWO FORKS DAMSITE . . . . .	84
5.13	RELATIONSHIP BETWEEN ROCK QUALITY DESIGNATION AND 3-D COMPRESSIONAL VELOCITY . . . . .	85
5.14	CORE PHOTOGRAPH OF A PORTION OF BORING F, TWO FORKS DAMSITE .	86
5.15	RELATIONSHIP BETWEEN ROCK QUALITY DESIGNATION AND ELECTRICAL RESISTIVITY BORING SB 5 . . . . .	88
5.16	RELATIONSHIP BETWEEN ROCK QUALITY DESIGNATION AND ELECTRICAL RESISTIVITY BORING SB 10 . . . . .	89
5.17	RELATIONSHIP BETWEEN ROCK QUALITY DESIGNATION AND ELECTRICAL RESISTIVITY BORING PM-2 . . . . .	90

# ILLUSTRATIONS (Cont'd)

<u>Figure</u>		<u>Page</u>
6.1	RELATIONSHIP BETWEEN ROCK QUALITY DESIGNATION AND CORE RECOVERY . . . . .	93
6.2	RELATIONSHIP BETWEEN VELOCITY INDEX AND CORE RECOVERY . . .	94
6.3	RELATIONSHIP BETWEEN ROCK QUALITY DESIGNATION (RQD NO. 1) AND VELOCITY INDEX - 3-D SONIC VELOCITY . . . . .	97
6.4	RELATIONSHIP BETWEEN ROCK QUALITY DESIGNATION (RQD NO. 1) AND VELOCITY INDEX - UP-HOLE SEISMIC VELOCITY . . . . .	99
6.5	RELATIONSHIP BETWEEN ROCK QUALITY DESIGNATION (RQD NO. 2) AND VELOCITY INDEX - 3-D SONIC VELOCITY . . . . .	100
6.6	RELATIONSHIP BETWEEN ROCK QUALITY DESIGNATION (RQD NO. 2) AND VELOCITY INDEX - UP-HOLE SEISMIC VELOCITY . . . . .	101
6.7	RELATIONSHIP BETWEEN ROCK QUALITY DESIGNATION (RQD NO. 3) AND VELOCITY INDEX - 3-D SONIC VELOCITY . . . . .	102
6.8	RELATIONSHIP BETWEEN ROCK QUALITY DESIGNATION (RQD NO. 3) AND VELOCITY INDEX - UP-HOLE SEISMIC VELOCITY . . . . .	103
6.9	RELATIONSHIP BETWEEN ROCK QUALITY DESIGNATION (RQD NO. 1) AND VELOCITY INDEX - TEHACHAPI . . . . .	106
6.10	RELATIONSHIP BETWEEN ROCK QUALITY DESIGNATION (RQD NO. 2) AND VELOCITY INDEX - TEHACHAPI . . . . .	107
6.11	RELATIONSHIP BETWEEN ROCK QUALITY DESIGNATION (RQD NO. 3) AND VELOCITY INDEX - TEHACHAPI . . . . .	108
6.12	RELATIONSHIP BETWEEN 3-D SONIC AND SEISMIC COMPRESSIONAL WAVE VELOCITIES . . . . .	109
6.13	RELATIONSHIP BETWEEN ROCK QUALITY DESIGNATION (RQD NO. 1) AND VELOCITY INDEX - COMBINED 3-D AND UP-HOLE DATA . . . .	111
6.14	RELATIONSHIP BETWEEN ROCK QUALITY DESIGNATION (RQD NO. 2) AND VELOCITY INDEX - COMBINED 3-D AND UP-HOLE DATA . . . .	112
6.15	RELATIONSHIP BETWEEN ROCK QUALITY DESIGNATION (RQD NO. 3) AND VELOCITY INDEX - COMBINED 3-D AND UP-HOLE DATA . . . .	113
7.1	TYPICAL CIVIL ENGINEERING PROBLEMS INVOLVING MODULUS OF DEFORMATION . . . . .	119
8.1	L.N.E.C. PLATE JACK TEST . . . . .	123
8.2	KARADJ DAM PLATE JACK TEST . . . . .	124
8.3	DWORSHAK DAM PLATE JACK TEST . . . . .	125
8.4	FLAT JACK TEST . . . . .	127

# ILLUSTRATIONS (Cont'd)

<u>Figure</u>		<u>Page</u>
8.5	CONCAVE DOWNWARD LOAD-DEFORMATION CURVE FROM PLATE JACK TEST . . . . .	131
8.6	CONCAVE UPWARD LOAD-DEFORMATION CURVE FROM A PLATE JACK TEST . . . . .	132
9.1	TYPICAL PRESSURE CHAMBER TEST SET-UP . . . . .	139
9.2	STRESS DISTRIBUTION AND DISPLACEMENTS AROUND PRESSURE CHAMBERS . . . . .	142
9.3	RADIAL JACK TEST . . . . .	145
11.1	IN-SITU TEST USING CABLE ANCHORS . . . . .	150
12.1	COMPARISON OF THE MODULUS OF DEFORMATION AND MODULUS OF ELASTICITY FROM IN-SITU STATIC TESTS . . . . .	155
12.2	COMPARISON OF PLATE JACK TEST MODULI MEASURED IN THE VERTICAL AND HORIZONTAL DIRECTION . . . . .	156
12.3	COMPARISON OF PLATE JACING TEST MODULI MEASURED PERPENDICULAR AND PARALLEL TO BEDDING . . . . .	158
12.4	COMPARISON OF IN-SITU TEST MODULI BEFORE AND AFTER GROUTING . . . . .	159
12.5	COMPARISON OF MODULI FROM BOREHOLE DEFORMATION AND PLATE JACKING TESTS . . . . .	161
12.6	COMPARISON OF MODULI FROM PRESSURE CHAMBER AND PLATE JACK TEST . . . . .	163
13.1	COMPARISON OF IN-SITU STATIC MODULUS OF DEFORMATION AND DYNAMIC MODULUS OF ELASTICITY . . . . .	166
13.2	COMPARISON OF IN-SITU STATIC MODULUS OF ELASTICITY AND DYNAMIC MODULUS OF ELASTICITY . . . . .	167
14.1	ILLUSTRATION OF A METHOD FOR OBTAINING A WEIGHTED ROCK QUALITY BENEATH A PLATE JACKING TEST . . . . .	170
14.2	COMPARISON OF IN-SITU STATIC MODULUS OF DEFORMATION AND ROCK QUALITY DESIGNATION . . . . .	171
14.3	COMPARISON OF IN-SITU STATIC MODULUS OF ELASTICITY AND ROCK QUALITY DESIGNATION . . . . .	172
14.4	COMPARISON OF IN-SITU PRIMARY WAVE AND SHEAR WAVE VELOCITY . . . . .	174
14.5	COMPARISON OF LABORATORY STATIC AND DYNAMIC MODULI . . . . .	175
14.6	VARIATION OF MODULUS RATIO, $E_d/E_{t50}$ , WITH ROCK QUALITY DESIGNATION . . . . .	177
14.7	VARIATION OF MODULUS RATIO, $E_e/E_{t50}$ , WITH ROCK QUALITY DESIGNATION . . . . .	178

# ILLUSTRATIONS (Cont'd)

<u>Figure</u>		<u>Page</u>
14.8	VARIATION OF MODULUS RATIO, $E_d/E_{dyn}$ , WITH ROCK QUALITY DESIGNATION . . . . .	179
14.9	VARIATION OF MODULUS RATIO, $E_e/E_{dyn}$ , WITH ROCK QUALITY DESIGNATION . . . . .	180
14.10	VARIATION OF MODULUS RATIO, $E_d/E_{t50}$ , WITH VELOCITY INDEX . . . . .	181
14.11	VARIATION OF MODULUS RATIO, $E_e/E_{t50}$ , WITH VELOCITY INDEX . . . . .	182
14.12	VARIATION OF MODULUS RATIO, $E_d/E_{dyn}$ , WITH VELOCITY INDEX . . . . .	183
14.13	VARIATION OF MODULUS RATIO, $E_e/E_{dyn}$ , WITH VELOCITY INDEX . . . . .	184
14.14	COMPARISON OF IN-SITU STATIC MODULUS OF DEFORMATION AND DEFORMATION RATIO (PROJECT SITES) . . . . .	186
14.15	COMPARISON OF IN-SITU STATIC MODULUS OF ELASTICITY AND DEFORMATION RATIO (PROJECT SITES) . . . . .	187
14.16	COMPARISON OF IN-SITU STATIC MODULUS OF DEFORMATION AND DEFORMATION RATIO (OTHER SITES) . . . . .	188
14.17	COMPARISON OF IN-SITU STATIC MODULUS OF ELASTICITY AND DEFORMATION RATIO (OTHER SITES) . . . . .	189
14.18	COMPARISON OF DEFORMATION RATIO AND ROCK QUALITY DESIGNATION . . . . .	191
15.1	COMPARISON OF IN-SITU TEST MODULUS AND MODULUS COMPUTED FROM DISPLACEMENT OBSERVATIONS OF STRUCTURES . . . . .	197
16.1	COMPARISON OF AVERAGE RATE OF ADVANCE FOR SINKING AND GROUTING SHIFTS AND ROCK QUALITY DESIGNATION, SHAFT, EAST COAST . . . . .	202
16.2	COMPARISON OF AVERAGE RATE OF ADVANCE FOR SINKING SHIFTS AND ROCK QUALITY DESIGNATION, SHAFT, EAST COAST . . . . .	203
16.3	COMPARISON OF GROUTING SHIFTS/50 FT INTERVAL AND ROCK QUALITY DESIGNATION, SHAFT, EAST COAST . . . . .	204
16.4	COMPARISON OF RATE OF ADVANCE AND JOINTS/10 FT, TUNNELS AT SITES NO. 1 AND 2, TEHACHAPI PROJECT, CALIFORNIA . . . . .	206
16.5	RATE OF CONSTRUCTION AND COST PER LINEAR FOOT PLOTTED AGAINST ELECTRICAL RESISTIVITY AND SEISMIC VELOCITY . . . . .	209
17.1	COMPARISON OF ROCK QUALITY AND TUNNEL SUPPORT, SITE NO. 3, TEHAGHAPI PROJECT, CALIFORNIA . . . . .	217
17.2	SET SPACING PLOTTED AGAINST ELECTRICAL RESISTIVITY AND SEISMIC VELOCITY . . . . .	218
17.3	COMPARISON OF ESTIMATED ROCK QUALITY DESIGNATION AND SUPPORT CLASSIFICATION FOR THE STRAIGHT CREEK TUNNEL PILOT BORE . . . . .	220
17.4	COMPARISON OF SUPPORT REQUIREMENTS BY WIDTH OF OPENING AND ROCK QUALITY . . . . .	223

## PRINCIPAL SYMBOLS

$E_d$	= modulus of deformation, field static test
$E_{dyn}$	= modulus of elasticity, laboratory dynamic test
$E_e$	= modulus of elasticity, field static test
$E_r$	= deformation modulus, field static test (includes $E_e$ and $E_d$ )
$E_{seis}$	= modulus of elasticity, field dynamic test
$E_{st}$	= modulus of elasticity, laboratory static test
$E_{t50}$	= tangent modulus of elasticity, laboratory static test
$k$	= permeability
$r$	= coefficient of correlation
RQD	= Rock Quality Designation (core logging parameter)
$S_e$	= elastic or recoverable deformation, field static test
$S_t$	= total deformation, field static test
SE	= standard error
SL	= level of significance
$V_F$	= field velocity
$V_L$	= laboratory velocity
$V_P$	= dilational wave velocity (P-wave)
$V_S$	= shear wave velocity (S-wave)
$\nu$	= Poisson's ratio
$\rho$	= mass density (unit weight/acceleration of gravity)

This page intentionally left blank.

PART A  
ENGINEERING CLASSIFICATION OF IN-SITU ROCK

SECTION 1  
INTRODUCTION

1. Nature of the Problem

The engineering properties of soil and rock are important factors in nearly every civil engineering project. The nature of geologic materials is considered in the foundation design of buildings, bridges, and dams. The design of highway, canal, and railroad cuts is based on an evaluation of the stability of natural materials. The properties of soil and rock are especially important in underground construction as they determine the design, method of construction, and cost of the project.

The requirements of modern civil engineering for a knowledge of the engineering properties of natural materials resulted in the development of first soil mechanics and more recently rock mechanics. Soil and rock mechanics are specialized branches of material science which is the study of the mechanics of man-made materials such as concrete and steel. Although both disciplines use analytical methods developed by material science, they must also use special techniques to deal with the heterogeneity of natural materials. The use of geologic studies to plan and evaluate field testing is one of the most important of these techniques.

Soil mechanics has developed methods for predicting the engineering behavior of soil based on soil classification, field and laboratory testing, and the observed behavior of engineering structures. All three elements are important, but the concept of soil classification is the unifying element. Soil classification provides a method for subdividing soil deposits into zones with engineering significance. Zoning assists in sample selection and the correlation of laboratory and field test results with measured engineering behavior. Soil classification is performed by classification or index property tests. These tests do not measure engineering properties of soil, but were chosen because they are simple, relatively inexpensive, and reproducible tests which correlate with the engineering properties of the soil mass. Examples are grain-size and relative density tests in coarse-grained soils and consistency in fine-grained soils.



While many properties of soil can be measured in the laboratory and field, the properties of greatest interest in engineering are permeability, strength, and compressibility of the in-situ material. These properties depend on the total character of the soil, the soil grains, and the grain-to-grain relationships. The engineering properties can normally be measured by laboratory tests. This fact greatly reduces the cost of soil testing as the cost of obtaining and testing representative samples in the laboratory is generally much lower than making corresponding measurements in the field.

The engineering behavior of the soil mass is determined by using the results of laboratory and field testing, the geometry of the soil mass determined by geologic studies, and the loads imposed by the structure. If the actual behavior is measured after construction, then a comparison can be made with the predicted behavior and future work can benefit from any modifications made in exploratory or analytical techniques.

Generally, the engineering properties of a rock mass cannot be predicted with the precision expected in soil investigations. Although there are many field and laboratory tests available, there are no widely accepted index properties which correlate with the engineering properties of the rock mass. In addition, the number of rock behavior measurements which quantitatively define the in-situ engineering properties of rock is rather limited.

These observations reflect a fundamental difference between soil and rock. Nearly all rock masses are not solid but consist of a series of partially interlocking blocks somewhat like a dry masonry wall. These blocks, often referred to as joint blocks, are roughly equivalent to the soil grain in a soil deposit. The joint blocks are created by the presence of natural surfaces of weakness such as joints, shear zones, bedding planes, and foliation surfaces. Collectively, these surfaces may be referred to as geological discontinuities for they are natural breaks in the continuity of the rock mass. The spacing of the geological discontinuities depends upon the rock type and the geologic history of the deposit. They are commonly spaced a few inches to a few feet apart. The character of the surfaces ranges from thin, discontinuous breaks which do not fully destroy the integrity of the rock, to wide fault zones with broken and altered rock which interrupt the continuity of the rock mass. The spacing and character of these surfaces determine whether the rock mass will have the properties of the individual joint blocks or those of residual soil.

A typical laboratory sample of rock is taken from a single joint block and the laboratory properties are those of the joint block and not the rock mass. This characteristic of laboratory testing is imposed by the requirements of sample preparation and the limited size of the sample which can be tested in laboratory equipment. The laboratory properties of such intact rock are similar to those of the rock mass only in the case of exceptionally good rock.

The limitation of laboratory testing in rock mechanics has convinced some investigators that field testing provides the only source of engineering information. However, field testing is expensive and only a small number of tests may be economically justified on even a large project.

Many of the field tests do not measure properties which are of immediate use to the engineer. For instance, core logs and geophysical tests provide data which must be interpreted before they can assist engineering design. This interpretation is presently based on the judgment of a geologist or engineer without the assistance of quantitative correlations. Each of the conventional exploratory tests is a potential index property of the engineering properties of a rock mass, but the science of rock mechanics has been impoverished by the lack of an engineering classification based on these tests.

In 1959 a proposal was submitted to the U.S. Air Force Weapons Laboratory, Kirkland Air Force Base, New Mexico, suggesting an investigation of this problem. A two-part investigation was proposed -- the first to provide a classification system for intact rock, and the second, a classification system for in-situ rock. It was suggested that both classifications be sufficiently general in scope that they could be used under a wide range of geologic conditions.

The first phase findings were reported in "Engineering Classification and Index Properties of Intact Rock" (Deere and Miller, 1966) published by the USAF Weapons Laboratory. The report is based on extensive laboratory testing of 13 rock types from 27 sites. The classification presented is based on two engineering properties of intact rock, the unconfined compressive strength and the tangent modulus of elasticity measured at a stress level 50 percent of the unconfined strength. Classification charts were presented which contained test data from that investigation and from the literature. The charts show that each rock type has a unique area in the classification indicating that lithologic descriptions can be used to estimate the engineering properties of intact rock. The report also showed that unit weight and the rebound hardness determined by

the Schmidt Concrete Hammer could be used as index properties to estimate the strength and tangent modulus.

The second phase, reported herein, consists of the collection and correlation of exploratory and laboratory data to develop index properties, an engineering classification for in-situ rock, and the correlation of the engineering classification with measurements of engineering behavior.

## 2. Scope of the Investigation

Field exploration data from twelve construction projects were obtained with the cooperation of the U.S. Bureau of Reclamation, U.S. Army Corps of Engineers, California Department of Water Resources, and several private companies. Additional information was obtained from private consulting files at the University of Illinois. The data collected include core logs, borehole photography, water pressure tests, and geophysical testing. These data were supplemented by additional core logging and geologic mapping performed by University of Illinois personnel, and geophysical testing performed by Birdwell Division of Seismograph Service Corporation, and the U.S. Air Force.

Data from in-situ engineering tests were obtained from the agencies listed above and the literature. These data include the results of plate jack, pressure chamber, and radial jack tests for in-situ deformability, measurements of deformation caused by engineering structures, and construction records.

Whenever possible, the cooperating agencies provided laboratory information. This information was supplemented by testing performed at the Rock Mechanics Laboratory, Department of Civil Engineering, University of Illinois.

Section 2 reviews previous classifications of in-situ rock. Sections 4 and 5 describe respectively the field and laboratory tests used in this investigation. Section 6 presents correlations between field tests and presents an engineering classification of in-situ rock.

The remaining Sections describe the various tests for the engineering properties of a rock mass. Sections 7 to 12 describe the static and dynamic engineering tests for in-situ deformation modulus. Section 13 presents correlations of in-situ moduli and the rock quality indices. Section 14 reviews measurements of deformation caused by engineering structures. Sections 15 and 16 compare rock quality measurements with factors taken from construction records. Section 17 presents a summary of the correlations. Section 18 presents conclusions and recommendations for future research.

### 3. Sites Studied

#### a. Introduction

The sites selected for field study are presented in Table 1.1 which also gives a listing of prior testing and testing performed during this investigation. The following paragraphs contain a brief description of the purpose and geologic conditions at each site.

#### b. World Trade Center

The data obtained at this site were compiled from the foundation investigations of the twin 110-story buildings to be constructed in lower Manhattan in New York City. The bedrock is gneiss, schist, and pegmatite of the Manhattan Schist Formation which is overlain by glacial drift and fill. The rock is generally fresh because it has been scoured by glacial activity. Local zones of weathered material exist which are probably located along the major joint systems.

#### c. Dworshak Dam

This project is located on the North Fork of the Clearwater River near Orofino, Idaho. The dam is a multipurpose power, flood control, and recreation facility that is 673 ft high with a crest length of approximately 3,000 ft. Rock mechanics investigations were completed in 3 test adits in the abutments to determine the in-situ deformation properties of the rock for design purposes. The rock is a massive granite-gneiss of the Orofino Series formed by the metamorphism of the Beltian Series sediments. The rock has been injected with quartz veins and occasional basaltic dikes.

#### d. Little Goose Dam

This dam, which consists of both earth fill and concrete sections and a 700-foot navigation lock, was designed by the Corps of Engineers for navigation, flood control, and power. The site is located on the Snake River near Starbuck, Washington. The rock is typical of the Columbia Plateau basalts, consisting of flow breccias, altered and vesicular basalts, and columnar basalts.

#### e. Two Forks Dam site

This proposed dam will be located on a tributary of the South Platte River near Conifer, Colorado, and is principally designed to avert flood damage in the Denver area. The Bureau of Reclamation is conducting in-situ rock mechanics tests in the left abutment to provide the necessary design information for a modified arch dam. The rock is a strongly foliated migmatitic gneiss and mica-hornblende schist.

TABLE 1.1

## SUMMARY OF ROCK MECHANICS DATA FROM PROJECTS UNDER INVESTIGATION

Site and Lithology	Laboratory Tests	Core Logging	Geologic Mapping	Seismic Surveys	Permeability Measurements	3-D Sonic Logging	Borehole Photography	In-situ Deformation
World Trade Center	1	1		2	2	2		
Dworshak Dam	1	1	1	2,3	2	3	2	2
Little Goose Dam	1	1	1,2		2			
Two Forks Damsite	1	1	1,2	2,3	2	3	2	2
Yellowtail Dam	1	1	1,2	2	2	3		2
Tehachapi Pumping Plant and Discharge Tunnels	1	1	1,2	2,3	2	2		2
Nevada Test Site	1	1				2		
Glen Canyon Dam	1	1	2	2				2
Morrow Point Dam	1	1	2	2				2
NW Illinois Power Plant	1	1	1	2		2		
Hackensack Gas Storage Facility	1	1	2	2	2			
Maryland Federal Center	1	1		2				

1 = Work performed by project  
personnel  
2 = Data obtained from coopera-  
ting agencies  
3 = Data obtained under con-  
tract to the project

f. Yellowtail Dam

This structure is a 575-foot modified arch dam located on the Bighorn River near Hardin, Montana. It was designed by the Bureau of Reclamation for water power, flood control, and recreation. Adits were driven into both abutments for grouting and inspection purposes and also to provide test sites for in-situ deformation tests. The rock is the massive Madison Limestone capped with soft Amsden Shale; the limestone being the foundation material. Solution activity has increased the width of some joints, and clay-filled cavities were discovered during the exploration program.

g. Tehachapi Pumping Plant and Discharge Tunnels

This pumping plant and discharge tunnels are part of a series of engineering projects designed to transport water from northern to southern California. The function of this project is to lift water about 2,000 ft up the north side of the Tehachapi Mountains where it will then flow by gravity through tunnels and siphons towards Los Angeles and San Diego. The tunnel linings must be designed to withstand pressures up to 1,000 psi and for this reason in-situ jacking tests were conducted to determine the modulus of deformation of the rock.

The rock consists of both diorite gneiss and sandstone at the pumping plant excavation; only gneiss is present in the tunnels. The quality of the rock is extremely variable because of the numerous local shear and fault zones that are probably associated with the larger Garlock and San Andreas Fault systems.

h. Nevada Test Site

A limited amount of information was available from exploratory borings in dacite and rhyolite on Pahute Mesa near Mercury, Nevada. The borings were part of a preliminary testing program to determine the physical properties of both intact and in-situ rock prior to nuclear experimentation studies.

i. Glen Canyon Dam

This dam was designed by the Bureau of Reclamation as a multipurpose structure for hydroelectric power, recreation and flood control. It is a 710-foot high concrete arch dam spanning the Colorado River near Page, Arizona. The rock is a rather soft, massive, friable sandstone of the Navajo Formation. Deformation measurements were made beneath the structure and on the abutments to determine the amount of permanent set of the rock due to annual variations in the loads transmitted by the arch action of the dam.

J. Morrow Point Dam

This project is a double-curvature, thin-arch dam located on the Gunnison River near Montrose, Colorado. Designed by the Bureau of Reclamation, this dam is 468 ft high, 52 ft thick at the base, and 12 ft thick at the crest. Its principal use is for hydroelectric power. The power house is located in the left abutment, 400 ft below the surface. The rock types described by the Bureau consist of mica schist, quartzite, and pegmatite. Extensive rock mechanics investigations were undertaken to provide information for the design of the power house.

k. Other Sites

These sites are grouped together because their engineering information consists only of borings and some seismic surveys. These projects include:

1. a northwestern Illinois nuclear power plant (Silurian limestone), 2. a cryogenic gas storage facility in Hackensack, New Jersey (Triassic sandstone and siltstone), and 3. a federal center at Olney, Maryland (gneiss).

## SECTION 2

### CLASSIFICATION SYSTEMS FOR IN-SITU ROCK

#### 1. Introduction

The engineering classification systems proposed for in-situ rock have been based on several factors. A common method has been to define the rock in terms of its intact unconfined compressive strength and modulus of elasticity. The anticipated mode of failure of the rock in underground excavations is then predicted on the basis of both deformational properties and the degree of fracturing. Other systems have compared the engineering behavior of the rock considering support requirements, blasting criteria, permeability, and slope stability with a qualitative description of jointing or bedding planes. The recent trend has been to quantitatively define geologic discontinuities either by core logging techniques, measurement of joint spacing, thickness of bedding planes, or by seismic or electrical resistivity measurements. These data have then been correlated with the engineering properties of the rock mass.

#### 2. Classification Systems

Terzaghi (1946) developed a system for classifying rock for the purpose of predicting tunnel support requirements. He used mining terminology to categorize the rock and to provide a description of each type (Table 2.1). His descriptive categories are based on joint spacing and weathering, but are not defined by measurements. His system is in general use today to evaluate rock for underground construction projects.

Coates (1964) criticizes this classification because it is dependent on use. The size of the tunnel with respect to the spacing of the joints will affect the choice of descriptive category for the rock. Because this classification does not use quantitative measurements, data are evaluated by individual interpretation. Terzaghi was undoubtedly well aware of these factors and probably intended that his system be modified to suit the dimensions of an underground opening.

A general classification for strength and stability analysis of a particular rock mass was given by John (1962). This was one of the first systems describing rock in terms of intact compressive strength, weathering, and the spacing of joints. On the basis of these properties he classified rock into



four groups: 1) sound; 2) moderately sound, somewhat weathered; 3) weak, decomposed and weathered; and 4) completely decomposed. For the hypothetical rock mass shown in Figure 2.1 the compressive strength ranges from 3,000 to 7,400 psi with a joint spacing from 3 to 40 inches. The rock mass would be classified as moderately sound with a blocky appearance which, according to John, should allow underground excavations of moderate spans without support. An engineering analysis for a material of this type should be based on principles of rock mechanics. For any material of an equivalent intact strength having a joint spacing less than 0.2 inch, soil mechanics techniques should be used for predicting material behavior.

TABLE 2.1  
TERMS DESCRIBING IN-SITU ROCK CONDITIONS

Category	Description
Intact	Rock containing no joints
Stratified	Rock consisting of individual strata with little or no resistance against separation along the planes of contact
Moderately jointed	Rock containing joints with blocks interlocked so that no lateral support is necessary for vertical walls
Blocky and seamy	A jointed rock mass composed of separated intact rock fragments which would require support for vertical walls
Crushed	Chemically unweathered rock reduced to small particle size
Squeezing	Rock that advances into a tunnel without perceptible volume increase
Swelling	Rock which exhibits a volume increase caused by minerals having a high swelling capacity

The classification system proposed by John is not in general use in the United States possibly because one of the variables, compressive strength, may have little relationship to the engineering performance of most rocks. A rock described as being "sound" on the basis of its intact strength may have a range of joint spacing from 20 feet to several inches. The engineering behavior of this material often depends upon the joint spacing, with the intact

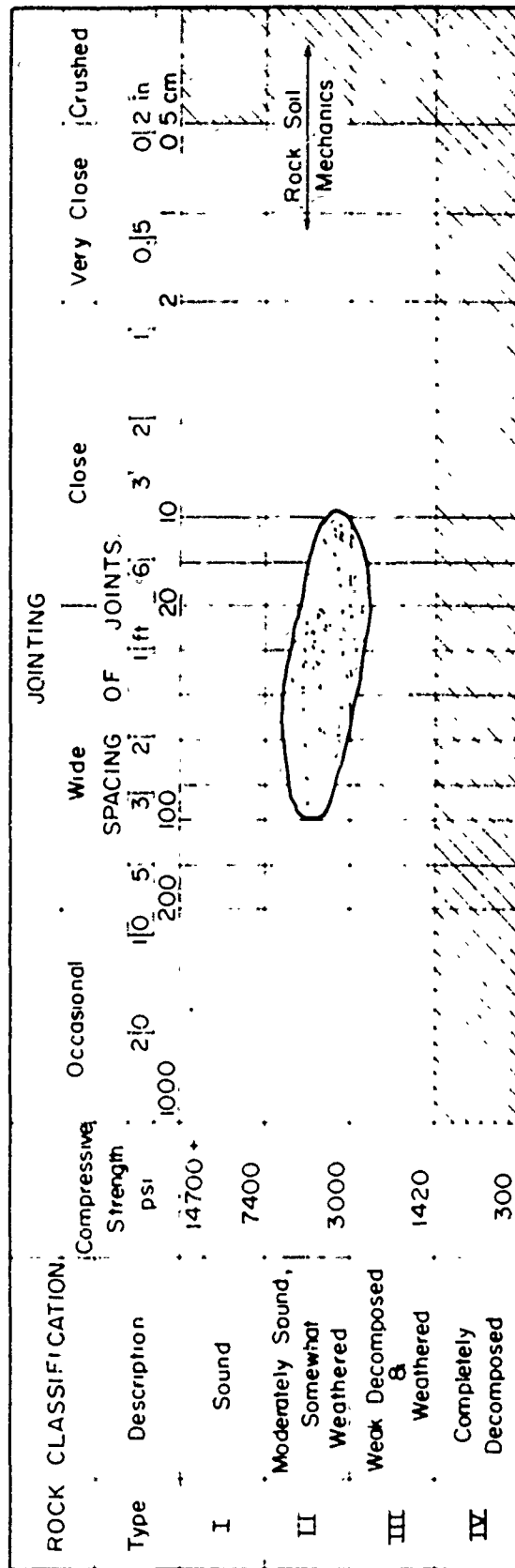


FIG. 2.1 REPRESENTATION OF STRENGTH OF A ROCK MASS (After John, 1962)  
Reproduced with the permission of A.S.C.E.

strength playing only a minor part in the engineering considerations. It would be misleading to define a rock mass with joints as closely spaced as 1 inch as a "sound" rock with close jointing.

Deere (1963) has recommended that the descriptive terminology of joint spacing and thickness of bedding be based on actual measurements. His criteria for boundaries are shown in Table 2.2.

TABLE 2.2  
DESCRIPTIVE TERMINOLOGY FOR JOINT SPACING  
AND THICKNESS OF BEDDING UNITS

Descriptive Term (joints)	Joint spacing or thickness of beds	Descriptive Term (bedding)
very close	< 2 in	very thin
close	2 in - 1 ft	thin
moderately close	1 ft - 3 ft	medium
wide	3 ft - 10 ft	thick
very wide	> 10 ft	very thick

Deere also suggested that the lengths of individual pieces of rock core should be measured because they are related to the joint spacing and bedding thickness in the rock mass. It is generally easy to locate core breakage influenced by drilling and these surfaces can be discounted. The tightness, irregularity, and filling material of joint surfaces have engineering importance and should be included in the core descriptions. He also recommends that the irregularity of these surfaces be described in terms of planeness (plane, curved, or irregular), and in degrees of smoothness (slick, smooth, or rough). This information could be useful in a consideration of slope stability, however, coefficients of friction should only be applied following field tests.

Coates (1965) proposed a method of classifying in-situ rock based on strength, deformation characteristics, and degree of continuity of the mass. He suggested that the first two factors be defined by laboratory tests because of the difficulty in measuring them in the field. He pointed out that a highly deformable rock would behave in a similar manner in the field, whereas a strong rock would be either strong or weak depending upon geologic discontinuities.

His classification system, shown in Table 2.3, should be supplemented with additional information such as joint orientation, permeability and porosity, and the presence of altered zones.

TABLE 2.3  
CLASSIFICATION OF IN-SITU ROCK

I. Strength		
	<u>Description</u>	<u>Unconfined strength (psi)</u>
	Very strong	> 25,000
	Strong	10,000 - 25,000
	Weak	5,000 - 10,000
	Very weak	< 5,000
II. Deformation properties		
A. Elastic		
- no creep or swelling tendencies		
- large amount of stored strain energy		
- a brittle fracture failure with explosive energy release		
B. Plastic		
- more than 25 percent total strain at any stress level is irrecoverable		
- some material will creep or swell on exposure and some will fail by yielding or rupture		
- includes viscous or time dependent strain materials (at constant stresses)		
III. Continuity		
	<u>Description</u>	<u>Joint Spacing</u>
	Massive	> 6 ft
	Blocky	1 ft - 6 ft
	Broken	3 in - 1 ft
	Very broken	< 3 in

The major contribution of Coates' classification is that it defines the continuity of a rock mass by actual measurement of joint spacing and therefore results in a quantity that is not dependent upon the size of a rock cut or underground opening. The strength and deformation parameters are based on laboratory measurements, which may have limited application to in-situ rock.

Onodera (1963) proposed a method of describing a rock mass by determining its in-situ dynamic modulus ( $E_{seis}$ ) by seismic tests and its

corresponding laboratory value ( $E_{dyn}$ ). The ratio of these moduli ( $E_{seis}/E_{dyn}$ ), was expressed as the soundness of the rock. For an unjointed material,  $E_{seis}$  should be approximately equal to  $E_{dyn}$ . However, the presence of discontinuities will reduce the seismic properties by a factor which is dependent upon the number of joints, the presence of weathering products, water conditions, and the openness of the features. His system is similar to that of Kudo (1965) who suggests that the relationship  $E_{dyn} - E_{seis}/E_{dyn}$  be called the crack coefficient of an in-situ rock mass. An evaluation of relative rock quality has been assigned to each numerical range of values (Table 2.4) and the corresponding geologic description is given in Table 2.5 (Onodera, 1963).

Onodera thought this technique could be used in the structural evaluation of a dam foundation or to measure the efficiency of consolidation grouting. He has offered a valid means of classifying in-situ rock by actually measuring a property of the mass. His geologic descriptions, however, give no indication of joint spacing.

Classification systems were developed at the Rosieres (Sudan) and Latiyan (Iran) Dam sites to categorize the complex geology of each region (Knill and Jones, 1965). The systems based on core logging, seismic surveys, in-situ deformation tests, permeability measurements, geologic mapping, and general rock behavior during construction, are presented in Table 2.6. Although there were several varieties of gneisses identified at this site, the amount of weathering was considered to be the significant engineering geologic feature. The description of each category was originally based on core examination. Excavations were made in many areas previously investigated by borings, and it was concluded that an accurate prediction of rock weathering could be made from cores even though only partial sample recovery was achieved.

A similar system was developed to describe the sandstone and quartzites (grades I-V) and shales (grades VI-VII) at the Latiyan Dam site (Table 2.7) (Knill and Jones, 1965).

Knill and Jones presented a map of the site showing the distribution of each rock grade. From this information subsurface conditions could be predicted. The results of in-situ jacking and seismic tests at Latiyan Dam were correlated with the various grades of rock quality by Lane (1964) (Table 2.8).

The classification of the rock at the Rosieres site is based on a subjective evaluation of the geologic conditions, and therefore is restricted

TABLE 2.4  
SOUNDNESS CLASSIFICATION OF ROCKS IN-SITU

Symbol	Grade	Soundness	Crack Coefficient
A	Excellent	0.75 - 1.00	< 0.25
B	Good	0.50 - 0.75	0.25 - 0.50
C	Available	0.35 - 0.50	0.50 - 0.65
D	Deficient	0.20 - 0.35	0.65 - 0.80
E	Bad	< 0.20	0.80 - 1.00

TABLE 2.5  
GEOLOGICAL DIAGNOSTICS OF ROCK GRADE

Grade	Geologic Description
Excellent	Fresh, no alteration, few joints
Good	More or less jointed, joints only slightly open, some weathering along surfaces
Available	More or less parted by joints with or without minor clay filling, rock fresh but joint surfaces weathered
Deficient	Joints rather widely opened containing clay fill, water in joints, rock more weathered
Bad	Advanced weathering, conspicuously jointed, cracked or crushed

TABLE 2.6  
CLASSIFICATION OF GNEISSIC ROCKS AT ROSIERES DAM

Grade	Description	Recovery (Percent)	Engineering Behavior
I	Fresh	> 90	Less blasting powder (by volume) needed for excavation than with II or III
II	Slightly weathered	70 - 100	Permeability 1 UL*
III	Highly or moderately weathered	15 - 70	Not suitable for concrete dam foundation; permeability generally 2 UL (but as high as 5 UL); material requires blasting; slopes stable up to 10 m
IV	Completely weathered	< 15	Very permeable; mechanically excavated; slopes disintegrate in wet conditions to angles between 25° - 30°

\* 1 UL = one Lugeon unit: a measurement of the groutability of rock based on the number of liters of water per minute pumped in a one meter length of test hole at a pressure of 10 atmospheres (1 UL corresponds approximately to a permeability of  $1 \times 10^{-5}$  cm/sec)

TABLE 2.7  
CLASSIFICATION OF ROCK AT LATIYAN DAM

Grade	Description	Engineering Properties
I	Sound, massive, widely spaced joints	Required blasting
II	Bedded with some shale layers	Required blasting; maximum stable slope - 70° up to 20 m high
III	Thinly bedded (5-15 cm) or flaggy rock with some shale layers	Required blasting
IV	Blocky, seamy rock, frequent intercalations of shale, some open joints	Required blasting; slopes stable at 45-50° up to 15-20 m
V	Broken, faulted or weathered, with some shale, generally found in a loose condition	Required blasting; slopes of 45-50° stable up to 15-20 m
VI	Thinly bedded	Required blasting; slopes fail at angles of 40° over 20 m high
VII	Friable clayshales	Mechanical excavation; slopes as in Grade VI

in its application. The method developed at Latiyan Dam combines construction experience and the results of in-situ rock mechanics tests. If a system of describing the joint spacing (John, 1962; Deere, 1963) had been combined with the in-situ measurements and observations, relationships might have been established for use on other engineering projects.

TABLE 2.8  
CORRELATION OF ROCK QUALITY AND THE RESULTS OF  
IN-SITU JACKING AND SEISMIC TESTS, LATIYAN DAM

Rock	Grade	$E_d$	$E_e$	$V_p$	$V_p/V_L$	Mean Core Recovery (Percent)
Quartzite and Sandstone	I	0.85	2.1	12,400	0.72	--
Sandstone	II	0.64	1.4	11,100	0.69	75
Sandstone	IV	0.21	0.58	8,500	0.59	55
Sandstone	V	0.26	0.29	6,600	0.50	24
Shale	VI	0.11	0.29	8,200	0.74	19

where

$E_d$  = in-situ secant modulus of deformation,  $\times 10^6$  psi

$E_e$  = in-situ modulus of elasticity (3rd load cycle)  
 $\times 10^6$  psi

$V_p$  = seismic velocity, ft/sec

$V_L$  = saturated laboratory sonic velocity, ft/sec

$V_p/V_{Lab}$  = fracture index

A method for quantitatively describing the nature of a rock mass from core borings was developed by Deere (1964). This system was designed to make the maximum use of drilling information because borings are required for almost all construction projects. The Rock Quality Designation (RQD) is obtained by measuring the total length of all unweathered pieces of core greater than or equal to 4 inches and dividing the total by the length of the particular core run. This quantity is expressed as a percent and is used to classify in-situ rock (Table 2.9).



The RQD is a measure of jointing and weathering of a rock mass and can be correlated with the seismic properties suggested by Onodera (1963). Such a relationship is shown in Figure 2.2. The velocity ratio has been squared to make the quantity proportional to a ratio of field and laboratory dynamic moduli ( $E_{seis} = \rho v_p^2 \frac{(1+\mu)(1-2\mu)}{(1-\mu)}$ ). An RQD was estimated from Onodera's geologic descriptions.

TABLE 2.9  
MODIFIED CORE RECOVERY AS AN INDEX OF ROCK QUALITY

RQD (Percent)	Description of Rock Quality
0 - 25	Very poor
25 - 50	Poor
50 - 75	Fair
75 - 90	Good
90 - 100	Excellent

The in-situ deformation properties of rock can be estimated using the RQD system (Deere, et al., 1957). This relationship is based on the premise that if the joint spacing is wide enough the deformation modulus of a rock mass will approach that of a laboratory sample. Therefore, as the RQD approaches 100 percent the modulus ratio approaches 1.0. Deere et al. (1967) have correlated the RQD with the results of in-situ seismic tests and have shown that either index can be used to determine rock quality. When indices are related to the results of field jacking tests, the anticipated deformation of a rock mass can be predicted.

Scott and Carroll (1967) classified the granite and metasedimentary rocks at the Straight Creek Tunnel site, Colorado, into five categories (Table 2.10). Seismic and electrical resistivity surveys were run in a pilot tunnel and in boreholes, and the results indicate that both the velocities and resistivities decrease as the rock becomes more jointed and weathered (Figure 2.3). These data were also compared with engineering properties of the rock such as support requirements, height of tension arch, stable rock loads, and rate of tunnel advance. The relationships between rock quality, geophysical data, and construction experience established in exploratory or preliminary

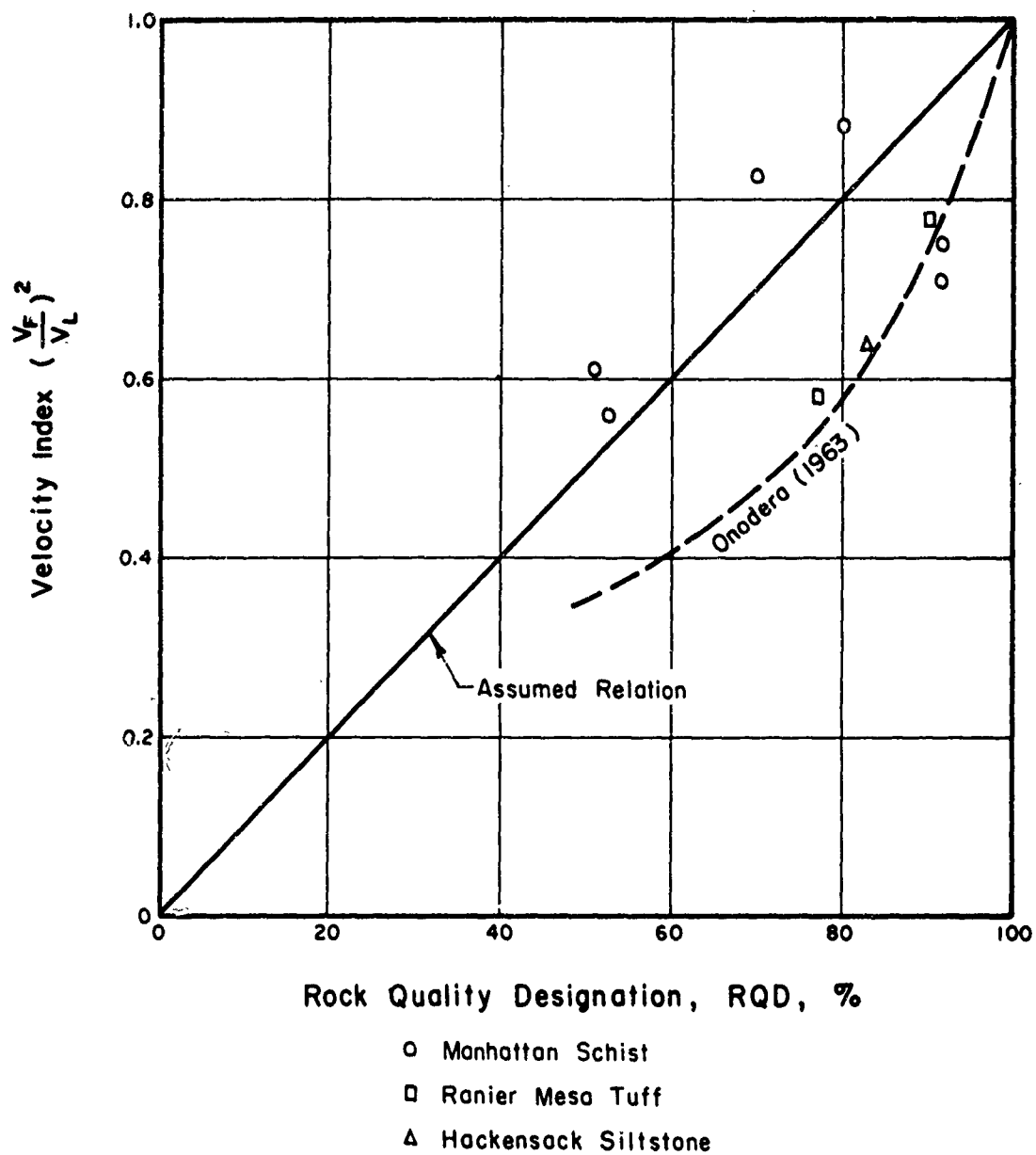


FIG. 2.2 CORRELATION OF ROCK QUALITY AS DETERMINED BY VELOCITY RATIO AND RQD (After Deere et al., 1967 ) Reproduced with the permission of A.I.M.E.

TABLE 2.10  
ROCK QUALITY BASED ON GEOLOGIC CHARACTERISTICS OBSERVED  
IN THE STRAIGHT CREEK TUNNEL PILOT BORE

Rock Quality (1 = best)	Fracture Spacing (feet)	Mineral Alteration (percent of rock)	Faulting	Foliation and Schistosity	Rock Type
1	> 3.0	< 5	None	None; predominant banding in migmatite	Predominantly granite or diorite dikes; sparse migmatite
2	1.0 - 3.0	5 - 10	Minor; a few slicks and minor gouge	Poorly defined; prominent banding in migmatite	Commonly granite; sparse gneiss and migmatite
3	0.3 - 1.0	10 - 15	Moderate; slicks common; minor gouge	Poorly to well defined; may be absent in granite	Granite and metamorphics, occurrences about equal
4	0.1 - 0.3	15 - 20	Moderate to severe; slicks and gouge on most surfaces	Well defined in metamorphics; may be absent in granite	Commonly schist, gneiss, or migmatite; sparse granite
5	< 0.1	> 20	Intense; frequency of gouge seams may be greater than fracture spacing	Very well defined; may be absent in granite	Predominantly schist; sparse granite

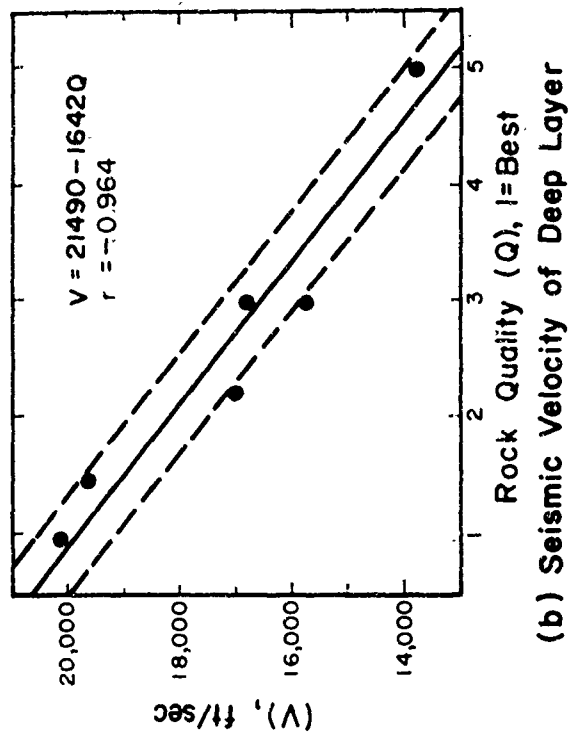
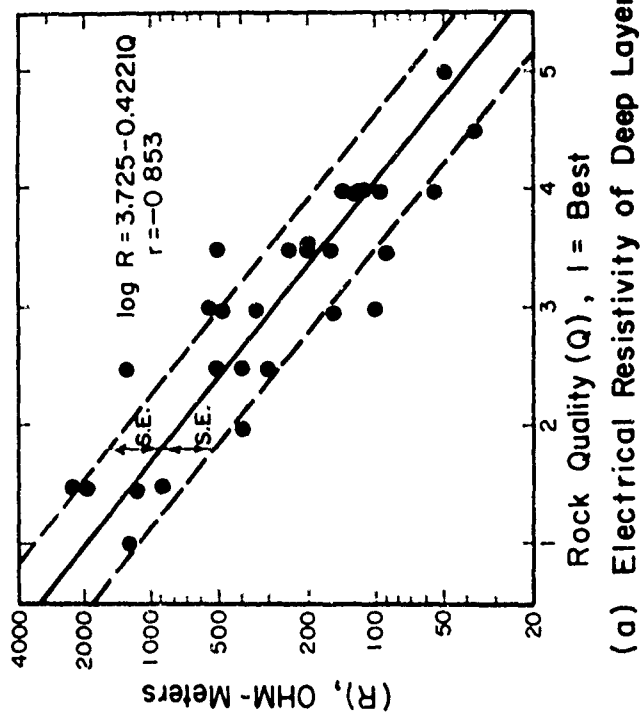


FIG. 2.3 ROCK QUALITY PLOTTED AGAINST ELECTRICAL RESISTIVITY AND SEISMIC VELOCITY (After Scott and Carroll, 1967)

stages of construction can be used later in the project to predict potentially hazardous rock conditions. By using these methods, it is also possible to make quantitative estimates of rock quality which aid the contractor in his bid estimates and construction techniques.

Obert and Duvall (1967) proposed a structural classification of rock by considering the combination of geologic and mechanical properties that influence the design and construction of underground openings. Their classification was subdivided into competent and incompetent rock as shown in Table 2.11.

TABLE 2.11  
STRUCTURAL CLASSIFICATION OF ROCK

I. Competent Rock	- capable of maintaining underground openings without structural support
A. Massive	
1. Elastic	- joint spacing greater than the critical dimensions of the opening
2. Inelastic	- tendency of the rock to creep or flow (halite, potash, trona)
B. Laminated	
1. Elastic	- thinly laminated but relatively elastic sedimentary and metamorphic rocks
2. Inelastic	- openings subject to heave or sag (oil shales, laminated evaporite deposits)
C. Jointed	- rock containing one or more sets of parallel joints
II. Incompetent Rock	- incapable of sustaining unsupported underground openings; degree of severity increases as the joints become more closely spaced and their surfaces become more altered or weathered

The authors state that the classification should be used with judgment because the size and depth of the structure influences the behavior of a rock mass. For example, a low-strength rock such as chalk would be classified as competent at depths of 100 feet (for a 30-foot diameter opening) but would be incompetent at a depth of 1,000 feet. Salt is relatively elastic at depths of

several hundred feet but is inelastic at a depth of several thousand feet. The boundary between competent and incompetent rock is based on joint frequency and weathering. The authors provide no quantitative descriptions of these parameters, and therefore, the system is limited to use by experienced field engineers.

Ege (1967) developed a core indexing system to relate boring data, the results of geophysical tests, and the engineering behavior of rock. Although no definite classification has yet been proposed, this method is now being used as a means of predicting tunneling conditions at the Nevada Test Site. The core index number is based on 10-foot coring intervals, and is calculated by adding the joint frequency and 0.1 of the percent values for core loss and broken core (pieces less than 3 inches). The purpose of using the multiplication factor of 0.1 is to keep the index number between 1 and 10. Joint frequencies seldom exceed 10 joints per foot.

Ege also calculated RQD values for his data. The relationship between RQD and the core index number is shown in Figure 2.4. The good correlation was not unexpected because each system measures essentially the same properties of the rock core. The calculations of the RQD are simpler and for this reason would be preferred for use in the field.

### 3. Conclusion

The classification systems for in-situ rock which have been proposed are based on either laboratory values of strength and deformation, or on some description of the jointing and weathering of the rock mass. These descriptions are either qualitative in terms of general geologic conditions or are quantitative measurements of discontinuities obtained by core logging or geophysical methods.

Laboratory properties are limiting values which are seldom attained in the rock mass. Classification systems based on laboratory properties have, therefore, limited field engineering value. It has been shown that jointing and weathering do influence engineering properties of in-situ rock and so the quantitative measure of these features is the most promising approach for future classification methods.

The next step in the development of an in-situ classification system is to determine which methods of measuring rock quality are the most sensitive to geologic discontinuities and can therefore be related to the engineering behavior of the rock mass.

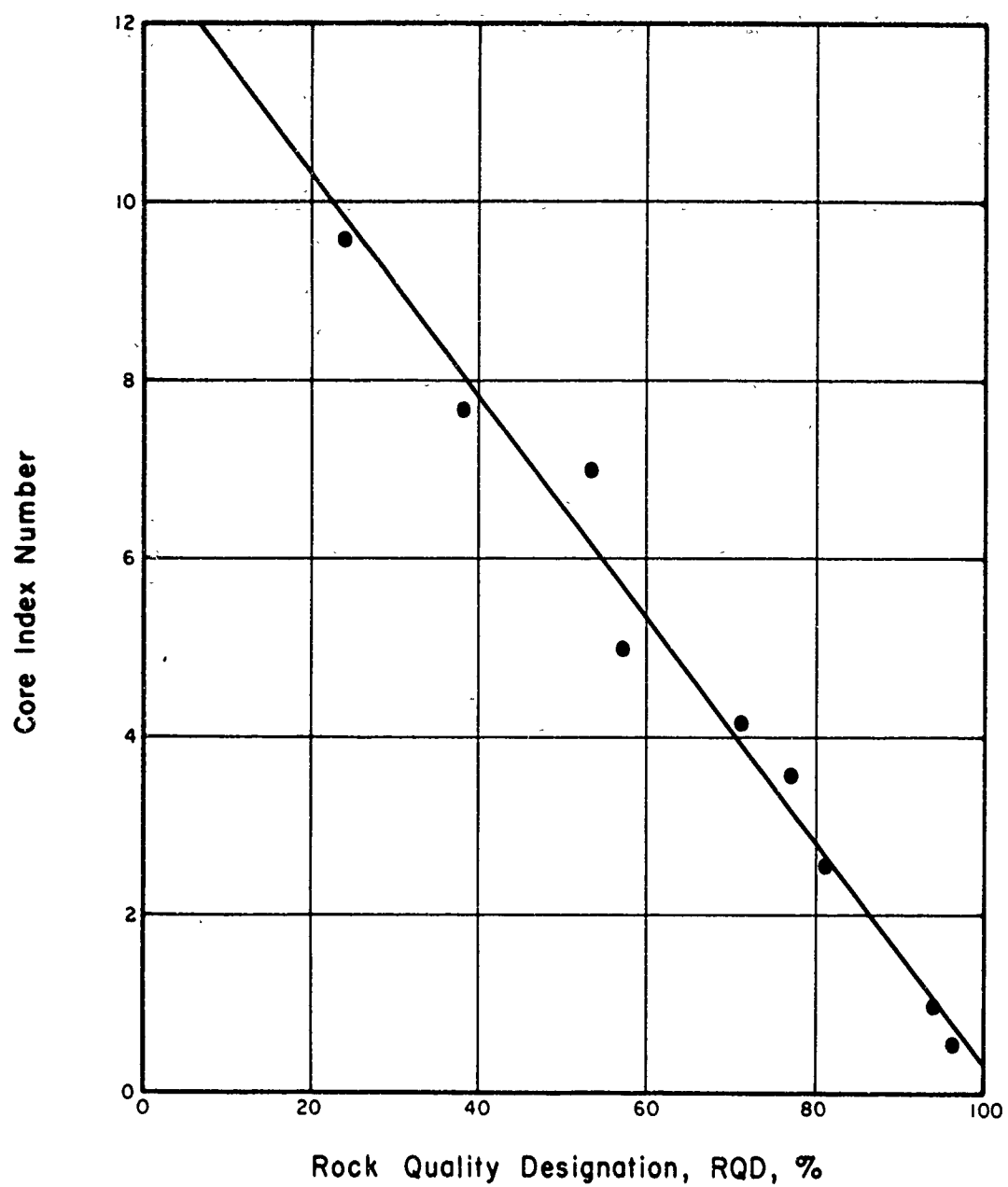


**FIG. 2.4 CORRELATION OF ROCK QUALITY DESIGNATION AND CORE INDEX NUMBER (After Ege, 1967)**

## SECTION 3

### FIELD INVESTIGATION METHODS

#### 1. Introduction

An accurate prediction of the engineering properties of a rock mass depends upon the use of a wide variety of exploration techniques. The information provided by cooperating agencies included boring logs, permeability measurements, and in some cases, bore hole photography and geophysical surveys. These data were supplemented with detailed core logging, geologic field mapping, and geophysical surveys where necessary. A description of the core logging procedure and field exploration techniques is presented in this section.

#### 2. Core Logging

Because core borings are the most common exploration method, a system should be developed to obtain from these borings the maximum available information about the rock. Boring logs usually provide a brief lithologic description, a qualitative description of joints and faults, and the percentage of core recovered during a particular core boring interval. Additional information often includes the type of drilling apparatus used: single-tube, double-tube, or wire-line core barrels; face or side discharge bits; and the size of stones in the diamond bit. These aspects of the drilling equipment may be important when the boring logs are used to determine in-situ rock conditions. In addition, the rate of drill advance can often indicate the abrasiveness or hardness of the rock.

##### a. Core recovery

Core recovery is the most commonly used method of expressing in-situ rock quality. The core recovery is the percentage of a cored interval which is represented in the core box by cylinders to gravel size pieces of rock. Because both sound and weak rock are included in core recovery, it is not a good method of evaluating in-situ rock quality. The driller, who often measures and is judged by core recovery, is encouraged to obtain higher recoveries by spreading out the zones of broken rock in the core box. In basalt, for example, it is common to find brecciated zones between massive layers. Core recoveries of nearly 100 percent have been reported from these zones as well as from the massive rock above and below. In zones of heavily jointed rock the core recovery may be high whereas the core itself is broken into many pieces less than one foot



in length. Low values of recovery are indicative of poor quality rock such as fault zones or weathering. However, if the recoveries are high (80-90 percent) it does not necessarily mean that the rock can be considered to be massive with uniform properties.

b. Modified core recovery

The method of core logging developed by Deere (1964) has an advantage over core recovery because his technique considers core loss and broken core as well as the degree of jointing and weathering of the recovered portion. His system, the Rock Quality Designation (RQD), counts only those pieces of unweathered rock greater than or equal to 4 inches, and divides their combined length by the length of the coring interval. The RQD system was used for describing the core borings in all sites investigated for this investigation.

The RQD is a function of the length of individual pieces of core therefore some discretion is necessary in determining whether the broken surfaces are the result of drilling procedure, improper handling, or actually represent joint planes. The broken surfaces of the core can generally be described as:

1. Clean regular surfaces which can be rejoined with only a hair-line separation
2. Irregular and rounded surfaces that reflect considerable grinding in the core barrel
3. Rather smooth surfaces that cannot be rejoined but which show no signs of weathering (foliation planes)
4. Surfaces showing weathering, hydrothermal alteration, or slickensides

The clean regular surfaces which could be rejoined (category 1) were considered to have been caused by the drilling procedure and were not counted as joints. It can not be determined whether all the core breaks described in categories 2 and 3 reflect significant discontinuities in the rock mass. Any weathering products that might have been present in category 2 would have been completely removed by the grinding action. These core breaks are not common and were considered to be joint surfaces because there was no way of knowing whether they represented an in-situ feature.

Core breakage along the thick bands of mica in foliated rocks, category 3, is considered to be a significant in-situ discontinuity. Even though these features are probably not open joints in the field, they may have a strong influence on tunneling conditions when they are parallel or sub-parallel to the

tunnel axis. Any weathered or slickensided pieces of core, category 4, are considered as major in-situ discontinuities.

All pieces of core bounded by surfaces described in categories 2, 3, and 4 were measured and recorded as part of the standard logging procedure adopted for this project. Intervals containing pieces less than 0.1 ft long were defined as broken zones and each surface was examined for evidence of weathering. Because joints and fractures have more engineering significance than do minor lithologic variations, greater care was taken in examining each feature and measuring its inclination than in recording subtle mineralogical changes.

Rather than using only a core base length of 0.35 ft (4 inches) as defined by Deere (1964) for his RQD (Figure 3.1A), base lengths of 0.1 ft, 0.2 ft, 0.5 ft, and 1.0 ft were used in this study to determine which joint spacing had the best correlation with the results of other types of borehole tests. In addition, five more rock quality values were calculated considering only the weathered surface of core (category 4) as representing in-situ joints (Figure 3.1B). The same five base lengths were used in these tests.

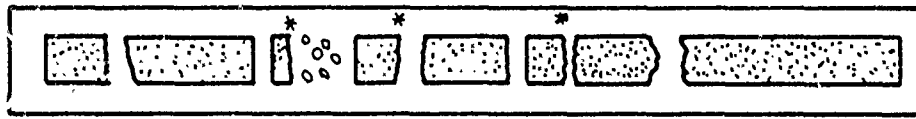
The situation could arise using the 0.35 ft base where the in-situ joints have a uniform spacing of 0.5 ft. In this case the rock quality would be 100 percent (assuming that the rock was unweathered and that there was no core loss in the run), but this close joint spacing might cause construction difficulties in underground excavations. To overcome this limitation of the other rock quality values, another value was calculated where the lengths of all core pieces 0.1 to 1.0 ft were squared to obtain a weighted core length. The new rock quality value was calculated by adding the weighted core length and dividing by the length of the core run (Figure 3.1C). This system can also be used when only weathered surfaces are considered as actual in-situ discontinuities (Figure 3.1D). The advantage of this system is that it is not necessary to select an arbitrary boundary below which all pieces are disregarded. The length of each piece is considered in the calculation of rock quality, but the longer pieces are given greater weight by the squaring process.

The core logging method proposed by Ege (1967) was also used, and the results from each of the sites studied were compared with the RQD. Figures 3.2 and 3.3 indicate a nearly perfect correlation between these two indices. Each system therefore measures essentially the same properties of the rock core.

There are many possibilities for statistical analyses of rock core. As the technique becomes more refined, however, the system becomes too complicated

# Rock Quality

Core Recovery	Rock Quality			
	(A) All Core Pieces (0.35 Base)	(B) Considering Only Weathered Surfaces (0.35 Base)	(C) Squaring Piece Lengths (0.1-0.99)	(D) Squaring Lengths Bounded By Weathered Surfaces (0.1-0.99)
0.35 ft.	0.35 ft.		.12 ft.	
0.70	0.70	1.15	.49	1.15 ft.
0.1			0.1	
0.2			.04	.04
0.2			.25	.49
0.5	0.50	0.70	.04	
0.2			.16	
0.4	.040			
1.4	1.40	1.80		1.80
4.05 ft.	3.35 ft.	3.65 ft.	2.51 ft.	3.48 ft.
405/5.0 = 81 %	3.35/5.0 = 67 %	3.65/5.0 = 73 %	2.51/5.0 = 50 %	3.48/5.0 = 70 %



Core Run  
= 5.0 ft.

\* Weathered Joint Surface

FIG. 3.1 TECHNIQUES FOR DETERMINING ROCK QUALITY FROM DRILL CORE

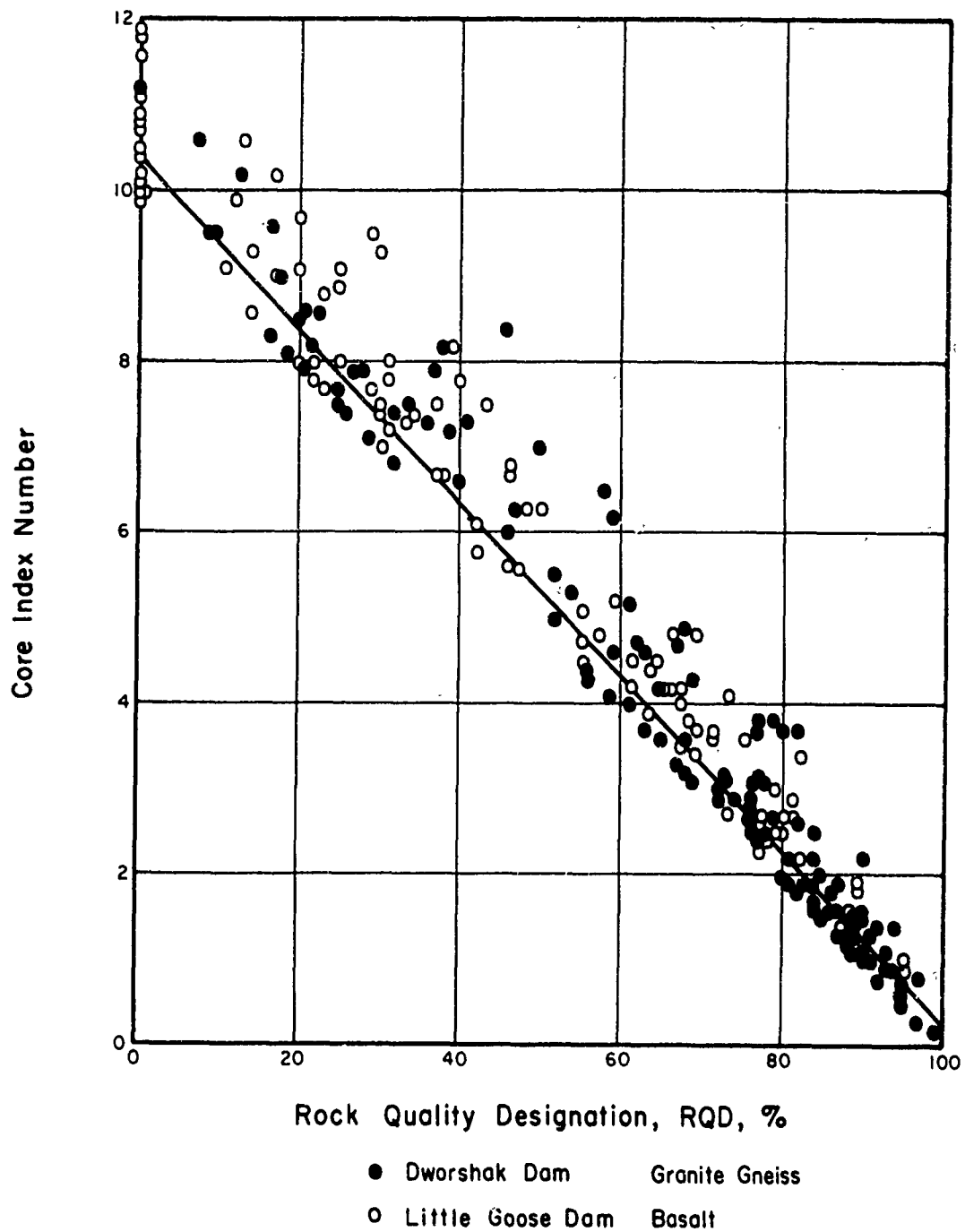


**FIG. 3.2 RELATIONSHIP BETWEEN ROCK QUALITY DESIGNATION AND CORE INDEX NUMBER—GRANITE GNEISS AND BASALT**

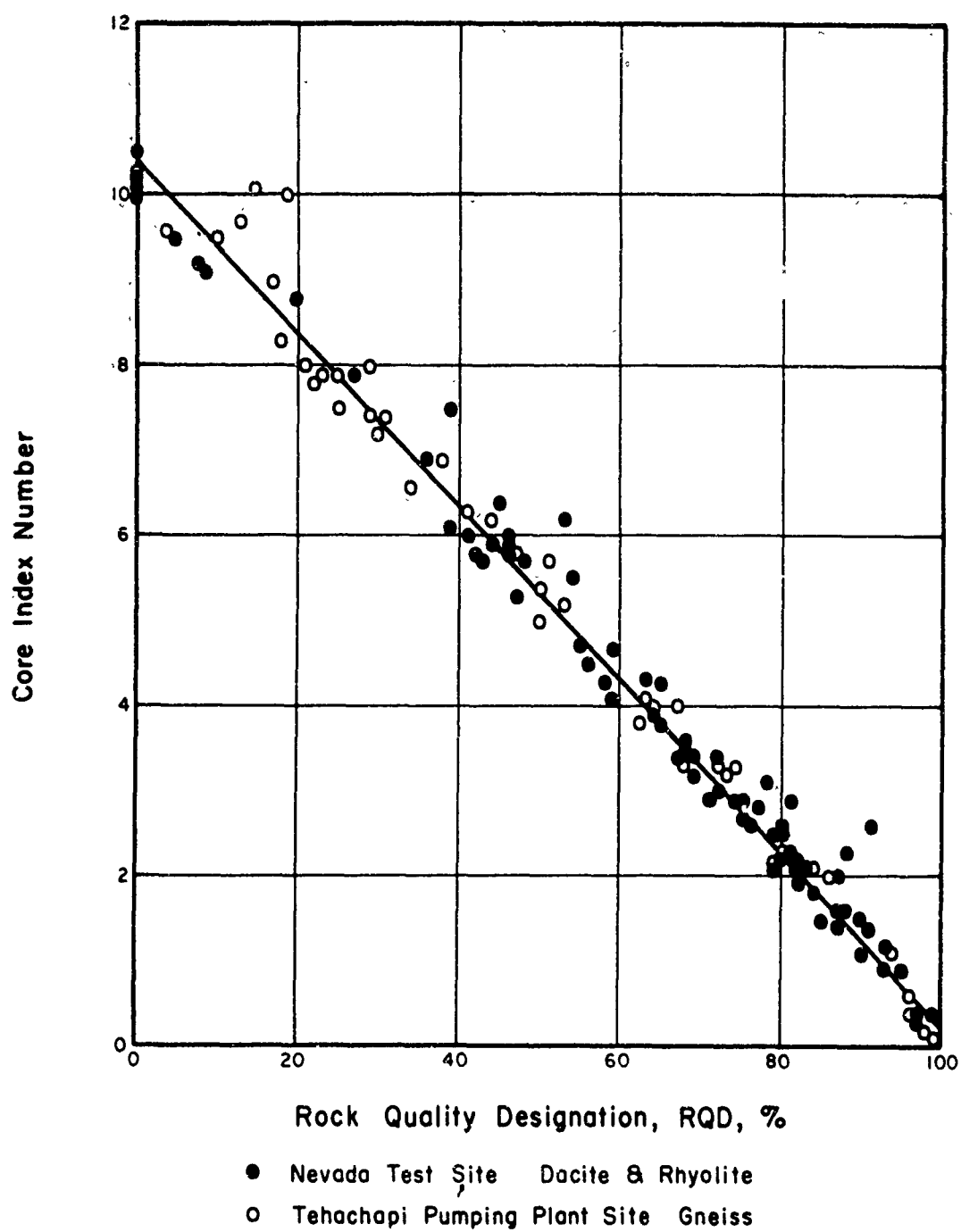


FIG. 3.3 RELATIONSHIP BETWEEN ROCK QUALITY DESIGNATION AND CORE INDEX NUMBER— GNEISS, DACITE, AND RHYOLITE

for efficient use in the field. The methods used in this project were chosen because of their simplicity both in the logging procedure and calculations.

### 3. Geologic Mapping

#### a. Introduction

The geologic mapping procedures used for this project were limited to the determination of fracture spacing, weathering, and the location of fault zones in underground excavations. Measurements were made only in areas where the results could be correlated with in-situ deformation data, seismic refraction surveys, or variations in tunnel support requirements.

#### b. Mapping procedure

The mapping procedure consisted of laying out a 100-foot cloth tape (graduated in 1/100 foot) along each wall of a tunnel to measure the fracture spacing. Orientation and inclination of the fractures were recorded as were details concerning their tightness and the presence of alteration products. A mappable fracture was considered to be one that appeared as a continuous planar surface for at least 3 feet. This length was selected in an attempt to avoid any smaller fractures that could have been caused by blasting.

Fracture spacing was measured along each wall and, in small diameter tunnels, along the crown. Where the joints strike nearly parallel to the tunnel axis it is difficult to measure their spacing in the walls and it becomes necessary to take the measurements in the crown or face. Joint spacing can be illustrated by plotting the data as a bar graph of either RQD or fracture frequency. Developed geologic sections can also be used to show the relationship between the different joint sets.

The lithology of the sites discussed in this report was uniform enough that minor variations in mineralogy along a test section were considered to be insignificant. The degree of jointing and weathering are the factors that influence the results of geophysical tests, in-situ deformation tests, and tunnel support requirements.

### 4. Borehole Photography

The borehole photography data mentioned below was supplied by the U.S. Army Corps of Engineers and the U.S. Bureau of Reclamation from exploratory work done at the Dworshak and Two Forks Damsites. The information was compared with the rock quality determined by logging the core from the same boreholes.

The development of borehole photography and television have provided important tools for examining the in-situ conditions of a rock mass. They are used to determine the strike and dip of joints as well as to locate weathered and faulted zones that are often not indicated in core logs because of poor recovery. Each system has its advantages, and both are currently being used in the United States by the Bureau of Reclamation, the Army Corps of Engineers, and numerous private consulting firms.

a. Borehole camera

The camera, developed by the Corps of Engineers, is designed to provide a 360-degree photograph of an NX (3-inch diameter) borehole using either color or black and white film. The following description of the borehole camera is condensed from Burwell and Nesbitt (1954). The instrument consists of a conventional 16 mm motion picture camera with a 15 mm lens, a high voltage circular flash tube, a hollow truncated conical mirror, and an oil damped compass. The camera unit is mounted in a stainless steel tube (31-1/2 in. long and 2-3/4 in. in diameter) with a circular quartz window which is opposite the conical mirror when the camera unit is in the tube.

The flash tube is actuated by a synchronizing pulse from the camera lowering apparatus, illuminating the boring and simultaneously exposing the film. The depth counter and pulse synchronizing wheel are mounted on the camera cable-wheel. The camera drive is synchronized by the same pulsing circuit. The image of the borehole is projected to the camera lens by the hollow conical mirror which also makes the compass, located below the mirror, visible to the camera lens. The camera takes 16 pictures per foot of boring. Each picture covers a 1 inch section of the boring, creating a 33 percent overlap. The 16 mm film spools have a capacity of 25 feet so that 75 feet of boring can be filmed without reloading. The photographs may be shown on a regular screen or projected onto a cylindrical frosted glass screen by means of a conical prism, thereby simulating the borehole. Strike and dip of joints can be determined by orienting them with respect to the north arrow and the thickness of the feature can be measured to within 0.0001 ft.

The system has many advantages over other exploration techniques, and there are also disadvantages. In zones of crushed or soft rock the hole may not remain open long enough to permit photography, and the record of these important portions of the boring is not obtained. Because the camera is focused for a known distance to the borehole wall, any hole enlargement caused by poor

rock will result in photographs that are out of focus. The water in the boring must be relatively clear to obtain useful pictures. This means that photography must be delayed until soil particles settle or the hole must be flushed with clean water. Camera photography has not been successful in holes inclined at an angle less than  $50^{\circ}$  to the horizontal because of the difficulty in sliding the instruments in the hole, the susceptibility of the quartz window to damage, and the severe tilting of the compass. The latter condition is important only for determining the attitude of joints and would not be critical if a quick inspection of the hole was sufficient.

b. Television camera

The Bureau of Reclamation initiated the use of the side-viewing television camera in the United States at the Morrow Point Dam site in Colorado. In addition to locating rock fractures, the camera was used to determine the effect of stress relief and blast damage in the rock around the perimeter of excavations (Dodd, 1967).

Pictures of the borehole wall are transmitted to the surface by closed-circuit television for instant viewing. The location, orientation, and inclination of fractures can be mapped during the test and a video tape provides a permanent record. Widths of features less than 0.003 ft can be measured. The field of view of the television camera is limited to approximately  $52^{\circ}$  in contrast to the  $360^{\circ}$  field of the borehole camera. The camera, however, can be rotated through  $360^{\circ}$  to observe all sides of the boring. The television camera has been used successfully in overhead borings as well as those inclined at  $10^{\circ}$  to the horizontal.

c. Evaluation of borehole photography

There are several advantages of the television camera over borehole photography. Fractures in the rock can be viewed while at the site, it can quickly be determined whether a useable record has been obtained, and the entire hole can be surveyed quickly and a detailed record taken of those portions deserving careful study. Hole enlargements can be kept in focus because the lens can be adjusted by surface controls. However, the borehole camera gives a  $360^{\circ}$  view of the hole without rotating the sonde and can use color film. The advantage of color film is that it shows lithologic changes and weathering along joints more clearly than black and white film. Both instruments are apparently portable enough for use in underground excavations.



An important value of either method is that a complete geologic description of the rock is obtained without the interpretive analysis often required by seismic surveys and core borings. The prominent geologic features are clearly presented and can be accurately described.

## 5. Permeability Measurements

### a. Introduction

Permeability tests were not conducted in this investigation, however, a large amount of water pressure test data was provided by the cooperating agencies. The core from each boring tested was logged and a value of rock quality was calculated for each test interval. A discussion of the equipment as well as testing procedures and data analysis is presented below.

### b. Open end tests

A known amount of water is added to the open end of a pipe whose base is set at the desired position for the test. Sufficient water is added to maintain a constant level under gravity flow conditions. A constant level is seldom maintained when testing above the water table, but a fluctuation of within a few tenths of a foot over a 5-minute testing interval is considered satisfactory (Zangar, 1953). The permeability can be calculated by:

$$k = \frac{Q}{5.5rH} \quad \begin{array}{l} k = \text{permeability, ft/min} \\ Q = \text{constant rate of flow, cu ft/min} \\ r = \text{internal radius of casing, ft} \\ H = \text{differential head of water, ft} \end{array} \quad (3.1)$$

The value of H for tests made below the water table is the difference in feet between the water table and the level of water in the casing. For tests above the water table H is the length of the column of water in the hole.

### c. Pressure Tests

The tests involve the pumping of water into a borehole with measurements being taken at quantity of flow for given pressure increments. A single packer test (Figure 3.4) may be used to determine the average permeability over the entire length of a boring or may be restricted to certain intervals. If the hole is to be tested at 10-foot intervals, the drill steel is removed after a 10-foot drilling run and the testing equipment inserted into the hole. The packer, mounted near the lower end of the water pipe, is placed 10 feet from the bottom of the hole and expanded against the wall by mechanical or pneumatic means.

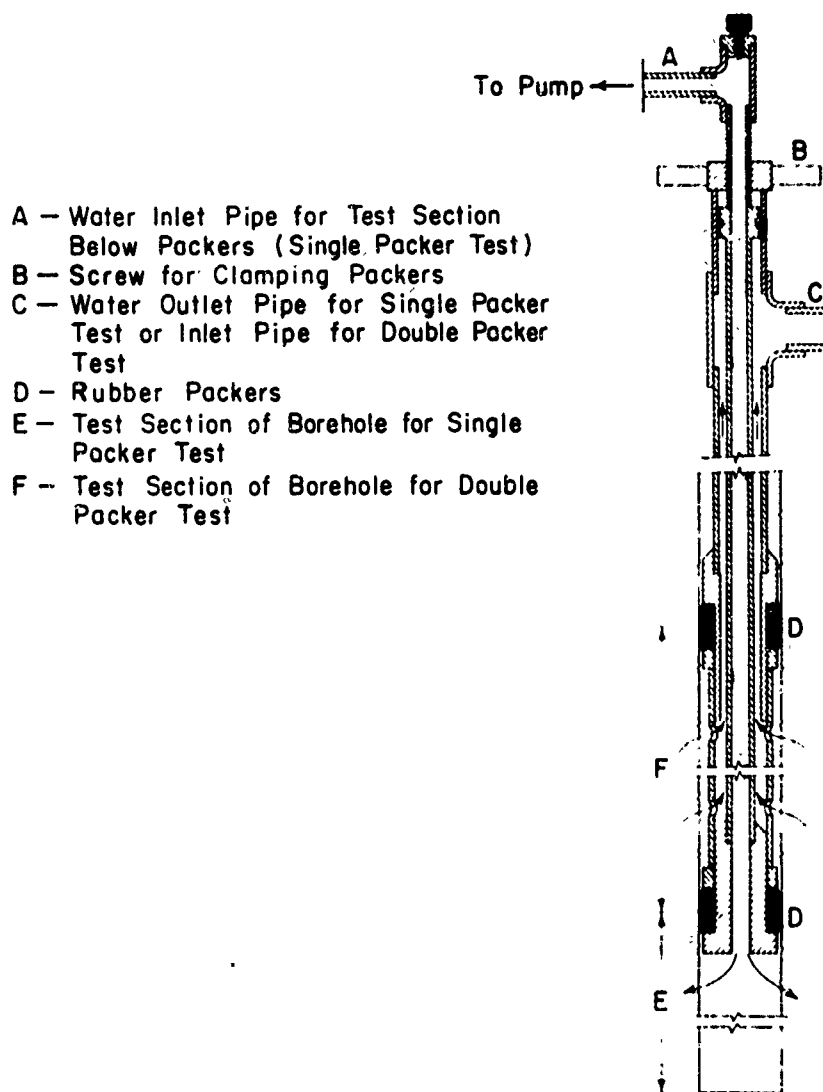


**FIG. 3.4 WATER PRESSURE TEST — DETAILS IN BOREHOLE (After Morgenstern & Vaughan, 1963)**

A double packer test is run after the hole has been drilled and is used in certain zones of suspected high permeabilities (Figure 3.4). These zones may be noted on the driller's logs as being locations of high drilling-water losses. For this test, two packers are spaced 5 feet to 10 feet apart at the lower end of the water pipe and are expanded against the borehole wall. Water is forced into the hole through ports located between the packers.

(1) Procedure for pressure testing

The joint surfaces must be free of any rock fragments or mud that were caused by drilling. The hole should be surged with clean water until the overflow is clear of suspended sediment. If possible the wash water should be at a higher temperature than the ground water to prevent air bubbles from forming in the rock voids, thereby, reducing the permeability.

It is common practice to run the test using different pressure increments. The pressure is allowed to build up to 50 to 60 percent of the desired level and held as constant as possible. Once the quantity of inflow has stabilized the initial readings of pressure, amount of water, and time are taken. After a 5-minute interval another set of readings is taken and the rate of inflow is computed. The pressure is then increased to the maximum value and a similar set of readings taken. The low pressure stage can be repeated to check earlier readings and to see if any damage has been done to the rock by the high pressures.

The maximum pressure recommended is governed by the amount of overburden above the test section and is generally set at 1 psi per foot of depth. If excessive pressures are used, the joints may be forced open and the rock surface may heave. Data from grouting tests showing the pressure required for rock fracturing versus the overburden pressure are given in Figure 3.5. These data indicate that the 1 psi per foot of overburden appears to be a safe pressure criterion.

If testing pressures are required above those of the overburden pressure, or if a check is desired to be sure that pressures are not excessive, in-situ tests can be made to determine the response of the rock to increasing pressure values. The amount of water loss is recorded in test holes for each increment of increasing pressure until failure of the rock occurs. The relationship should be linear (Figure 3.6a) prior to failure. When the pressure exceeds the shear strength of the rock mass the joints open and leakage suddenly increases (Figure 3.6b). The results of these tests can then be used as a guide for pressure requirements in other boreholes.

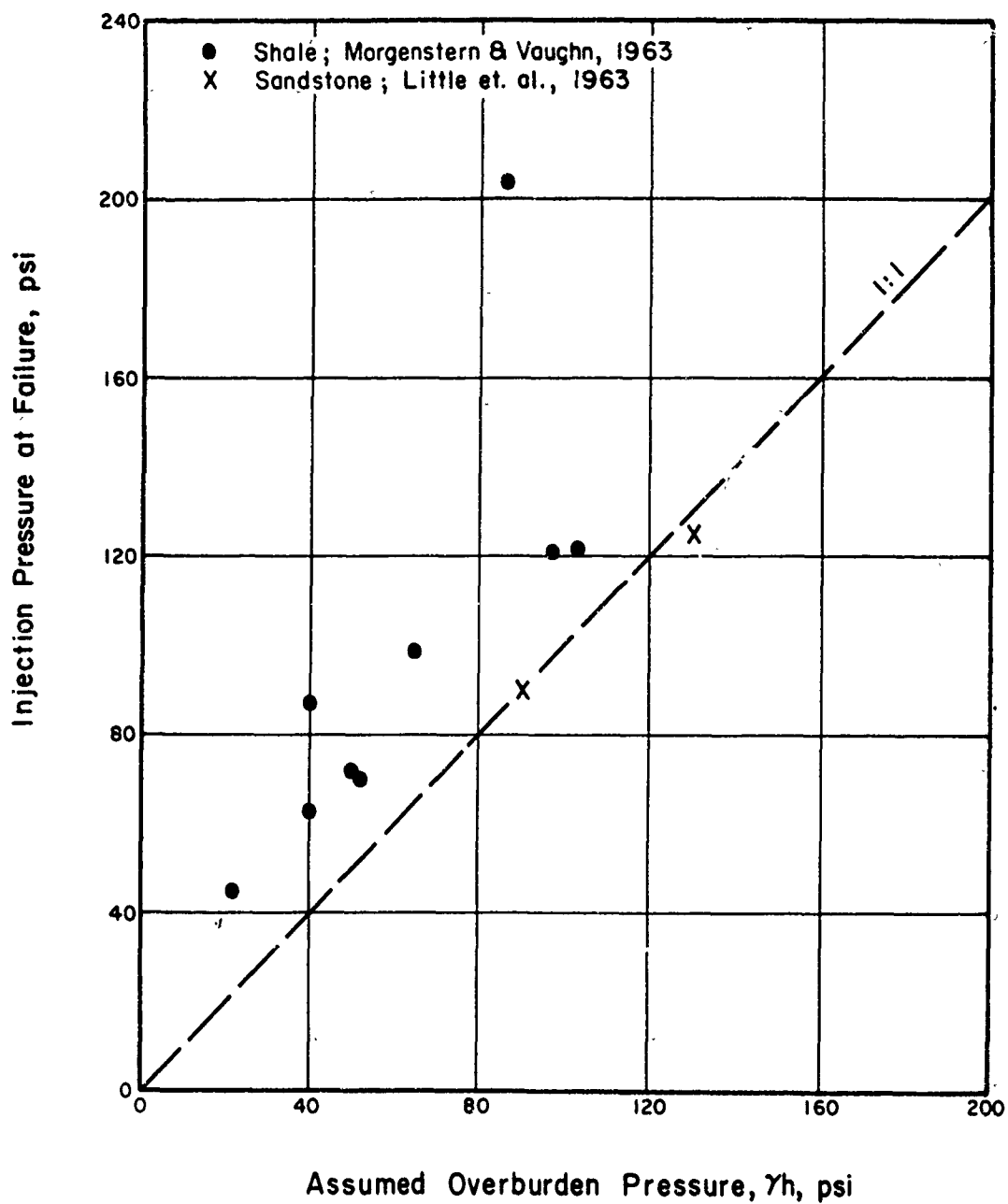
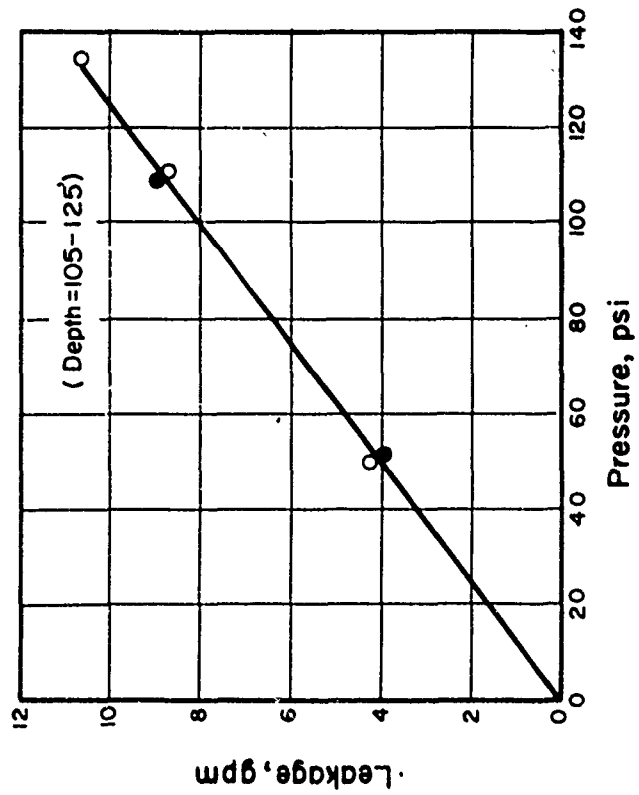
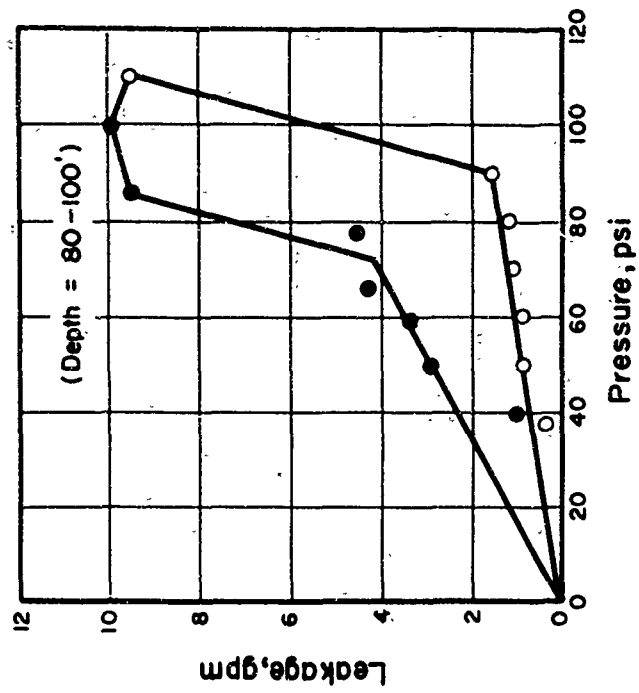


FIG. 3.5 RELATIONSHIP BETWEEN ASSUMED OVERBURDEN PRESSURE AND INJECTION PRESSURE AT FAILURE



a.) Linear Increase in Leakage With Increasing Pressure



b.) Failure of Rock Along Joint Planes Caused by Excessive Pressure

FIG. 3.6 WATER PRESSURE TESTING - LEAKAGE vs. PRESSURE (After Little et al. 1962)

Friction head losses may amount to a significant portion of the initial pressure depending upon the internal diameter, roughness, and length of the water pipe, and the amount of flow. For this reason it is recommended that the water pipes be laid out on the ground, and a relationship be determined between water flow, length of pipe, and the difference in pressure between the ends of the system.

There are no standard specifications concerning the capacity of water pumps for these tests because of the variations in permeability that may exist in rock. As a general rule the capacity should be at least 50 gpm to cover a wide variety of conditions.

## (2) Calculations of permeability

The formulas for calculating permeability are most valid when the thickness of the stratum tested is at least five times the length of the test interval and when the test is run below the water table (U.S. Bureau of Reclamation, 1963). The following formulas used to compute permeability are based on the assumption that the flow is radially outward into the rock under steady state conditions.

$$k = \frac{Q}{2\pi LH} \log_e \frac{L}{r} ; \quad L \geq 10r \quad (3.2)$$

$$k = \frac{Q}{2\pi LH} \sin h^{-1} \frac{L}{2r} ; \quad 10r > L \geq r \quad (3.3)$$

where:  $k$  = permeability, ft/min  
 $Q$  = constant rate of flow into the hole, cu ft/min  
 $L$  = length of test section, ft  
 $H$  = differential head of water, ft  
 $r$  = radius of hole, ft  
 $\log_e$  = natural logarithm  
 $\sin h^{-1}$  = arc hyperbolic sine

When the test length is below the water table,  $H$  is the distance in feet from the water table to the swivel plus the gage pressure in units of feet of water. When the test length is above the water table,  $H$  is the distance in feet from the center of the length tested to the swivel plus the applied pressure in units of feet of water.

Simplified versions of the above formulas are given by the U.S. Bureau of Reclamation (1963) where the relationships of hole diameter and length of test interval have been calculated and expressed in tables. The formulas are reduced to the form:

$$k = \frac{C_p Q}{H} \quad (3.4)$$

where  $C_p = 4900$  for an NX hole tested at 10-foot intervals.

Monahan and Sibley (1965) further simplified the calculations by presenting a nomograph for pressure test computations.

### (3) Evaluation of pressure tests

The construction of water pressure testing apparatus is generally left to the ingenuity of the driller. There are seldom any standards set for equipment and testing procedures and the quality of the test data is variable.

The failure of maintaining a tight seal between the packers and the rock is the principal reason for testing difficulties. The packers are made from felt or rubber and vary in length from 2 inches to 4 feet. Although many variations of packers have been used in successful tests, it is recommended that they be at least 18 to 24 inches long and preferably expanded against the wall by pneumatic means. Pressures to 125 psi have been used to insure a tight seal.

In addition to leakage between the packer and the rock, water may bypass the packer through open joints that form a connection between the test interval and the rest of the boring.

The best results can be obtained by using the single packer technique and pumping water into a small test section (5 to 10 ft.) between the packer and the bottom of the hole. The drilling operation, however, must stop each time the required depth is reached, and the drill-steel removed. Single packer tests can also be made after the hole has been drilled by placing the packer at successively higher 10-ft intervals until the entire length of the boring has been tested. Where zones of high water takes are encountered a double packer system can be used for the permeability tests.

It has been noted (Bussey, 1963) that grout takes were less in holes drilled with percussion tools than in those drilled with rotary rigs. Comparative tests made in a massive diorite at the Karadj Dam indicate that percussion drilling fills the joints with rock fragments which cannot be removed by a thorough flushing of air and water. This factor should be recognized if percussion drilled holes are considered for permeability tests. Rocks with moderate to low permeabilities are especially affected by the small rock chips produced by percussion drilling.

## 6. Geophysical Testing

### a. Introduction

Geophysical surveys are commonly used in civil engineering practice as a means of determining the depth of overburden or surface weathering for foundation studies. The seismic velocities can also be used to calculate in-situ dynamic moduli of the rock for the design of dam foundations, underground installations, or high pressure water tunnels. Seismic velocities and electrical resistivity values, because they are influenced by discontinuities and weathering, can indicate variations in rock quality in boreholes.

The geophysical measurements conducted in this investigation included continuous velocity logging in boreholes, up-hole and cross-hole seismic surveys, and seismic refraction tests on the ground surface and in tunnels. Data on dynamic moduli were also obtained from locations of in-situ deformation tests for purposes of relating the static and dynamic properties of the rock mass.

The continuous sonic velocity measurements at the Dworshak, Two Forks, and Yellowtail Damsites were made by a 3-D sonic logger owned by the Birdwell Company of Tulsa, Oklahoma. Their 3-D sonic velocity logger was chosen for these measurements because it provides a continuous record of both compressional and shear waves. Birdwell also performed up-hole, cross-hole and refraction surveys using conventional seismic equipment. An Air Force Weapons Laboratory geophysical team, under the direction of Richard Zbur, provided additional seismic information at the Two Forks and Tehachapi sites. The remainder of the seismic data was obtained from the records of the Bureau of Reclamation, the Corps of Engineers, and the California Department of Water Resources.

### b. The 3-D sonic logger

The 3-D sonic logger is so named because the logs show the amplitude and time of arrival of the sonic energy for a given distance of travel. The 3-D sonde used in NX boreholes is 2-1/4 inches in diameter, 12 feet long, and weighs 150 pounds. Borings can be logged at a rate of from 30 to 100 feet per minute. The tool can withstand pressures of 7,500 psi and temperatures of 250°F.

A sonic pulse is generated by a cylindrical magnetostrictive type transducer, which is a coil wrapped around a rod with magnetostrictive properties. A magnetic field caused by AC current in the coil deforms the rod producing a sonic pulse which travels into the rock. The pulse rate is approximately 20 repetitions per second and the resonance frequency of the transducer is 22 kc/sec. Cylindrical piezoelectric crystals are used as receivers. They



are located within the tool at a distance of 3 and 6 feet from the transmitter. Acoustic isolators between the transmitter and receivers prevent the sonic energy from traveling down the body of the tool. The arriving pulse deforms the crystals and produces the electricity necessary to record the energy arrival.

The generated pulse travels through the fluid in the borehole as a compression wave and strikes the rock face. According to Christensen (1964), a portion of the energy of the waves incident normal to the borehole travel along the formation-fluid interface as boundary waves, whereas the remaining part is carried directly into the rock and is attenuated. Those incident at the critical angle as defined by Snell's Law travel up and down the borehole as compressional waves, whereas those striking at a greater incident angle undergo mode conversion and are propagated as shear waves (Figure 3.7). Regardless of the mode in which these three waves travel through the rock, they are refracted out of the rock and recorded as compressional waves. The twice refracted compressional wave, the twice mode-converted shear wave, and the twice mode-converted boundary wave are distinguished by their respective travel times. The compressional wave has the shortest travel time, the shear wave travel time is intermediate, and the boundary wave has the longest travel time.

The arrival times are transmitted to the surface, amplified and shown on an oscilloscope as an amplitude modulated display (Figure 3.8A). For continuous recording of travel times that are more easily interpreted, the amplitude modulated display is converted to an intensity or variable density display and presented as a series of dots and dashes (Figure 3.8B). Positive deflections appear as light zones and the negative deflections as the dark zones. The intensity of lightness or darkness indicates the relative amplitude whereas, the distance between similar portions of light or dark zones indicates the frequency of the wave. The delay characteristics of the system have been internally compensated and the time displayed on the oscilloscope represents fluid and formation travel time.

The intensity modulated data are projected onto 220 mm film whose movement is synchronized with the speed of the sonde in the hole. The 220 mm film permits a greater resolution of the data than 35 mm or 70 mm films because an equivalent display is spread out over a greater distance. A fiber optics system is used to project the variable density displays onto the film. The high image resolution of this instrument reduces the distortion that accompanies normal projection methods.

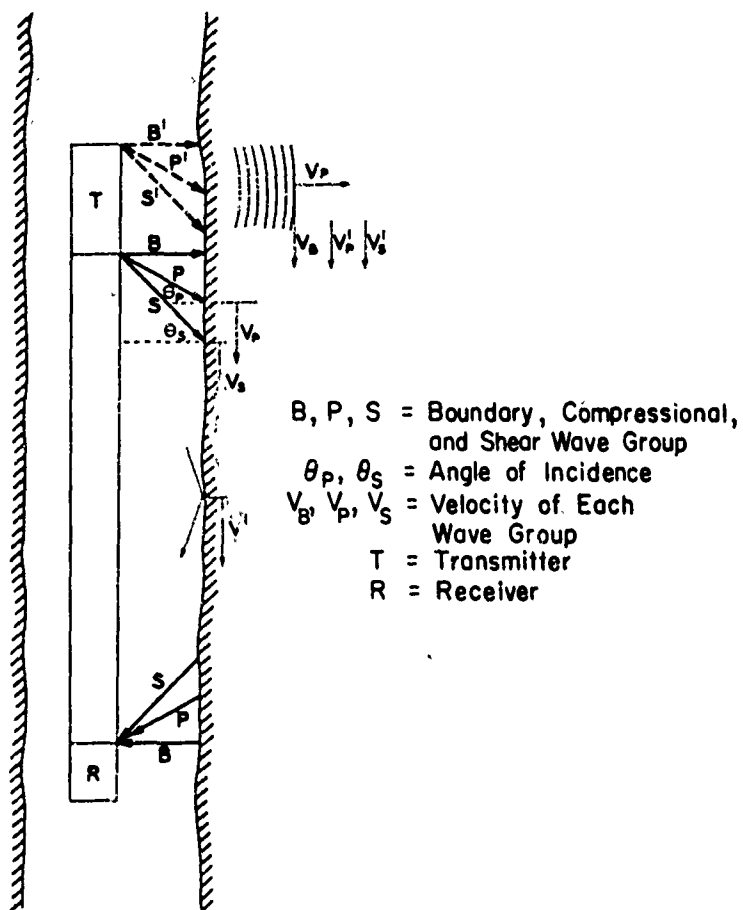
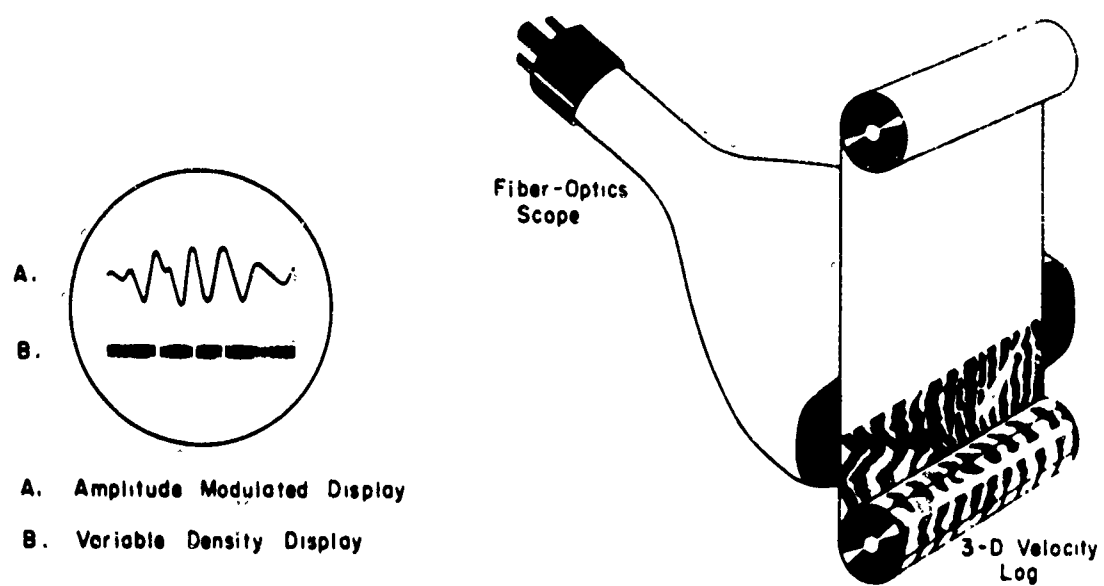


FIG. 3.7 TWO-DIMENSIONAL CONFIGURATION OF 3-D SONDE-BOREHOLE GEOMETRY ( After Christensen, 1964 ) Reproduced with the permission of the Society of Professional Well Log Analysts



**FIG. 3.8 VARIABLE DENSITY LOGGING SYSTEM ( Lawrence, 1964 )**

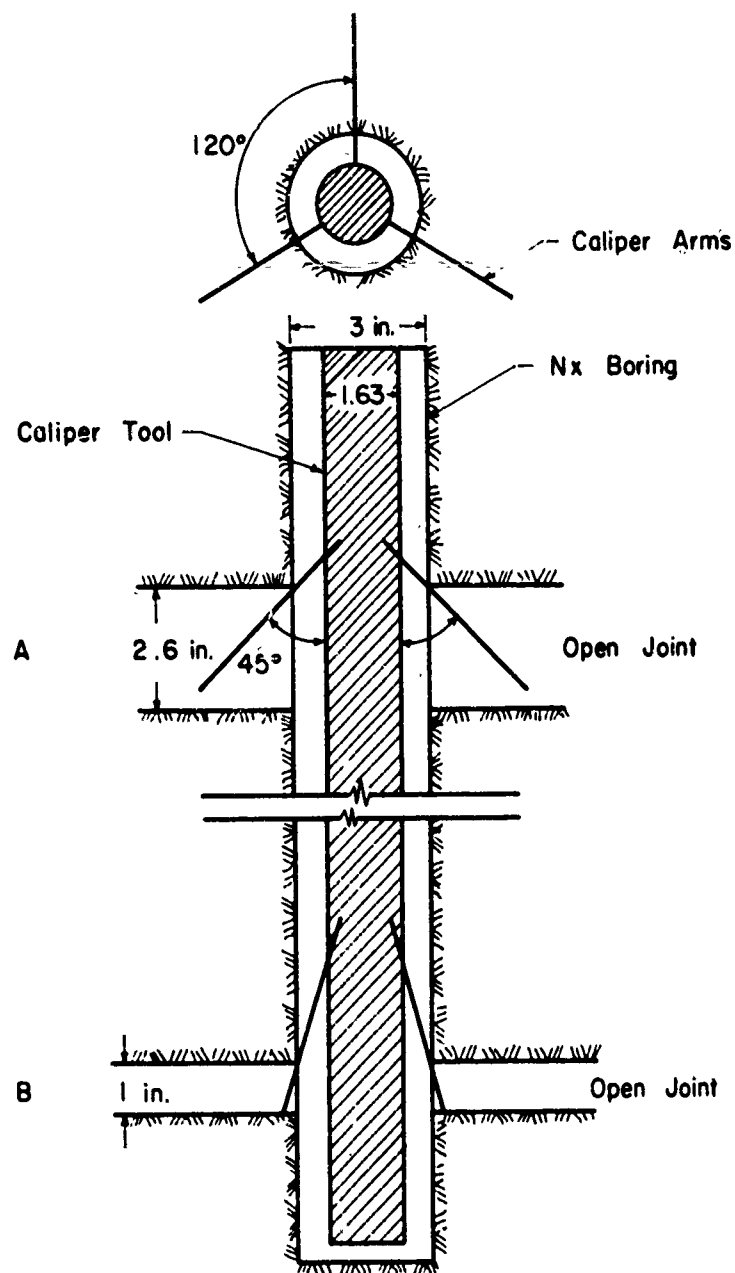
### (1) Analysis of the data

The density of the rock and variations in the hole diameter must be determined before the velocities or elastic constants can be calculated. For this reason caliper and gamma-gamma density logs are run in conjunction with the 3-D sonic logging.

The caliper logger is approximately 4 feet long and 1-5/8 inches in diameter. Three independently operating spring-loaded arms are mounted around the tool at 120° intervals, and extend outward in contact with the borehole wall. The arms are pointed down so they will not catch on irregularities in the rock as the tool is drawn up the hole. The diameter logged is twice the average radius measured by the three arms. The arms are 4 inches long and have a maximum extension angle of 45°. The largest change in diameter that can be measured is 7.2 inches, which is possible only where the open zone is at least 2.6 inches high (Figure 3.9). The tool is calibrated on the surface using steel cylinders of known diameter and lowered to the bottom of the hole. As the tool is raised a continuous graph of hole diameter is made which is probably accurate to within 1/8 inch. The logging speed of this instrument is about 20 ft/min.

The in-situ density is determined by measuring the amount of back-scattering that occurs when gamma rays strike the rock. The sonde used in this study is approximately 5 feet long and 1-5/8 inches in diameter. A cesium 137 source is placed in the bottom of the tool 22 inches below a scintillation counter. Gamma rays collide with the atoms of the rock and are either absorbed, randomly scattered, or backscattered at the angle of incidence. The frequency with which this scattering occurs is proportional to the density of the material. The greater the degree of random scattering and absorption the higher the density of the rock and the lower is the response at the detector (Pickell and Heacock, 1960).

The sonde is calibrated in the laboratory with a number of different density materials. It is calibrated again in a block of plaster before and after each run in the field. Thus, a standard is established and minor variations in the performance of the tool can be accounted for in the final calculations. The performance of the system is dependable only where the borehole remains in gage, and therefore, readings from zones of caved hole cannot be considered accurate. For this reason a caliper log is recommended to aid in the interpretation of the density log. The accuracy of this system was checked by determining the laboratory density of samples taken from the same position in borings logged by



Maximum Measurable Diameter      Joint A = 7.2 in.  
    Joint B = 3.6 in.

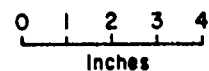


**FIG. 3.9 MAXIMUM HOLE DIAMETER MEASURABLE  
 BY CALIPER TOOL FOR DIFFERENT  
 SIZE JOINTS**

the density tool (Figure 3.10). In the majority of cases the laboratory values are 5 to 10 percent higher than the field values.

## (2) Computation of velocities and dynamic elastic constants

The compressional and shear wave velocities cannot be calculated directly from the field logs. Borehole diameter, rock density, and the theoretical depth of energy penetration into the rock must be considered in addition to the original travel time. Once the velocities have been determined the dynamic elastic constants can be calculated by the following relationships:

$$\mu = \frac{V_p^2 - 2V_s^2}{2(V_p^2 - V_s^2)} \quad \begin{array}{l} \mu = \text{Poisson's ratio} \\ V_p = \text{compressional wave velocity} \end{array} \quad (3.5)$$

$V_s =$  shear wave velocity

$$E_s = \rho V_s^2 \quad E_s = \text{shear modulus} \quad (3.6)$$

$$E_y = 2 E_s (1 + \mu) \quad \rho = \text{specific gravity} \quad (3.7)$$

$$E_y = \rho V_p^2 \frac{(1 + \mu)(1 - 2\mu)}{(1 - \mu)} \quad E_y = \text{Young's modulus} \quad (3.8)$$

$$E_B = \rho V_p^2 - 4/3 E_s \quad E_B = \text{Bulk modulus} \quad (3.9)$$

If a gamma-gamma log has not been run, the density can be approximated by the following (Lawrence, 1964):

$$\rho' = \frac{\rho_f V_f^2 V_T}{V_s^2 (V_F^2 - V_T^2)} \quad \begin{array}{l} \rho' = \text{formation density} \\ \rho_f = \text{fluid density} \\ V_f = V \text{ fluid} \\ V_T = V \text{ tube wave} \\ V_s = V \text{ shear wave} \end{array} \quad (3.10)$$

Porosity can be calculated when the bulk density of the rock is known (Alger et al., 1963):

$$\phi = \frac{\rho_g - \rho_b}{\rho_g - \rho_f} \quad \begin{array}{l} \phi = \text{porosity} \\ \rho_g = \text{grain density of the rock matrix} \\ \rho_b = \text{bulk density of the rock from the log} \\ \rho_f = \text{density of the fluid in the pores} \end{array} \quad (3.11)$$

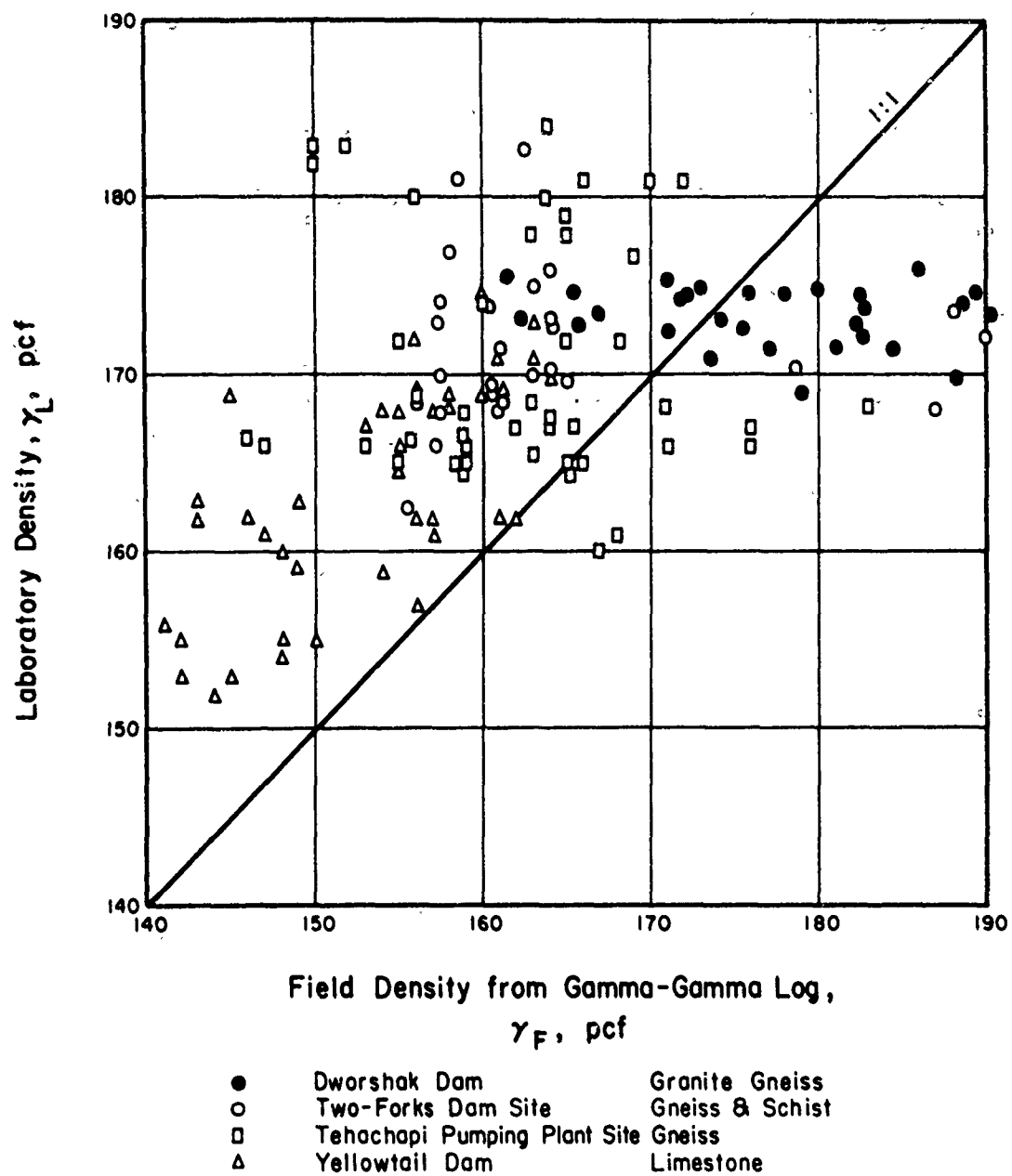


**FIG. 3.10 RELATIONSHIP BETWEEN FIELD (GAMMA-GAMMA) AND LABORATORY DENSITIES**

### (3) Evaluation of the 3-D sonic velocity logger

The major advantage of the 3-D system is that it provides a very detailed record of the entire wave train produced by the pulsing device. The arrival times of the compressional and shear waves are more easily determined than in other sonic logging devices currently being used. The dynamic elastic constants can be calculated if the density of the rock mass is known. The density can be determined either by using a gamma-gamma density log or by using a laboratory density of representative core samples.

The 3-D method measures the dynamic properties of the rock close to the walls of the borehole. The depth of penetration of the energy between transmitter and receiver is on the order of 1 to 1-1/2 ft for the 3 ft spacing and 2 to 2-1/2 ft for the 6 ft spacing. Because the 3-D sonic survey tests only a very small percentage of the total rock mass the velocities are generally higher than those obtained from either up-hole or cross-hole seismic surveys.

The apparatus is not presently suited for efficient use in rough terrain. The system is run from a 12-ton truck which contains all the electronic equipment normally used by Birdwell for oil well logging. The truck has a 4-wheel drive and a power winch which allows its use on unimproved roads, but its size and weight limit its mobility.

Normally the tool is connected directly to the van by means of a heavy 7-conductor cable that provides power for the transmitter, has a channel for the returning signal, and controls the movement of the sonde in the hole. A selsyn wheel mounted directly over the hole on an A-frame and connected to the van by a second cable synchronizes the tool movement with the camera drive. The logging depth must be measured in this way because of tension variations in the conductor cable between the van and the boring. The operator controls the sonde movement with a power winch. The logging procedure is simple when the van can be parked beside the hole. However, at the Dworshak, Two Forks, and Yellowtail projects, borings on the abutments and in test adits were up to one-half mile from the van. The selsyn cable, which is only used as an electrical conductor, was quickly laid along the ground between the operating van and the selsyn wheel. The signal cable, which is both a conductor and the means of moving the 3-D sonde, was routed between the van and the boring through sheaves at each abrupt change in slope or bend in the tunnel. In addition to the time required to set up the test, the logging time was also increased. Although the power winch was able to lift the sonde in a boring one-half mile away the sonde was lowered for



additional logging runs by pulling additional cable from the truck. This proved to be an exhausting and time-consuming job. Because the logging charges for this type of work were based on a daily rate rather than on the total footage, this sonic testing was very expensive.

A significant improvement in the logging procedure was made at the Two Forks site with the use of a portable hand-operated winch. The rate of logging was controlled by the hand winch and the depths were recorded by means of the selsyn cable and measuring sheave as before. The power cable was routed to the winch on the van in a slack condition, eliminating the need for sheaves at each bend or change in slope of the tunnel and the necessity of pulling additional cable from the truck for each run. The hand-operated winch, which has 300 ft of cable, was used to log borings drilled from test adits and surface borings which could not be reached by the van. The portable winch reduced the time on site by approximately 50 percent.

The 3-D system has the disadvantage that it can only be used in the fluid-filled portion of a hole. If the water table is low in the area, the upper portion of the hole cannot be logged and this section is often the most important for foundation investigations. Another disadvantage is that material such as grout or cellophane-stringers used to reduce the permeability of the rock during drilling, will affect inhole velocity measurements. The cellophane material traps air in the rock and causes severe attenuation of the transmitted energy (Nugent and Banks, 1965). Grout superficially fills rock defects which masks the influence of these defects on the velocity log.

The 3-D system has a filtering device which can eliminate low-level background noises. For this reason, vehicular traffic will not affect the log. However, drilling and blasting in the immediate vicinity must be stopped while logging.

The operating cost to bring the Birdwell Company into the field is as follows: travel time and site operation for 3-D, sonic, caliper, and density logs, \$700/day; data reduction, \$100/boring; computer time, \$40/hour; supervising engineer, \$125/day plus travel expenses. Birdwell generally charges by the boring (unit cost) when logging deep holes in oil fields or other readily accessible areas. This cost method is not practical for most engineering projects because of the roughness of the terrain and the long set-up times required for numerous shallow borings.

c. Seismic surveys

(1) Refraction surveys

Seismic refraction surveys are used to determine the extent of surface weathering, the depth to a more dense geologic stratum, or the thickness of the zone of loosened rock (destressed zone) around an underground opening. Refraction surveys were used for this investigation to measure seismic velocities of the gneisses and schists in a tunnel at the Two Forks Dam site and to determine the depth of surficial weathering away from the tunnel portal. It was also used to obtain velocities of the sandstone and gneiss at the Tehachapi Pumping Plant site for correlation with the 3-D values.

The refraction survey measures the arrival time of seismic energy at a number of geophones placed at known distances from the shot point. A set-up for a typical refraction survey is shown in Figure 3.11. The input energy depends upon the seismic velocity of the rock and the depth of penetration desired. For detailed work in a small area, an 8-pound sledge-hammer striking a steel or aluminum plate is sufficient, whereas a blasting cap or dynamite is usually necessary for testing intervals of 100 ft or more.

The hammer-type seismographs used by the Bureau of Reclamation at the Glen Canyon, Morrow Point, and Two Forks dam sites have only one recording channel and the distance between the shot point and the geophone must be increased with each shot to get a complete record. A trip-switch on the hammer initiates the timing mechanisms and the first energy arrival at the geophone stops the counter. Most seismographs have a number of channels with one geophone for each channel which enables the entire survey to be run with one shot. The time of blasting must be synchronized with each of the recording channels so that the arrival times at the geophones can be measured. A blasting console is wired into the recording instrument, and the final record has the instant of the shot marked on the trace of each channel. As the energy arrives at each of the successive geophones, the trace shows a sudden increase in amplitude. A plot of the time versus distance (Figure 3.11) can be used to calculate seismic velocities and the depths to strata of greater density.

(2) Up-hole seismic surveys

In an up-hole seismic survey a light charge (Water Works booster, blasting cap, or nitromon primer) is ignited at a given depth in a borehole. The first energy arrivals are measured at a number of geophones whether in the same hole or on the surface. The charges can be located at various depths but

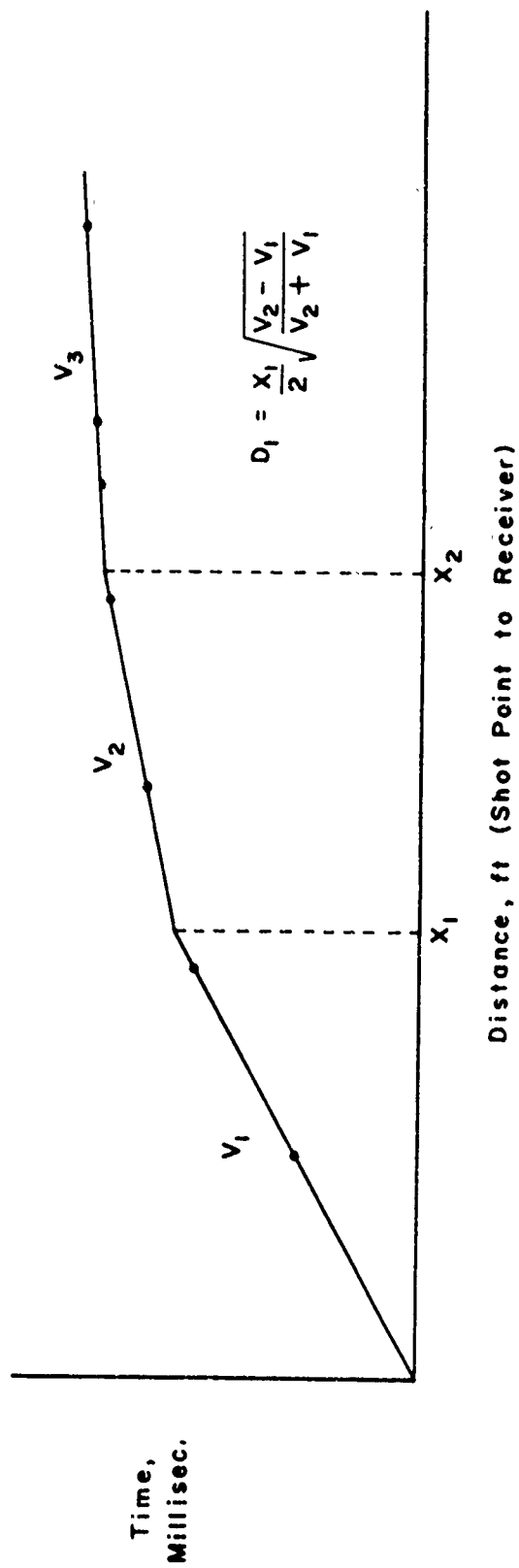
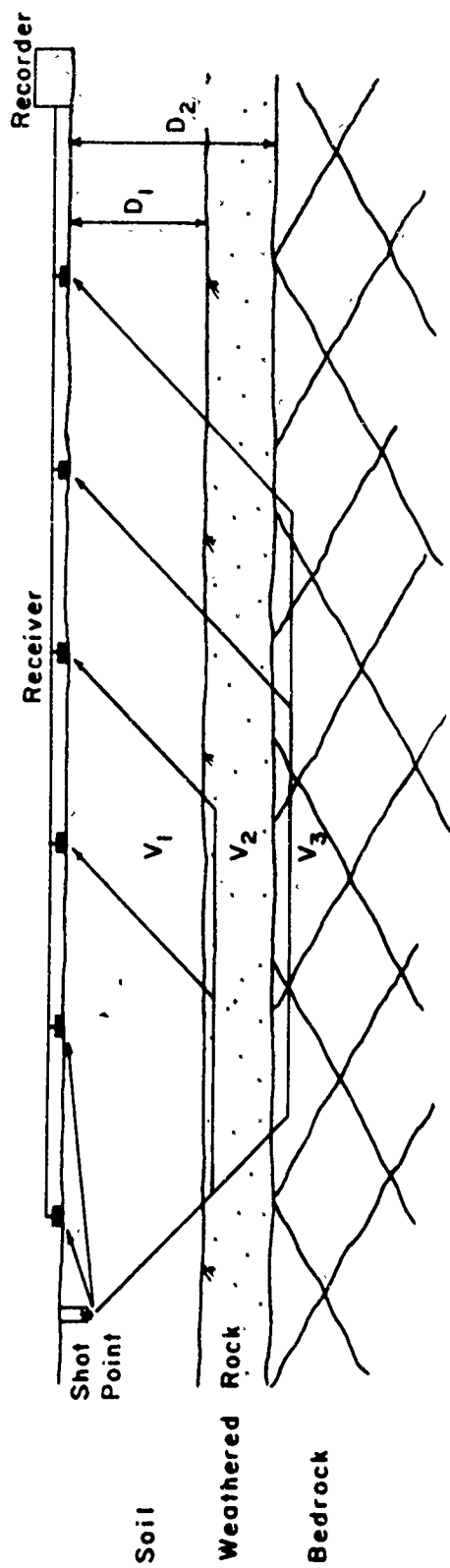


FIG. 3.11 REFRACTION SEISMIC SURVEY

the initial shot is usually placed at the bottom with successive ones at higher levels. If the geophones are at the surface it is recommended that they be in direct contact with the rock and be placed at least 5 feet from the collar of the hole. Successive shots should not be made from the same position in the hole because blast-induced damage of the rock may result in anomalously low velocities. An array of the surface geophones can be used to obtain additional information from the test. Two or three geophones spaced equidistant from the collar measure the velocity along the borehole. Other geophones located along lines which radiate outward from the boring measure the velocity of the rock behind the walls of the boring.

The method can be modified by placing several geophones in the hole and shooting from the bottom (Figure 3.12). In this case, the strength of the charge should be kept low to prevent damage to the geophones. The dynamite can also be placed on the surface, away from the collar of the hole, and the same geophones used.

#### (3) Cross-hole seismic surveys

Information on rock quality between adjacent borings can be obtained by measuring the seismic velocity of the rock between holes. Various shot and geophone spacings can be used. For parallel shooting, the depth of the dynamite and the geophone (in adjacent holes) are the same. Fan shooting measures the arrival time from one shot point to a number of geophones (Figure 3.12).

#### (4) Evaluation of seismic methods

Detailed measurements of seismic velocities in shallow borings or along tunnel floors require an instrument with high sensitivity. For example, to measure a 20-foot hole behind a jacking test in a tunnel, the first velocity readings should be obtained within 3 to 5 ft of the surface. If the rock is anticipated to have a velocity of 15,000 ft/sec, the recorder must be able to measure travel times of 0.2 to 0.3 milliseconds. The same sensitivity is needed for measuring the depth of the distressed zone around tunnels. At the present time, there are few commercially made instruments with this resolution. Because most of the geophysical apparatus is designed for oil field use, it may not have the sensitivity required for detailed engineering work. Consequently, the aims of the project should be made clear to the geophysical company before the contract is signed.

The sensitivity of the recording apparatus is often expressed in "paper speeds". An oscillograph with a paper speed of 25 in/sec displays a

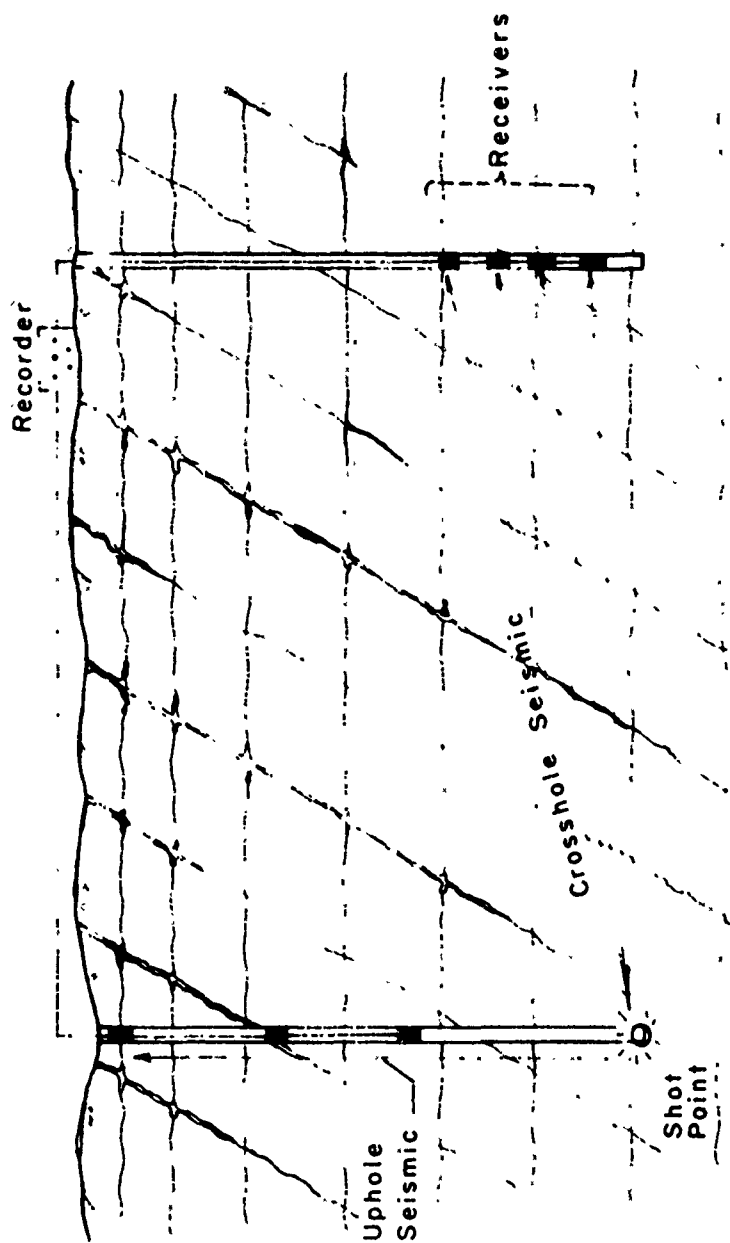


**FIG. 3.12 UP-HOLE AND CROSS-HOLE SEISMIC SURVEYS**  
 (After Deere et. al., 1967) Reproduced with the  
 permission of A.I.M.E.

10-millisecond time interval over 0.25 inch of recording paper. In this case, the readings of the first energy arrivals can only be accurately read to about 2 milliseconds. Therefore, if the rock has an anticipated velocity of 15,000 ft/sec, it is not possible to obtain an accurate measurement of energy arrival times if the geophones are spaced within 30 feet of the shot point. Paper speeds of up to 250 in/sec are needed for the detailed seismic surveys mentioned above. Such sensitivity would display a 4-millisecond interval over 1 inch of paper, and the time of energy arrivals can be read as low as 0.25 milliseconds.

The hammer seismograph has an advantage over seismographs that use dynamite as the source of energy because of strict control of explosives in heavily populated areas. This instrument is equipped with a dual polarity geophone with a flat or spike base. The spike base is not recommended for tunnel work because there is seldom enough soft material in which to set the spike. Its engineering versatility would be greatly increased if an inexpensive inhole geophone was developed by the manufacturer. It would be possible to make detailed inhole velocity measurements with this type of geophone. Seismic surveys could also be made in feeler holes ahead of a tunnel face to locate zones of low velocity or poor quality rock. An inhole geophone should be coupled to the rock by an expanding arm that would force the instrument tightly against the bore-hole wall. If the system does not have this feature, the hole must be filled with water for proper coupling. The disadvantages of having to rely on a high ground water table are obvious.

d. Electrical resistivity

Electrical logging operates on the principle that any change in the conductivity of geological material will alter the flow of current in the rock and, therefore, will increase or decrease the electrical potential between measuring electrodes.

Electrical conductivity in most rocks is essentially electrolytic. Conductance takes place through the water in the voids of the material which contain dissolved salts. Resistivity of a rock depends on the resistivity of the electrolytes and is inversely proportional to the porosity. In massive crystalline rocks, unless the water is saline, the degree of fissuring is the most important factor controlling resistivity (Griffiths and King, 1965).

The conventional resistivity logs are obtained by measuring the change in voltage caused by the flow of current between two electrodes. The resistivity

( $r$ ) of a formation is defined as the resistance ( $R$ ) between opposite faces of a unit cube of that material (Dobrin, 1960). Therefore, for a conducting cylinder of length ( $x$ ) and cross-sectional area ( $x^2$ ):

$$r = \frac{Rx^2}{x} \quad (3.12)$$

If a current ( $I$ ) is emitted from an electrode, the resulting equipotential surfaces are spheres concentric with the electrode. The potential at any spherical surface of radius ( $x$ ) from the electrode (Gaskell and Threadgold, 1960):

$$V = IR \quad (3.13)$$

$$= \frac{Irx}{4\pi x^2} \quad (3.14)$$

$$= \frac{Ir}{4\pi x} \quad (3.15)$$

The resistivity of a rock mass can be determined in a borehole by measuring the change in voltage ( $\Delta v$ ) across two electrodes a known distance apart ( $x$ ). Several different types of resistivity logs can be obtained by varying the spacing of the current and potential electrodes. The tests commonly run in boreholes produce normal and lateral resistivity curves.

#### (1) Normal curves

The configuration shown in Figure 3.13a is a schematic of the apparatus used for normal resistivity curves. If electrodes A and M are closely spaced and B and N are far apart, the potential between A and M is the one of importance. Therefore, with the normal configuration the potential from A to M is as follows:

$$V = \frac{Ir}{4\pi AM} \quad (3.16)$$

For logging purposes the potential is measured at the reference level 0, which is halfway between A and M.

#### (2) Lateral curves

The electrode configuration for lateral logging is shown in Figure 3.13b. In this case, A is 18 ft 8 in. from 0 (the mid-point between M and N), M and N are close together (32 in.), and B is far enough from AMN that it has little influence on them.

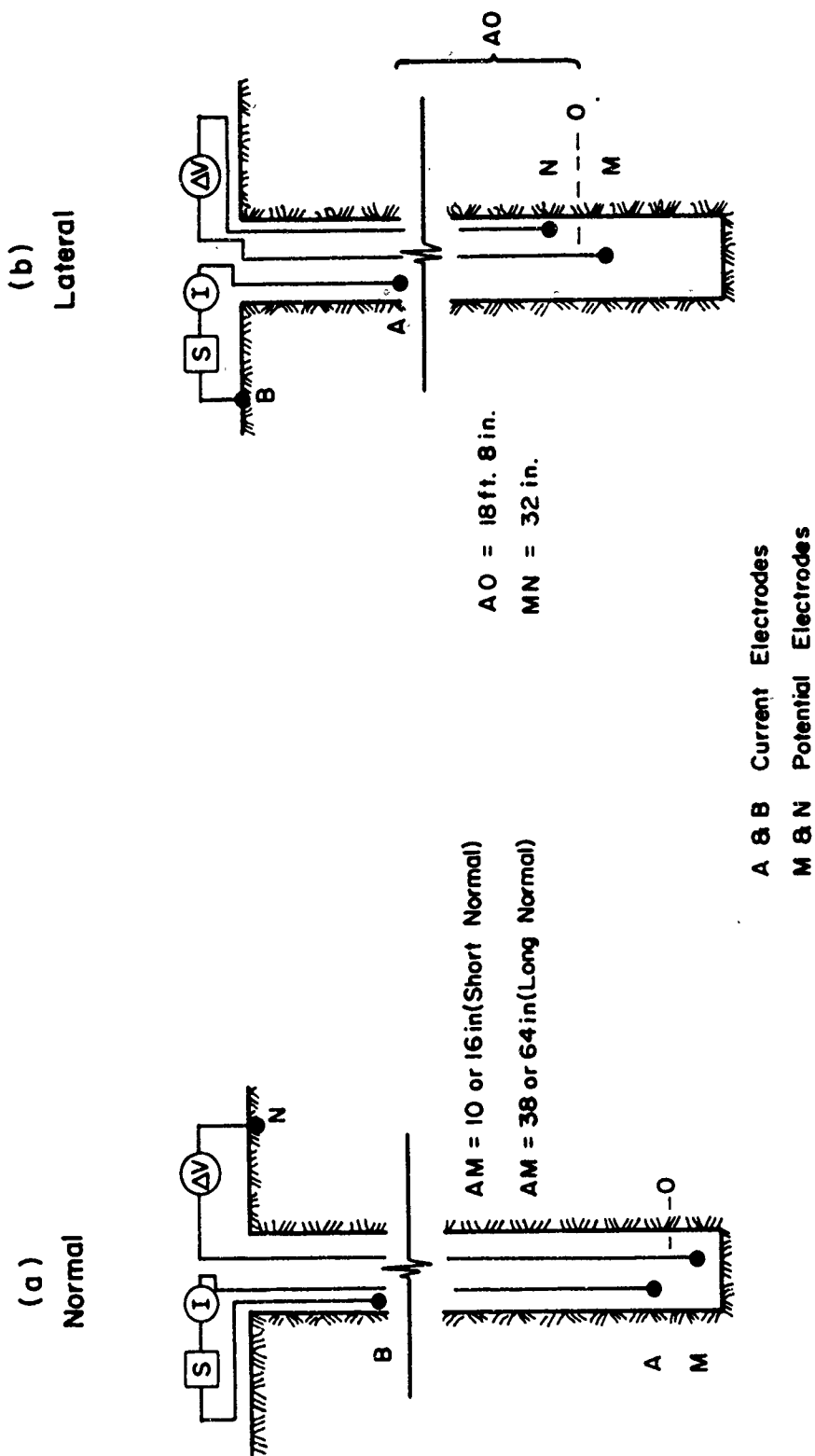


FIG 3.13 SCHEMATIC ELECTRODE CONFIGURATION FOR RESISTIVITY CURVES (After Pirson, 1963) Reproduced with the permission of Prentice-Hall Inc.



The voltage difference transmitted to MN is:

$$V = \frac{Ir}{4\pi} \left( \frac{1}{AM} - \frac{1}{AN} \right) \quad (3.17)$$

The long spacing on this type of log was designed so that the resulting depth of penetration would be great enough that resistivity values would not be influenced by the invaded zone. This zone is located around the borehole and represents the encroachment of drilling mud and fluid into the formation.

### (3) Evaluation of electrical resistivity

The resistivity values measured by these logs are apparent resistivities because they are influenced by factors other than the electrical properties of the formation. These include: 1) the resistivity of the drilling mud, 2) diameter of the borehole, 3) the location of the electrode array with respect to changes in rock resistivities, and 4) the depth of the invaded zone (for normal logs only). Factors 1 and 4 apply to oil field conditions where drilling muds are extensively used. Correction curves are available for each of these factors to determine the true resistivity of the rock.

## SECTION 4

### LABORATORY INVESTIGATIONS

#### 1. Introduction

Laboratory tests are used to define a rock in terms of intact engineering properties such as strength, modulus of elasticity, density, and compressional velocity. The tests were selected to provide laboratory data that could be correlated with corresponding in-situ properties. Laboratory samples represent the rock in its most homogeneous and isotropic state and when tested, and compared with field data, provide a method of measuring the effects of discontinuities.

#### 2. Sonic Pulse Velocities

The compressional wave velocities of samples collected at field sites were measured in both a dry and saturated condition under successive uniaxial stress levels of 0, 50, 100, 200, 400, 1,000, 3,000, 1,000, and 0 psi. The 3,000-psi limit was chosen so that all samples could be tested without failure of the weaker rocks. A violent failure could damage the transducers and reduce the reliability of the subsequent velocity data. Saturation is defined as the water absorbed by the specimen under the following laboratory procedures:

1. Oven-dry the sample for 24 hours at 105°C.
2. Place the specimen in a bell-jar for 3 hours under a partial vacuum of approximately 28 inches of mercury.
3. Cover the sample with water while it remains under partial vacuum for another 3 hours.
4. Allow the sample to sit for 18 hours under water at atmospheric conditions.

This saturation procedure is based on the results of saturation tests presented in Table 4.1. These tests on dense rocks, which should have long saturation periods, show that a 3-3-18 hour cycle provides the same percent absorption as the 24-24-48 used by Deere and Miller (1966).

Following saturation, the samples were weighed and tested. After being oven-dried for 24 hours their dry weight and velocity measurements were taken again. In both sonic tests the ends of the samples were covered with a thin film of silicone grease to improve acoustic coupling.

The complete details of the pulse velocity apparatus are given by Deere and Miller (1966) and the same equipment was used without modification for this laboratory program. A brief description of the apparatus taken from their report is given below.

TABLE 4.1  
PERCENT ABSORPTION FOR SEVERAL SATURATION CYCLES

ROCK TYPE	% ABSORPTION			
	CYCLE TIME, HOURS			
	0-0-2	2-2-2	3-3-18*	24-24-48
GRANITE	0.09	0.11	0.14	0.14
GNEISS	0.50	0.57	0.57	0.57
	0.11	0.25	0.25	0.25
SCHIST	0.12	0.20	0.19	0.20
and GNEISS	0.05	0.15	0.17	0.17
	0.08	0.08	0.10	0.10
LIMESTONE	0.94	4.15	4.17	4.15
	0.19	0.62	0.62	0.62

\* selected cycle time as explained above

$$\% \text{ Absorption} = \frac{P_2 - P_1}{P_1} \times 100$$

$P_2$  = weight of saturated specimen

$P_1$  = weight of oven-dried specimen

The schematic diagram (Figure 4.1) represents the relationships of the major components of the pulse velocity measuring equipment. A short duration, high voltage (1,000 volts maximum) pulse was applied to the transmitting crystal from a high-gain, high-pass signal amplifier. The transducers consist of barium titanate piezoelectric crystals (natural frequency = 200 to 300 kc/sec) fastened to the inside of stainless steel transducer cups. These cups are labelled transmitter and receiver in the diagram, but can be used interchangeably. The input pulse causes the crystal to expand and contract rapidly, thereby imparting a stress pulse to one end of the sample. In this way a series of

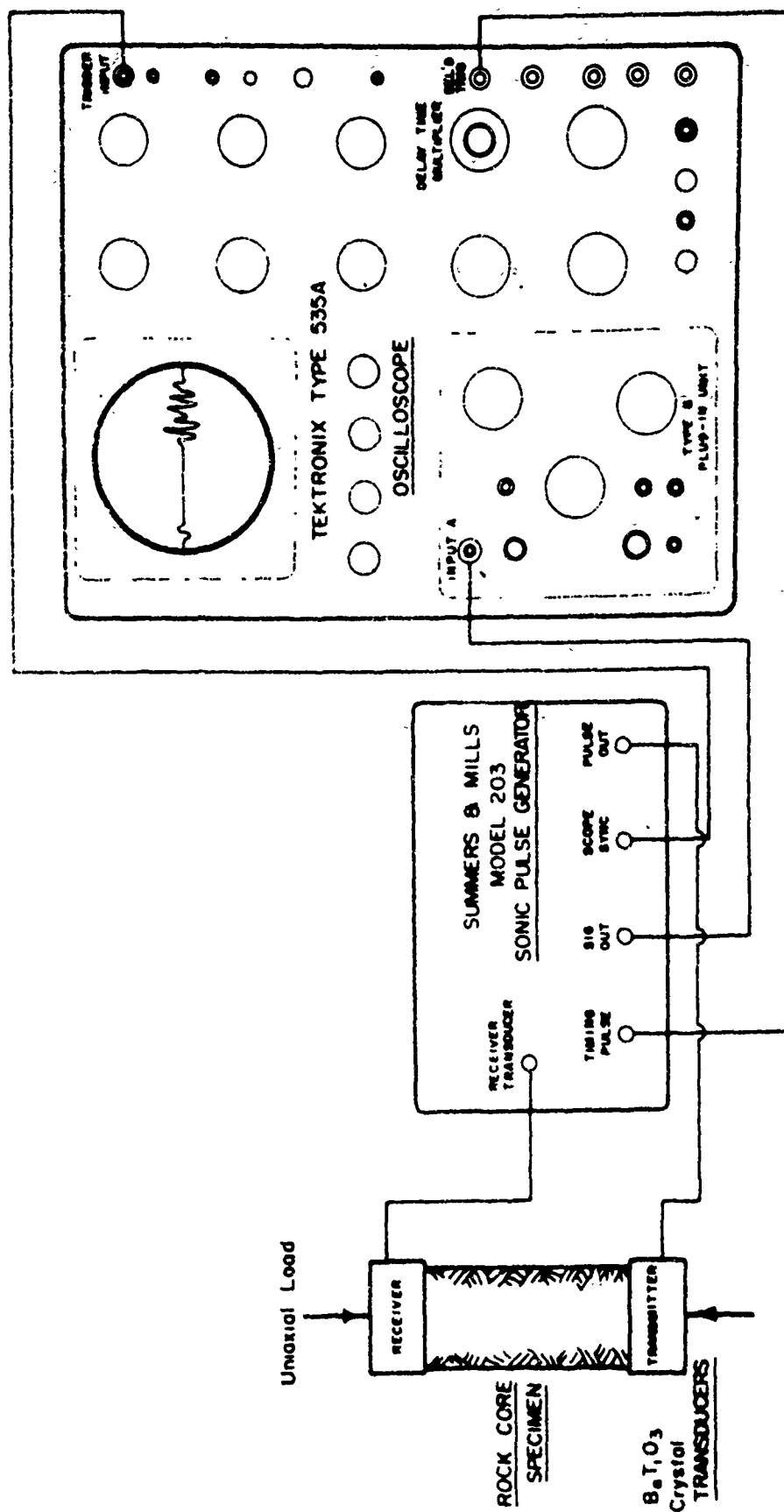


FIGURE 4.1 SCHEMATIC INTERCONNECTION DIAGRAM FOR SONIC PULSE VELOCITY MEASURING EQUIPMENT (After Deere & Miller, 1966)

ultrasonic wave trains are propagated through the sample to strike the receiving transducer at the other end. The arrival of these pulses causes the mechanical deformation of the crystal which generates a voltage across the crystal face. The energy is amplified and displayed on the cathode-ray tube of the oscilloscope. The start of the signal sweep must be related to the time of the initial input pulse because the sweep must appear as a stationary wave-form on the screen. These calibrated sweeps cause the horizontal distance on the screen to represent a known interval of time. Therefore, the time of the first arrival of a sonic pulse on the oscilloscope can be measured directly.

The saturated and dry velocities are calculated by dividing the length of the sample by the first arrival time corrected for instrument delay. The dynamic elastic modulus can be calculated.

$$E_{\text{dyn}} = \rho V_{\text{Lab}}^2 \frac{(1+\nu)(1-2\nu)}{(1-\nu)} \quad (4.1)$$

where

- $E_{\text{dyn}}$  = dynamic modulus of elasticity
- $\rho$  = mass density
- $V_{\text{Lab}}$  = compressional wave velocity
- $\nu$  = Poisson's ratio

### 3. Unconfined Strength and Modulus of Elasticity

Unconfined compressive strengths and moduli of elasticity were determined for 280 samples representing the entire range of rock types studied during the project. Many of these samples were taken from the areas of in-situ jacking tests to compare in-situ and laboratory moduli. The loads were applied by a 300-kip Riehle hydraulic testing machine and measured by a 600-kip capacity load cell. Axial strains were measured by two SR-4 electrical resistance gages mounted vertically on opposite sides of the sample and wired in series. The load cell and SR-4 gages were connected to a Moseley X-Y Recorder, model 2D, which plotted a stress-strain curve as each test progressed. The samples were tested to failure at a loading rate of approximately 60 psi/sec.

### 4. Evaluation of Test Results

Young's modulus or the modulus of deformation for rock is a function of the applied stress and may depart from the simple proportionality of stress and strain that applies to many engineering materials (Deere and Miller, 1966). These

authors chose to use the modulus that represented the slope of the stress-strain curve at 50 percent of the ultimate unconfined strength. This procedure was used in an effort to reduce the influence of microfractures in the sample which close at low stress levels and produce a concave upward slope in the stress-strain curve. The same procedure was followed in analyzing all stress-strain properties of rock core for this investigation.

The results of sonic velocity tests showed that in all cases the compressional velocities increased as the stress level increased and were higher for the saturated samples than for dry ones. This has been observed by many researchers including Walsh (1965), Birch (1960), Wyllie et al. (1958, 1956), Hughes and Kelley (1952), and Deere and Miller (1966).

It was observed that the percent of velocity increase with increasing axial load could vary widely in similar samples. If the closing of microfractures in the rock is responsible for the increase in velocity with load, the stress-strain curve should reflect the presence of these features.

A comparison of Figure 4.2 and Figure 4.3 (granite-gneiss) shows the latter to have a pronounced concave upward stress-strain curve at stress levels between 0 and 3000 psi, whereas the former is straight to convex upward within the same stress range. These are data from identical appearing samples taken from the same site.

The non-linear stress-strain curves at low stress levels can be attributed to the closing of fissures in the rock. These microfractures are thought to be the result of changes in the stress environment to which the rock has been subjected. They may originate from the different elastic properties of the minerals, which would cause differential elastic rebound upon unloading. The effect of these features is also apparent in the dry velocity curves as those samples that have the non-linear stress-strain curve show a greater increase in velocity with increasing load than do those samples with linear stress-strain properties. The saturated samples do not show as great an increase in the compressional velocity as do the dry samples even though the stress-strain curves indicate the presence of microfractures. The same relationships can be shown for the limestone in Figures 4.4 and 4.5.

The effect of pore fluids on the acoustic properties of rock has been studied in detail by petroleum geophysicists (Mann and Fatt, 1960; Wyllie et al., 1958, 1956; Hughes and Kelley, 1952; King, 1966). The presence of air-filled voids retards the propagation of elastic waves between adjacent grains due to the

Rock Type Granite Gneiss; Dworshak Dam

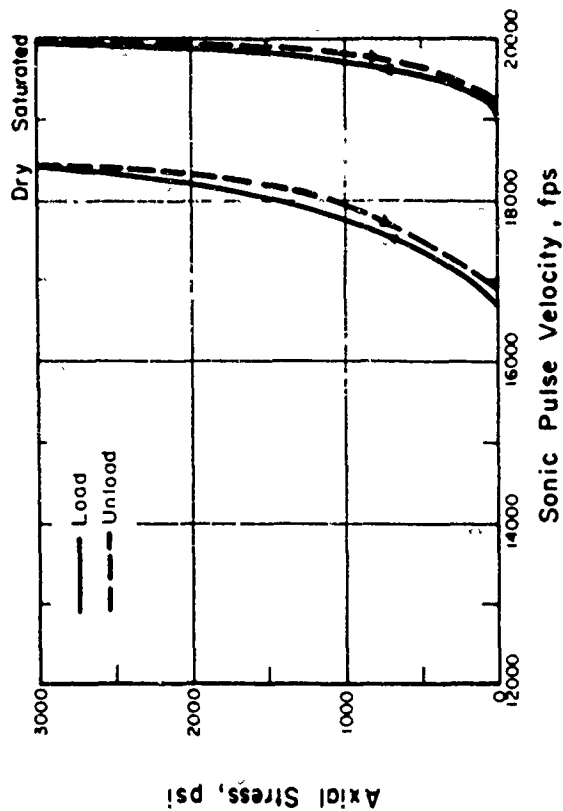
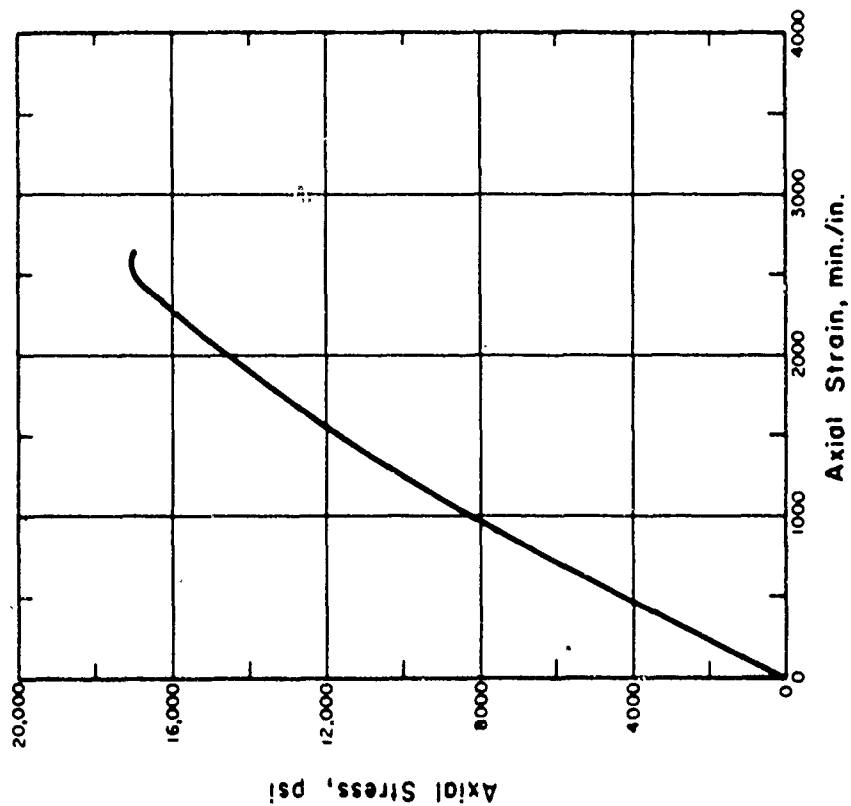
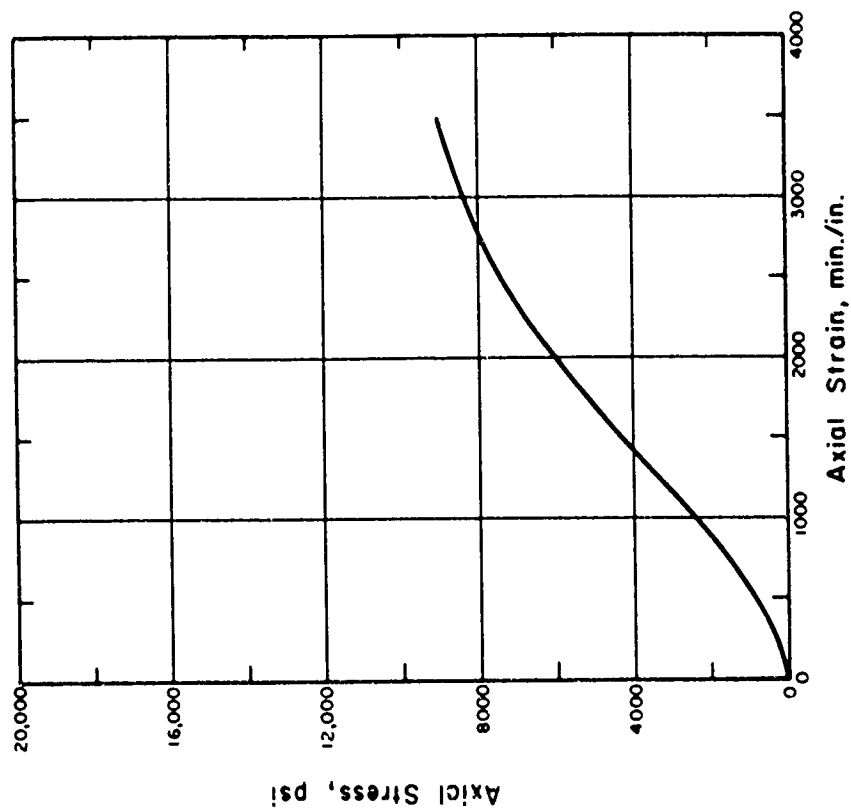


FIG. 4.2 STRESS-STRAIN BEHAVIOR AND SONIC PULSE VELOCITY FOR ROCK IN UNIAXIAL COMPRESSION - DWORSHAK I



Rock Type Granite Gneiss; Dwarshak Dam

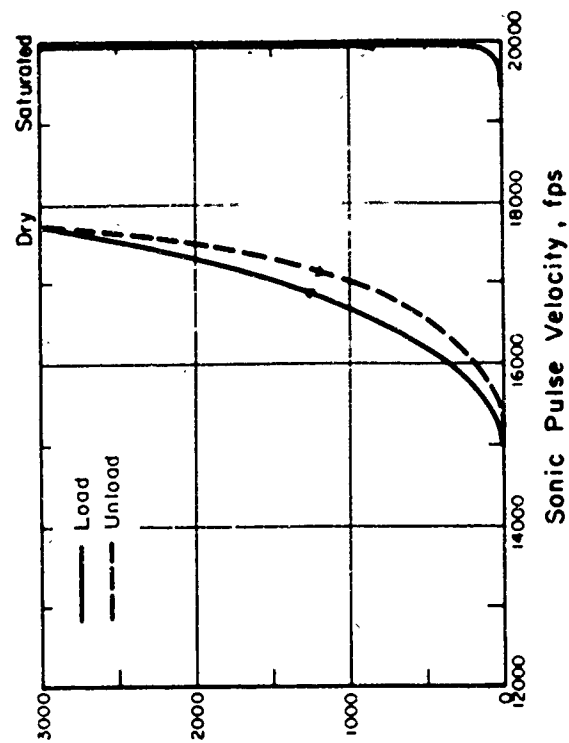
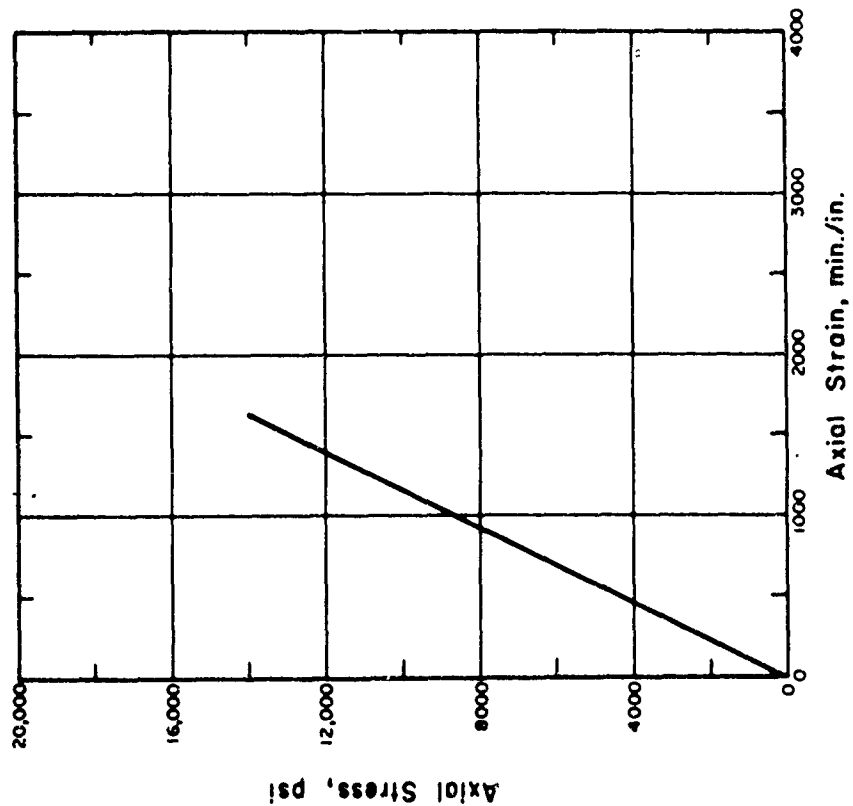


FIG. 4.3 STRESS-STRAIN BEHAVIOR AND SONIC PULSE VELOCITY FOR ROCK IN UNIAXIAL COMPRESSION - DWORSHAK 2





Rock Type : Limestone ; Yellowtail Dam

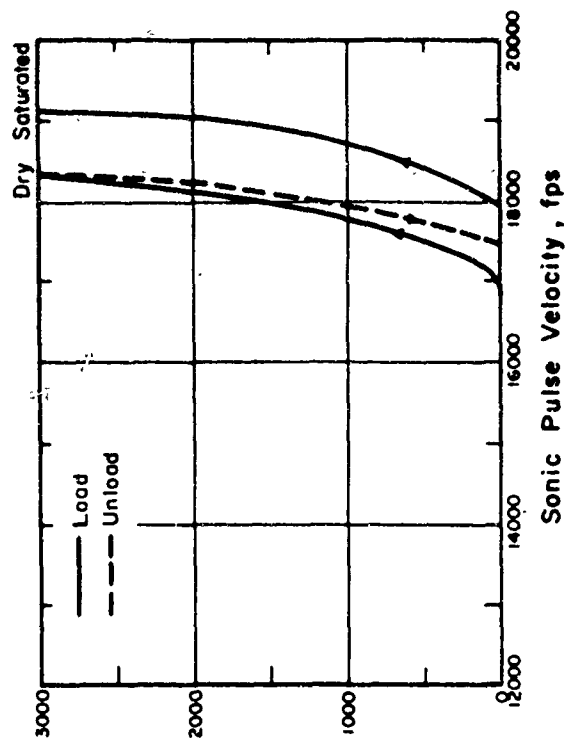
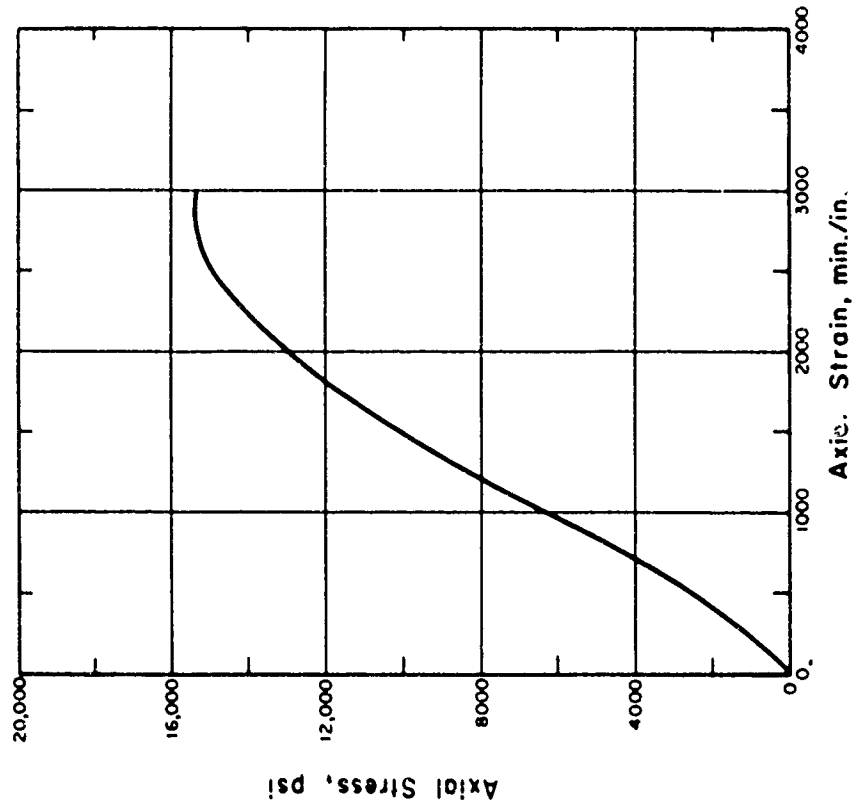


FIG. 4.4 STRESS-STRAIN BEHAVIOR AND SONIC PULSE VELOCITY FOR ROCK IN UNIAXIAL COMPRESSION - YELLOWTAIL I



Rock Type Limestone ; Yellowtail Dam

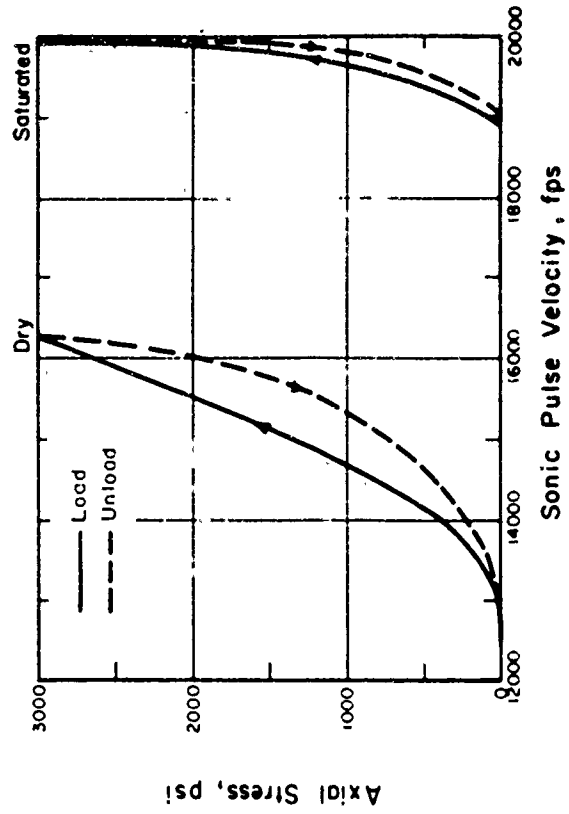


FIG. 4.5 STRESS-STRAIN BEHAVIOR AND SONIC PULSE VELOCITY FOR ROCK IN UNIAXIAL COMPRESSION - YELLOWTAIL 2

high acoustical impedance across the rock-air interface. The attenuation of the signal may cause a great enough decrease in the amplitude of the first arrival that it cannot be identified on the oscilloscope. Therefore, the secondary phase of the compressional wave may be mistaken for the first arrival. The energy also travels the more indirect path entirely through the grains of the rock. In both cases the arrival time of the compressional wave will be later than if the rock contained no voids or cracks. When the sample is saturated, the air has been driven out of the void spaces. Any subsequent velocity measurements will be higher than those in the dry rock because the acoustic impedance across the water-rock boundary is less than that across the air-rock interface.

The velocities of the saturated samples were chosen for correlation purposes because 3-D velocities and most data from up-hole and tunnel seismic surveys were obtained from saturated material. The selection of the proper stress level at which to measure the compressional velocities is important because all rocks show an increase in velocity with pressure. Intuition might suggest that the stress level be governed by the estimated overburden pressure acting at the depth from which the sample was obtained. These velocities would be expected to be compatible with the 3-D sonic velocities at the same depth. However, the assumption that the pressure at a certain depth is equal to the overburden may not always be justified. The in-situ stress state is related to tectonic forces as well as the overburden pressure. In addition it appears that a short term axial pressure which duplicates the overburden pressure would not restore the sample to its in-situ condition. Therefore, it was considered most reasonable to select a stress level that resulted in the maximum increase in the velocity for all rock types. All laboratory velocities used in this report were measured at 3,000 psi. In the majority of cases the increase in velocity for the saturated rock had leveled off at this point. Triaxial tests of saturated rock cores up to 10,000 psi have shown a continual velocity increase throughout the entire test (Wyllie et al., 1958; King, 1966) although in many cases at least 90 percent of the velocity increase has taken place by 3,000 psi.

SECTION 5  
RELATIONSHIP OF ROCK QUALITY  
AND IN-SITU TEST RESULTS

1. Introduction

The results of the in-situ tests described in Section Three depend, at least in part, on the character of the geological discontinuities of the rock mass. The sensitivity and reliability of each test can be judged by comparing test results with core logs. In this section borehole photography, permeability tests, 3-D sonic tests, and resistivity tests are compared with the location of joints or faults or the rock quality defined by the RQD. The RQD used in this section is the one suggested by Deere (1966).

2. Borehole Photography

The number of joints identified by borehole photography is less than the number of core breaks seen in a boring (Figure 5.1). This may be caused by several factors: 1) breakage during drilling, 2) separation along potential planes of weakness such as foliation or bedding, and 3) tight joints that can not be identified on the photographs. If a joint surface has been weathered it is readily recognized on the photographs because of color differences. However, if no weathering is present or if the water is cloudy it would be difficult to identify tight joints. Because a joint is tight in a borehole does not mean that a similar feature would remain closed in the vicinity of a large underground opening. Stress relief movements would occur primarily along such surfaces.

Borehole photography has provided an invaluable tool for observing large in-situ discontinuities and for measuring their orientation and inclination. However, it should not be assumed that those joints seen in photographs represent the only planes of potential weakness in the rock mass.

3. Permeability

The values of rock permeability were determined from either single or double packer pressure tests run in 5 or 10-foot sections of the borehole. The rock types included gneiss, schist, and sandstone so that for the majority of data permeability was dependent upon open joints. The data in Figures 5.2 to 5.6 show that there is a very poor correlation between RQD and permeability.

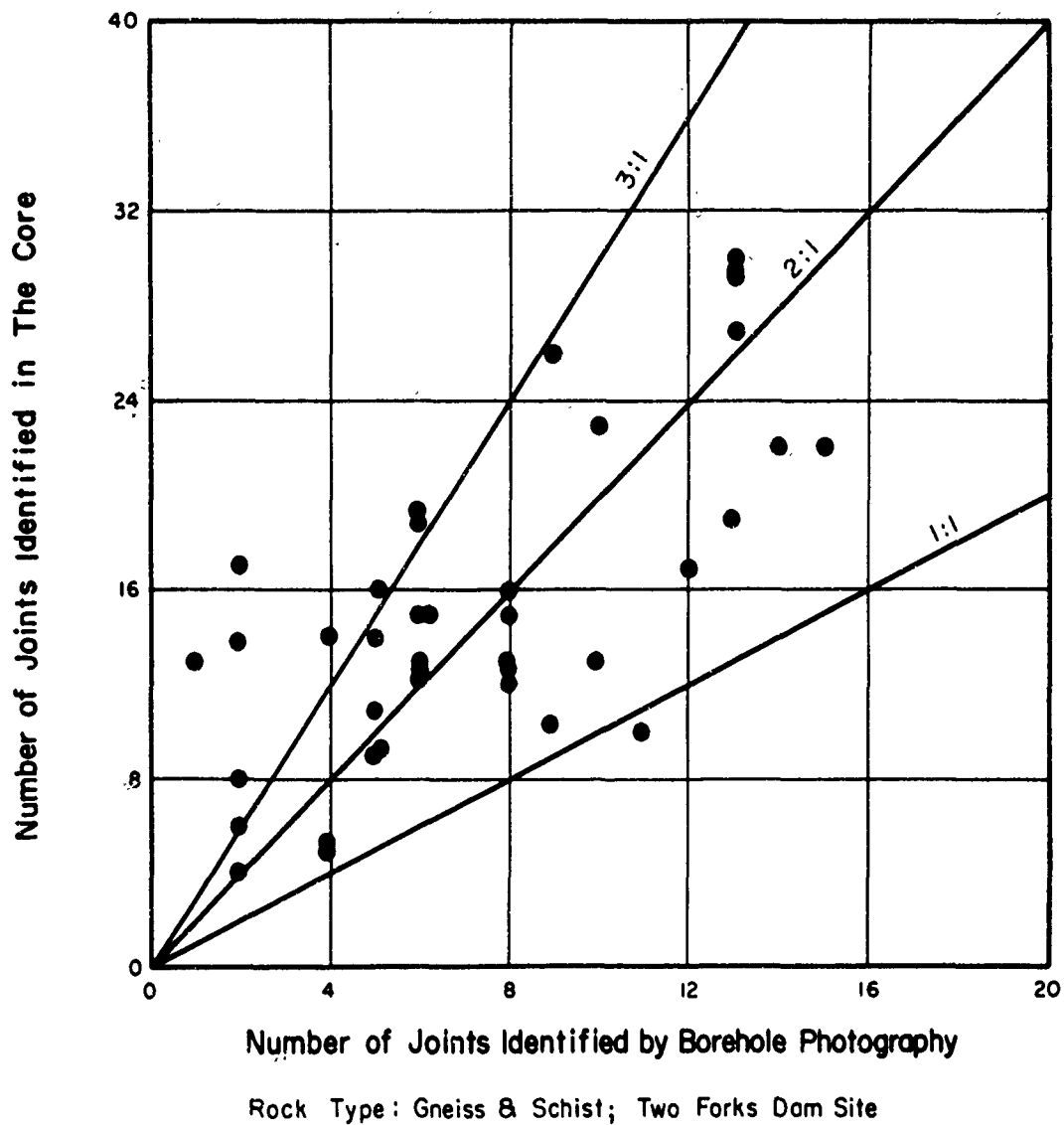


FIG. 5.1 RELATIONSHIP BETWEEN NUMBER OF JOINTS IDENTIFIED BY BOREHOLE PHOTOGRAPHY AND THOSE IDENTIFIED IN THE CORE



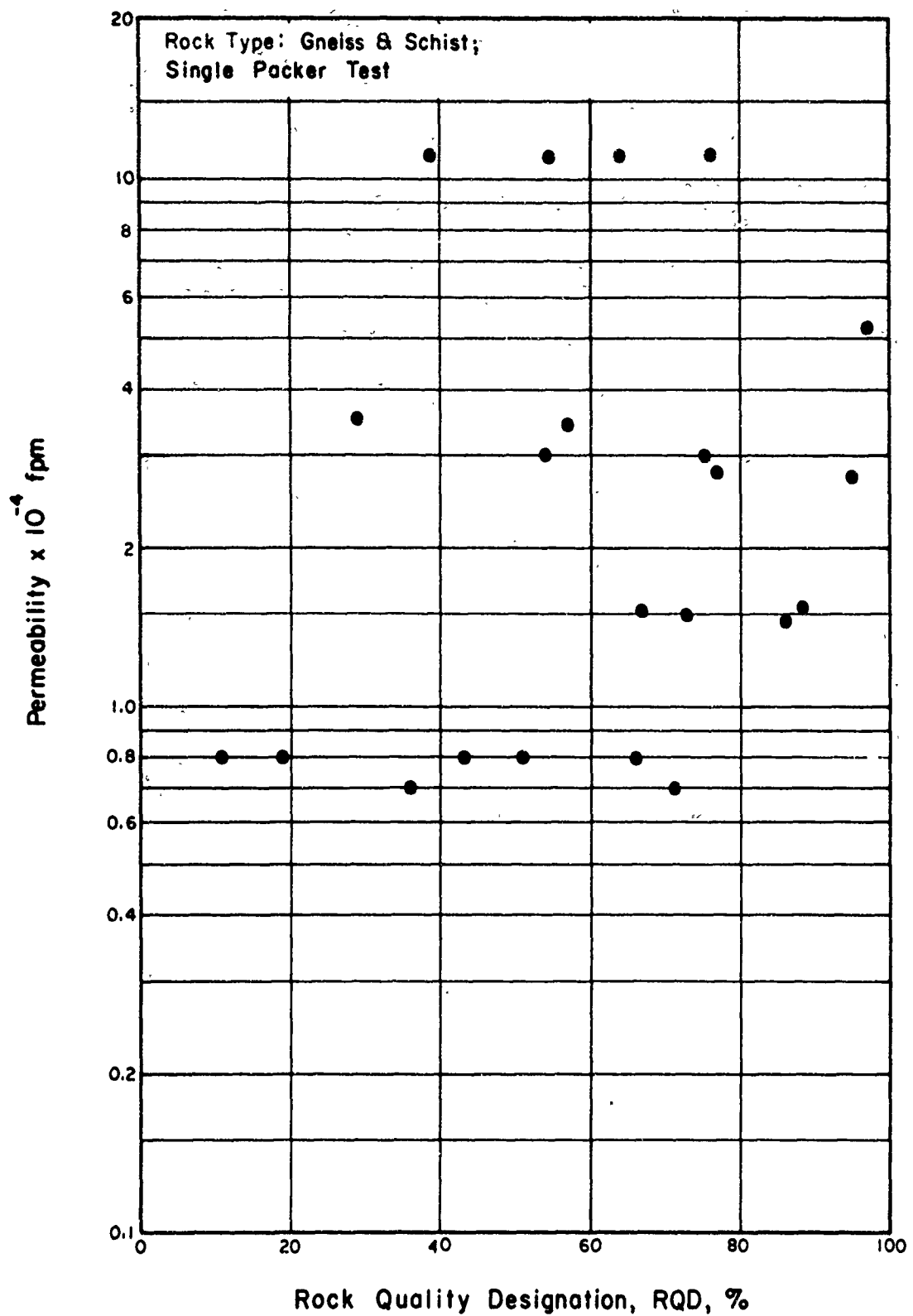


FIG. 5.3 RELATIONSHIP BETWEEN ROCK QUALITY DESIGNATION AND PERMEABILITY—TWO FORKS DAMSITE

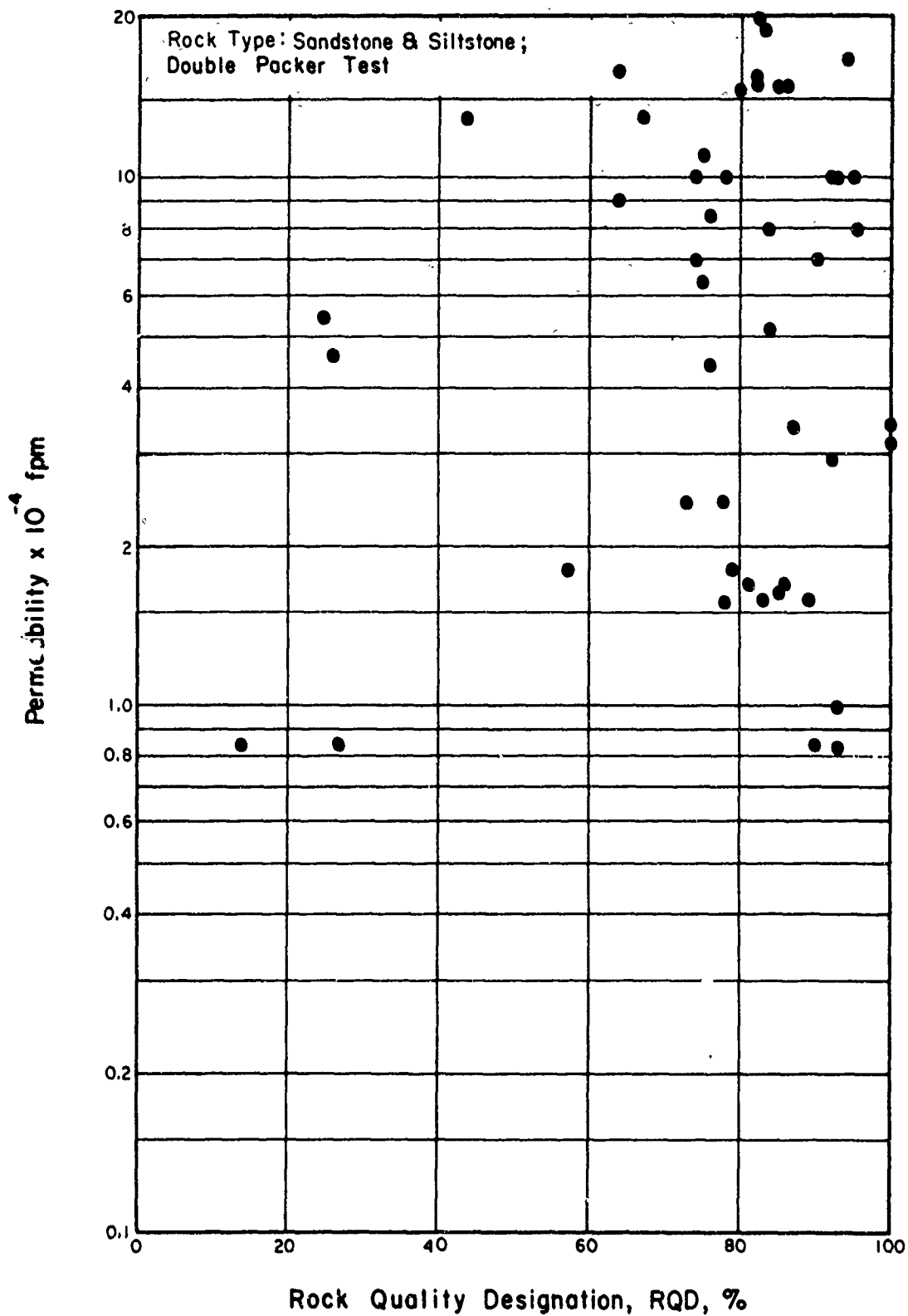


FIG. 5.4 RELATIONSHIP BETWEEN ROCK QUALITY, DESIGNATION AND PERMEABILITY—HACKENSACK GAS STORAGE FACILITY



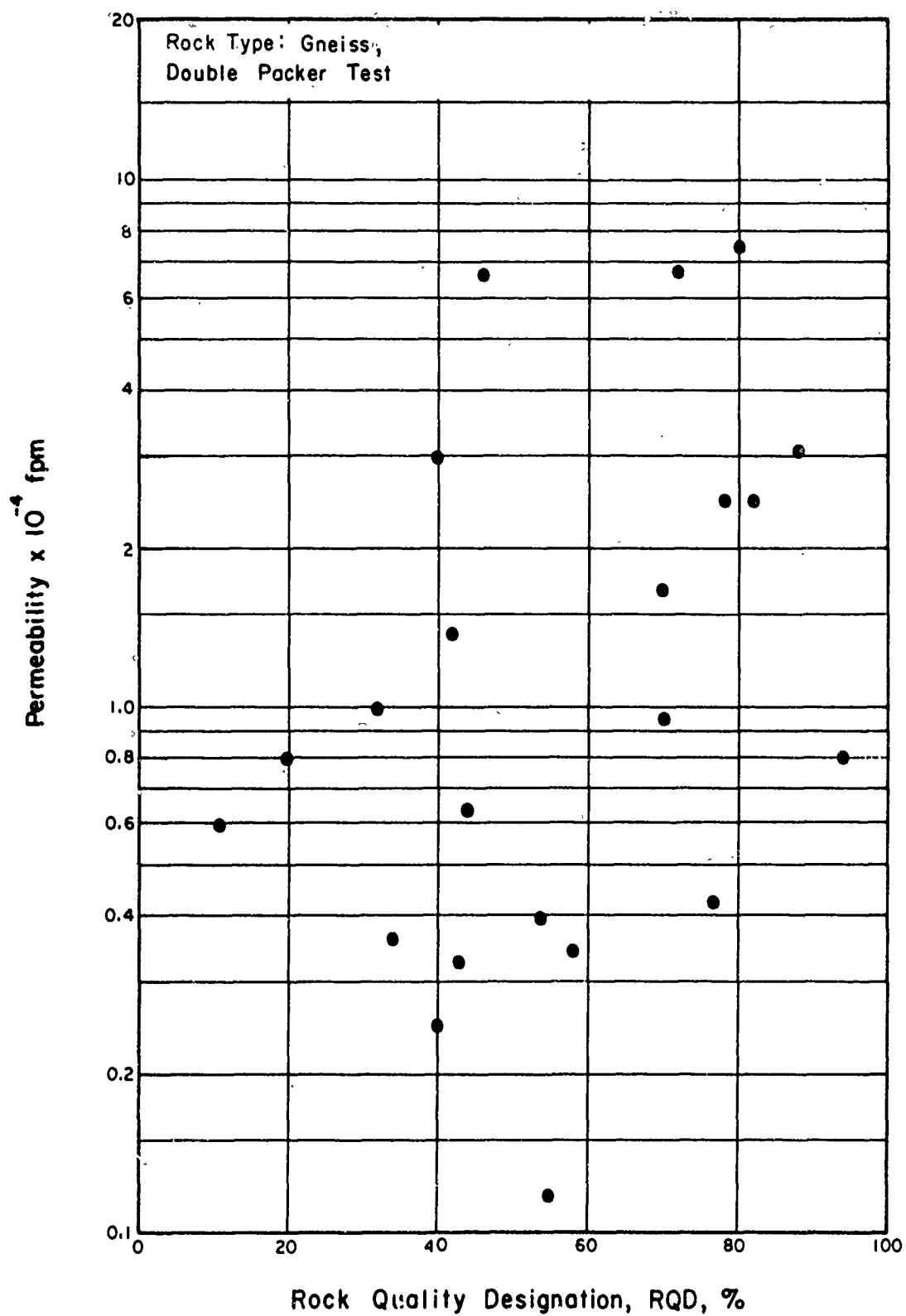


FIG. 5.5 RELATIONSHIP BETWEEN ROCK QUALITY DESIGNATION AND PERMEABILITY — WASHINGTON SUBWAY

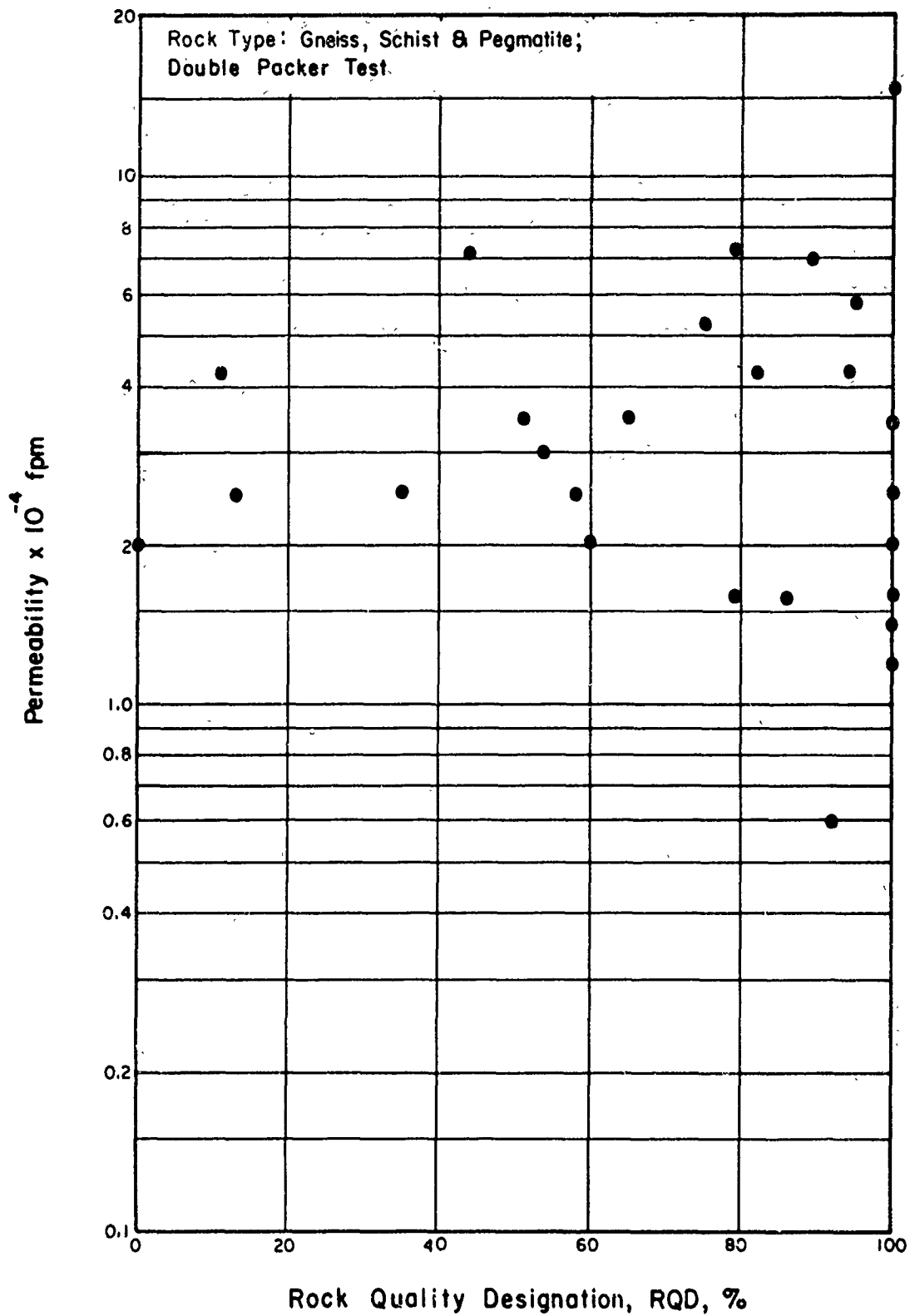


FIG. 5.6 RELATIONSHIP BETWEEN ROCK QUALITY DESIGNATION AND PERMEABILITY—WORLD TRADE CENTER SITE

There is either a wide range of permeabilities for a nearly constant RQD or a restricted range of permeabilities for a wide variation in RQD. There is apparently no relationship between the type of test and the degree of correlation because similar trends were obtained from data of both single and double packer tests. The tests represented in Figure 5.5 were run using 4-foot long leather packers expanded against the rock at pressures exceeding 120 psi. This method should have given the most reliable data because leakage between the packers and the rock should have been minimal. It was not possible to determine whether packer leakage occurred in any of the tests or whether the pressures were high enough to enlarge the fractures in the rock.

The data indicate that the RQD can not be used as a means of predicting in-situ permeability. The RQD is an index of joint frequency and weathered rock and while these factors affect permeability it is likely that the more important factor is the width of open joints. Joints 1/8 to 1/2 in. in width would not necessarily influence the RQD but could be responsible for high permeability.

The establishment of a relationship between permeability and the openness and frequency of joints requires a direct measure of these features by borehole or television cameras. The hole should be examined before and after pressure testing to determine if any separation has occurred along joint surfaces during the test. The rate of water intake should also be correlated with the increase in pressure for the same reason (Figure 3.4). Drilling fragments may penetrate fissures and obscure them from recognition on photographs. These fissures might be washed clean during the pressure tests and anomalously high water losses would result.

These water pressure data indicate that permeabilities of in-situ rock can vary from  $1 \times 10^{-6}$  to  $1 \times 10^{-3}$  ft/min even though the rock is generally of high quality. For this reason no assumptions should be made of in-situ permeabilities on the basis of an RQD or other evaluations of rock based on fracture frequency or the amount of weathering.

#### 4. 3-D Sonic Logs

The variations of the wave form patterns in a 3-D log can provide qualitative information about the rock that may be as useful as the sonic velocity in an engineering evaluation. The presence of solution cavities, joints, and faults that do not intersect the boring may be inferred by a careful study of the logs. An approximate angle of inclination of intersection

or nearby joints and faults may also be determined by observing the wave pattern. A particular wave pattern depends upon the reflection of sonic energy at the discontinuity. If these features are not within the immediate vicinity of the boring, it is necessary to extend the sweep time of the oscillograph so that time is available for the energy to reach the feature and be reflected back to the sonde. The normal sweep time of a 3-D log is about 1,200 microseconds and it could be increased to 2,500 or 5,000 microseconds to locate features within 30 feet of the hole. The expanded time scale will, however, compress the energy display on the log and make it difficult to identify the arrivals of the primary and shear waves.

The 3-D log in Figure 5.7 shows what is interpreted to be a nearly vertical fracture that was recorded when the time scale was expanded to 5,000 microseconds. These features may also appear as thin lines on the log. If a nearly vertical fracture cuts across the boring or is within the influence of the depth of penetration of primary or shear energy, the arrivals of the sonic pulses from different sides of the borehole may be slightly out of phase. This causes a split of the dark streaks on the log which occurs with little increase in travel time (Figure 5.8). These features may also be caused by foliation in metamorphic rocks that dip at high angles.

The diagonal lines in Figure 5.9 that tend to converge at the left side of the log are interpreted (Walker, 1964) as reflections from a density interface or joint that intersects the boring at nearly right angles. Figure 5.10 is a schematic representation of the origin of these lines. As the logging sonde approaches the interface, the reflected wave arrives at the receiver at progressively shorter time intervals. When the transmitter moves beyond the joint, the opposite pattern is formed on the log and the overall appearance is that of a "W". When the transmitter is opposite the reflecting surface, only the normally transmitted energy reaches the receiver and this continues until the receiver has passed the surface. The area showing no reflection corresponds to the length of the tool. These reflection features are common in many 3-D logs and are observed more readily where the sweep time has been increased.

The principal causes of a decrease in sonic velocity are zones of closely spaced joints and faults or the presence of abrupt changes in lithology such as clay-filled solution cavities or fault gouge. The shear wave is generally more affected by jointing than is the primary wave because the former

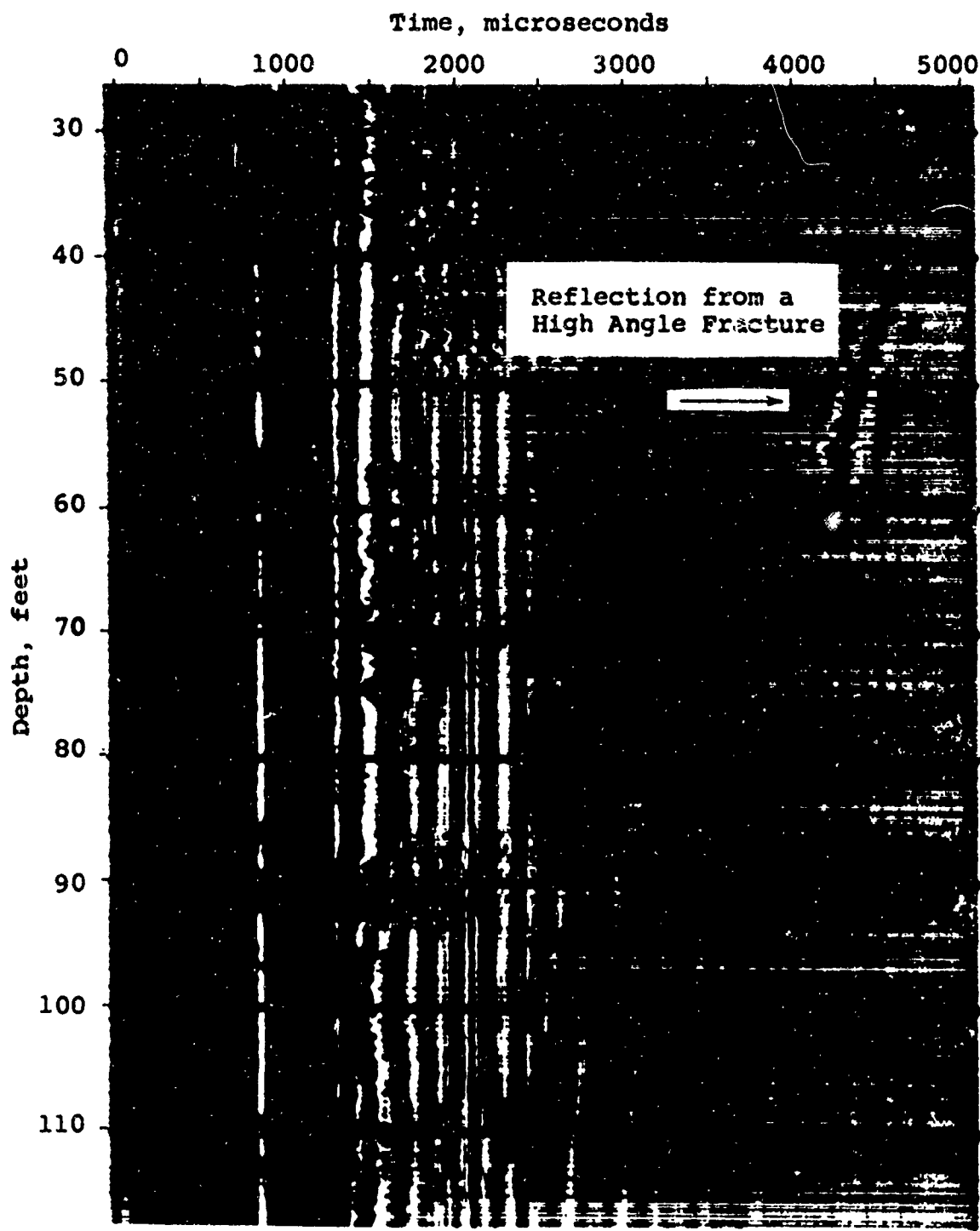


FIG. 5.7 3-D SONIC VELOCITY LOG - REFLECTION PATTERN CAUSED BY A HIGH ANGLE FRACTURE AT SOME DISTANCE FROM THE BOREHOLE, DWORSHAK DAM

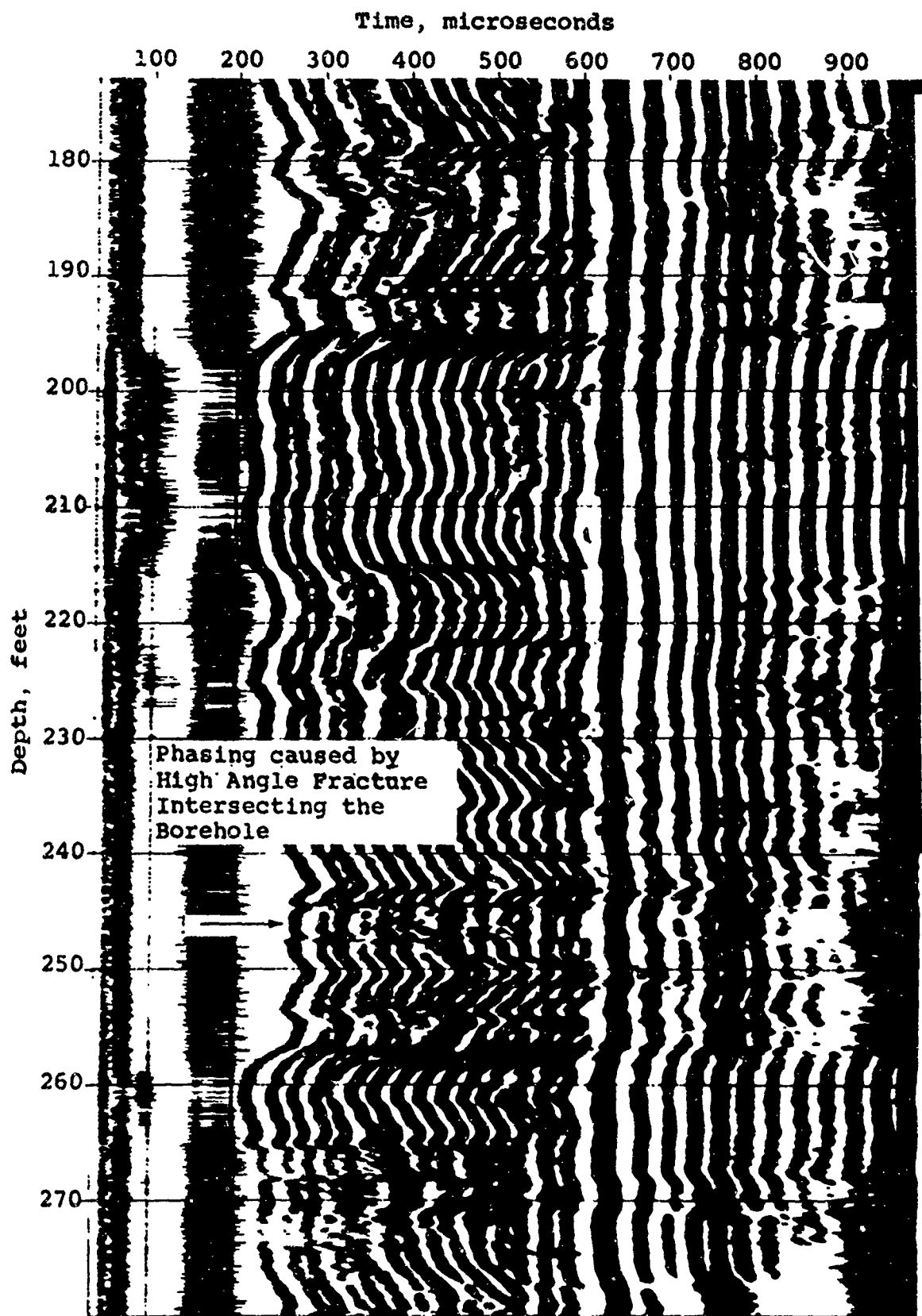


FIG. 5.8 3-D SONIC VELOCITY LOG - PHASING PATTERN  
CAUSED BY HIGH ANGLE JOINTS INTERSECTING  
THE BOREHOLE, YELLOWTAIL DAM

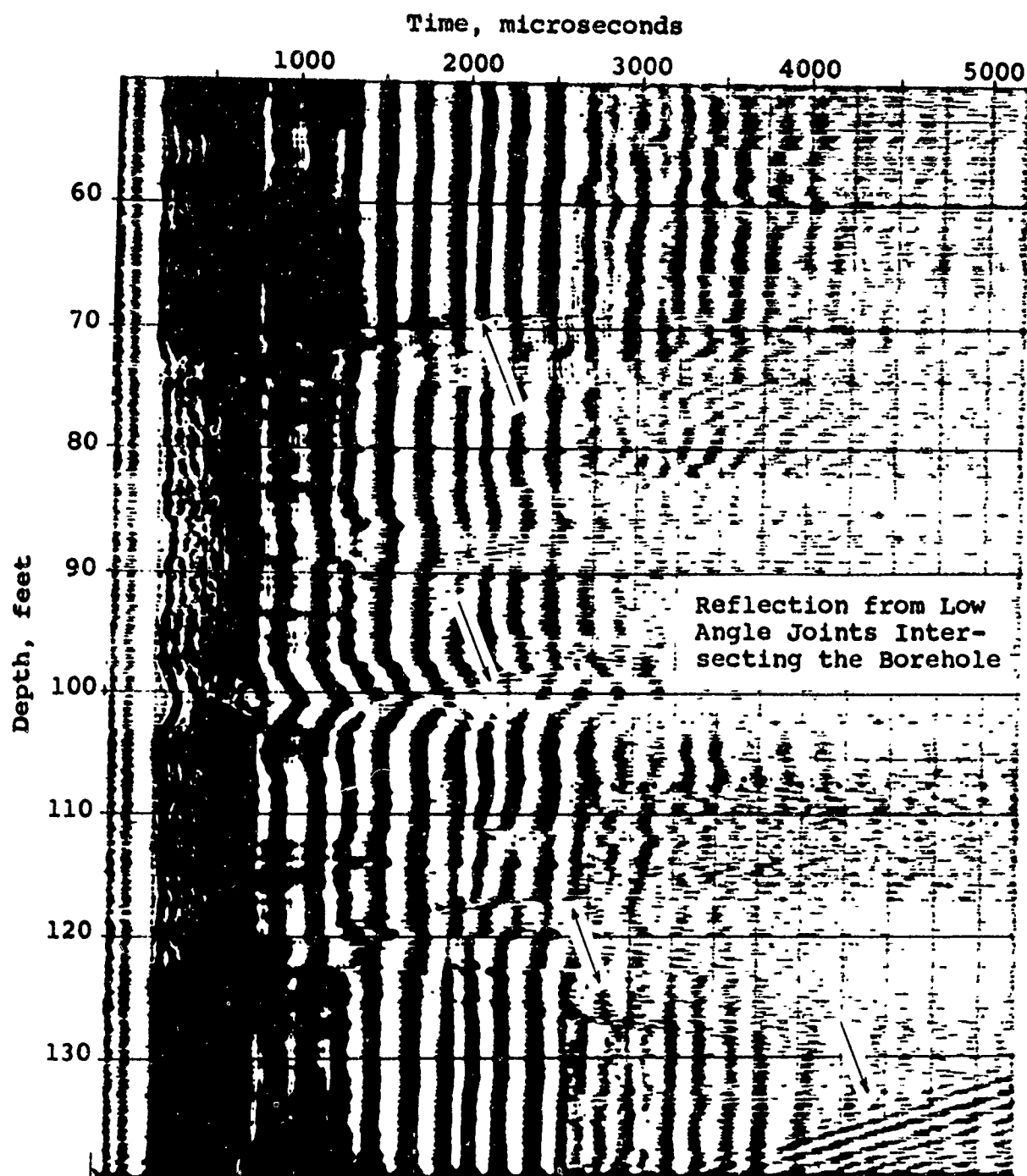
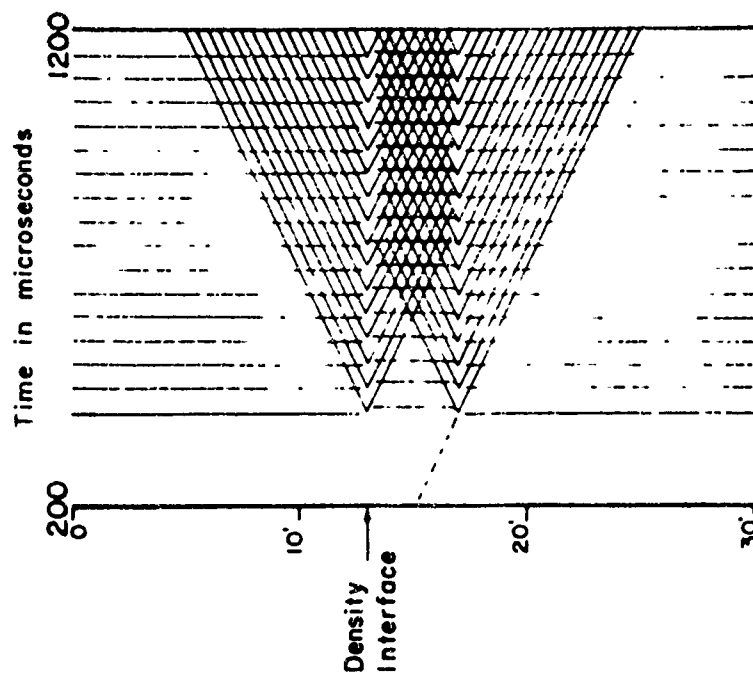
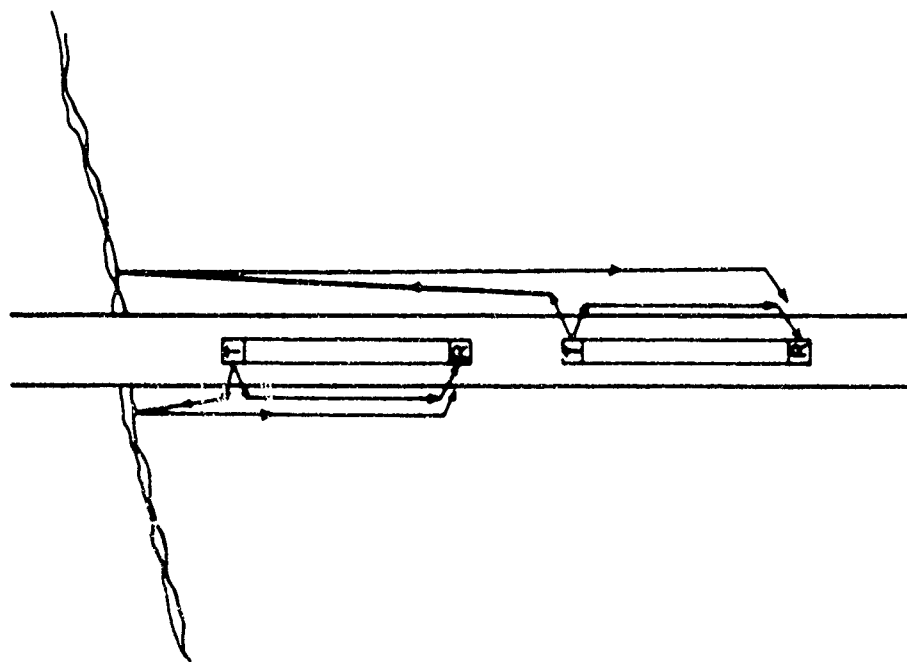


FIG. 5.9 3-D SONIC VELOCITY LOG - REFLECTION PATTERN CAUSED BY LOW ANGLE JOINTS INTERSECTING THE BOREHOLE, TWO FORKS DAMSITE



Acoustic Tool Approaching a Density Interface

FIG. 5.10 SCHEMATIC DIAGRAM OF "W" PATTERN CAUSED BY ENERGY REFLECTION FROM A DENSITY INTERFACE (After Walker, 1964)

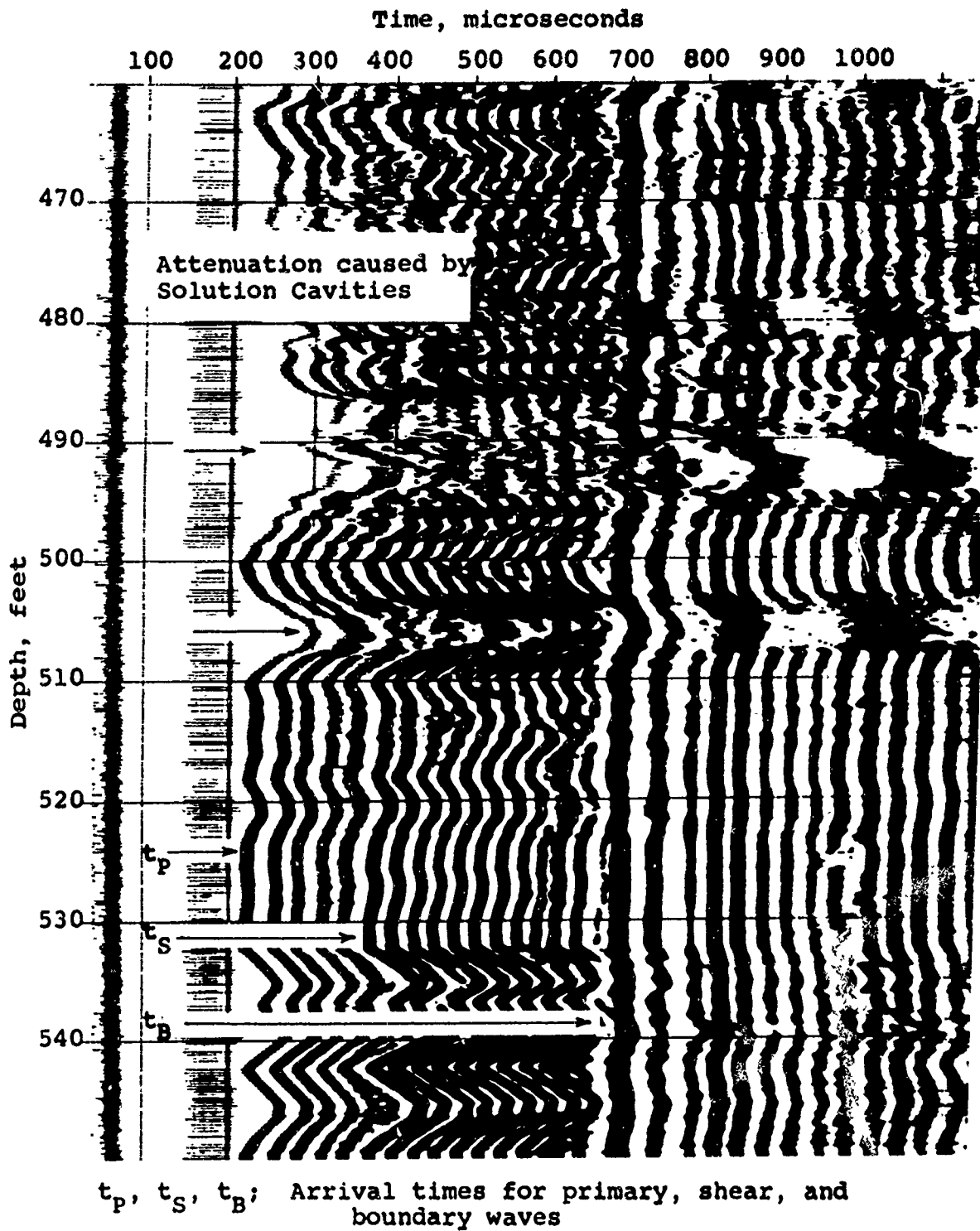


is attenuated by the water in open fissures. This facilitates the identification of the shear arrival when the differences in amplitude of the primary and shear waves are small. Jointing and solution features influence the appearance of the boundary or Stoneley wave that generally appears at a time of 700 to 800 microseconds for a 3-foot tool spacing. Any changes in hole diameter caused by caved-in rock or voids will cause an irregular-appearing boundary wave because these waves travel along the surface of the borehole.

A portion of a 3-D log from limestone is shown in Figure 5.11. The clear sharp wave patterns indicate a dense homogeneous material. However, this formation has numerous solution cavities and brecciated zones, two of which are located at 490 and 505 feet. The primary and shear energy have been so attenuated that it is difficult to distinguish between them. The boundary wave is also distorted which suggests an increase in hole diameter. Other velocity logs run in the same formation have shown a complete loss of signal in these cavities. Variations of the velocity in this rock are primarily related to shale-filled cavities or to solution enlarged joints and not to the presence of numerous fissures.

The log shown in Figure 5.12 represents a heavily jointed metamorphic rock with foliation planes that dip from  $30^{\circ}$  to  $90^{\circ}$ . Phasing splits in the primary and shear wave patterns are common throughout the record because the majority of fractures dip at angles ranging from  $50$  to  $90^{\circ}$ . The high amplitudes in the 28 to 38-foot interval were caused by energy transmission through a local zone of dense unjointed mica hornblende schist. The increase in arrival times and the signal attenuation in the 39 to 45 ft and 55 to 63 ft intervals are a result of closely spaced joints, and the 72 to 123 ft interval represents a fault zone with gouge and a high fracture frequency. The loss of the boundary wave signal at 102 ft suggests that the hole has been enlarged. This was verified by the results of both caliper and density logs. The variations of arrival times in this log are primarily caused by joint frequency as shown on the graph of RQD and velocity (Figure 5.13). These structural interpretations of the rock were based on an examination of the core borings. A photograph of the heavily fractured core from a depth of 67 to 110 ft is shown for this boring (Figure 5.14).

The examples presented above show that the core log, and the 3-D sonic, caliper, and density logs can be used together to obtain a much clearer impression of rock conditions in a boring. Comparisons other than RQD versus sonic velocity are, however, basically qualitative.



$t_p$ ,  $t_s$ ,  $t_b$ ; Arrival times for primary, shear, and boundary waves

FIG. 5.11 3-D SONIC VELOCITY LOG - SIGNAL ATTENUATION CAUSED BY SOLUTION CAVITIES IN LIMESTONE, YELLOWTAIL DAM

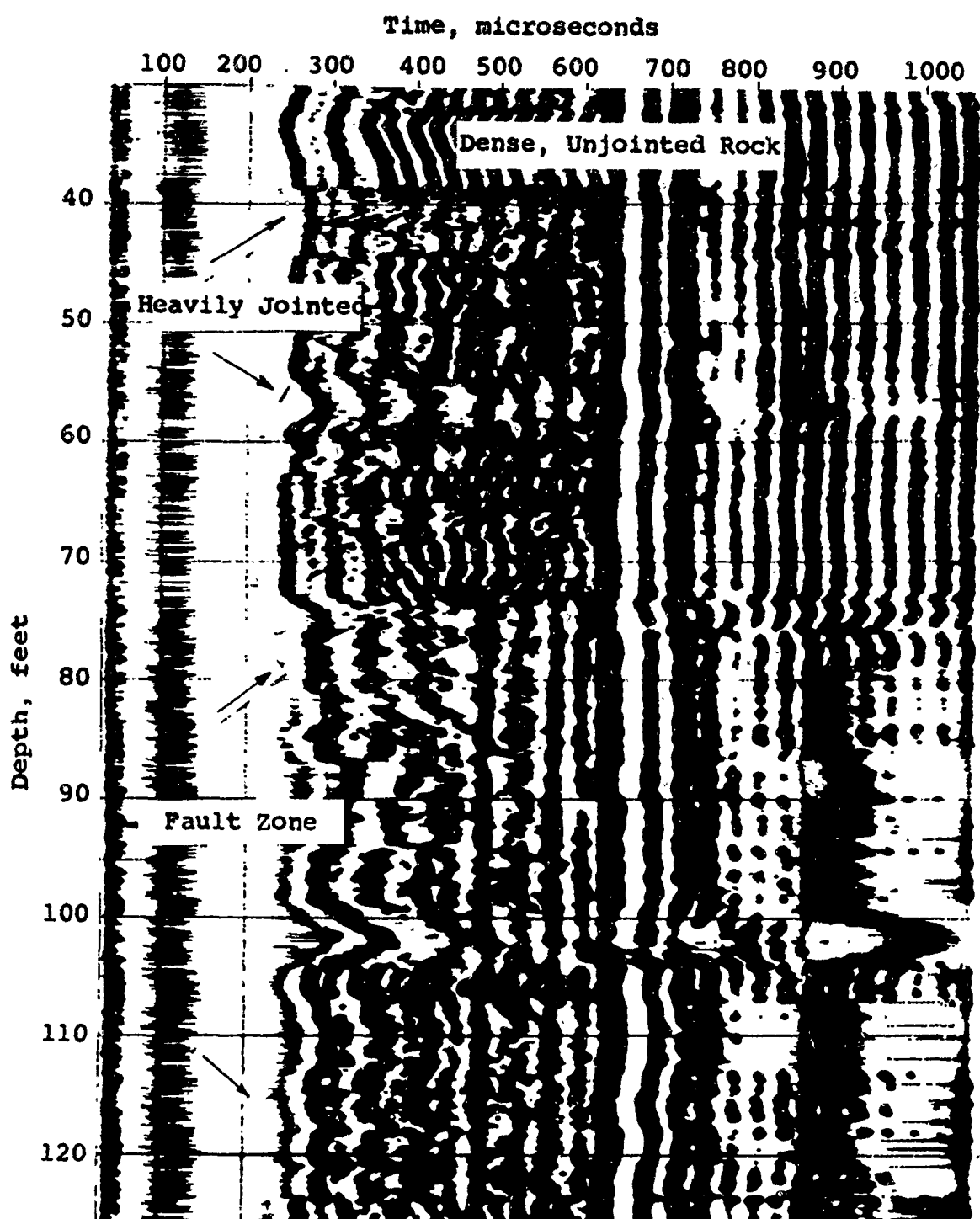


FIG. 5.12 3-D SONIC VELOCITY LOG - INCREASED TRAVEL TIME AND SIGNAL ATTENUATION CAUSED BY FAULTING AND JOINTING, BORING F, TWO FORKS DAMSITE

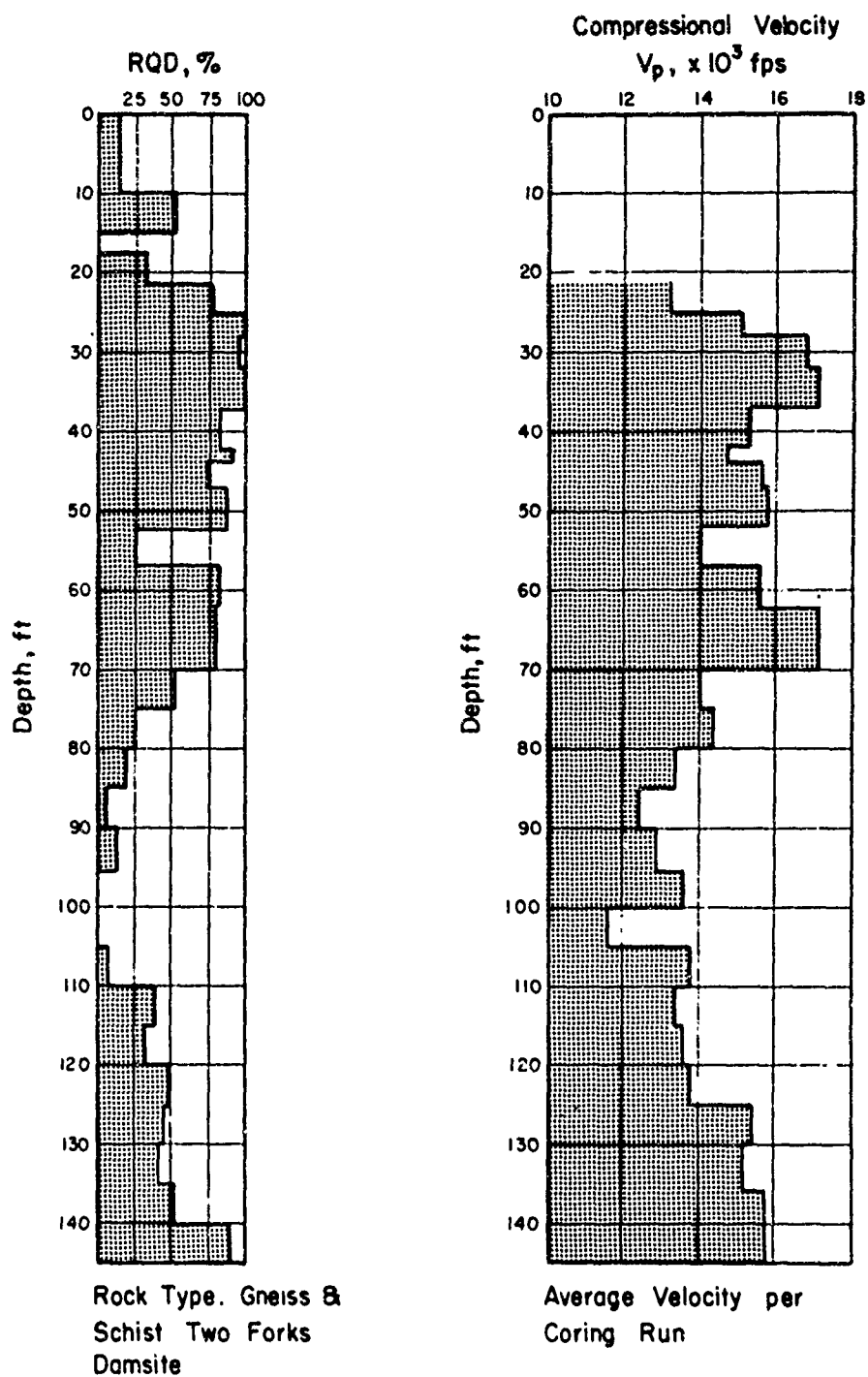


FIG.5.13 RELATIONSHIP BETWEEN ROCK QUALITY DESIGNATION AND 3-D COMPRESSIONAL VELOCITY.



FIG. 5.14 CORE PHOTOGRAPH OF A PORTION OF BORING F,  
TWO FORKS DAMSITE

## 5. Electrical Resistivity

Electrical resistivity surveys were not carried out under this contract but a limited amount of data was available from private consulting files (Deere, 1967, private communication). Resistivity logs were run in two borings in granite as part of an exploration program for a pressure tunnel. A Widco in-hole logger with a 2-inch electrode spacing (normal configuration) was used in each boring. The lithology is constant throughout each boring and any deviations on the log are considered to be the result of jointing or faulting. The data from the two borings (Figures 5.15 and 5.16 respectively) show a general trend of increasing resistivity with an increase in the RQD. Electrical conductance occurs most readily through water-filled pores or fissures and will therefore be higher in heavily fractured zones. The absolute resistivity values in Figure 5.16 are higher than those in Figure 5.15 even though the lithology is the same in each boring. A possible explanation is that the chemistry of the ground water may be different considering that the borings are 1 mile apart. The variation in dissolved salts can be an important factor when analyzing resistivity data. The resistivity data shown in Figure 5.17 from dacite and rhyolite were obtained by using a logger with a lateral electrode configuration (9-foot spacing). The points fall within the range shown in Figure 5.15 and have the same trend of increasing resistivity with an increase in RQD.

The regression line determined by the resistivity measurements at the Straight Creek Tunnel (Scott and Carroll, 1966) is shown on each of the figures and in all cases the slope is steeper than that of the other data. These measurements were made along tunnel walls in gneiss, schist, and pegmatite with a Gish-Rooney apparatus using a Wenner electrode arrangement. This equipment is limited to use on the ground surface or along tunnel walls.

Although there is considerable scatter in the resistivity values, the data do indicate that this method is sensitive to heavily jointed areas in borehole or along tunnel walls. It appears that either lateral or normal logs can be used effectively if the spacing between measuring electrodes is small. The short electrode spacing used in the Widco apparatus is preferred for exploration because thin shear or fault zones can be recorded that otherwise might go unnoticed with a device having a longer electrode spacing. The spacing of the electrodes should be less than the degree of detail required for joint mapping with a 2 electrode (normal) device (Wyllie, 1963).

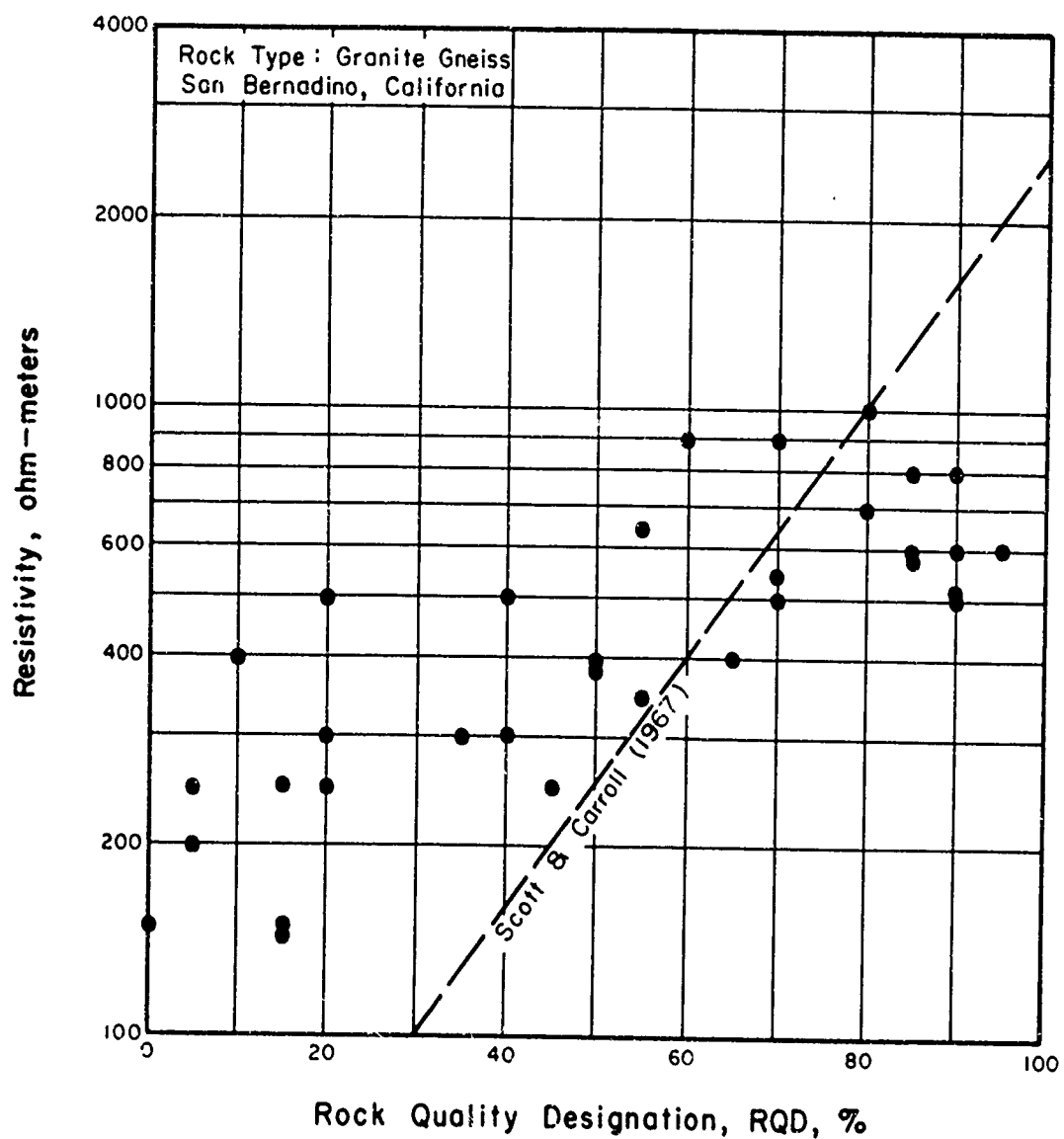


FIG. 5.15 RELATIONSHIP BETWEEN ROCK QUALITY DESIGNATION AND ELECTRICAL RESISTIVITY BORING SB 5

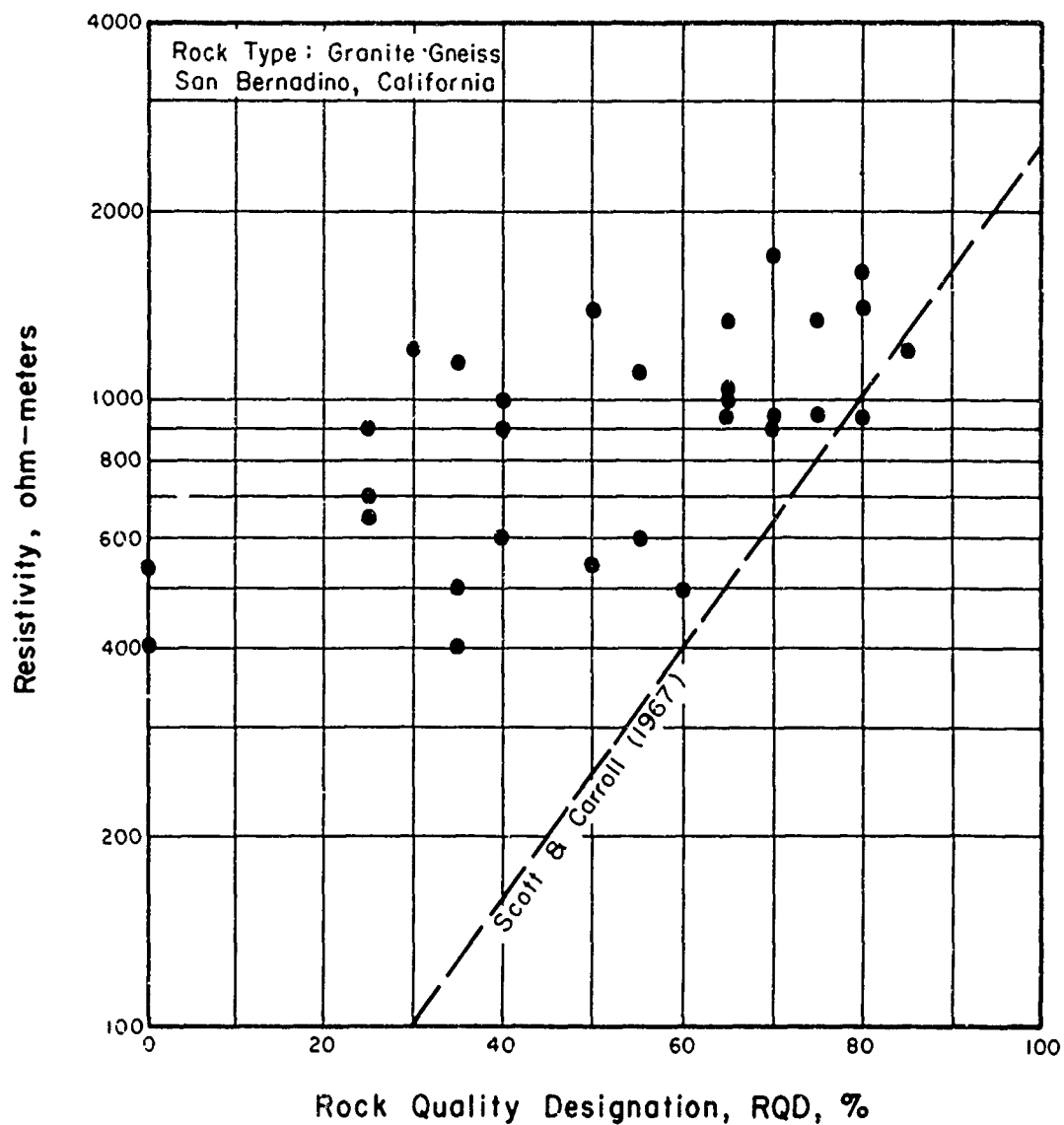


FIG. 5.16 RELATIONSHIP BETWEEN ROCK QUALITY DESIGNATION AND ELECTRICAL RESISTIVITY BORING SB 10



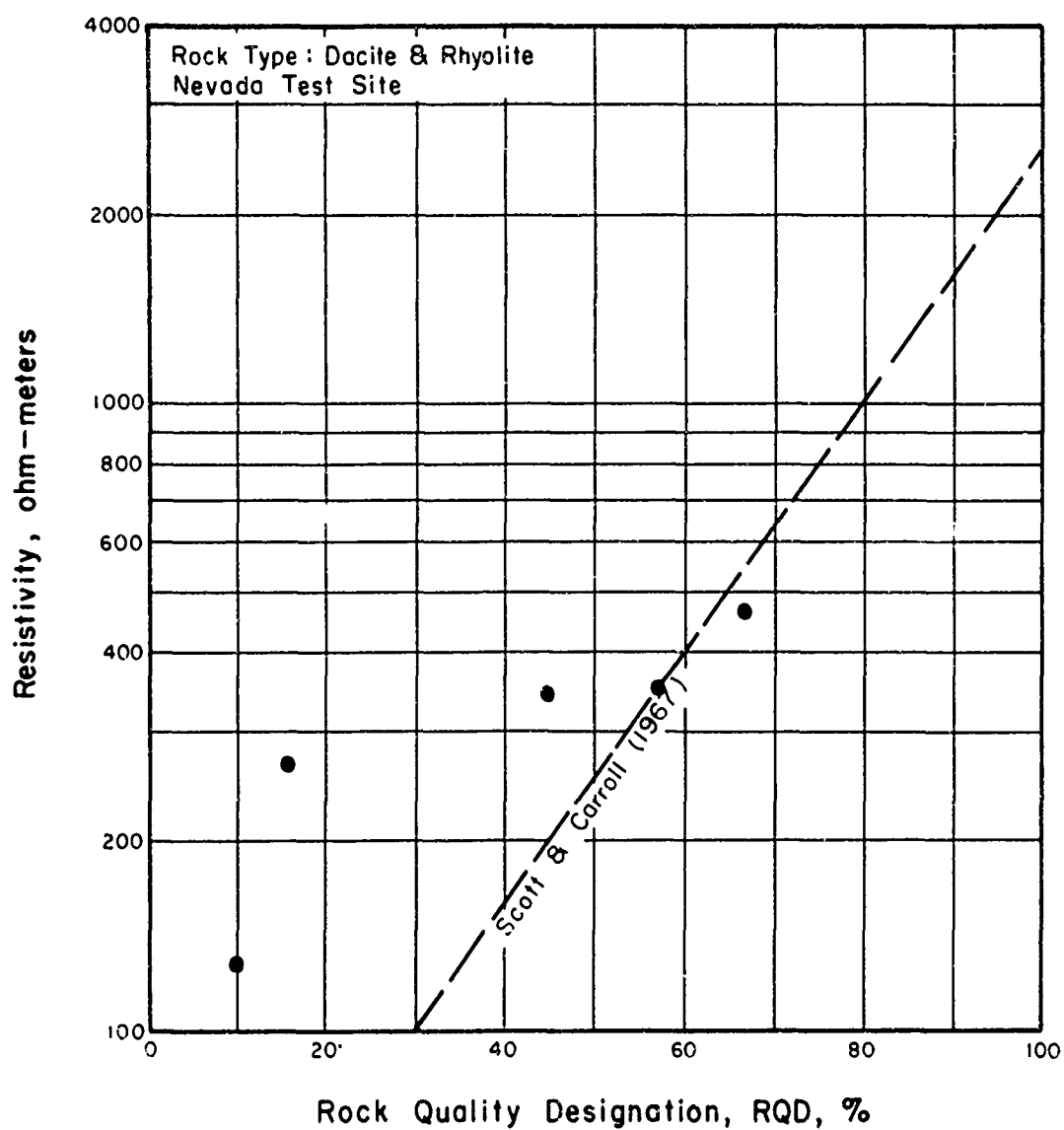


FIG. 5.17 RELATIONSHIP BETWEEN ROCK QUALITY DESIGNATION AND ELECTRICAL RESISTIVITY BORING PM-2

These records show that resistivity logs can be used to identify fractured zones in rock, especially if the rock type does not change within the boring. More information is necessary before a definite correlation can be established between RQD and resistivity or before recommendations can be made for the best type of testing equipment.

## 6. Conclusions

The data presented in this section have shown that sonic velocity and resistivity measurements can be correlated with rock quality defined by the RQD. While visual examination of drill core is the most direct method for determining rock quality, the correlation between these tests and rock quality may be used to supplement and in some cases replace core logging. Sonic velocity or resistivity measurements could, for instance, provide rock quality estimates in zones of core loss or in deep borings where rock bit drilling is less expensive than core drilling. Although both methods can be correlated with the RQD, sonic logging was used in this investigation because it is less sensitive to slight changes in the lithology and texture of the rock and the chemistry of the ground water.

The graphs of RQD and permeability indicate that in-situ permeability cannot be estimated from fracture spacing. Apparently fracture spacing and permeability are independent properties of a rock mass and both must be measured to determine the in-situ conditions. The poor correlation between the frequency of fractures determined by the RQD and borehole photography indicates that the two methods do not measure the same discontinuities. Borehole photography records the orientation and openness of major discontinuities while core logging provides a record of the inclination (but not orientation) and spacing of both the major discontinuities and planes of incipient fracturing. Borehole photography may be correlated with in-situ permeability although data is not available to establish the correlation. It should be valuable for assessing stability problems involving major discontinuities. The RQD can be used to assess the properties of a rock mass which depend on all the geological discontinuities.

## SECTION 6

### ENGINEERING CLASSIFICATION FOR IN-SITU ROCK

#### 1. Introduction

A classification system is presented that is based upon index properties of in-situ rock. These indices are a measure of the discontinuities in the rock mass and were developed using (1) a modified core recovery technique (the Rock Quality Designation, RQD) and (2) the results of field and laboratory seismic and sonic velocity tests (Velocity Index). Two methods are therefore available for determining rock quality and each provides a check on the accuracy of the other. The RQD, for example, may be affected by the drilling procedure whereas velocity measurements are not. The term rock quality pertains to the engineering suitability or the response of the material to construction procedures. Its application extends to situations where jointing or weathering are important in design considerations such as in-situ deformation, depth to suitable foundation material, tunnel support criteria, or general rock conditions throughout a site for pre-bid information.

#### 2. Indices of Rock Quality

##### a. Core recovery

Core recovery is often used as a means of evaluating rock conditions. Its determination is left to the discretion of the driller and can not always be used with confidence. It represents the amount of rock removed from a particular coring interval but indicates nothing about the condition of the core. This limitation of core recovery is evident in Figure 6.1, RQD versus Core Recovery, and Figure 6.2, Core Recovery versus Velocity Index. While the RQD ranges from 30 to 100 percent and the Velocity Index from 0.3 to 1.00, the core recovery values are almost uniformly 80 to 100 percent. For these reasons it is not recommended that core recovery alone be used as the basis for estimating in-situ rock conditions.

##### b. Rock quality designation (RQD)

Twelve methods of computing a value of rock quality were described in Section Three. These data were calculated on a 709<sup>4</sup> IBM computer from measurements of over 8,000 ft of core borings. The results of each method were correlated with the others to determine unique values of rock quality. For example,

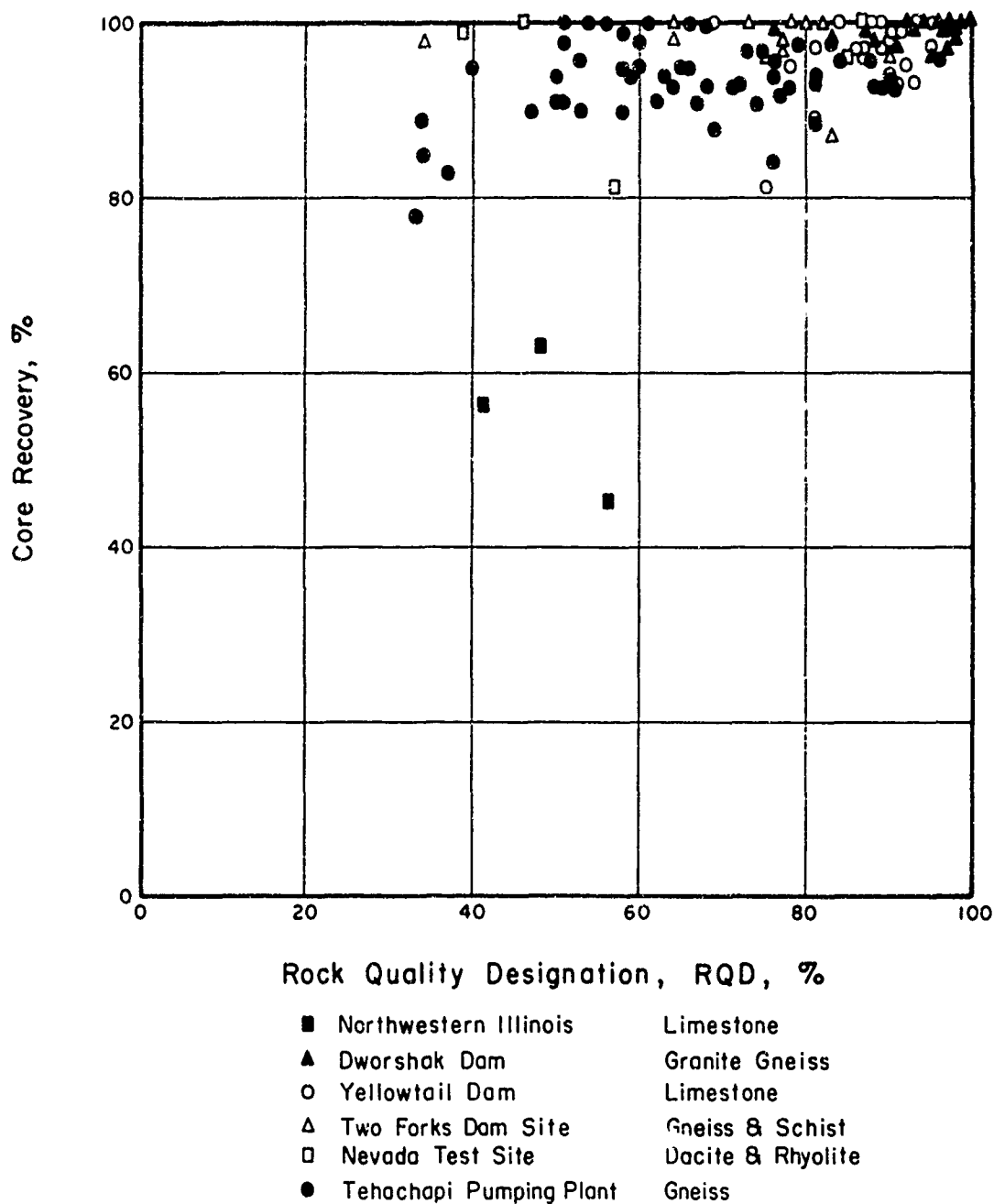


FIG. 6.1 RELATIONSHIP BETWEEN ROCK QUALITY DESIGNATION AND CORE RECOVERY

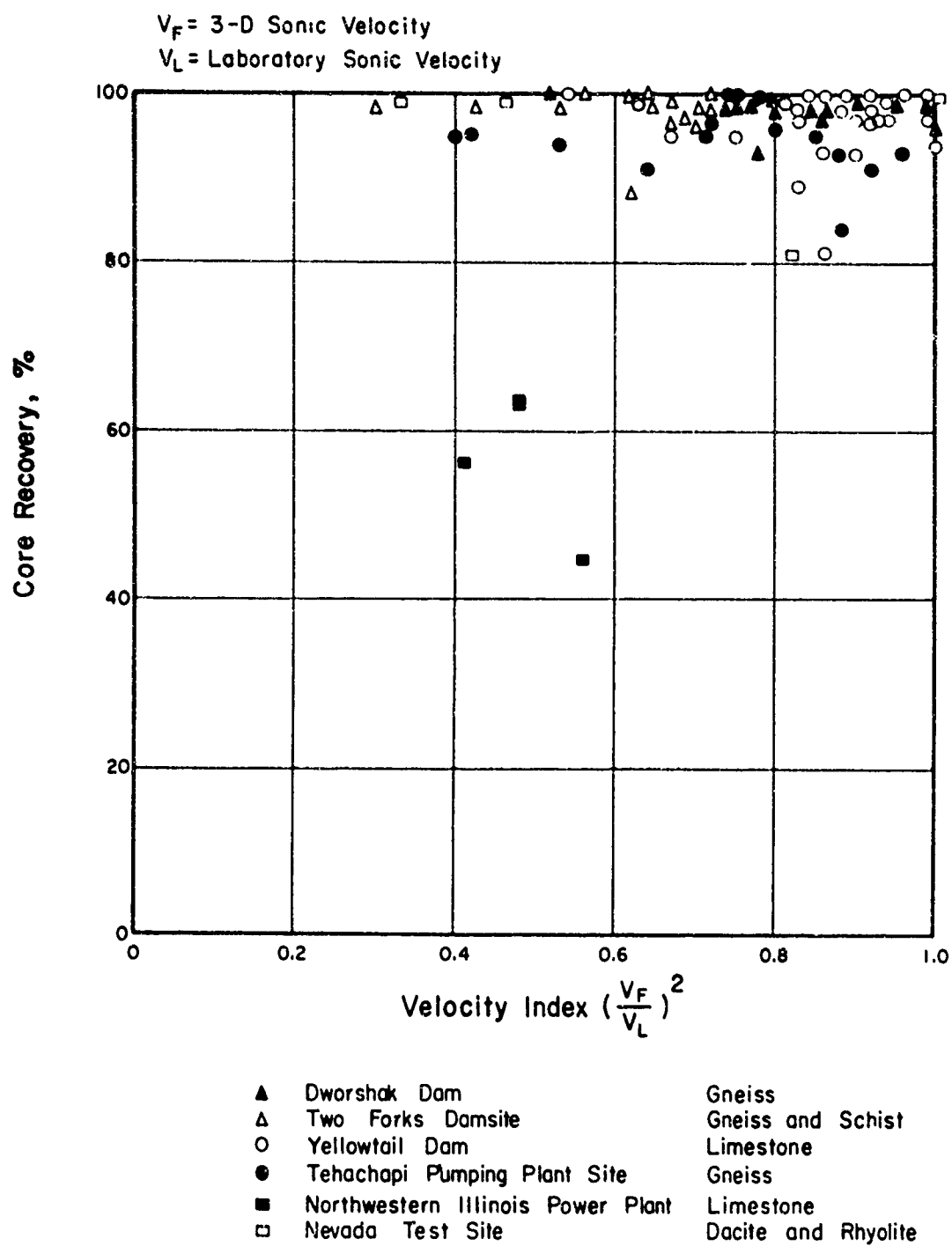


FIG. 6.2 RELATIONSHIP BETWEEN VELOCITY INDEX AND CORE RECOVERY

if an RQD using a core length of 0.2 ft correlated well with an RQD using a base of 0.5 ft only one of these values was considered for additional correlation with other properties such as the Velocity Index and permeability. By this process the unique RQD values were determined to be those based on core lengths of 0.35 ft, 0.5 ft and the weighted method of squaring the lengths of pieces less than 1.0 ft (Figure 3.1). These values will be referred to in the following discussion as RQD No. 1, RQD No. 2, and RQD No. 3 respectively. The original use of the RQD (Deere, 1964) was with the 0.35 ft length, i.e., RQD No. 1.

c. Velocity index

The Velocity Index is defined as the square of the ratio of in-situ to intact compressional wave velocities. The field velocities consist of either in-hole sonic (3-D) values or the results of up-hole seismic surveys. These sonic and seismic data were normalized by using a laboratory value in the denominator to counteract the influence of lithology. If the field velocity alone was used, a heavily jointed granite could have the same velocity as an unjointed friable sandstone. The ratio of the velocities will approach 1.0 as the number of joints decrease and the rock improves in quality. The ratio was squared so that the Velocity Index is equivalent to the ratio of the dynamic moduli. A particular zone of low quality rock will have a proportionally greater effect on the RQD in a core run than it will on the velocity in the same interval. The squaring of the velocity ratio tends to offset this difference and the RQD and Velocity Index decrease on a nearly equal basis with increased jointing.

All the sonic and seismic velocities used in this report were measured in saturated rock. The difference between dry and saturated laboratory velocities has already been mentioned in Section Four. A similar comparison for in-situ rock was made at one site. In a moderately fractured gneiss, up-hole seismic tests were performed in two borings, one in dry rock and the other below the water table. The velocities of the saturated rock were 60 percent higher than those in the dry rock. There is not enough information available to determine whether the differences would be as great at other sites.

3. Correlation of Rock Quality Indices

Velocity measurements from up-hole seismic and 3-D sonic tests were correlated with RQD to determine if these rock quality indices could be used interchangeably. To make these comparisons it was necessary to adjust the scale of the test intervals. The sonic logs, for instance, contain foot-by-foot

velocity values while RQD is based on core runs of 5 to 10 ft. To compare these data, the sonic velocities were averaged for each core run. A Velocity Index calculated from the average sonic velocity and a laboratory sonic test was compared with RQD values. The seismic tests, on the other hand, have test intervals of 10 to 75 ft and it was necessary to compare the average RQD for the interval with a Velocity Index based on the seismic velocity and one or more laboratory tests.

The preliminary determination of the best-fit line through the data was made by using two statistical methods, the least square regression and the reduced major axis analysis (Miller and Kahn, 1962). The former method requires that one of the axes be the independent variable. If X is made the independent variable, the method fits a line to the data that minimizes the sum of the squares of the distances to the line measured perpendicular to the X-axis. Conversely, the regression of X on Y can be defined as the line that minimizes the sum of the squares of the deviations from the line, the distance being measured perpendicular to the Y-axis. The regression line of Y on X is not necessarily the same as the line for X on Y although they both intersect at a point representing the mean values of the two variables.

The use of the least square regression method assumes that the scatter of the data is caused by deviations of one variable. This is not the case when considering the RQD and Velocity Index because each term is dependent upon the amount of jointing and not on each other. The reduced major axis analysis minimizes the sum of the areas of the triangles formed by lines drawn from each point to the desired line and parallel with the X- and Y- axes. It makes no assumptions of dependence. The reduced major axis line appears more reasonable than do either of the least square lines (Figure 6.3). This statistical method was used to determine the best-fit line for all the data presented herein.

The degree of correlation between X and Y can be expressed by the correlation coefficient,  $r$ , which is a measure of the intensity of association or relationship between variables. The quantity,  $r$ , varies between -1 and +1, which are the values for a perfect correlation. The signs + and - are used for positive linear correlations and negative linear correlations respectively. The correlation coefficient is shown on each of the graphs in this section.

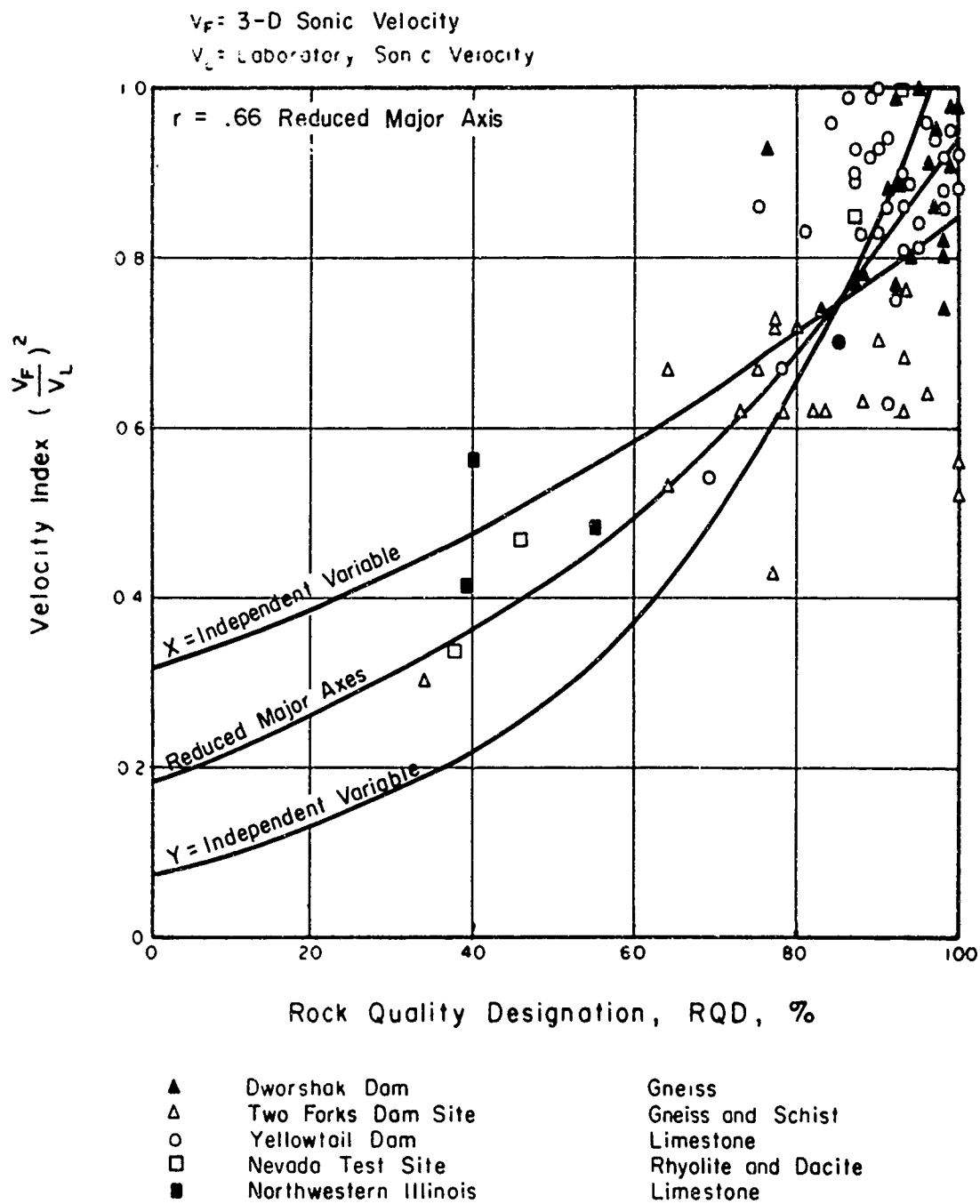


FIG. 6.3 RELATIONSHIP BETWEEN ROCK QUALITY DESIGNATION (RQD NO. 1) AND VELOCITY INDEX — 3-D SONIC VELOCITY



The significance of a correlation coefficient depends on the number of data points used in its calculation. Fisher (1963) presents a table of significance levels which expresses the probability of having a random distribution, i.e., no correlation. From the table, knowing the number of data points and the correlation coefficient, it is possible to estimate the probability of a non-correlation from 100 per thousand to 1 per thousand (significance levels 0.10 and 0.001, respectively). A significance level of less than 0.05 is considered significant and one less than 0.01 is considered highly significant. It can be noted that the significance levels shown on the graphs (S.L.) are generally 0.001 indicating highly significant correlations.

The correlation of rock quality indices is discussed for each of the RQD's calculated from different base lengths. The data for each RQD are presented on 2 graphs; the first is based on 3-D sonic velocities and the second on up-hole measurements.

The relationship of RQD No. 1 and the Velocity Index is shown on Figure 6.3 (based on 3-D sonic velocity) and Figure 6.4 (based on up-hole velocities). A logarithmic curve has been used as a best-fit line. These data indicate that the 0.35 ft base RQD is apparently not as sensitive as is the 3-D logger in measuring joint frequency because of the larger variation in the Velocity Index (0.6 to 1.0) with respect to a smaller change in the RQD (80 to 100 percent). Both the RQD and velocity data are generally lower (at the same site) on the up-hole velocity graphs than those on the 3-D graphs. These seismic velocities are measured over a greater portion of the rock than are the 3-D values, and therefore are influenced by more fractures. The RQD values are representative of average conditions over the length of the boring and will not have the high values typical of smaller intervals tested by the 3-D logger.

The use of RQD No. 2 (based on core lengths of 0.5 ft) reduces the cluster of points that characterized RQD No. 1 and spreads the data into a more linear trend (Figures 6.5 and 6.6). However, this method also produces considerable scatter in the RQD for a Velocity Index range of 0.8 to 1.0 suggesting that the 0.5-ft base length might be too severe and that the RQD is too low because of the large amount of core that is being omitted from consideration.

The distribution of data in Figures 6.7 and 6.8 which is based on RQD No. 3 (weighted values) is similar to that shown in Figures 6.5 and 6.6 except

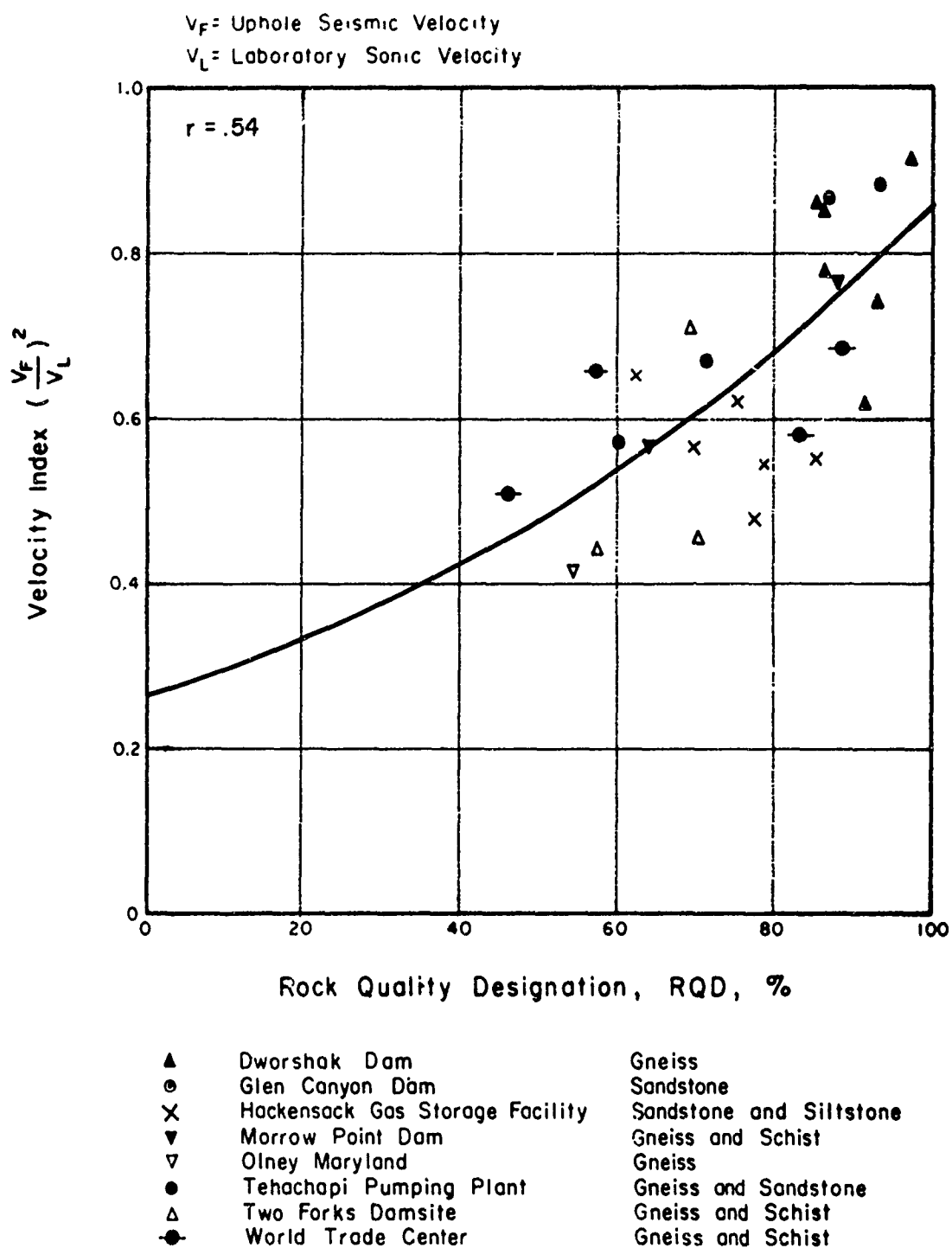


FIG. 6.4 RELATIONSHIP BETWEEN ROCK QUALITY DESIGNATION (RQD NO.1) AND VELOCITY INDEX — UP-HOLE SEISMIC VELOCITY

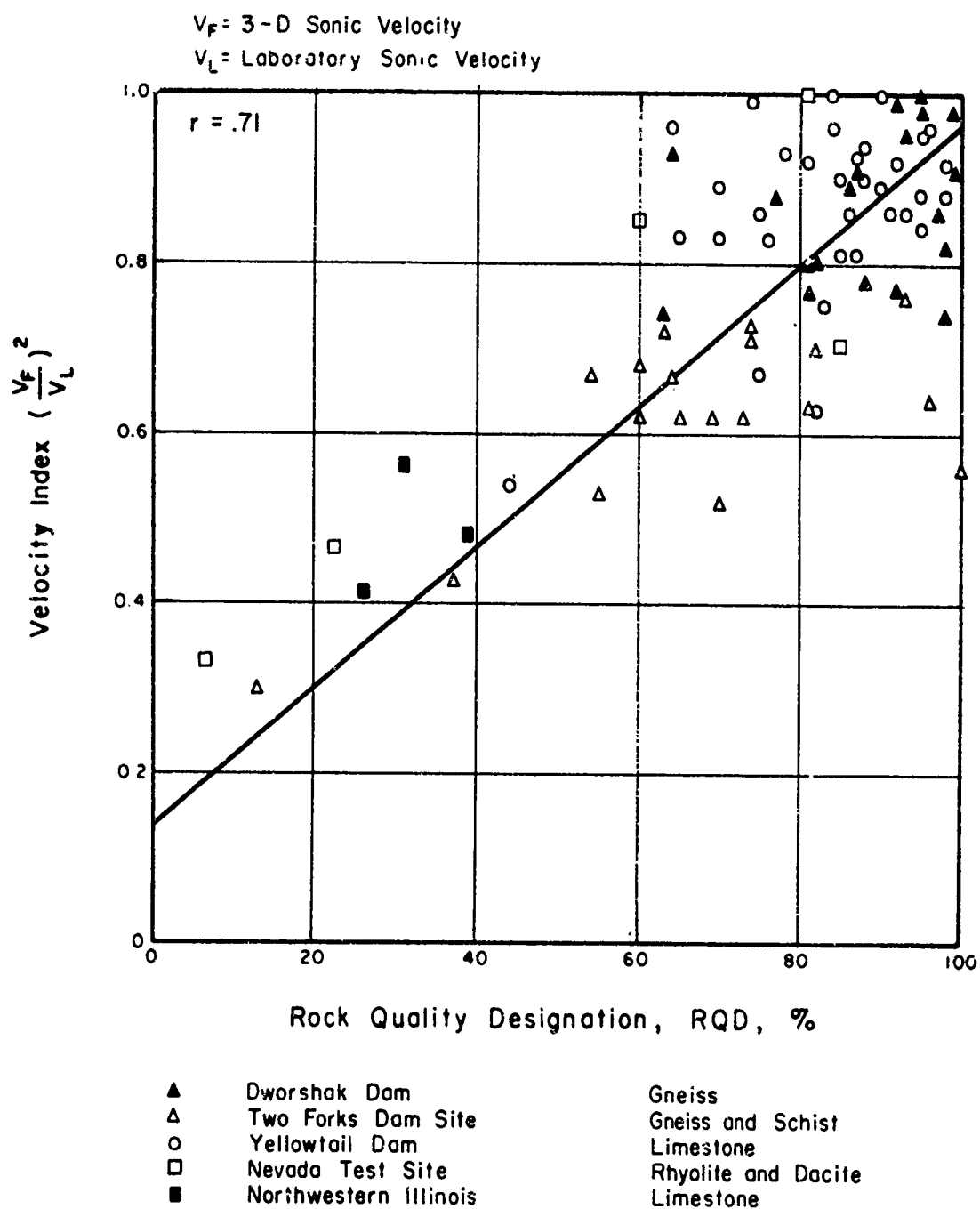


FIG. 6.5 RELATIONSHIP BETWEEN ROCK QUALITY DESIGNATION (RQD NO. 2) AND VELOCITY INDEX - 3-D SONIC VELOCITY

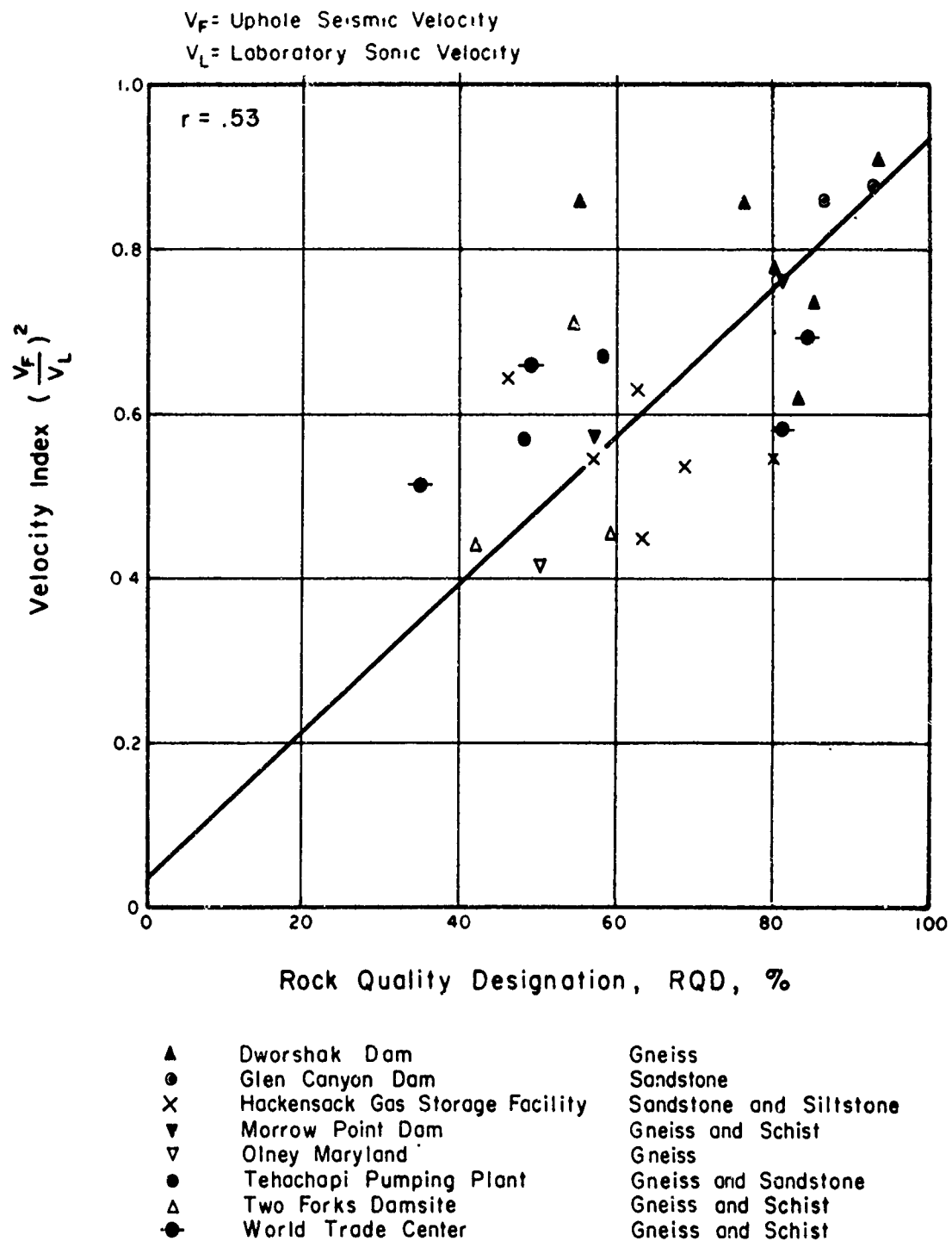


FIG. 6.6 RELATIONSHIP BETWEEN ROCK QUALITY DESIGNATION (RQD NO. 2) AND VELOCITY INDEX - UP-HOLE SEISMIC VELOCITY

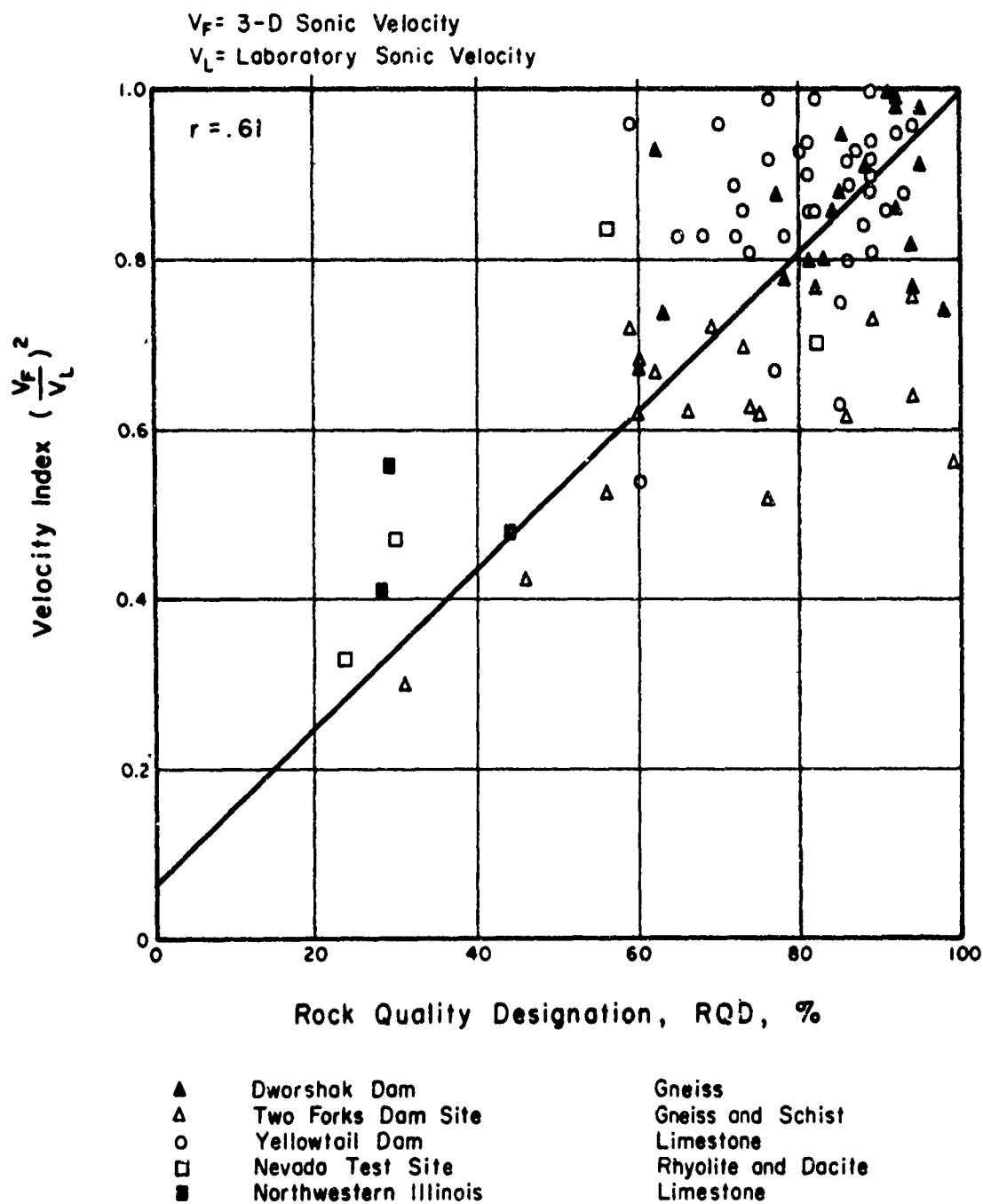


FIG. 6.7 RELATIONSHIP BETWEEN ROCK QUALITY DESIGNATION (RQD NO. 3) AND VELOCITY INDEX - 3-D SONIC VELOCITY

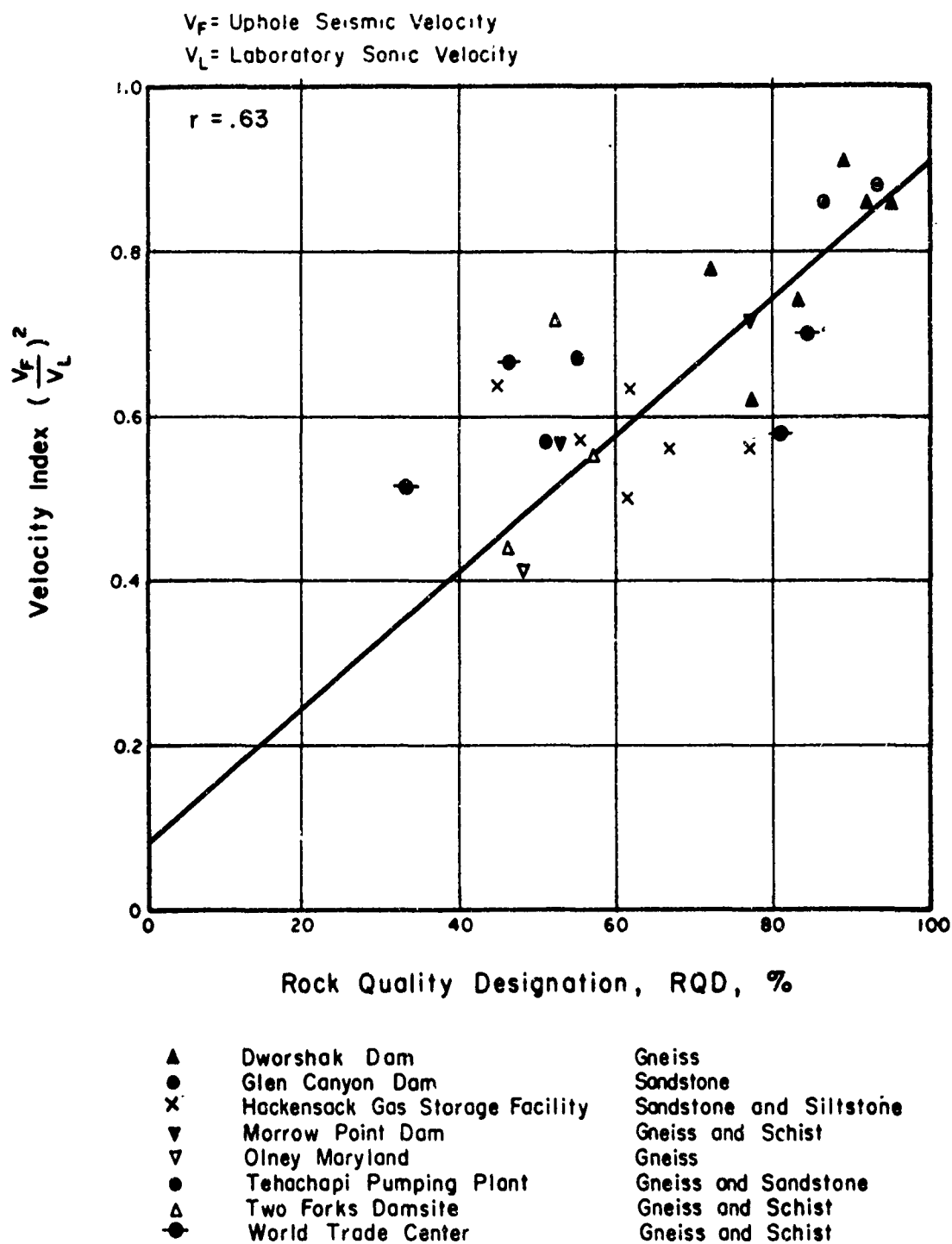


FIG. 6.8 RELATIONSHIP BETWEEN ROCK QUALITY DESIGNATION (RQD NO. 3) AND VELOCITY INDEX--UP-HOLE SEISMIC VELOCITY

in the low and extremely high ranges. The absence of RQD No. 3 values in these ranges is expected because a coring run would have to consist of fault gouge to have an RQD close to 0 percent and conversely, the RQD will seldom be 100 percent because core pieces greater than 1.0 ft are relatively uncommon.

All graphs show that the Velocity Index approaches 1.0 as the RQD approaches 100 percent. It is not anticipated that the Velocity Index would consistently exceed 1.0 because of the careful preparation of the laboratory samples in contrast to the rock conditions expected in boreholes. The samples are subjected to higher pressures in the laboratory than exist in the field and in addition, the higher frequencies and pulsing rate of the laboratory equipment as opposed to either the 3-D sonic or the seismic methods may also tend to produce higher velocities. A Velocity Index of approximately 0.2 at an RQD of 0 percent is in agreement with the anticipated behavior of faulted or extremely weathered rock. For a dense material such as granite, an intact velocity of 19,000 ft/sec can be assumed. Weathering or faulting may reduce the rock to a soft porous state or even to a clay gouge. In these instances saturated in-situ velocities of 8,000 to 10,000 ft/sec would be expected. The corresponding Velocity Index would be approximately 0.2 and the RQD of this material would be nearly 0 percent.

As was explained in Section Three, core pieces bounded by weathered joints, severely ground surfaces, and breaks that could not be perfectly matched were included in the measurements of rock quality. It is not possible to determine if all these surfaces represent in-situ discontinuities or are artificial breaks caused by drilling. If the latter were the case in a significant proportion of the borings, there would be a decrease in rock quality with no change in the Velocity Index. The RQD of a rock mass does not indicate the degree of openness of the joints or the presence of soft filling along these surfaces. These features can cause attenuation of seismic energy and can be responsible for low compressional velocities. It was anticipated, therefore, that numerous cases could occur where the Velocity Index would decrease rapidly while the RQD remained constant. This does happen to a limited extent in Figure 6.3 and could reflect either openness of joints or that the critical joint spacing is greater than 0.35 ft. It might also be suspected that water could couple the seismic energy across the joints with no signal loss. The Velocity Index would thereby remain nearly constant

whereas the RQD would decrease. The linear relationships of these graphs indicate that joint spacing seems to be the controlling factor of the RQD and Velocity Index.

The data plotted on Figures 6.9 through 6.11 represent the range of values of rock quality from the Tehachapi site. This information was not plotted on the other graphs because of their inconsistency. The up-hole seismic values, however, were consistent with the relationships established at the other sites. The slope of the best-fit line is nearly the same as in the other graphs, but it has been displaced upward along the Y-axis. If the relationships established for the other sites is representative of the behavior of rock, the Tehachapi data are anomalous. The distribution of the data points indicates that either the RQD values are too low or that the 3-D sonic velocities are too high. The low RQD might have been caused by core breakage during drilling. These holes were drilled with a wire-line core barrel which can provide high core recovery when operating correctly, but a mis-latch of the core barrel can produce severe core breakage. A number of zones of low core recovery are known to be the result of mis-latch, but this factor is probably less important than the character of the rock. The boring logs indicate that the rock is heavily jointed with weathered surfaces on most core pieces. It is believed that the core logging did indicate the degree of jointing in the rock mass and that the problem lies with the sonic logging apparatus.

The sonic velocities are consistently higher than less jointed rocks of similar composition from other sites. The anomalous velocities may be the result of a malfunction of the instrument or the assumptions made during the analysis of test data are not valid. The assumption that the tool was centered in the holes during logging may not be valid. If the deep holes are not vertical, the tool would have been resting against the rock during the tests and the energy would have traveled through a thinner fluid zone than expected. The assumed fluid travel time would be too large and the corrected travel time too small. This could cause an apparent high rock velocity.

A comparison was made between the seismic and sonic (3-D) velocities at 4 sites (Figure 6.12). These measurements were made over exactly the same portion of their respective borings and indicate that the seismic velocities are generally lower than their sonic counterparts. The information from the



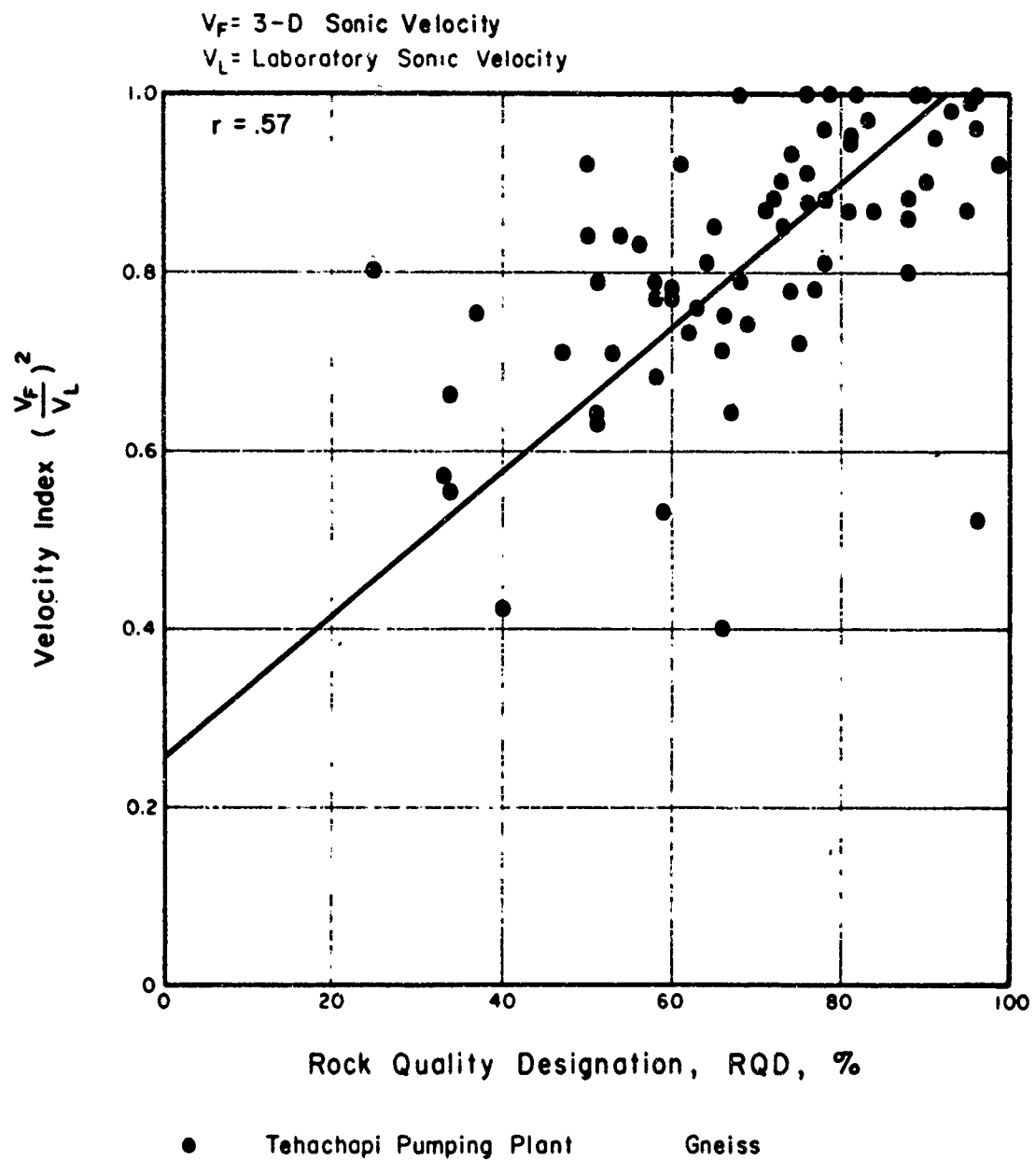


FIG. 6.9 RELATIONSHIP BETWEEN ROCK QUALITY DESIGNATION (RQD NO. 1) AND VELOCITY INDEX—TEHACHAPI

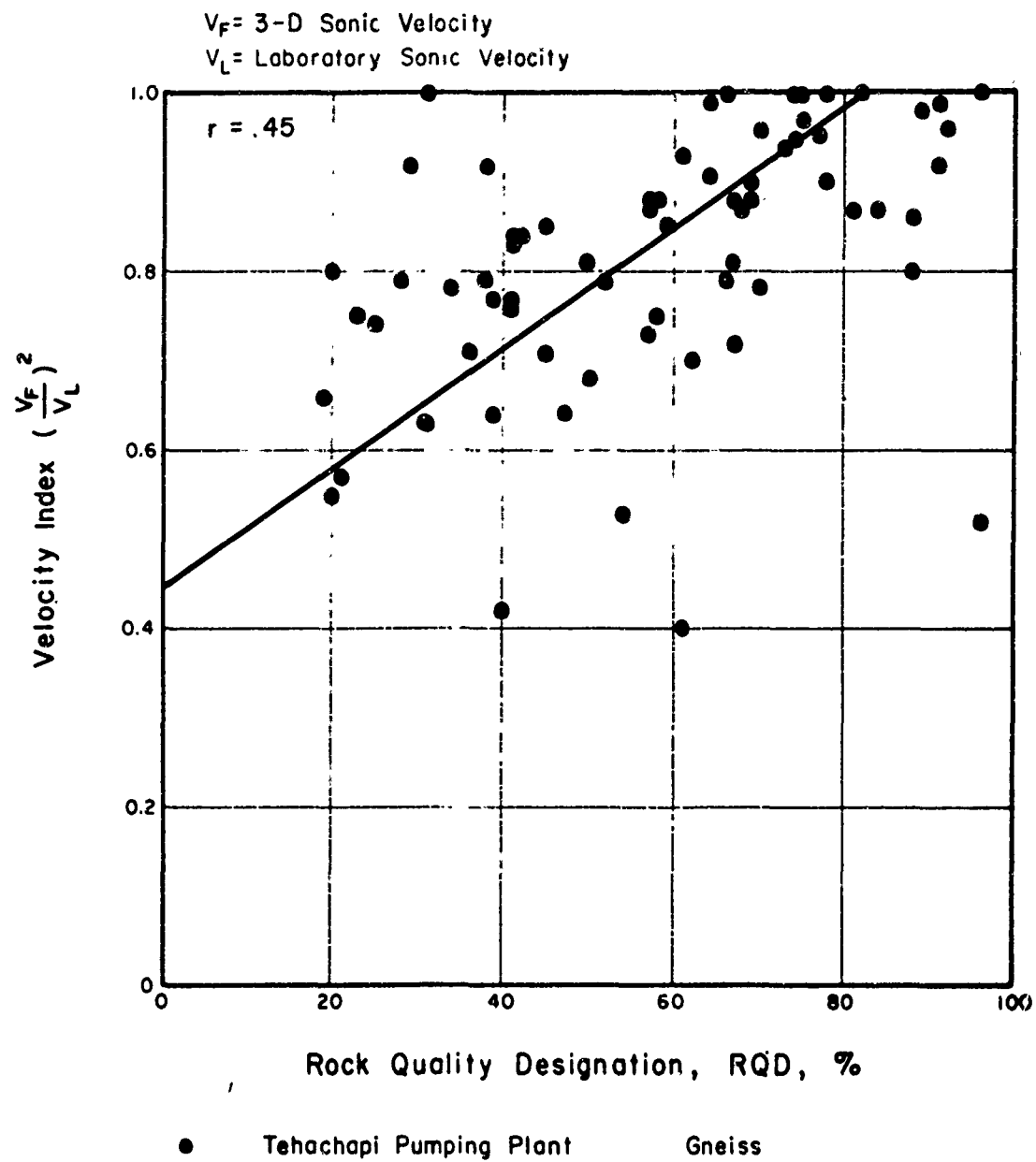


FIG. 6.10 RELATIONSHIP BETWEEN ROCK QUALITY DESIGNATION (RQD NO. 2) AND VELOCITY INDEX-TEHACHAPI

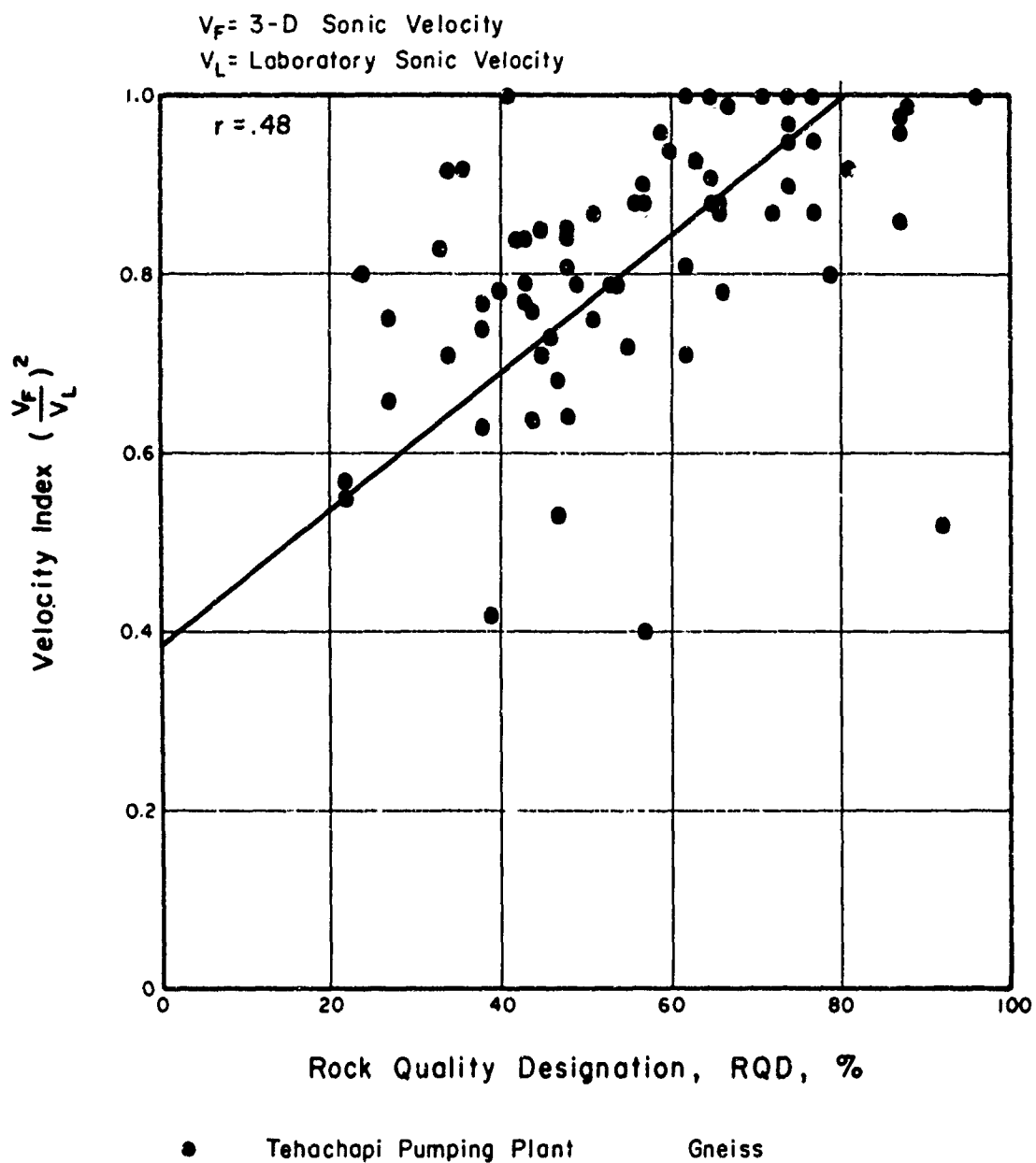


FIG. 6.11 RELATIONSHIP BETWEEN ROCK QUALITY DESIGNATION (RQD NO. 3) AND VELOCITY INDEX-TEHACHAPI

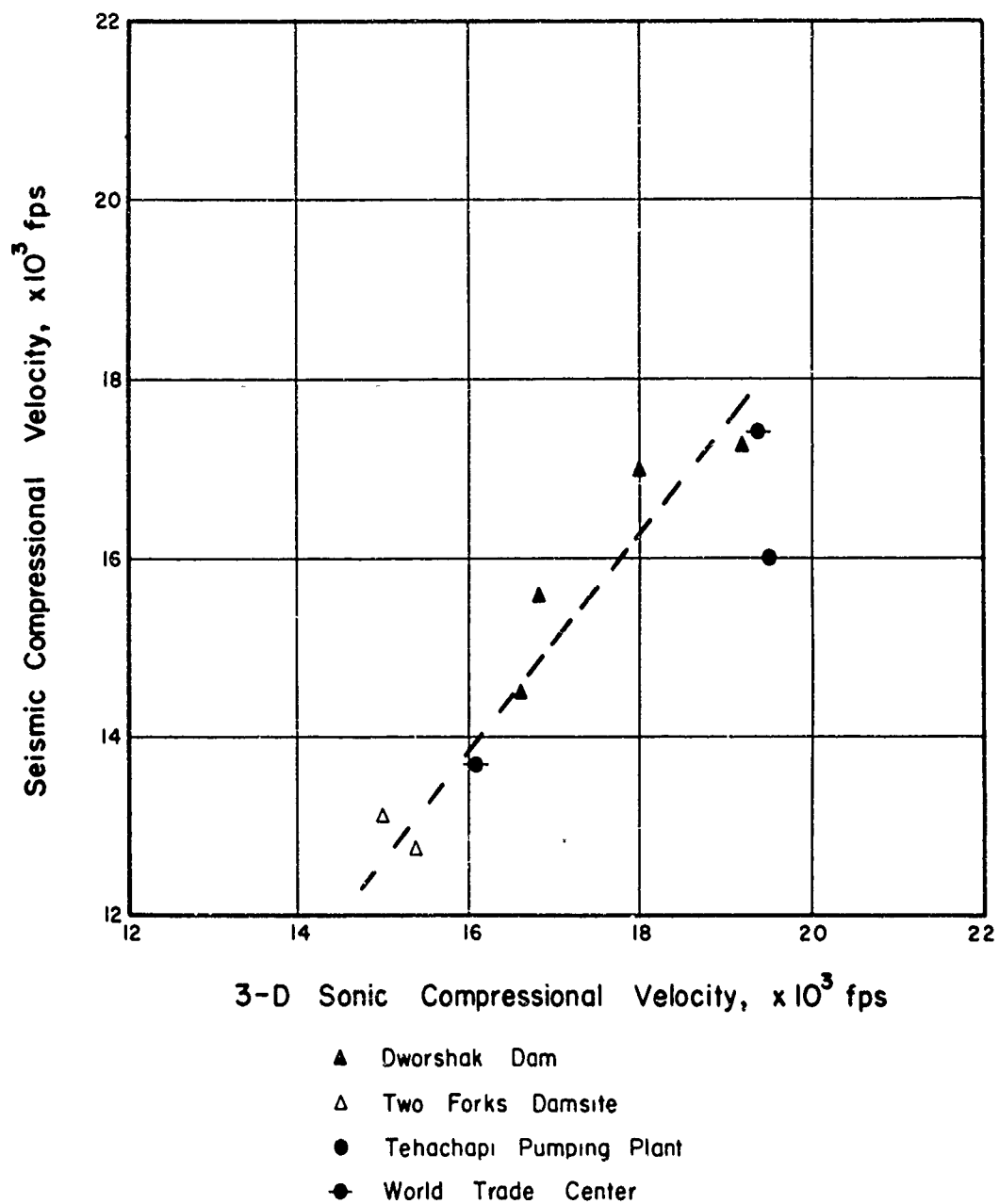


FIG. 6.12

RELATIONSHIP BETWEEN 3-D SONIC AND SEISMIC COMPRESSIONAL WAVE VELOCITIES

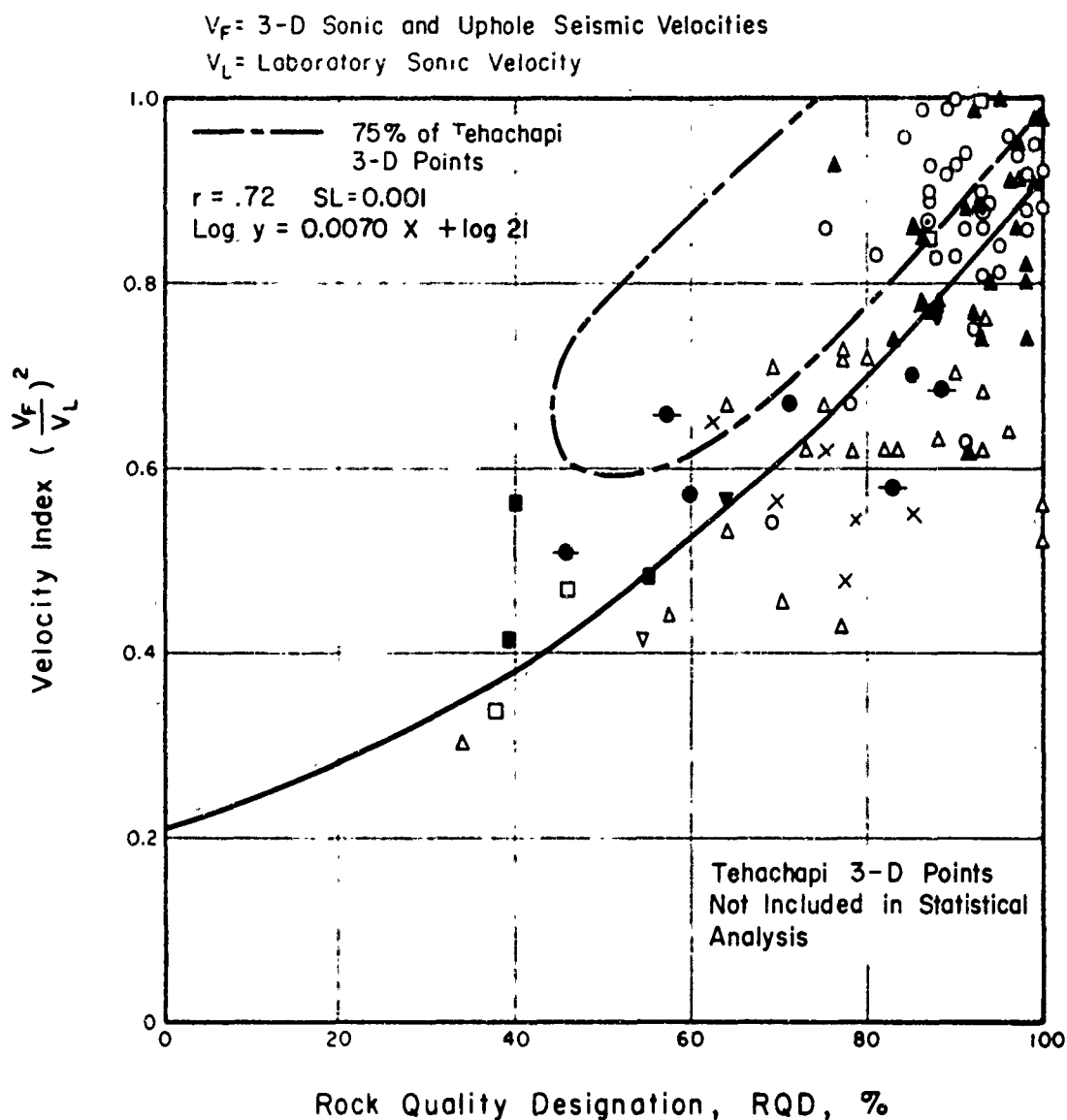
Tehachapi site falls away from the trend of the rest of the data indicating that the sonic velocities are higher than the seismic values would imply. The 3-D velocity could be as much as 13 percent higher than would be expected according to the other data. If all the 3-D data from the Tehachapi site are reduced by 13 percent and a new Velocity Index determined for each point and compared with the RQD, the results are in accord with the trends established from the other sites. The modified velocity values have not been used in the classification system because there is not enough information available to determine whether or not the 13 percent figure is valid.

#### 4. Engineering Classification

The Velocity Index values for uphole seismic and 3-D sonic are combined with each RQD in Figures 6.13 through 6.15. Although the test interval is much larger for the uphole tests, the points for both uphole seismic and 3-D sonic tests generally have the same trend. One exception is the 3-D sonic tests at Tehachapi. These values are anomalous to the trend established by the uphole seismic at Tehachapi and seismic and sonic at other sites. For this reason they are not plotted individually and are not included in the statistical analysis. The location of the Tehachapi sonic data is shown by a dashed 75 percent line. A reduced major axis correlation line and correlation coefficient are shown on each graph. A best-fit line has been drawn through the points, and considering the distribution of data, the graph can be conveniently subdivided into descriptive categories of rock quality. The selection of the boundary lines is an arbitrary matter. However, an attempt has been made to set these boundaries on the basis of a general impression of the rock conditions observed at each site. This could include the degree of jointing seen in rock slopes or excavations, the amount of weathering along joint surfaces, general tunneling conditions, and any other engineering or construction difficulties caused by geologic features.

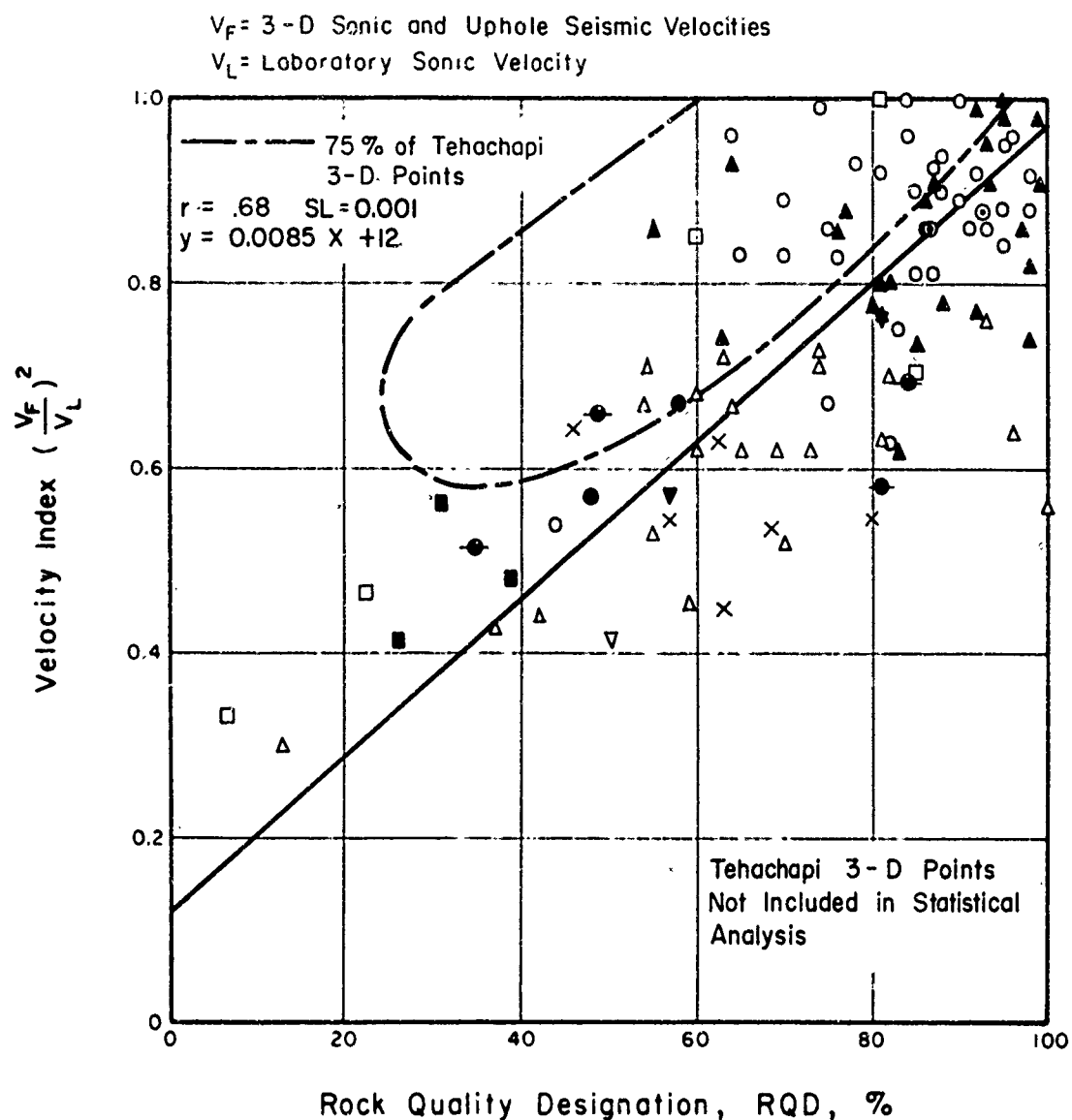
If the graphs are subdivided on the basis of RQD only (Table 6.1) a classification can be developed that is independent of the type of rock under consideration.

It is shown that the granite gneiss at the Dworshak Dam can be described as of Excellent Quality whereas the gneiss at the Tehachapi, World Trade Center, and Morrow Point projects can vary from Good to Poor Quality. This variation is strictly a function of the amount of jointing and weathering



- |     |                                 |                         |
|-----|---------------------------------|-------------------------|
| ▲   | Dworshak Dam                    | Gneiss                  |
| △   | Two Forks Dam Site              | Gneiss and Schist       |
| ○   | Yellowtail Dam                  | Limestone               |
| □   | Nevada Test Site                | Rhyolite and Dacite     |
| ■   | Northwestern Illinois           | Limestone               |
| ⊙   | Glen Canyon Dam                 | Sandstone               |
| X   | Hackensack Gas Storage Facility | Sandstone and Siltstone |
| ▽   | Morrow Point Dam                | Gneiss and Schist       |
| ∇   | Olney Maryland                  | Gneiss                  |
| ●   | Tehachapi Pumping Plant         | Gneiss and Sandstone    |
| —●— | World Trade Center              | Gneiss and Schist       |

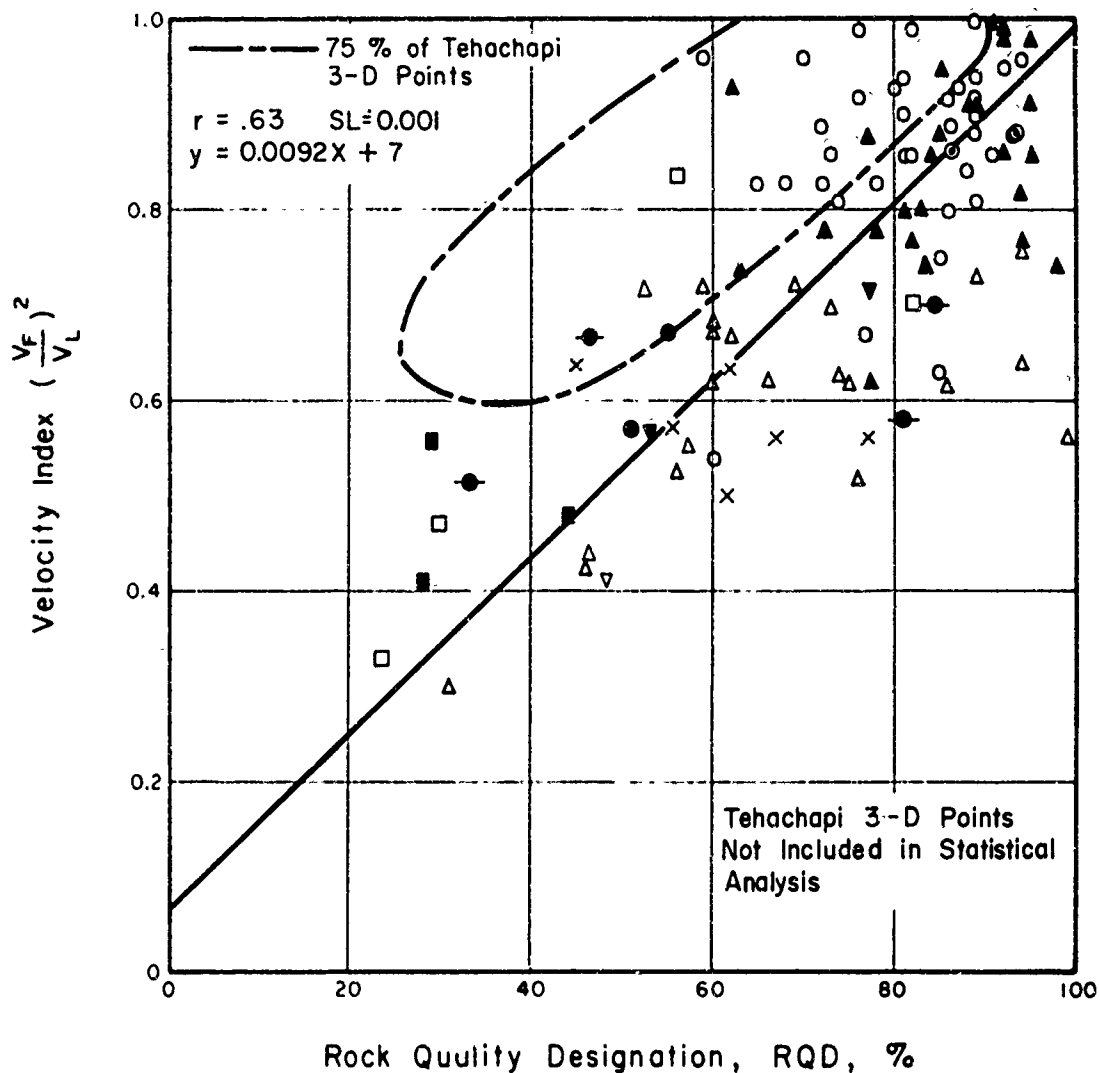
FIG. 6.13 RELATIONSHIP BETWEEN ROCK QUALITY DESIGNATION (RQD NO. 1) AND VELOCITY INDEX-COMBINED 3-D AND UP-HOLE DATA



- |   |                                 |                         |
|---|---------------------------------|-------------------------|
| ▲ | Dworshak Dam                    | Gneiss                  |
| △ | Two Forks Dam Site              | Gneiss and Schist       |
| ○ | Yellowtail Dam                  | Limestone               |
| □ | Nevada Test Site                | Rhyolite and Dacite     |
| ■ | Northwestern Illinois           | Limestone               |
| ⊙ | Glen Canyon Dam                 | Sandstone               |
| X | Hackensack Gas Storage Facility | Sandstone and Siltstone |
| ▼ | Morrow Point Dam                | Gneiss and Schist       |
| ▽ | Olney Maryland                  | Gneiss                  |
| ● | Tehachapi Pumping Plant         | Gneiss and Sandstone    |
| ◆ | World Trade Center              | Gneiss and Schist       |

FIG. 6.14 RELATIONSHIP BETWEEN ROCK QUALITY DESIGNATION (RQD NO. 2) AND VELOCITY INDEX—COMBINED 3-D AND UP-HOLE DATA

$V_F$  = 3-D Sonic and Uphole Seismic Velocities  
 $V_L$  = Laboratory Sonic Velocity



- |   |                                 |                         |
|---|---------------------------------|-------------------------|
| ▲ | Dworshak Dam                    | Gneiss                  |
| △ | Two Forks Dam Site              | Gneiss and Schist       |
| ○ | Yellowtail Dam                  | Limestone               |
| □ | Nevada Test Site                | Rhyolite and Dacite     |
| ■ | Northwestern Illinois           | Limestone               |
| ⊙ | Glen Canyon Dam                 | Sandstone               |
| X | Hackensack Gas Storage Facility | Sandstone and Siltstone |
| ▼ | Morrow Point Dam                | Gneiss and Schist       |
| ▽ | Olney Maryland                  | Gneiss                  |
| ● | Tehachapi Pumping Plant         | Gneiss and Sandstone    |
| ● | World Trade Center              | Gneiss and Schist       |

FIG. 6.15 RELATIONSHIP BETWEEN ROCK QUALITY DESIGNATION (RQD NO. 3) AND VELOCITY INDEX-COMBINED 3-D AND UP-HOLE DATA



which are two significant geologic features that must be considered in an engineering evaluation of in-situ rock. In a similar comparison, the massive limestone at Yellowtail Dam falls in the Good to Excellent categories whereas the limestone at the Northwestern Illinois site is generally of a Poor Quality. Intense weathering at the latter site is the primary reason for this variation. The frequency of jointing is responsible for the different engineering properties of the sandstone at Glen Canyon Dam as opposed to a similar rock type at the Hackensack site. The rock at the Two Forks site can be described as Fair to Good Quality based on the majority of points although some of the data fall into the Poor category. These latter values are representative of the RQD and Velocity Index in the fault zone shown on Figure 5.14 at a depth of 95 to 105 ft.

TABLE 6.1  
DESCRIPTION OF IN-SITU ROCK QUALITY

<u>RQD</u> (Percent)	<u>Description</u>
0-25	Very Poor
25-50	Poor
50-75	Fair
75-90	Good
90-100	Excellent

A consideration of Figures 6.13 through 6.15 indicates that RQD No. 1, No. 2, or No. 3 could be used interchangeably with the Velocity Index to predict in-situ rock quality. The tight distribution of points in Figure 6.13 (RQD No. 1) would indicate that this method is preferable over RQD No. 2 or RQD No. 3. However, the correlation between the variables is not linear at high values of RQD because the Velocity Index decreases faster than the RQD in this range. The graph of RQD No. 2 (Figure 6.14) has a more linear trend but there is considerably more scatter of the data points. The graph of RQD No. 3 might be a compromise between these two systems because of its linearity and slightly less scatter of the data than that shown for RQD No. 2. This method, however, is slightly more complicated than either of the other two systems

because of the additional calculations of squaring the lengths of the core pieces.

Considering these factors, it is recommended that RQD No. 1 (base length of 0.35 ft) be used as the method of describing rock core for engineering purposes. The data have the least amount of scatter of any of the other systems and do not require any weighting process for pieces of varying lengths. The relationship with the Velocity Index is such that either index can be used to describe the properties of a rock mass. RQD No. 1 is the technique described by Deere (1964). The non-linear nature of these points suggests that the RQD No. 1 and Velocity Index should not be subdivided using the same boundaries as shown on Table 6.1. If such a system were used, a rock mass with an RQD of 80 percent would be described as being of Good Quality whereas its anticipated Velocity Index (based on the graph) would indicate a Fair Quality rock. By changing the boundaries on the Velocity Index axis the two systems are compatible. This method is suggested as the basis for the classification system (Table 6.2).

TABLE 6.2  
ENGINEERING CLASSIFICATION FOR IN-SITU ROCK

RQD (Percent)	Velocity Index	Description
0-25	0-0.20	Very Poor
25-50	0.20-0.40	Poor
50-75	0.40-0.60	Fair
75-90	0.60-0.80	Good
90-100	0.80-1.0	Excellent

A system is presented whereby in-situ rock quality can be determined either by seismic measurements or core logging procedures. The variations in the nature of the rock at any site can be measured using either method and an estimate of the relative percentages of each category can be made for a general evaluation of the rock. Although no quantitative engineering information is implied by these descriptive categories, they can be used to determine the

relative amounts of rock of varying quality. This should be the logical result of any exploration program for engineering projects.

The ultimate decision of the applicability of this classification system to field conditions must be based on its correlation with in-situ properties such as deformation, tunnel stability, or other engineering parameters.

PART B  
CORRELATION OF ENGINEERING BEHAVIOR AND THE  
ENGINEERING CLASSIFICATION OF IN-SITU ROCK

SECTION 7  
ENGINEERING PROPERTIES OF IN-SITU ROCK

1. Introduction

The properties of the rock mass which are important in rock engineering are compressibility, permeability, and strength. The particular physical property of interest depends upon the nature of the problem. For instance, for the design of a cut-slope in rock or an underground opening the strength characteristics are of prime importance. On the other hand, in the design of the abutments of an arch dam all three of the aforementioned mass properties may be important.

Each of these mass properties is measured by in-situ tests. Compressibility is measured by various static tests or dynamic tests such as seismic surveys or sonic logging. Permeability is measured by the water pressure or pumping tests described in Section Three. Strength, which is commonly the shear strength along geological discontinuities, is measured by a static test. The results of these tests can be safely used in the design of engineering structures only if the rock tested is representative of the rock mass. For this reason, field tests are much larger than conventional laboratory tests and usually involve a substantial investment of time and money.

Unfortunately rock masses are rarely homogeneous. They are normally comprised of zones which can be characterized by the spacing and type of discontinuities, rock type, and degree of weathering. A complete engineering evaluation of a rock mass would require a large number of in-situ tests so that statistical average properties of each zone could be determined. This approach is economically impractical and the field tests are commonly performed only in critical areas. The engineering evaluation of a rock mass would be more complete if exploratory observations and tests could be used to estimate the engineering properties of the rock in areas outside the in-situ test sites. The possibility of using the proposed engineering classification for this purpose is examined in Part B of this report.

## 2. Deformation Characteristics of In-Situ Rock

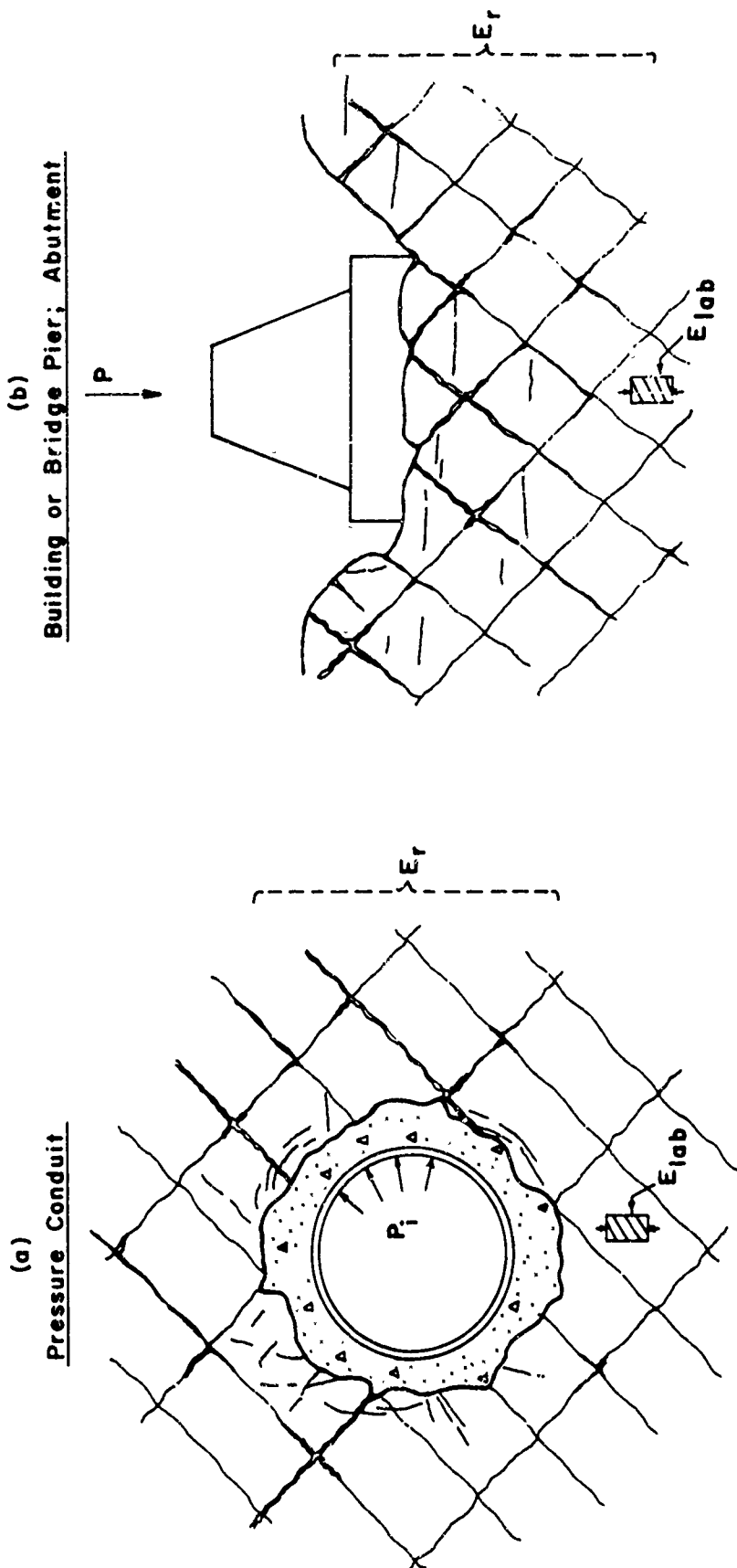
The deformation characteristics of a rock mass depend upon the nature of the intact rock and the characteristics of the geological discontinuities within the zone affected by the load. Because the deformability depends upon the average characteristics of the rock mass, the rock quality indices should be of value for predicting in-situ deformability.

Figure 7.1 illustrates two problems encountered in civil engineering practice where the deformability of rock, expressed as a deformation modulus, plays a major role in determining the design of the structure. The first is a lined pressure conduit such as an underground penstock. The liner plate may be designed by assuming no exterior support but a thinner plate can be used if the rock is assumed to resist a portion of the internal pressure. The second problem is the case of a building, bridge pier, or abutment founded on rock. The dimensions of the foundation are determined from an estimate of settlement, especially differential settlement, the structure can withstand. An accurate appraisal of the in-situ deformation modulus can result in a more economical foundation design.

The deformation characteristics of in-situ rock are determined by several types of static tests which are described and compared in Sections 8 to 12. Section 13 presents comparisons between static and dynamic tests performed at the same sites, while Section 14 presents correlations between these tests and rock quality measurements. A comparison of field test results and the deformability of foundation rock determined by deformations caused by engineering structures is presented in Section 15.

## 3. Permeability of In-Situ Rock

The data presented in Section 5 indicate a poor correlation between field permeability measurements and the rock quality of the tested interval. While the reasons for this poor correlation have not been investigated in detail, it is apparent that permeability depends upon the width and interconnection of fractures in the rock mass. As both of these factors are not measured with sufficient precision by rock quality indices, the possibility of extrapolating field permeability measurements by means of the proposed rock quality indices is not promising.



$E_r$  = Modulus of Rock Mass

$E_{lab}$  = Modulus of Intact Specimens

$E_r / E_{lab} = ?$

FIG. 7.1 TYPICAL CIVIL ENGINEERING PROBLEMS  
INVOLVING MODULUS OF DEFORMATION  
(After Deere et al., 1967) Reproduced  
with the permission of A.I.M.E.

#### 4. Shear Strength of In-Situ Rock

Field tests have shown that the shear strength along discontinuities depends to a large degree upon the geometry of the opposing joint-block surfaces and the characteristics of the filling material. Rock quality measurements are not sufficiently detailed if a failure can occur along a single persistent and adversely oriented geological discontinuity. When the rock movement involves a large number of discontinuities such as the raveling of a rock slope or the walls of an underground opening, rock quality measurements may provide a means of estimating the probability and magnitude of a potential failure.

Sections 16 and 17 examine two construction problems which are related to the shear strength of a rock mass. The relationship between the rate of construction of a tunnel and rock quality measurements are examined in Section 16. In Section 17 the support requirements of underground openings are compared with rock quality measurements.

## SECTION 8

### PLATE JACK TEST

#### 1. Introduction

The in-situ deformation modulus was first measured statically by the plate jack method. The earliest static test referred to in the literature reviewed was made in 1935 by the Irrigation Department of Algeria (Mayer, 1963). The first tests in this country were jack tests performed by the USBR at Davis Dam in 1948 (U. S. Bureau of Reclamation, 1948 and 1951).

Before that time, it was common design practice to assume that the modulus of the rock mass was twice that of concrete. This assumption was based on the observation that the laboratory modulus of elasticity measured on intact core samples is commonly higher than the laboratory modulus of concrete. The experience gained from hundreds of plate jack tests in nearly all rock types shows that this assumption was not conservative. The tests indicate that the in-situ modulus of rock is generally from one-half to one-tenth of the intact rock modulus and the majority of jack test moduli are less than the modulus of concrete. The low in-situ deformation modulus is primarily caused by movements along discontinuities in the rock mass. The following pages contain descriptions of various aspects of plate jack tests including site preparation, test setup, and conduct and analysis of the test.

#### 2. Site Preparation

The first concern in choosing a jack test site is to obtain a location where, depending on the purpose of the test, the rock represents the average or the extreme of rock quality encountered at this site. Because evaluation of rock quality is based on geologic information of a qualitative nature, subjective judgment has a large influence on the site chosen.

Rocha (1955), states that the site should be free of open joints as such joints which would be filled by grouting operations. This suggestion may seem unconservative until one examines the deformations measured in plate jack tests. Typically, the maximum deformations are only a small fraction of an inch. One open joint can easily double this deformation and halve the calculated deformation modulus.



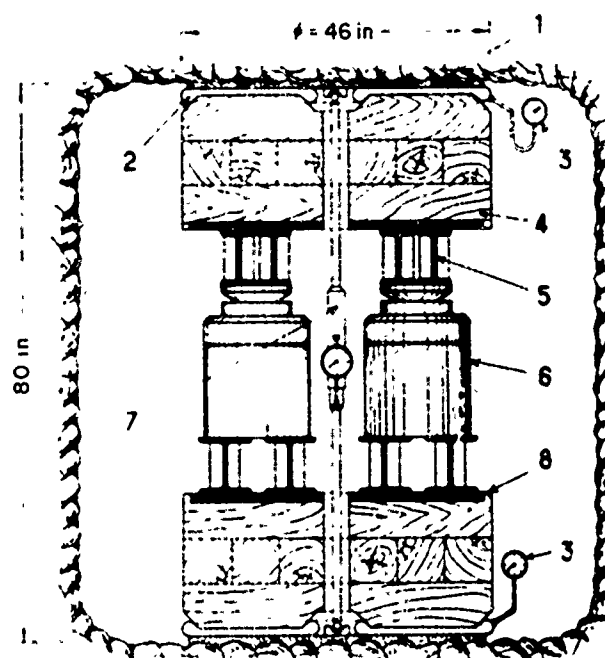
If an open joint can halve the plate jack modulus, what influence would it have upon structural deformations? Waldorf et al. (1963) examine this problem and show that individual joints under a major structure probably do not affect the structure, but the foundation deformations under the structure are a response to the deformation characteristics of the joints collectively. Thus, a test dominated by one adverse joint does not represent the average deformation characteristics of the rock mass.

Additional site requirements are imposed by the limitations of methods used to analyze the test results. The elastic equations used to calculate moduli from deformation measurements assume that the loaded area is an infinite half-space. This assumption is not completely valid if the loaded surface is of limited extent. Rocha (1955) suggests that test sites in adits be at least five tunnel diameters from the entrance, to obtain essentially an infinite surface in one direction. The diameter of the tunnel should also be at least several times the diameter of the jack plate but this ideal situation is often not attained due to the expense of driving large diameter tunnels.

Seismic investigations and borehole photography almost invariably show that the rock surrounding an underground opening is cracked for a distance up to ten feet or more behind the rock face. This cracking is caused by stress redistribution in the rock mass due to the presence of the opening, and of blast-induced fracturing. It will be shown later that the rock immediately behind a jack plate dominates the deformations measured in the tests and it is advantageous to minimize the influence of the cracked rock. Although the formation of the "distressed zone" can be only partially controlled, the blast-induced fracturing can be controlled. For this reason, it is common practice to use special techniques in excavating the test area. The test adit is usually driven through the test area by blasting with light charges. The adit is then enlarged to the size required by the test equipment using hand or pneumatic tools. At Morrow Point Dam, the test surfaces were excavated 18 to 24 inches behind the adit wall to avoid the zone of blast-induced fractures. This was accomplished by drilling holes on 3 in. centers and removing the remaining rock with a pavement breaker and chipping hammer (Dodd, 1967).

### 3. Test Setup

Figures 8.1 to 8.3 illustrate three types of plate jack equipment. The setup in Figure 8.1 has been used for a number of years by LNEC (Laboratorio



- (1) Mortar
- (2) Oil Filled Metallic Cushions
- (3) Pressure Gauges
- (4) Timber Packing
- (5) H- Section Irons
- (6) Hydraulic Jack
- (7) Extensometer For Measuring Changes  
In Distance
- (8) Iron Plate

FIG. 8.1 L.N.E.C. PLATE JACK TEST ( After Rocha, 1955 )

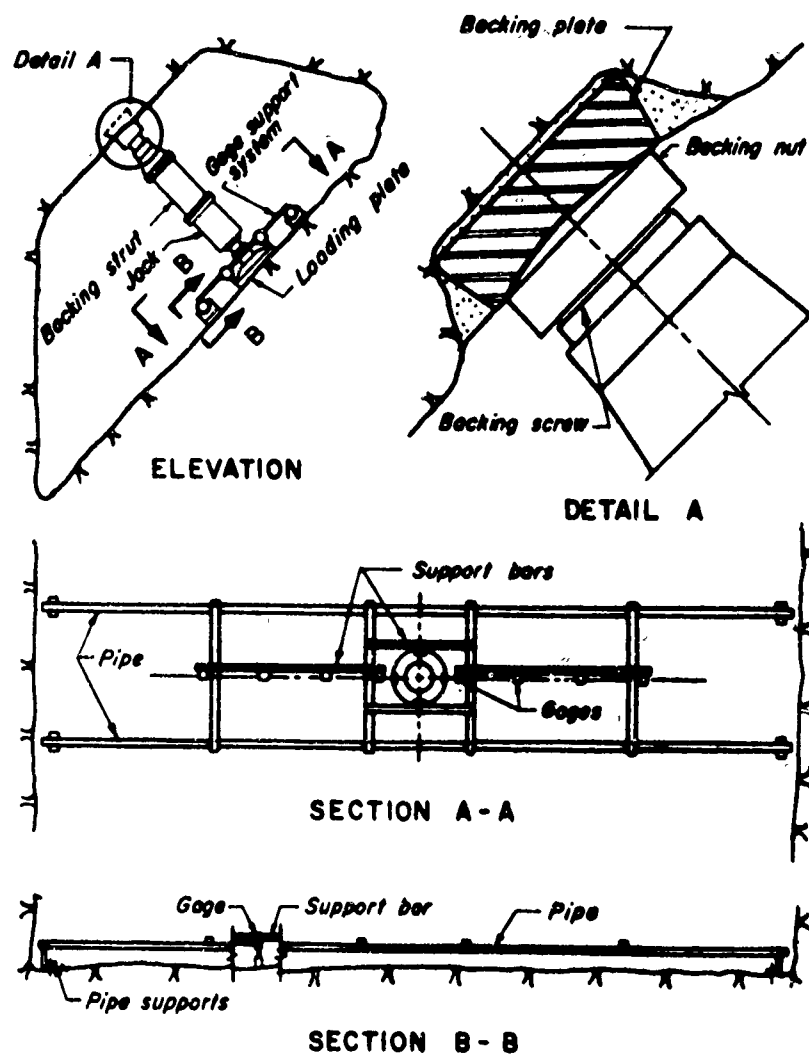


FIG. 8.2 KARADJ DAM PLATE JACK TEST  
(After Waldorf et. al., 1963)  
Reproduced with the permission  
of A.S.C.E.

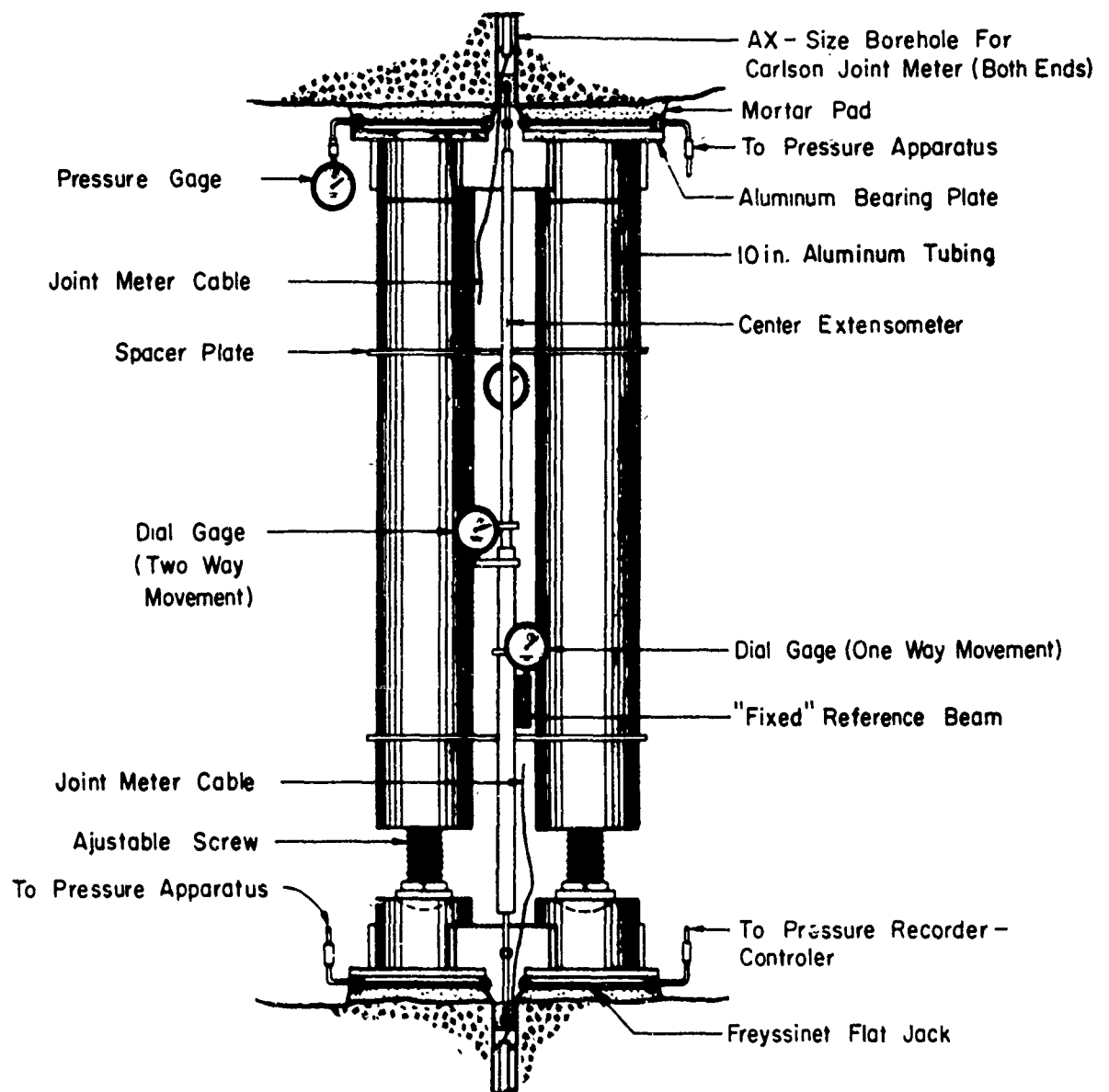


FIG. 8.3 DWORSHAK DAM PLATE JACK TEST ( After Shannon and Wilson , 1964 )

Nacional de Engenharia Civil, Lisbon, Portugal) for tests in foundation galleries of arch dam sites (Rocha, 1955). The equipment shown in Figure 8.2 was used at Karadj Dam, Iran (Waldorf et al., 1963), and that shown in Figure 8.3 was used at Dworshak Dam, U.S.A. (Shannon and Wilson, 1964).

Although the setups differ in detail, they have four essential parts: (a) a concrete pad to provide a smooth test surface, (b) jack plates, (c) hydraulic jacks, and (d) a reaction system. The jack plate in Figure 8.1 is an oil-filled metallic cushion or Freyssinet flat jack while the jack plate in Figure 8.2 is a rigid metal plate. The setup used at Dworshak Dam employs a Freyssinet flat jack as both a jack plate and a hydraulic jack. The reaction systems are quite different in the three setups: with timber in the LNEC setup, a metal strut in the tests at Karadj Dam, and the aluminum tubes at Dworshak Dam. In addition, each setup includes one or more dial gages for measuring rock deformation.

Figure 8.4 shows a jack test setup which uses a flat jack cemented in a slot formed by closely spaced drill holes in the floor of a test adit (Kujundzic, 1966). Although site preparation is more complicated, the equipment used in the test is simple and fairly portable. Deformations associated with the test are measured by noting the amount of air required to maintain the pressure in the flat jack. Rocha (1966) has suggested a modification of this technique which should provide faster and less expensive testing. He uses a rock saw to cut the slot and a thin, close-fitting, semi-circular flat jack which does not require cement to obtain close contact with the rock.

The choice of the jack plate is very important for it determines the validity of the moduli and the method of analysis. The first consideration is the size of the plate. Tests reported in the literature have been conducted using plates from 8 to 36 in. in diameter. Serafim (1968) reports that L.N.E.C. has performed some tests with 63 in. diameter plates. The plate should be of such size that it loads a significant volume of rock. The literature contains very few concrete suggestions on the size of the plate, but it appears desirable to use a plate diameter several times the average joint spacing. In highly fractured rock, a plate of small to medium size can be used to obtain representative deformations. In rock with rather wide joint spacing even large diameter plates cannot load a representative volume of rock.

Grimm et al. (1966) illustrated this problem with a report of jack tests on schist and iron ore. The jack plate size in each case was the same,

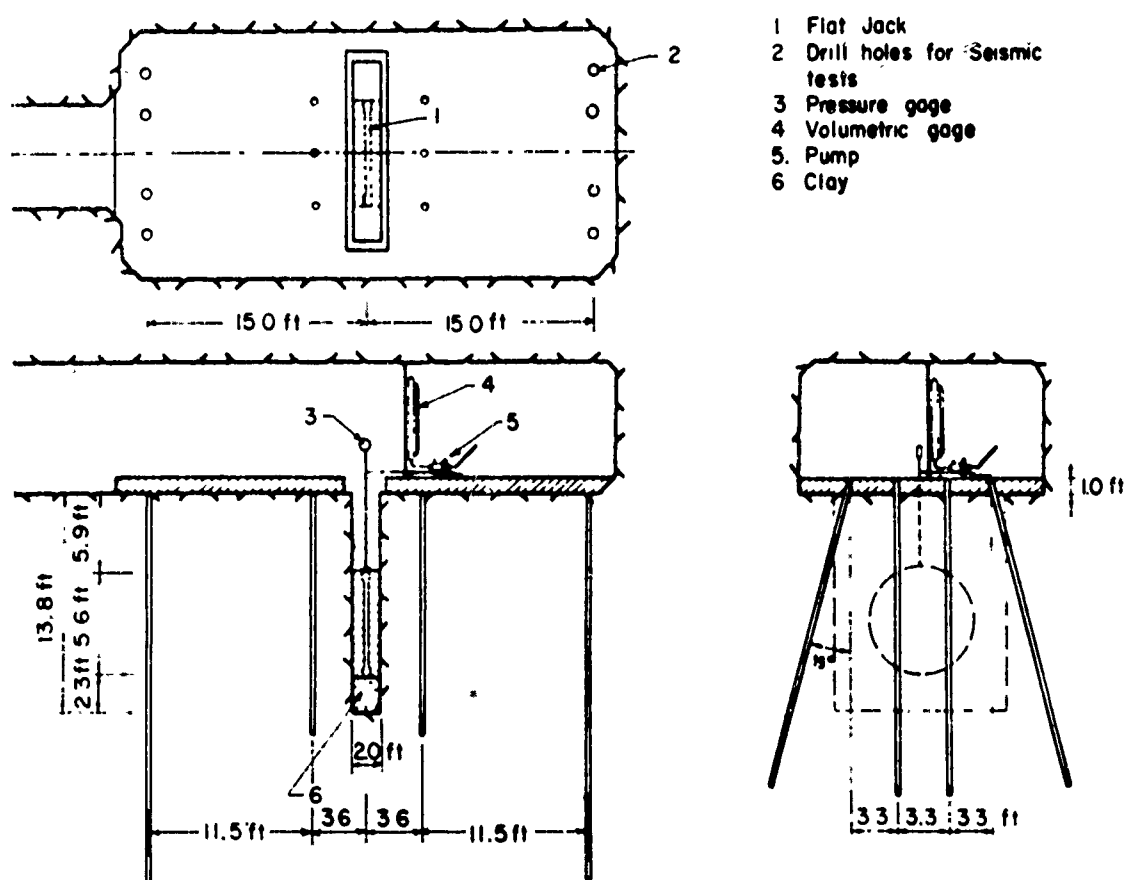


FIG 8.4 FLAT JACK TEST (After Kujundzic, 1966 )

but the average joint spacing in the iron ore was about equal to the diameter of the plate while it was a small fraction of the plate diameter in the schist. The jack modulus of the iron ore was about equal to the laboratory value while the field modulus of the schist was one-thirtieth of the laboratory value. The authors state that the latter value was valid but the former was high largely because of the scale of the test.

The rigidity of the jacking plate compared with that of the rock tested is important as it determines whether the results can be analyzed by rigid or flexible plate elastic solutions. The rigid plate analysis is appropriate for small diameter cast iron plates. The advantage of small rigid-plate jacks is that relatively high loads can be placed on the rock by means of a single hydraulic jack. Gicot (1948), and Talobre (1961) have used 8 to 10-in. rigid plates with small hydraulic jacks to obtain a relatively portable plate jack apparatus.

The use of small diameter rigid jack plates can be criticized from two points. The first is that the small plate may not give representative values because it does not load a significant volume of rock, i.e. at least several joint blocks. The second shortcoming is that the rigid plate exerts a high but unknown pressure on the rock. Elastic studies show that the stress distribution under a rigid plate loading an ideal elastic material produces high peripheral stresses and low stresses under the center of the plate. The fact that rock will not behave as an ideal elastic material makes it impossible to predict the stress distribution under the plate.

When the diameter of the jack plate is increased to test a more significant volume of rock, the rigid plate assumption is less valid. The stress distribution beneath the plate is the function of the modulus of the loaded media as well as the modulus, thickness, and radius of the plate. The problem of evaluating the semi-rigid case has been eliminated by Rocha (1955), and Dodd (1967) by placing a rubber pad or an oil-filled metallic cushion between the jack shoe and the mortar pad to obtain a uniform stress distribution. Shannon and Wilson eliminated the hydraulic jack completely and used a Freyssinet flat jack to load the rock directly. These jack plates exert a relatively uniform load on the rock, and therefore are analyzed by solutions for flexible plate loading on an elastic media.

The load applied to the jacking pad is obtained by using one to four hydraulic jacks, each having a capacity of 50 to 300 tons or a Freyssinet jack.

The number and size of the jacks depend on the size of the loading area and the magnitude of loads required. The most distinguishing feature of the hydraulic systems of various setups is the method of controlling the load on the rock. As the rock deforms the jack must be extended to maintain a constant load. This can be done manually, but for long-term tests which investigate the creep characteristics of the rock, an automatic pressure control system is required. The Shannon and Wilson setup employed a pressure regulator connected with a gear type hydraulic pump to maintain the pressure in the Freyssinet jack. The Bureau of Reclamation jack apparatus used at Morrow Point (Dodd, 1967) had two fluid systems. The first, called the active system, included the hydraulic jacks and an air operated hydraulic pump. The second, the reactive, consisted of a Freyssinet jack under the loading shoe and hydraulic lines connecting it to the air system. The ratio of the air pressure to oil pressure was set at 1:150 so that the hydraulic jacks exerted the desired load on the Freyssinet jack and, in turn, on the rock. When rock deformation caused a reduction in the oil pressure in the Freyssinet system, the pressure ratio was upset and the pump automatically turned on and restored the balance.

The required jack reaction can be obtained in several ways. In the case of jack tests conducted in test pits, the restraint can be developed against beams anchored in the rock or by jacking against a structure, such as a wooden crib filled with rock, which is heavy enough to resist the jack. Several systems used in underground tests are shown in Figures 8.1 to 8.3.

#### 4. Deformation Measurements

Figure 8.3 illustrates a gage designed to measure changes in the diameter of the tunnel. It consists of two telescoping metal tubes each grouted in the rock behind the center of a jack plate. Commonly, this diametral rod is made of invar, an alloy with a very low coefficient of thermal expansion. By avoiding large artificial lights in the test area during tests, the temperature changes can be limited to 1 to 3° C. Temperature corrections are, therefore, generally unnecessary. The movement of each plate is measured in this case by using one dial gage on the diametral rods to measure total deformations and a second attached to a fixed reference beam to measure movements of one rod.

Deformation measurements can also be made using dial gages to monitor movements of the jacking plate or the rock near the plate. In each case, the gages must be attached to a fixed reference point which is commonly a metal beam



parallel to the axis of the test adit. If the reference beam is anchored three to five plate diameters on either side of the test setup, it is assumed that it is outside the zone of influence of the test. Normally, three or four gages spaced at equal intervals around the periphery of the plate are used to measure jack plate movement. Movements of the rock surface are obtained by measuring vertical movements of pins grouted into the rock with dial gages attached to the reference beam.

Deformation measurements can also be made within the rock mass either in boreholes behind the jack plate or outside the jack plate area. Measurements of this type are reported by Shannon and Wilson (1964), the Multipurpose Dam Rock Testing Group of Japan (1964), and by Judd (1965). The Japanese tests used a Carlson strain meter with a gage length of 4 in. The Shannon and Wilson measurements were obtained by using a Carlson joint meter installation. The upper end of the gage was placed within 2 ft of the surface while the lower end of the gage was fixed at a depth of 18 ft. The jointmeter, because of its longer gage length, measures the average deformation of a large mass of rock. The strain meter will give quite different measurements depending on whether it is located in a joint block or spanning a joint. These measurements, which exclude at least a portion of the influence of the distressed zone, yield moduli which are more suitable to the design of arch dams.

##### 5. Testing Procedure

The pressure in the jack system is raised to the maximum testing load in three to four increments. In the Dworshak tests where the maximum load was 1,000 psi, the increments were 250, 500, 750, and 1,000 psi. Initially, the load was raised to 250 psi and maintained there until creep deformations had ceased. This generally required about 24 hours. Then the load was removed and the no-load conditions were maintained until creep had ceased. The cycles to 500, 750, and 1,000 psi followed the same form. The entire test required about 1 week.

Examples of load-deformation curves are shown in Figures 8.5 and 8.6. Deformations measured during loading and unloading are clearly indicated, as well as deformations under constant load. The modulus rosette-diagram is very helpful for checking various moduli. The load-deformation curve shown in Figure 8.5 has an overall concave downward form. This indicates that shearing displacements along the geological discontinuities beneath the plate are

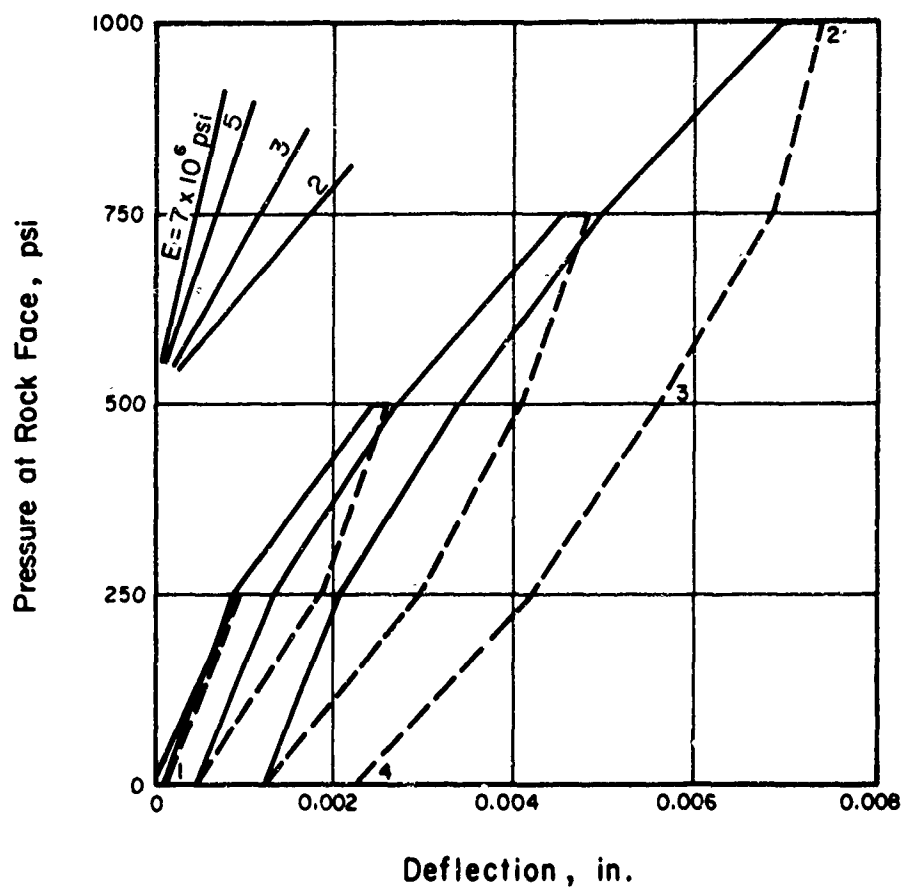


FIG. 8.5 CONCAVE DOWNWARD LOAD-DEFORMATION CURVE FROM PLATE JACK TEST (After Shannon and Wilson, 1964 )

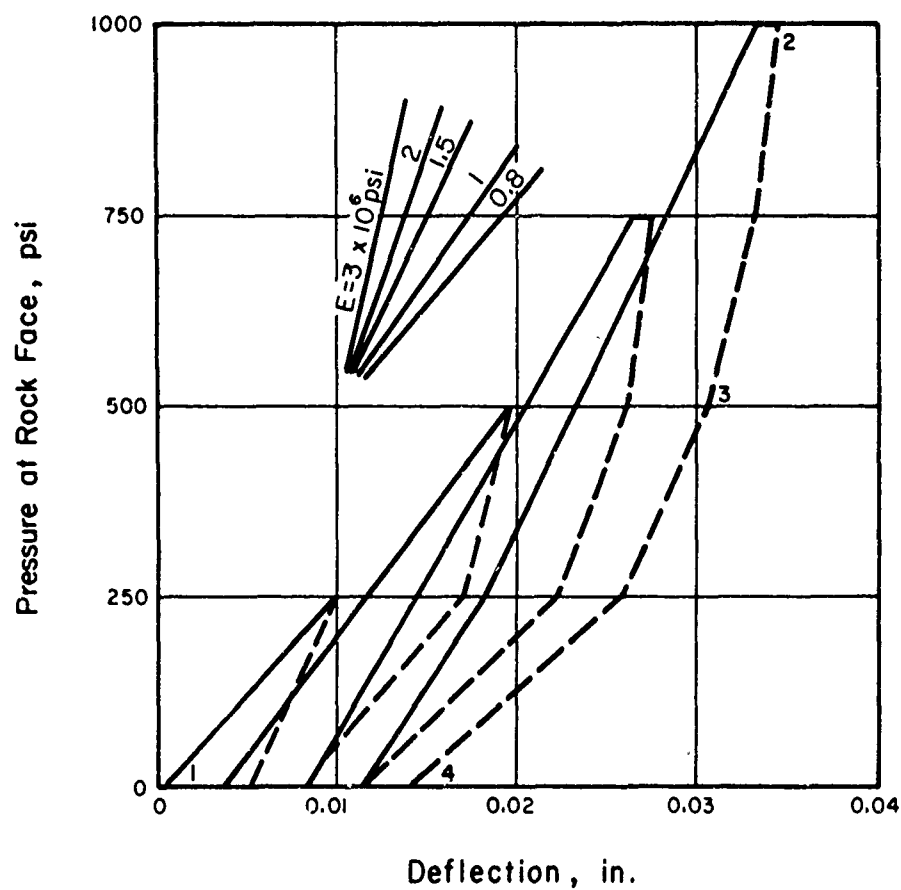


FIG. 8.6 CONCAVE UPWARD LOAD-DEFORMATION CURVE FROM A PLATE JACK TEST (After Shannon and Wilson, 1964)

increasing with pressure. Figure 8.6, on the other hand, has a form which is generally concave upward. In this case, the joints have closed at relatively low pressures and the moduli of the later cycles of the test are approaching that of the intact rock.

In both types of load-deformation curves it is not uncommon to observe rather peculiar movements during the first interval of loading. Exceptionally large deformation, abrupt changes in the rate of deformation, and even expansions are sometimes noted. This behavior is evidently the result of joint closure and joint block rotation which are local details and not representative of the average deformation characteristics of the rock mass.

The form of the unloading curve depends upon the surface forces tending to keep the joints closed. The magnitude of these forces depends upon the geometry of the joints, i.e., the amount of interlocking which prevents expansion, and the action of absorbed water on the two surfaces. Most commonly, the unloading curve is very steep during the removal of the first half of the load and then essentially parallels the loading curve to zero pressures.

Lane (1966) discusses the types of deformation observed in load-deformation curves. The first type is elastic movement which is an immediate response to changes in loading. In this, he groups the deformations noted during application and removal of load. The second type, or the plastic deformations, occur during periods of constant load. The third type of deformation is what he calls recoverable plastic. This type of movement occurs during unloading and at zero pressures at the completion of the test.

## 6. Interpretation of Test Results

Once the load-deformation curve has been defined, the engineer is faced with the problem of obtaining a design modulus from the test data. The test modulus is directly proportional to a slope on the load-deformation graph. However, the load-deformation graph can be interpreted in several ways. The engineer may use the total deformation and maximum load,  $E_{1-2}$ , the slope of the upper half of the unloading curve,  $E_{2-3}$ , or the slope of the entire unloading curve,  $E_{2-4}$  (see Fig. 8.6). While these moduli do not represent all possible interpretations they represent those commonly used.

$E_{1-2}$  is generally the lowest, and therefore, the most conservative value to use. It includes deformation during loading and constant load. Depending upon the general shape of the load-deformation curve, this modulus

increases or decreases with increasing stress levels, but is normally lower than  $E_{2-3}$  and  $E_{2-4}$ . This modulus will be referred to as the modulus of deformation,  $E_d$ .

The two moduli measured from unloading curves can be taken at any cycle of the test but as the loops are quite similar they are commonly measured on one of the cycles to maximum load.  $E_{2-3}$  is the highest, and it has been noted that it often corresponds to the modulus calculated from seismic tests.  $E_{2-4}$  is lower, with a range between the seismic modulus and the modulus of deformation. Of the two rebound moduli  $E_{2-4}$  seems the most useful as it is less affected by the characteristics of the joint surfaces during unloading. Herein, it will be referred to as the field static modulus of elasticity,  $E_e$ .

Moduli are calculated from the load-deformation curve using the assumption that the rock acts as a semi-infinite elastic medium. The assumption that a rock mass can be treated as an elastic medium can be justified only by the observation that within the range of loads imposed by conventional plate jack tests, the load-deformation relationship is approximately linear. The semi-infinite boundary condition is satisfied if the rock surface, which is loaded by the test, is considerably larger than the loading pad. Waldorf et al. (1963) suggests that the minimum dimension of the surface should be at least five plate diameters. Most of the diagrams of jack setups indicate that this requirement is not fulfilled. The expense of enlarging a test adit opening to obtain the five diameter requirement is probably prohibitive especially if a large number of tests are to be run. Shannon and Wilson (1964) partially compensated for the fact that the test adits at Dworshak were approximately two plate diameters wide and two and one-half diameters high by placing line drilled holes along the edge of the floor and crown of the tunnel to minimize the effect of the adjacent rock surface. Serafim et al. (1966) has suggested that the restraint caused by adjacent surfaces could be excluded by applying a reduction factor of 0.75 to the moduli calculated from load-deformation curves.

The rigid plate tests are interpreted by the Boussinesq rigid punch solution:

$$E_r = \frac{P}{2} \frac{(1 - \nu^2)}{\delta a} \quad (8.1)$$

where  $E_r$  is the deformation modulus of the rock,  $P$  is the total force applied,  $\nu$  is the Poisson's ratio of the rock,  $\delta$  is the measured displacement, and  $a$  is the radius of the rigid punch.

The elastic solution for displacement at the center of the circular and flexible Freyssinet jack is:

$$E_r = \frac{2q}{\delta} (1 - \nu^2) (a_z - a_1) \quad (8.2)$$

where  $q$  is the unit load,  $a_z$  is the area of the jack, and  $a_1$  is the area of the central hole. This formula is used to analyze the diametral measurements. The general solution for the Freyssinet jack which can be applied to deep readings is:

$$E_r = \frac{q}{\delta_z} [(1 + \nu)(z^2)] \left[ \frac{1}{(a_2^2 + z^2)^{1/2}} - \frac{1}{(a_1^2 + z^2)^{1/2}} \right] + [2(1 - \nu^2)] [(a_2^2 + z^2)^{1/2} - (a_1^2 + z^2)^{1/2}] \quad (8.3)$$

where  $\delta_z$  is the measured displacement at any depth  $z$ .

The formulas above require a Poisson's ratio which must be measured by another test or estimated. Rice (1964) suggests that Poisson's ratio can be estimated from laboratory and seismic tests. Sonic and seismic tests indicate that the Poisson's ratio for in-situ rock is commonly in the range of 0.1 to 0.3 (see Section 14) with 0.25 a reasonable average value. The effect of Poisson's ratio, however, is relatively small as it is squared in both the rigid and flexible plate equations.

Deformations measured across the diameter of the opening or from the jack plate are dependent to a large degree upon the deformability of the distressed zone. If the jack test moduli are to be used in the design of a tunnel lining, the influence of the distressed zone must be included. When the jack test moduli are to be used in the design of structural foundations, the influence of the distressed zone can yield a modulus which is too conservative. Because of the relative size of the pressure bulbs created by the in-situ test and the structure, the effect of a few feet of distressed rock is much more pronounced on the in-situ test. A more realistic in-situ modulus can be obtained for foundation studies if the influence of the distressed zone is minimized.

Theoretical elastic analysis indicates that the deformations measured outside the loaded area are less sensitive to the surface layers and they provide a better indication of the deformation characteristics of the deeper rock. However, deformations outside the loaded area are often so small that

they approach the limits of accuracy of the dial gages. Another method of determining the deformability of the deeper layers is to use gages such as the Carlson jointmeter installed in a drillhole behind the loaded area. The influence of the distressed zone is diminished by increasing the depth of embedment of the top of the gage. However, the depth of embedment is limited by the fact that the stress created by the surface load decreases with depth. The Dworshak Dam tests (Shannon and Wilson, 1964), indicate that a gage with an embedment of only 1 to 2 ft can provide deformation values approaching those of the undisturbed rock. The moduli calculated from buried gage measurements were commonly 100 percent higher than the moduli obtained from surface gages. Therefore, it appears that the influence of the distressed zone can be minimized most efficiently by using buried gages.

The literature provides few comparisons of rigid and flexible plate jack test results. Serafim et al. (1966) feel that there should be little comparison between the two methods but that the rigid plate values would be higher. The only direct comparison was made by the Japanese Multipurpose Dam Rock Testing Group (1964) where a rigid jack and a flexible jack test were performed in adjacent sections of a concrete gallery at Yuda Dam.

A concrete gallery offered an ideal test site for this comparison as mass concrete closely approximates the homogeneous elastic medium assumed for the analysis of plate jack tests. Laboratory values showed that the modulus of the concrete is  $3.8 \times 10^6$  psi.

Each test was instrumented with both surface and buried gages. The deformation within the concrete was measured by 4-in Carlson strain meters in a boring drilled along the center axis of the plate. Depth of embedment is not given.

Table 8.1 contains a summary of the moduli calculation from displacements. In the rigid plate test the surface moduli are lower than the laboratory value by a factor of three while the deep moduli are high by 50 percent. The flexible plate tests, on the other hand, yielded surface and deep moduli which are from 10 to 25 percent high. The load-deformation curves for both rigid tests had very low slopes under initial loads and the slope increased rapidly at higher load levels. The flexible tests yielded load-deformation curves with nearly uniform slope and the almost overlapping load and rebound curves for both surface and deep readings. The Japanese Multipurpose Dam Rock Testing Group concluded that the rigid plate made rather poor contact with the rock

mass in spite of the concrete pad and jack friction may be responsible for the erroneous test results. The flexible plate test on the other hand gives moduli which are slightly high but almost uniform for both surface and deep measurements.

TABLE 8.1  
COMPARISON OF MODULI MEASURED BY RIGID  
AND FLEXIBLE PLATE JACK TESTS

Type of Measurement	Modulus of Elasticity, psi x 10 <sup>6</sup>	
	Rigid Plate Jack	Flexible Plate Jack
Surface gages	1.2 to 1.4	4.3 to 4.5
Buried gages	4.7	4.3 to 4.8
Laboratory test	3.8	3.8

#### 7. Special Uses of the Plate Jack Test

While many references present load-deformation curves which show the magnitude of creep, only one reference contains information on creep rate. Serafim (1961) presents the results of a creep test that lasted 80 hours. The results plotted as deformation versus log of time revealed a nearly straight-line relationship. This information would be valuable in ascertaining the deformation due to long-term loading.



## SECTION 9

### PRESSURE CHAMBER TESTS

#### 1. Introduction

Pressure chamber tests are the largest in-situ static test of the deformation modulus. The pressure chamber test was first performed at pressure tunnel sites to determine if the rock could support part of the hydrostatic load, and thus, reduce the thickness of the liner. It has since been used in the abutments of arch dams to obtain the deformability characteristics of the rock for the design of the concrete arch.

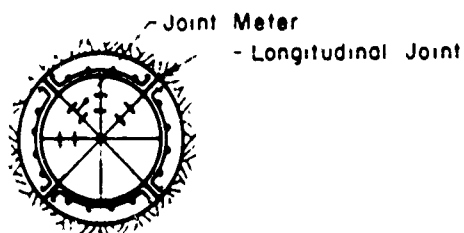
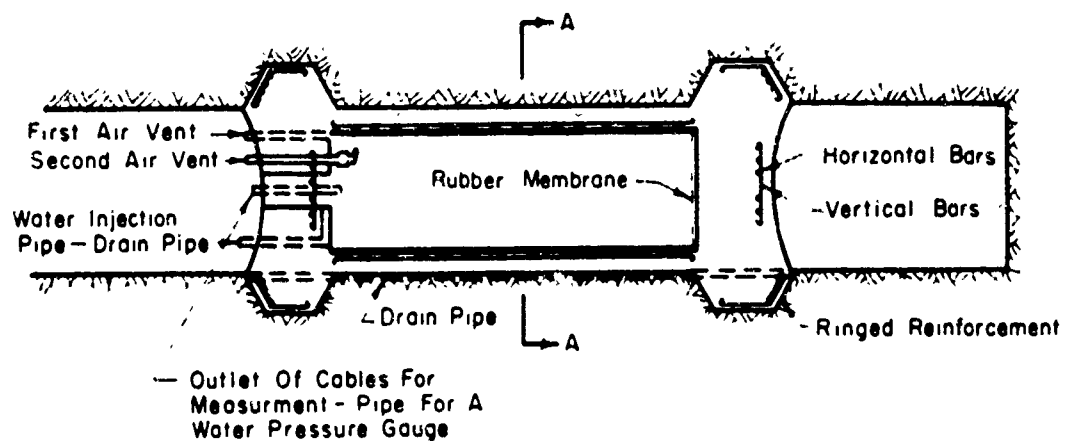
Because of the size of the area tested, pressure chamber tests are especially valuable in testing rock masses with large joint spacing. However, the test is expensive, and it is normally limited to large projects where an accurate determination of the deformation characteristics of the rock can result in substantial savings in the design of the structure.

#### 2. Site Preparation

The site preparation is similar to that of the jack test except the test area is much larger. The ideal test site would have a circular cross-section with walls smooth enough to allow the use of a thin flexible liner. However, this is nearly impossible to achieve because of irregularities caused by bedding and by joint surfaces. In foliate rocks, it may be necessary to use a rectangular cross-section (Talobre, 1961); but this cross-section requires a correction factor in the analysis that can be avoided by careful blasting and hand trimming to get a near circular cross-section.

#### 3. Test Setup

A typical pressure chamber setup is shown in Figure 9.1. The first setup in building the pressure chamber is the construction of one or two reinforced concrete bulkheads to isolate the test section. Some economy can be realized by placing the chamber at the end of the test adit and using a single bulkhead. The bulkhead toward the tunnel portal is equipped with an access portal covered during the test by a steel door, water pipes, air outlets, and wires for instrumentation within the chamber.



SECTION A-A

FIG. 9.1 TYPICAL PRESSURE CHAMBER TEST SET-UP (After Deere et al., 1967 )  
Reproduced with the permission of A.I.M.E.

The most critical part of the test chamber construction is the installation of an impermeable lining. Some of the earlier chamber tests (Rocha, 1955) were unlined and it was evident in examination of the chamber after the test that water had moved into bedrock joints and caused some of the joint blocks to move and rotate. This created a significant scatter in deformation readings.

The ideal liner material would be completely impermeable and yet would offer no resistance to the load. Rubber has these properties, but it cannot be placed directly on the rock as the irregularities of the rock surface puncture the rubber as soon as the chamber is pressurized. Bituminous material is reasonably impermeable, does not resist loads, and has been used successfully as a liner material (Rocha, 1955). Lightly reinforced concrete is reasonably suited for pressure chamber linings except for the fact that numerous fine cracks form at high pressures admitting some water to the rock, and the lining can develop hoop stresses which can resist a portion of the hydrostatic load. Thus, an acceptable liner would use a combination of these materials. A lightly reinforced concrete lining, which is jointed longitudinally so that it cannot develop hoop stresses, with an inner rubber lining to make it impermeable, appears to offer the best solution to the problem.

When the pressure chamber test results are used for design of a pressure tunnel lining, the test section may be a short section of the finished tunnel or an exploratory drift with trial lining. The test area should be excavated by the same construction techniques that will be employed in the tunnel. Trial linings are normally concrete or steel liner sections grouted to the rock mass. The test location may be chosen to represent the average or extreme rock conditions encountered, and the rock may be tested with or without consolidation grouting. Because of the cost of the test, only a few of these variables can be economically investigated at one site.

#### 4. Deformation Measurements

In order to minimize the influence of the ends of the loaded area, deformations are often measured in the middle one third of the chamber. The deformations are measured by diametral or buried deformation gages that are equipped with hydraulic or electrical systems which provide remote readout.

Typically, the diametral gages are installed in closely-spaced groups of two to four gages so that the deformations measured occur essentially

within a plane. Three such groups are often used with each group consisting of one gage in vertical orientation, a second in a horizontal orientation, and the third and fourth in 45-degree orientations.

The moduli determined from diametral gage measurements may be directly applied to the design of a pressure tunnel. A pressure chamber test at an arch dam site, however, should also be instrumented to obtain deformations within the rock mass where a destressed zone does not dominate the results. This can be accomplished by using buried gages as explained in the previous section.

Deformation measurements can also be obtained by carefully metering the water pumped into the chamber and measuring any leakage around the bulkhead. However, this method is not as sensitive as diametral and borehole gages and cannot be used if the lining has leaked. At best, this method offers only a crude check on the other deformation values.

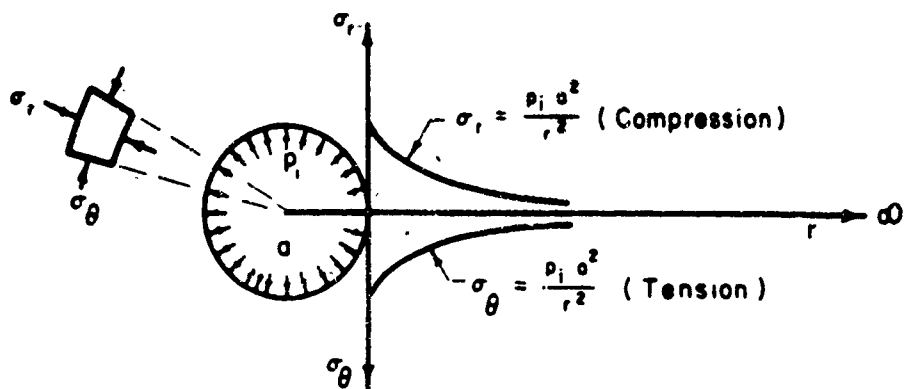
#### 5. Testing Procedure

The pressure chamber is filled by using a port near the bottom of the bulkhead. An open port near the top of the bulkhead provides a vent for the air displaced by the water. Because of the size of the opening and the small magnitude of rock displacements caused by test pressures, it is important to avoid movements due to heat exchange between the rock and the water. The water may be stored in the tunnel until it has equilibrated with the temperature of the adit, or it may be heated or cooled as it is pumped into the chamber. Once filled, the pressure chamber test is conducted quite similarly to the plate jack test, and the load-deformation curves are presented in the same way.

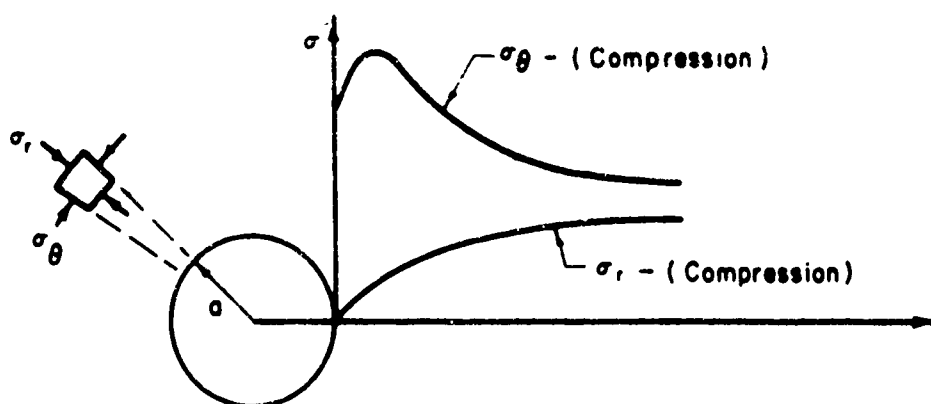
#### 6. Interpretation of Test Results

The analysis of the pressure chamber tests is based on the elastic solution of the thick-wall cylinder problem. This solution is valid if the deformations created by internal pressure can be considered a two-dimensional case. This is approximately valid when deformation measurements are made near the middle of a chamber at least 5 or 6 diameters long and sufficiently remote from the ground surface that its influence can be ignored (Rocha, 1955).

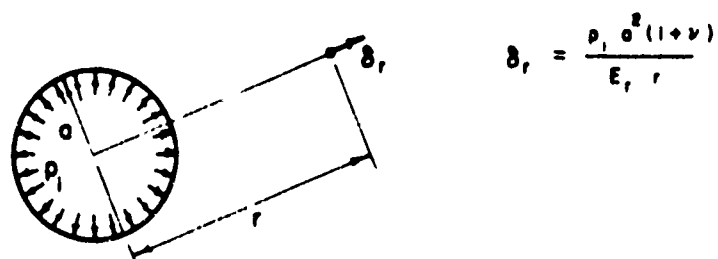
The application of the thick-walled cylinder solution is discussed by Deere et al. (1967). The following quotation refers to Fig. 9.2.



(a) Changes In Stress Distribution From Application Of The Chamber Pressure.



(b) Approximate Initial Stress Distribution Around A Pressure Chamber



(c) Radial Displacement Resulting From Application Of The Chamber Pressure

FIG. 9.2 STRESS DISTRIBUTION AND DISPLACEMENTS AROUND PRESSURE CHAMBERS (After Deere et al., 1967) Reproduced with the permission of A.I.M.E.

The application of an internal pressure,  $p_i$ , at the internal radius,  $a$ , of an infinitely thick cylinder causes changes in stress distribution as shown in Figure 9.2(a). The change in circumferential stress at the inner fiber is a tensile stress equal to the applied radial stress,  $p_i$ . Since a rock mass cannot transmit a tensile stress, some investigators (Bleifuss, 1955) have objected to the use of elastic theory to interpret the results of pressure chamber tests. It should be pointed out, however, that the initial stress distribution around an opening at depth consists of a compressive circumferential stress which peaks very near the opening as shown in Figure 9.2(b). Consequently, within the ranges of pressure normally used in pressure chamber tests (200-500 psi) the tensile change in circumferential stress due to the internal loading only serves to decrease the high initial circumferential compressive stresses. Therefore, the use of single elastic thick-walled cylinder theory for the interpretation of pressure chamber results is considered adequate provided the chamber is 5 to 6 diameters long.

The elastic solution for the thick-walled cylinder problem is

$$E_r = \frac{P_i a}{\delta_a} (1 + \nu) \quad (9.1)$$

where  $E_r$  is the modulus of the rock,  $P_i$  is the internal pressure,  $a$  is the radius of the chamber,  $\delta_a$  is the deformation of the wall of the chamber, and  $\nu$  is Poisson's ratio. A modulus can be calculated from buried gages using the relationship

$$E_r = \frac{P_i a^2}{\delta_r r} (1 + \nu) \quad (9.2)$$

where  $\delta_r$  is the deformation measured behind the wall of the chamber at a radius  $r$ .

Other relationships have been developed to account for the load carrying capacity of the chamber lining and the deformations caused by the distressed zone. These equations require additional assumptions and give higher and thus less conservative modulus values. These refinements of analysis are rarely justified and most tests are analyzed using equations 9.1 or 9.2. Equation 9.1 is most appropriate for pressure tunnel design, while equation 9.2 can be applied to foundation design.

## 7. Radial Jack Test

In recent years, the radial jack test has been used by several investigators (U.S. Bureau of Reclamation, 1966; and Lauffer and Seeber, 1966) to

combine the advantages of the relatively simple test setup of a plate jack test and the large mass of rock loaded by a pressure chamber test. The radial jack is installed in a section of test adit approximately one tunnel diameter long which has been carefully excavated and smoothed by a circumferential concrete pad. The jack consists of a number of longitudinal Freyssinet jacks, 6 to 8 ft long and approximately 1-1/2 ft wide, held against the rock by wooden beams that are in turn supported by a framework of ring beams (Figure 9.3). The test is usually instrumented like a pressure chamber test with diametral gages and gages within the rock. Unlike the pressure chamber test the diametral gages can be set up for direct reading as access to the test area is available during the test.

Because the test setup is only one diameter long, the two-dimensional plane strain assumption used in analyzing the pressure chamber test is no longer valid. The test is analyzed by a modification of existing elastic solutions by using additional deformation measurements taken outside the loaded area.

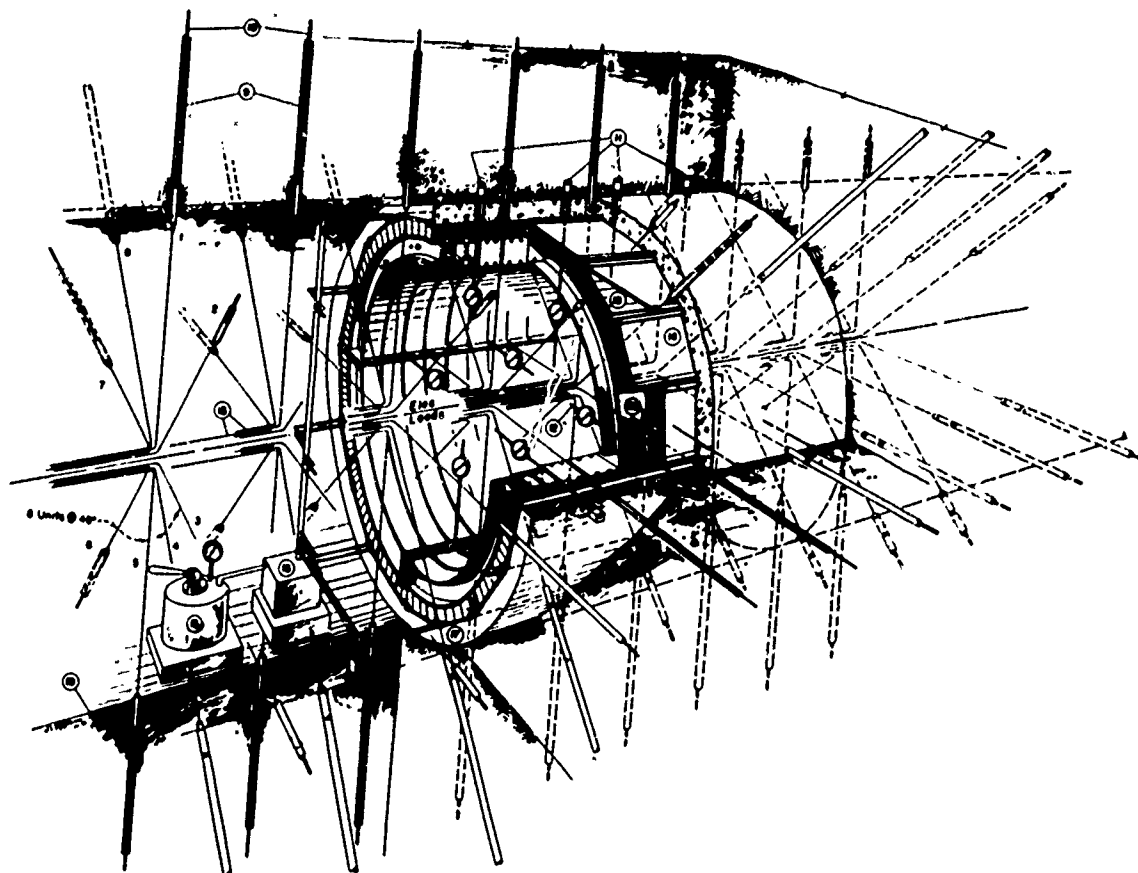


FIG. 9.3 RADIAL JACK TEST ( After USBR, 1966 )



## SECTION 10

### BOREHOLE DEFORMATION TESTS

#### 1. Introduction

Pressure chamber tests and large diameter jacking tests are expensive to perform because of extensive site preparation and elaborate testing equipment. Therefore, their use is generally limited to major construction projects. The need for a static deformation testing device that will give rapid, inexpensive in-situ modulus values has stimulated the development of a number of borehole deformation devices. At present, there are about six different instruments used to perform rapid deformation tests in borings of small to medium size. In the following sub-sections, these will be briefly described as reported in the literature.

#### 2. The CEBTP Apparatus

The CEBTP apparatus, developed by Dawance, uses the flat jack principle (Mayer, 1963). The apparatus consists of a hollow steel cylinder split by an axial cut into two halves. Within the hollow space are a pair of oil-filled rubber bags, which are so arranged that changes in oil pressure push the half cylinders apart. The movements of the half cylinders are measured by an induction extensometer located between the bags which is sensitive to movements of 0.004 in. The load exerted on a rock surface can be calculated from the pressure in the hydraulic system. No information is given on the size of the instrument except that it is about 29 in. in diameter. It is reasonable to assume that the instrument is from 3 to 4 times longer than its diameter, or 7-1/2 to 10 ft long. The method of analyzing load-deformation curves is not given, but the reference states that the instrument has been calibrated in blocks of concrete and gypsum.

#### 3. The Janod-Mermin Apparatus

The Janod-Mermin apparatus was developed about 15 years ago by engineers of Electricite de France (Mayer, 1963). It consists of a steel tube 30 in. long, 6-1/2 in. in diameter with a wall thickness of about 0.4 in., and a sleeve of annealed aluminum which encloses the tube leaving a hollow space between. Ring seals at both ends allow pressurizing of the hollow space by

water. Deformations are measured by a pair of transverse extensometers which pass through water seals in the steel tube and contact the aluminum sleeve. It is reported that the instrument can be used at internal pressures up to 3,500 psi.

#### 4. The Sounding Dilatometer

The sounding dilatometer, developed by Kujundzic (1964), consists of a steel cylinder 40 to 47 in. long surrounded by a rubber envelope making the complete diameter of the tool 8 to 12 in. Test loads are obtained by filling the space between the rubber and the steel tube with water. Testing pressures range from 600 to 1,000 psi. Deformations are measured either by a pair of centrally located extensometers, which pass through glands in the wall of the instrument, or by measuring the water pumped into the instrument. The volumetric method is used only in testing soft rocks. The smaller diameter tool is portable and decreases the cost of drilling test holes. However, Kujundzic states that a smaller diameter device does not stress a large enough volume of rock, and the local influence of one or more discontinuities can give "a totally erroneous picture of the rock at the point tested."

#### 5. Menard Pressure Meter

The Menard Pressure Meter consists of a cylindrical probe containing three pressure cells (Menard, 1966). The cells are cylinders of equal size arranged one above the other in the probe and normally inflated by compressed air or water. The middle cell is used for deformation measurements that are recorded by either feeler gages or the volumetric method. The upper and lower cells, or guard cells, are used to increase the length of the loaded area so that the deformation measurements are not disturbed by end effects. Various models of the pressure meter are available for tests in borings from 1-1/2 to 4-in. diameter.

#### 6. Summary

All the devices described above are, essentially, miniature pressure chamber tests. However, the CEBTP exerts a load through a rigid plate while the Janod-Mermin, Kujundzic, and Menard devices exert the load through flexible membranes. In each test, an elastic analysis of the results is based on the assumption that the measurements are made in the center of a rather long loaded area.

These instruments have the advantage that site preparation is simple, measurements can be made beyond the distressed zone of an adit, and they measure moduli deep in the rock mass without the expense of a test adit. Comparisons between borehole deformation measurements and jacking tests (Duffant and Comes, 1966, and Dvorak, 1967) indicate that the borehole tests yield a higher modulus with about the same scatter associated with the plate jack tests. The principal criticisms of this type of testing are that the load in a vertical hole is exerted horizontally while it is the modulus in the vertical direction which is normally required, and that the volume of rock affected by the test is smaller than large diameter jack tests.

## SECTION 11

### OTHER STATIC TESTS

#### 1. The Cable Method

A limitation of the plate jack tests described in Section 8 is that they can only be used efficiently in underground openings where the opposite wall of the opening can be used to provide restraint for the hydraulic jacks. A few surface plate jacking tests have been performed, but they require cumbersome arrangements of dead weight to provide reaction for the jacks. Such systems are limited to tests of relatively compressible rock. If hydraulic jacks could be used more efficiently in surface plate jack tests, the test could be used at sites for large buildings where a test adit is unjustified and could provide additional test sites at arch dam sites without the expense of driving more adits.

Jaeger (1961), Fergusson et al. (1964), and Deere (1965), have suggested that the required reaction for surface loading tests can be obtained by the use of cable tendons. Cable tendons are high strength steel cables anchored in a boring by means of a mechanical device or a grouted section. Techniques for installing cable tendons have been developed in recent years to provide inexpensive supports for slopes and underground openings. It is reported that loads up to 4,000 tons can be supported by this method (Jaeger, 1961).

The only documented large scale in-situ deformation test using cable reaction is reported by Zienkiewicz and Stagg (1966, 1967). Their test setup is shown in plan and section view in Figure 11.1. The setup consists of two pairs of cubic concrete loading pads each 3 ft on a side. The blocks are placed in a square configuration with 3 ft spaces left between them. The load is applied to each block by three 100-ton hydraulic jacks restrained by means of a cable tendon and cylindrical steel cable head. The load is transferred from the jack to the concrete block through a Freyssinet load cell. The maximum pressure in each test is 390 to 450 psi.

A pair of loading pads was used because deformations between the blocks are greater than those near a single loading block. An additional advantage of this setup is the blocks can also be loaded horizontally by means of tie bars and hydraulic jacks. A horizontal deformation modulus can be calculated from

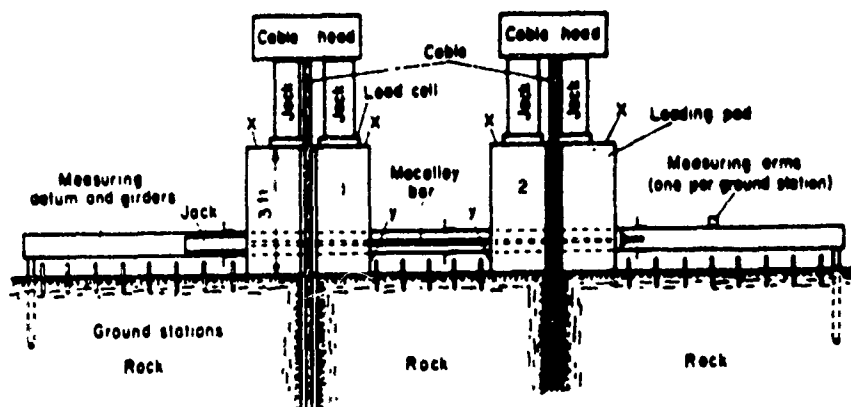
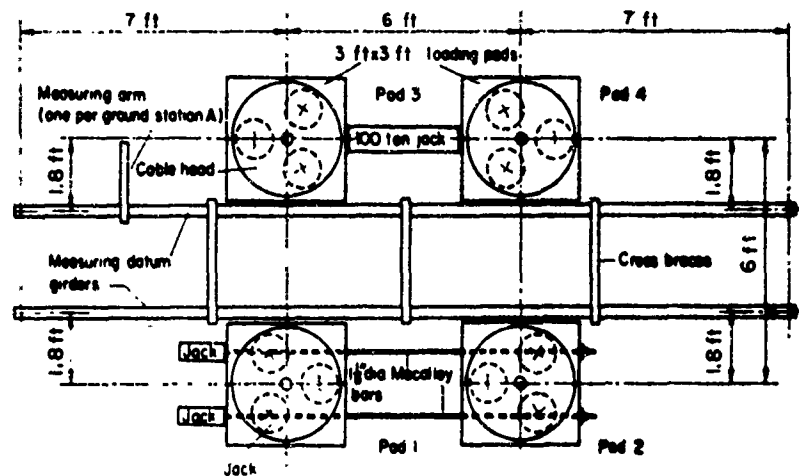


FIG. 11.1 IN-SITU TEST USING CABLE ANCHORS (After Zienkiewicz and Stagg, 1967 ) Reproduced with the permission of Pergamon Press

lateral displacements of the blocks. With two moduli measured in perpendicular directions Zienkiewicz and Stagg feel that important corrections for anisotropy can be obtained, which can in turn be applied to each set of values.

The main deformation measuring system is a series of sensitive dial gages supported on a reference rod 20 ft long which is supported by pins located outside the area affected by the load. The gage points are pins grouted several inches into the rock surface. In addition, vertical movements of the loading pads are measured by dial gages mounted on either side of the concrete block and attached to the same reference rod.

The reported test was performed in a limestone quarry in Derbyshire, Wales. The rock is a coarse crystalline limestone with massive bedding 30 to 60 ft thick. It contains two major joint sets intersecting at approximately 75 degrees with an average joint spacing for each set of approximately 3 ft.

The test site was located at the top of the quarry to obtain rock free of cracks due to production blasting. The soil and three feet of rock were removed to obtain the test surface. At this level, the joint blocks were sound, but the joint planes showed significant weathering. The significance of this weathering is shown by the low measured value of the deformation modulus,  $0.31 \times 10^6$  psi.

The size of the individual loading pads in this test are about the same as large diameter jack tests. Because of wide joint spacing at this site, the tests involved only a small number of joint blocks. Under these conditions, a heavily reinforced concrete pad, 10 by 10 ft loaded by 8 to 10 cable tendons, would provide an even more representative test. In this type of loading arrangement, deformation measurements in boreholes beneath the loaded area would provide information for calculating a deformation modulus.

The use of large loading tests can be justified if the results allow the use of a less costly foundation design when savings are substantially greater than the cost of the test. The test would be even more attractive, economically, if the loading pad can be used as one of the column footings. It would be particularly advantageous to put the test blocks on the poorer rock encountered because the maximum test loads can be maintained or adjusted during construction so that very small deformations occur.

## 2. Tank Test

A large in-situ static test is being conducted at the proposed site for a proton synchrotron near Thetford, England (Building Research Station, 1967). This accelerator will consist of several miles of horizontal beam tunnels and several experimental areas with permanent buildings. While the loads are not exceptionally high, it is said that the magnets which focus the proton beam must remain within 0.006 in. of position for every 150 to 300-ft section of tunnel. With such exacting requirements, it is mandatory to use a site with uniform bedrock having predictable deformation characteristics. The geologic investigations indicate that the Thetford site, located on the middle chalk formation, is adequate for the proposed structure. Quantitative information on the deformation characteristics will be obtained from a number of 3-ft diameter plate loading tests, and from one large scale in-situ test.

A large scale load test is being performed using a 59-ft diameter welded steel tank. During the test, the tank is filled with water so that it exerts an average load of approximately twenty-five psi. Deformation measurements will be made in man-size boreholes up to 100 ft deep beneath and adjacent to the tank. Remote recording inductive transducers will be used to monitor the strains created by the load. It is felt that a complete site evaluation can be made by comparing the results of the large-scale test with plate jack and laboratory tests.

An in-situ test of this scale will certainly provide unique information on the relationship between the intact and the in-situ properties of a rock mass. However, it should be noted that the test can only be used on relatively compressible rock due to the low load levels.

## SECTION 12

### COMPARISON OF IN-SITU STATIC TESTS

#### 1. Introduction

The literature on in-situ static tests is quite extensive although these tests have been performed only within the last two or three decades. The tests reported were performed in a variety of rock types ranging from clay shales to granites and quartzites. The geologic setting ranged from mountainous areas, where folding, faulting, and high tectonic stresses are found, to plains areas where the rock is essentially undisturbed. The range of rock types and geologic setting partially explains the observation that the lowest and highest moduli reported are separated by a factor of one thousand.

A survey of in-situ test results indicate, as would be expected, that a representative modulus range cannot be assigned to a particular rock type. It appears that a factor of ten may also separate the low and high values obtained by the same test techniques at one site in the same rock type. Several authors, notably Rocha et al. (1955), Serafim and Nunes (1966), Multipurpose Dam Rock Testing Group (1964), have presented data which show that this wide range of moduli is caused by the way the test is performed, the orientation of the test, and the characteristics of the rock mass.

In this section, a few of the factors which influence the calculated static modulus are discussed and illustrated by data from the literature. The values used in this discussion appear in Appendix A. Many of the graphs presented in this and the following sections best fit lines determined by reduced major axis analysis. Each best-fit line is accompanied by a correlation coefficient,  $r$ , a significance level,  $SL$ , and for important relationships, the equation of the best-fit line. Many of the graphs also contain reference lines with slopes of 1:1, 1:2, or 1:5 to assist the reader in evaluating the data presented.

#### 2. Comparison of the Modulus of Deformation and the Modulus of Elasticity

Of the many possible moduli which can be calculated from load-deformation curves, the deformation modulus ( $E_d$ ) and the modulus of elasticity ( $E_e$ ) are the most useful (See Section 8). The modulus of deformation may be the most appropriate value for design as it is the lowest and, therefore, the



most conservative value obtained from the test. It does contain the effects of crack closure, cyclic loading, and some creep deformation. The modulus of elasticity, on the other hand, is considered to be unrealistically high for use in design. It does correlate well with the seismic modulus but both are thought to be too high because they do not contain the effect of crack closure, and time-dependent displacements.

Figure 12.1 is a plot of  $E_e$  versus  $E_d$  for plate jack tests, borehole deformation, and radial jack tests. The correlation coefficient is 0.947. The graph shows that the ratio between the two moduli is relatively constant for the wide range of test types and in-situ moduli. Significant deviations from the correlation are evident only in rock with a low in-situ modulus. It should not be inferred that different types of static tests will give corresponding moduli at the same test site. This comparison is made later in this section.

The regression line shown in Figure 12.1 is dominated by the large number of plate jack tests. However, seven points representing radial jack tests at one site indicate that the same relationship is valid. The same trend is also indicated for four borehole deformation tests.

The relationship indicates that the ratio between the modulus of deformation and the modulus of elasticity changes with the value of the modulus of elasticity. When  $E_e$  is near  $10 \times 10^6$  psi the ratio is about 0.9. When  $E_e$  is near  $0.3 \times 10^6$  psi the ratio is about 0.3. This change suggests that  $E_d/E_e$  could be used as a rock quality parameter.

### 3. Comparison of Moduli Measured in the Vertical and Horizontal Directions

Rocha et al. (1955) and Serafim (1964) have reported that jack test moduli measured at a test site are commonly lower in the vertical direction than in the horizontal direction. Deere et al. (1967) attribute this behavior to the fact that gravity forces open the geologic discontinuities in the roof of the underground opening, and thus lower the modulus in the vertical direction.

In Figure 12.2 the modulus measured in the horizontal direction is compared with the modulus measured in the vertical direction. The majority of points show that the horizontal modulus is greater than the vertical modulus. In a few cases, the horizontal modulus is considerably smaller than the vertical modulus. These anomalies may be explained by the concept that the quality of the rock mass has changed significantly in the short distance between the two

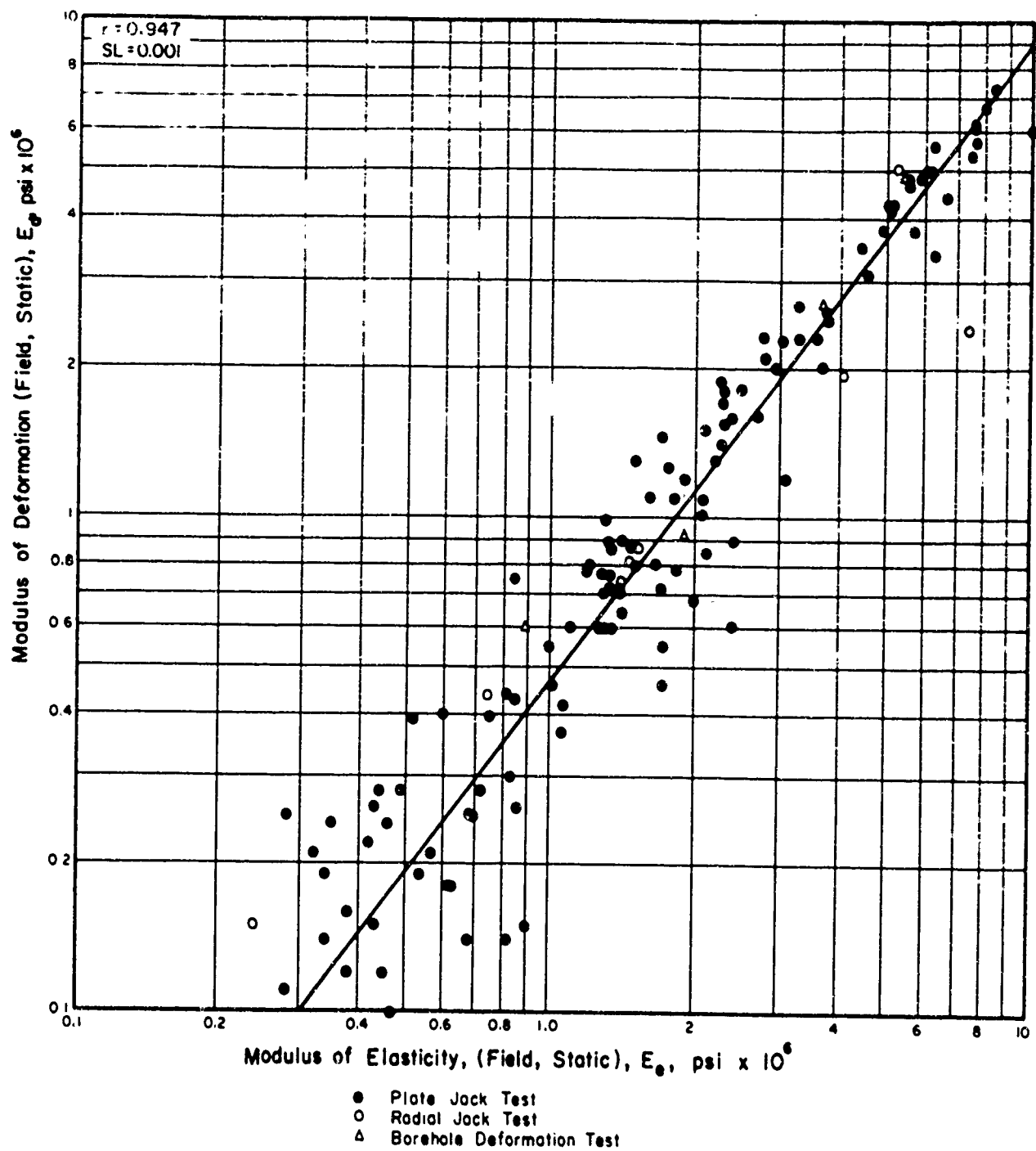


FIG. 12.1 COMPARISON OF THE MODULUS OF DEFORMATION AND MODULUS OF ELASTICITY FROM IN-SITU STATIC TESTS

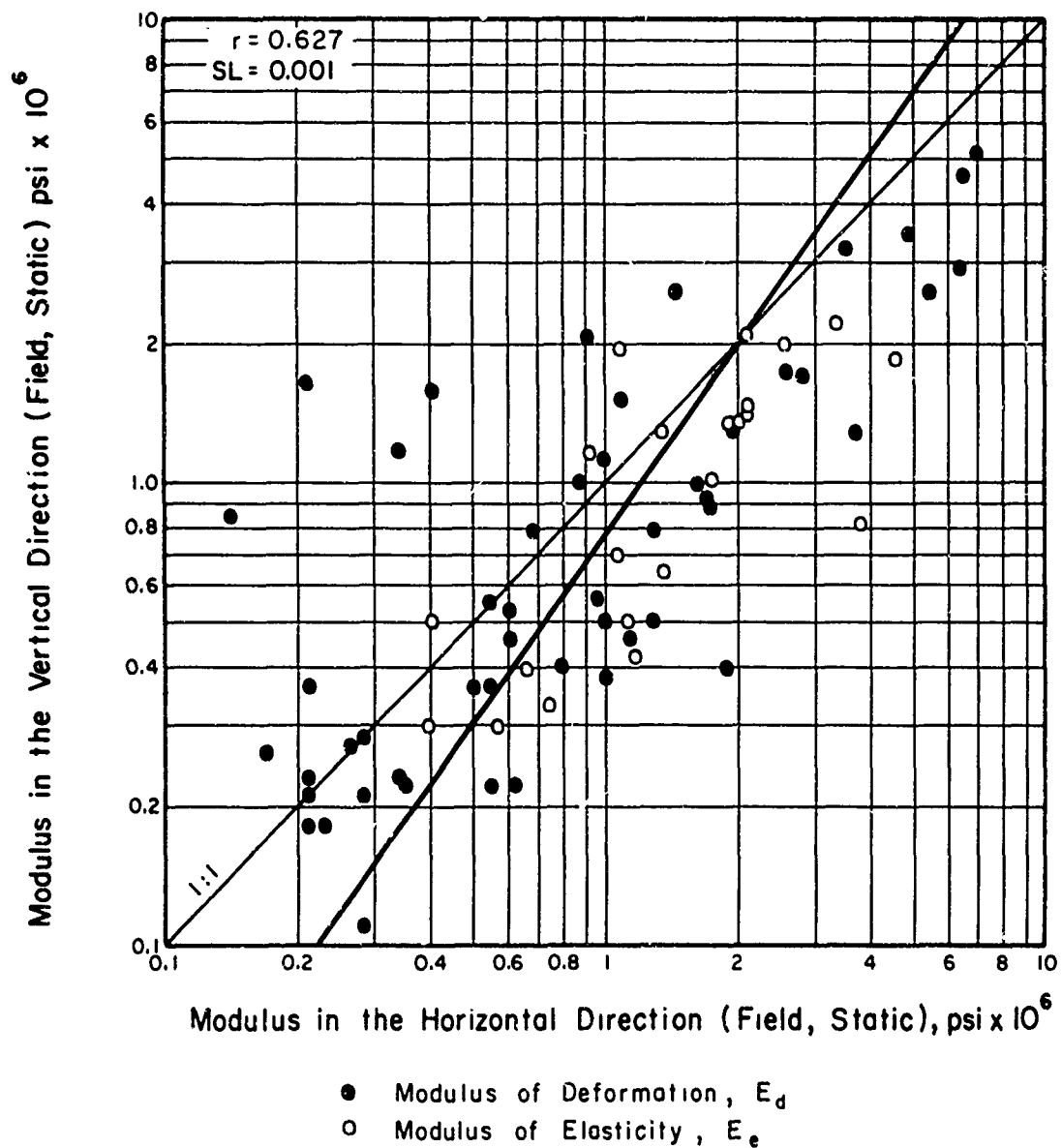


FIG. 12.2 COMPARISON OF PLATE JACK TEST MODULI MEASURED IN THE VERTICAL AND HORIZONTAL DIRECTION

tests and this change has masked the influence of test orientation. The effect of direction of stratification may also explain some of the anomalies.

#### 4. Comparison of Moduli Obtained Perpendicular and Parallel to Stratification

Bernard (1966) and Chapman (1961) have shown that the modulus measured perpendicular to stratification is lower than that obtained in the parallel orientation. In Figure 12.3, the moduli measured perpendicular to stratification are plotted against the corresponding parallel measurements. More than half of the data shows that the parallel values are up to 100 percent higher. However, the remaining points show that the moduli measured perpendicular to stratification are higher. These anomalies indicate that discontinuities other than bedding planes have influenced the test results. Perhaps extension fractures, which can form perpendicular to stratification in the destressed zone, are the major reason for the occasionally lower moduli measured in the parallel orientation.

#### 5. Comparison of Moduli Obtained Before and After Grouting

In Figure 12.4 moduli determined by plate jack, pressure chamber, radial jack test moduli, and field seismic measured after grouting are plotted against the moduli at the same location before grouting. In the majority of cases, the modulus after grouting is from one to two times the modulus before grouting with several values ranging up to five or higher.

A few values show lower moduli after grouting which indicates that the grouting operation is not always effective in consolidating the rock mass and apparently can be detrimental. This is most common for rock masses with an in-situ modulus before grouting of less than one million psi. The low initial modulus in these cases is probably the result of clay filled joints within the pressure bulb of the test. This clay filling is quite resistant to water flushing which commonly precedes grouting. Although flushing is more effective if the wash water is charged with compressed air to increase the turbulence in the fractures, the usefulness of grouting under these geologic conditions should be viewed critically. If substantial amounts of the clay filling are not removed by flushing, it will block grout penetration. In addition, the clay fillings drastically reduce the stability of the joint blocks, and it is possible that the pressure exerted by the grout can cause rotation of some of the joint blocks, resulting in a lower modulus.

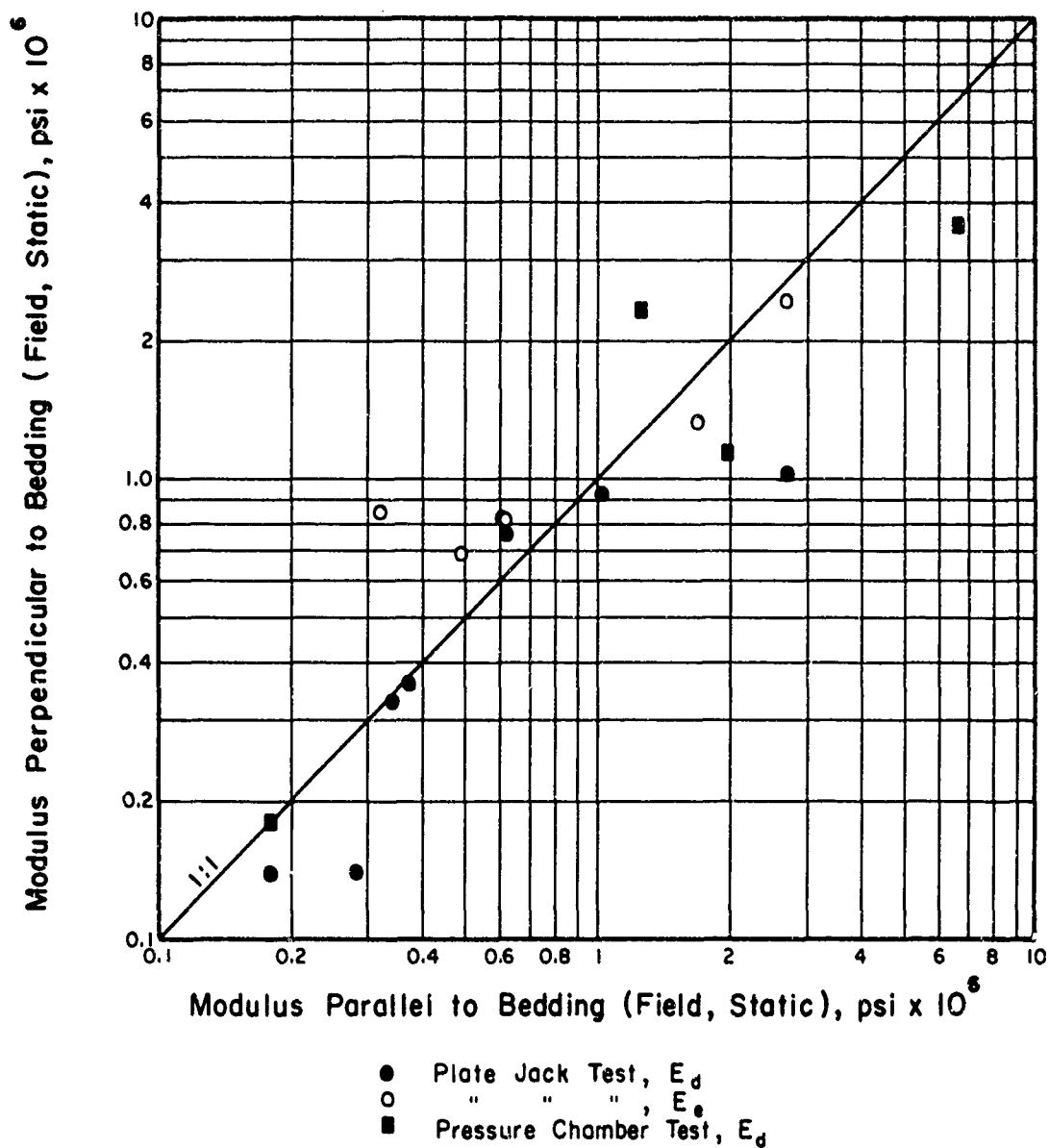


FIG. 12.3 COMPARISON OF PLATE JACKING TEST MODULI MEASURED PERPENDICULAR AND PARALLEL TO BEDDING

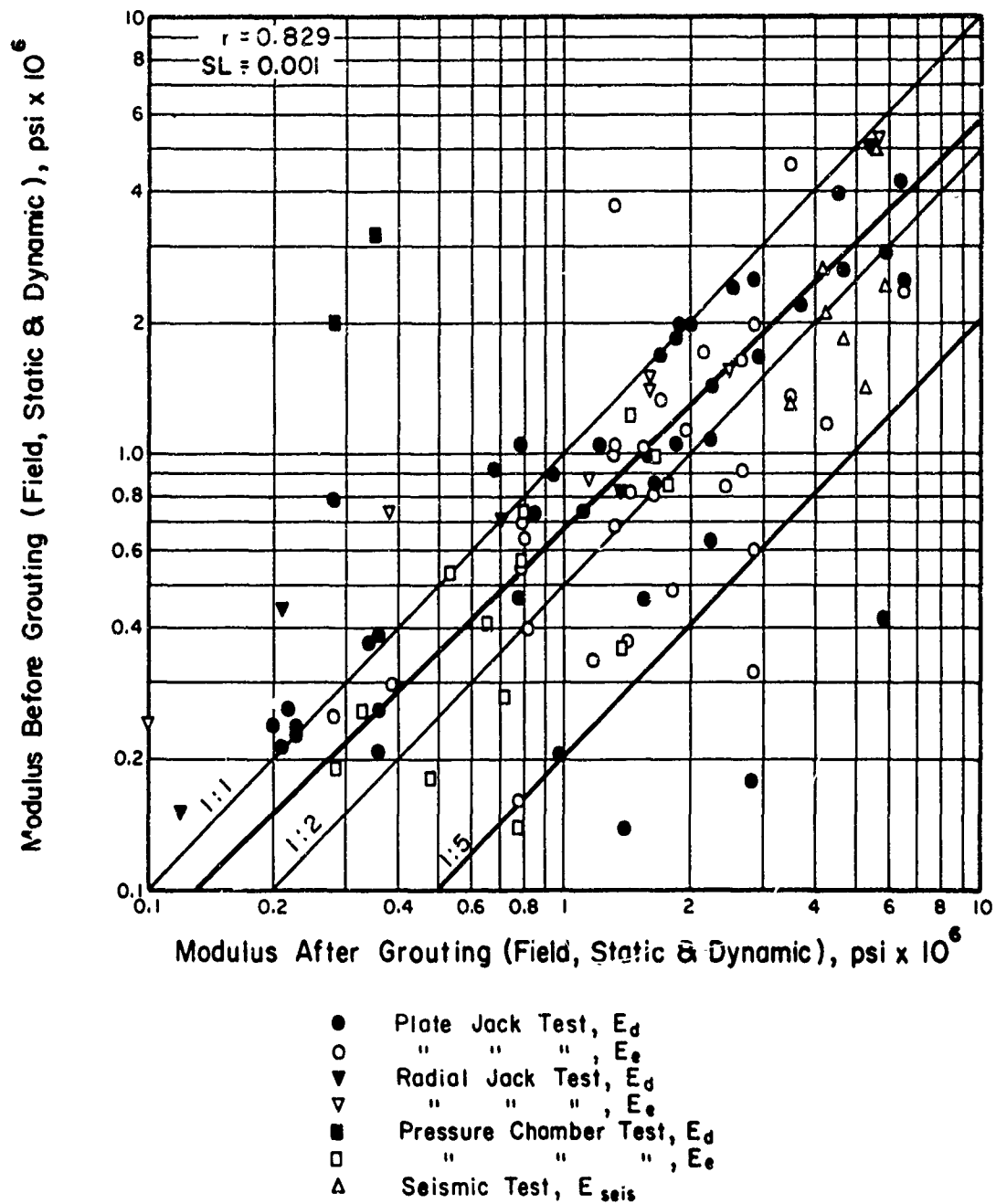


FIG. 12.4 COMPARISON OF IN-SITU TEST MODULI BEFORE AND AFTER GROUTING

The amount of improvement from grouting shown in Fig. 12.4 should be viewed critically from another point of view. Lauffer and Seeber (1966) measured the improvement from grouting by using two radial jack tests in adjacent areas of apparently similar rock quality. The results are included in Figure 12.4. Most of the tests indicate only small improvement in modulus grouting and a few show a lower modulus after grouting. The advantage of using two sites is that the after-grouting test is performed on rock which has not been prestressed by a previous static test. It is possible that some of the improvement in deformation characteristics from grouting reported at other sites is the result of prestress caused by the test before grouting.

#### 6. Comparison of Moduli Obtained by Borehole Deformation and Plate Jack Tests

In a limited number of cases, direct comparisons have been made between moduli obtained by plate jacking tests and borehole deformation measurements. Comparisons of these tests are presented by Duffaut and Comes (1966) and Dvorak (1967). Figure 12.5 contains a summary of the reported values. The borehole deformation moduli are consistently higher than the jack test moduli as would be expected by comparing the size of the stressed area. Because the borehole deformation technique stresses a smaller volume of rock than jack tests, the values, in general, should fall between the jack moduli and those of the intact rock. The data presented suggest that the borehole deformation modulus is from 50 to 100 percent higher than the corresponding plate jack modulus.

Although the data show a fairly consistent trend, this relationship is probably fortuitous. When the joint spacing is greater than the length of the borehole deformation device, a wide range of deformation moduli should be measured. In some tests, the instrument will be situated essentially within a joint block and the measured modulus will approach that of the intact specimen. In other tests, the measured deformations will be largely the result of movements along one joint. If this joint is open and oriented at an acute angle to the boring, the deformations will be high and the calculated modulus low.

#### 7. Comparison of Moduli Obtained by Pressure Chamber and Plate Jack Tests

The pressure chamber test, because of the large loading area, stresses a large number of joint blocks and the moduli are representative of an in-situ modulus. A plate jack test yields a valid in-situ modulus only when the joint spacing is some fraction of the loading plate diameter. When the joint spacing

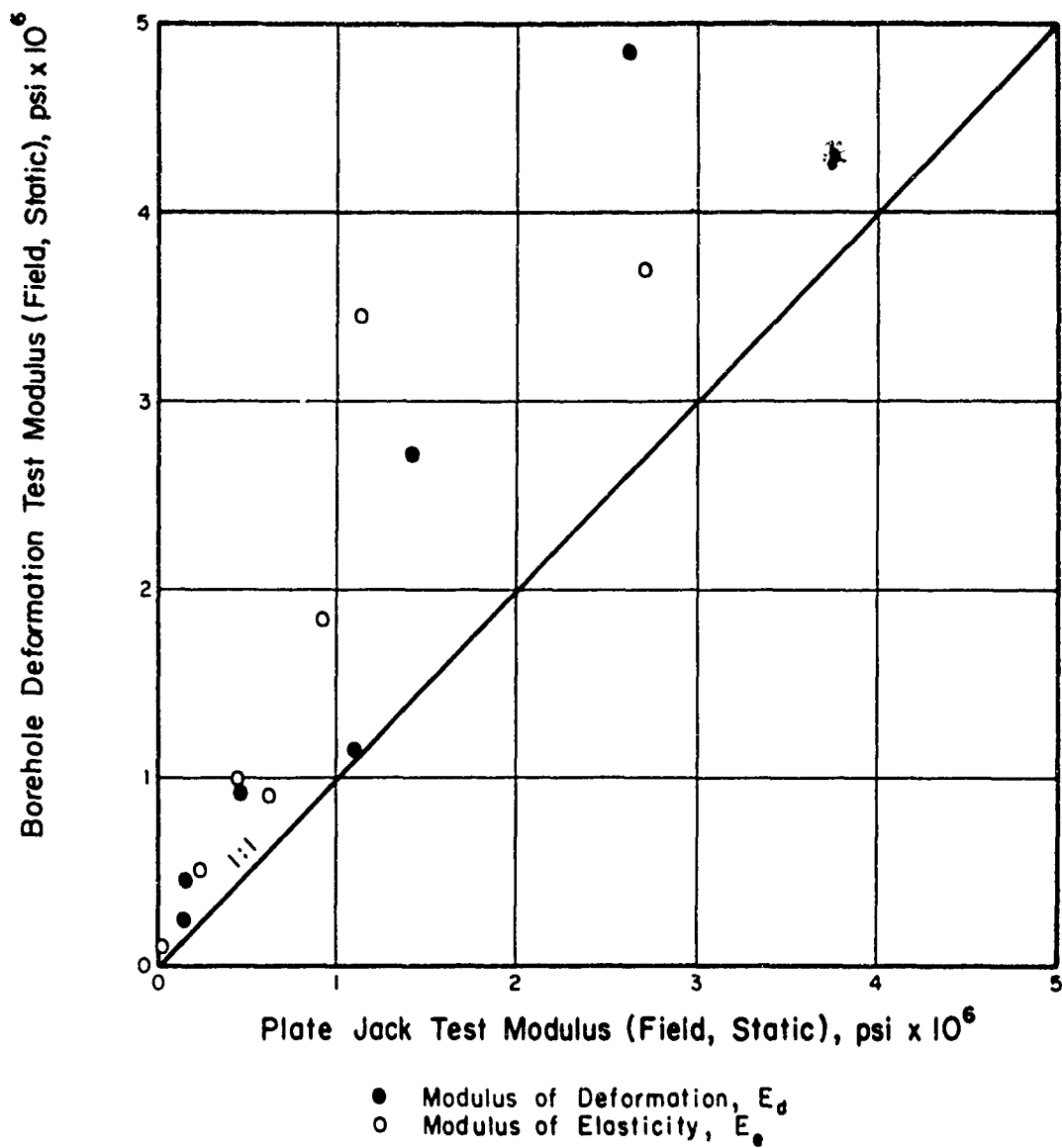


FIG. 12.5 COMPARISON OF MODULI FROM BOREHOLE DEFORMATION AND PLATE JACKING TESTS



is smaller than the plate, the plate jack and pressure chamber results should be similar. When the joint spacing approaches or exceeds the diameter of the loading plate, then the jack test moduli may be either higher or lower than corresponding pressure chamber moduli.

Unfortunately, the number of comparisons between these two test techniques is quite limited and the comparison (Figure 12.6) is not conclusive. More than half the data show that the pressure chamber moduli are equal to or less than the plate jack moduli.

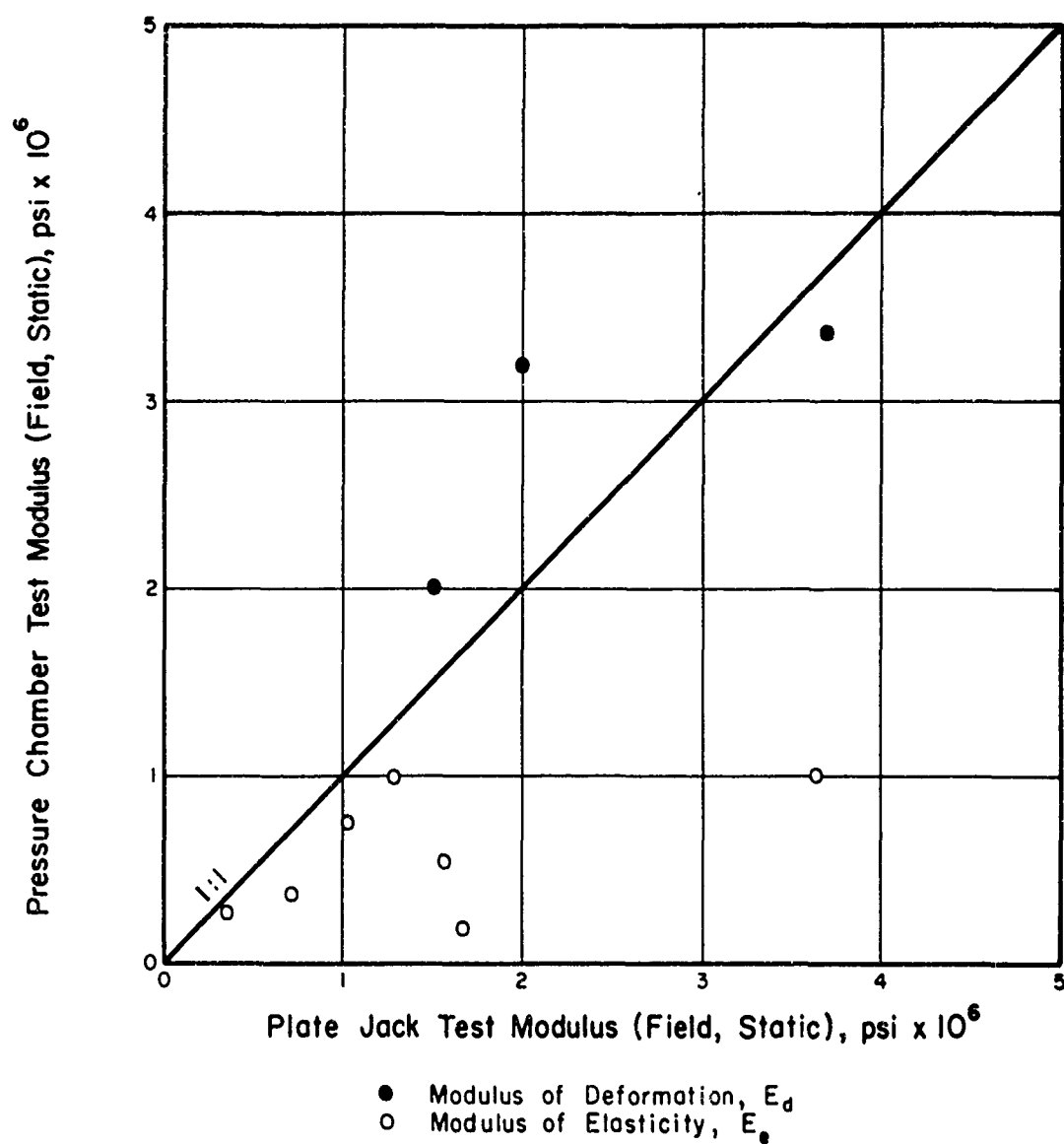


FIG. 12.6 COMPARISON OF MODULI FROM PRESSURE CHAMBER AND PLATE JACK TESTS

SECTION 13  
THE RELATIONSHIP BETWEEN STATIC AND DYNAMIC  
MODULUS MEASUREMENTS

1. Introduction

The usefulness of the field seismic technique to identify and delineate zones of relatively uniform rock quality is widely appreciated and frequently quoted in the literature. However, many authors express concern that dynamic moduli calculated from seismic velocities are significantly higher than corresponding moduli from static tests. This discrepancy between dynamic and static moduli can be explained by the considerable difference in the load level and the duration of loading used in the two techniques. The dynamic moduli are calculated from loads of a few pounds per square inch applied for a fraction of a second, while the static technique employs pressures of hundreds of pounds per square inch and load periods of from hours to days. Rusch (1960) and Serdengecti and Boozer (1961) show that the duration of loading has a significant effect on the moduli obtained for specimens tested in the laboratory. The data presented in this chapter show that dynamic moduli are higher than static moduli for field measurements.

Kitsunezaki (1965) suggests that a closer correlation of the two moduli can be obtained if the dynamic modulus is calculated from the velocity in the distressed zone. Because the plate jacking test essentially measures the modulus of the distressed zone, this approach seems quite reasonable in theory. However, surface velocity measurement from Carroll and Scott (1966), Scott and Carroll (1967), and Wantland (1963) show that the surface zone velocities are quite erratic and are apparently not related to geologic estimates of rock quality. In contrast, the deep zone velocities are related to the general rock mass quality (Scott and Carroll, 1967). In addition, the moduli calculated from surface velocity measurements are an order of magnitude lower than those calculated from deep zone velocities. On the other hand, test moduli calculated from surface deformations are generally about one-third to one-half of the moduli calculated from measurements beneath the jack plate.

## 2. Comparison of In-Situ Dynamic and Static Moduli

Figure 13.1 shows a relationship between modulus of deformation from static tests and the seismic modulus calculated from seismic velocities measured at or near the test site. Figure 13.2 presents the relationship between the modulus of elasticity and the seismic modulus. The scatter noted in both graphs may be due, in part, to the variable quality of the tests reported. It appears that much of this scatter is due to the relative size of the areas tested.

Seismic velocities are generally measured over intervals of from 10 to over 100 ft. The dynamic modulus calculated for this interval is therefore an average value for a large volume of rock. Plate jack test moduli are largely influenced by a few tens of cubic feet of rock directly behind the plate. Therefore, it is not surprising that direct comparison of the dynamic and static moduli from a number of sites presents a great deal of scatter.

Obviously, seismic surveys using much shorter geophone spacing would be of great assistance in making these comparisons. The recorder resolution required for such small scale seismic testing, however, is so high that the testing would be a research effort rather than a standard engineering test.

Despite their limitations, Figures 13.1 and 13.2 provide a means of estimating the in-situ deformation modulus or modulus of elasticity from seismic tests. It is realized that such estimates should not be used in design without some independent check of their validity. The correlations shown are valid only for the sites used in this investigation.

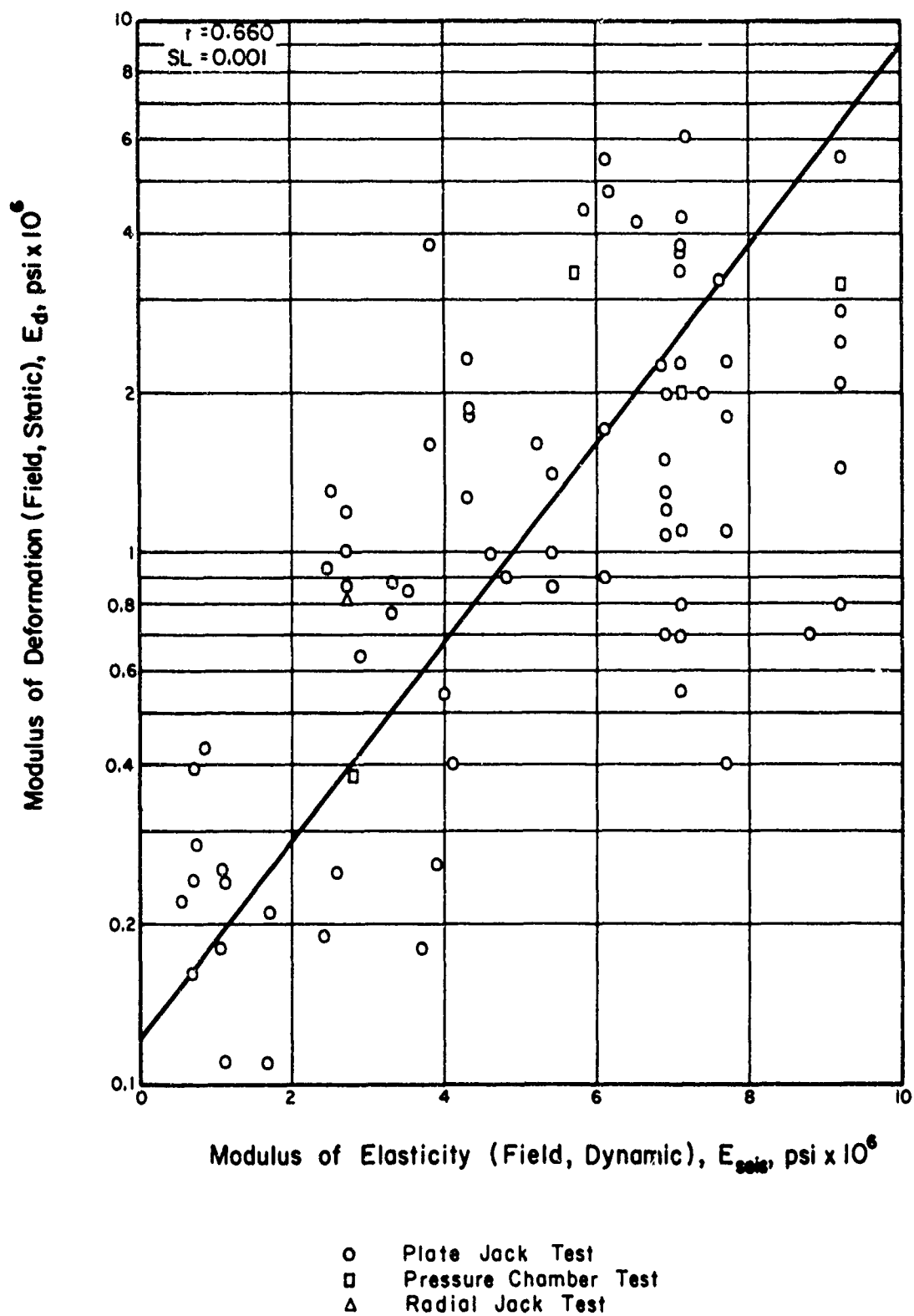


FIG. 13.1 COMPARISON OF IN-SITU STATIC MODULUS OF DEFORMATION AND DYNAMIC MODULUS OF ELASTICITY

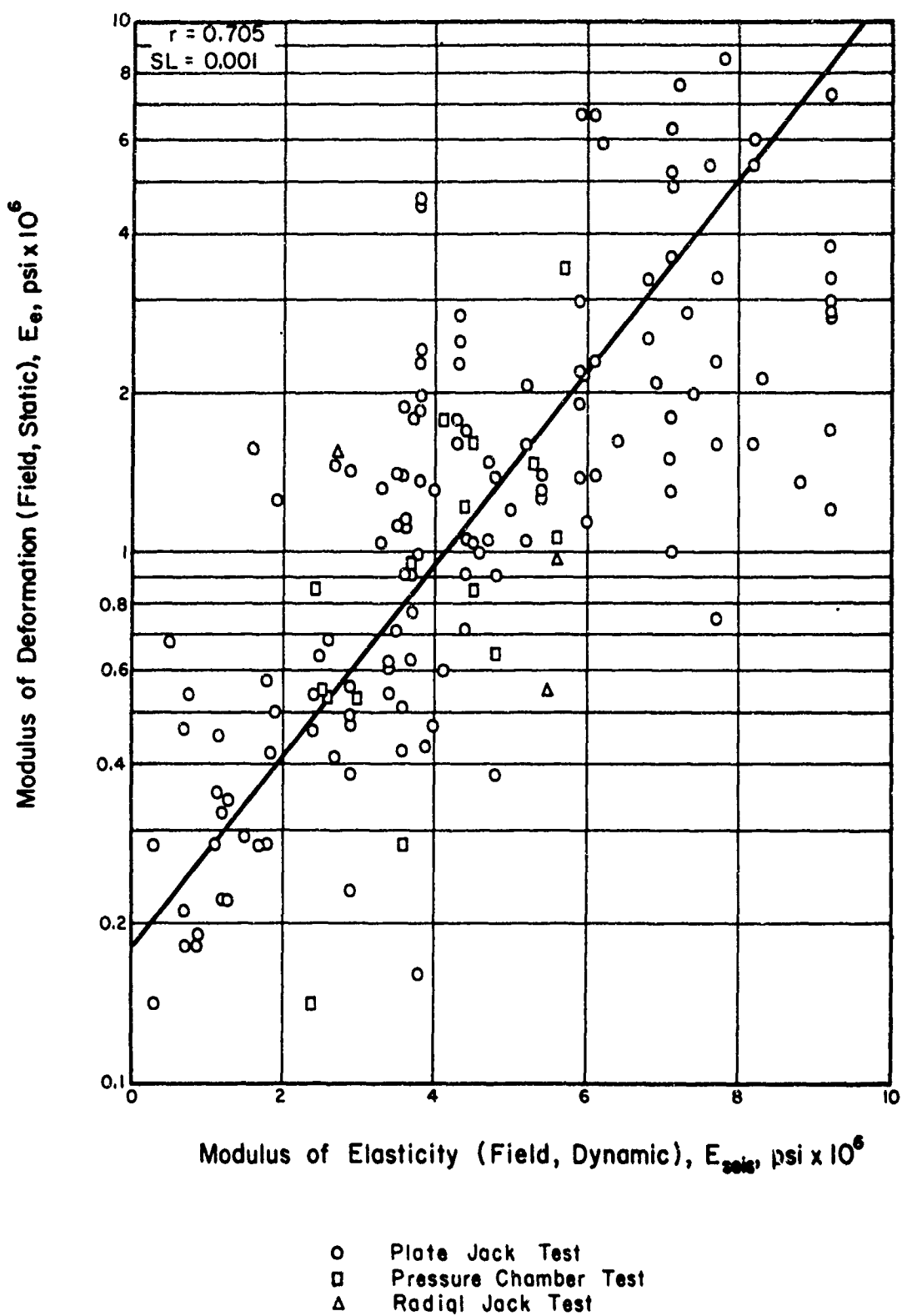


FIG. 13.2 COMPARISON OF IN-SITU STATIC MODULUS OF ELASTICITY AND DYNAMIC MODULUS OF ELASTICITY

SECTION 14  
THE RELATIONSHIP BETWEEN IN-SITU STATIC  
MODULI AND ROCK QUALITY

1. Introduction

The graphs presented in Section 12 indicate that data from various sites and various in-situ tests can be organized to determine the general characteristics of in-situ rock deformation. The relationships between the static modulus of deformation and modulus of elasticity, modulus in the vertical and horizontal orientation, modulus before and after grouting, and moduli determined by different in-situ tests on the same site, suggest some of the factors which determine the in-situ deformability of rock. However, none of the graphs provide an adequate measure of the character of the rock itself. It is the purpose of this section to show how the in-situ modulus changes with rock quality measured by the RQD and Velocity Index.

The pronounced influence of rock quality on the in-situ modulus is well illustrated by the plate jack test moduli obtained at Dworshak Dam (Shannon and Wilson, 1964). These tests offer a unique opportunity to determine the influence of rock quality because the rock is lithologically uniform and the tests were performed in a uniform manner. A total of 24 tests yielded moduli ranging from 0.7 to  $10 \times 10^6$  psi. This range includes most of the in-situ moduli reported in Appendix A.

It is apparent that increasing the number of tests without some measure of the rock quality for each test increases the uncertainty regarding the modulus to be used in design. The use of an average modulus seems reasonable, but test values showing moduli about one-fifth of the average might influence the engineer to apply a large factor of safety at some point in his calculations. On the other hand, the use of the minimum value for design might result in an overconservative design.

Rock quality measurements may be assigned an even more important role than comparing in-situ tests. If rock quality can be correlated with test moduli, then the rock quality measurements can be used to estimate the deformability of the rock mass at any location accessible by exploratory borings. This correlation would substantially reduce the number of in-situ tests required while at the same time providing the design engineer with a much better picture of the modulus variation within the rock mass.

The  $E_{\text{seis}}$  to  $E_d$  and  $E_e$  relationships in Chapter 13 represent one means of defining rock quality for this purpose. The relationships are, however, of limited usefulness for two reasons. In the first place, the scale of the seismic test is too large to define the rock quality at the static test site. Secondly, the range of the static and dynamic moduli in these relationships is the result of changes in both rock type and rock quality. The influence of rock quality can be determined by expressing the dynamic characteristics in terms of the ratio of in-situ to laboratory moduli, i.e., the Velocity Index.

## 2. Comparison of RQD and In-Situ Moduli

The RQD offers a method of determining rock quality which is independent of laboratory tests. As core borings are part of the exploration program on most major engineering projects, a correlation of in-situ test results with RQD could be made for just the small cost of core logging by the RQD method. The accuracy of the correlation between deformability and rock quality depends upon the accuracy of rock quality determination at the test site. For this purpose, a 10- to 20-ft core boring drilled behind the center of the jack pad is recommended.

Theoretical studies show that changes in stress because of a load at the rock surface decreases rapidly with depth. Therefore, near surface fractures have much more pronounced effect on the deflections measured than the deeper fractures. For this reason, the RQD measurements should be weighted according to depth. The data presented herein have been weighted by the Boussinesq stress distribution beneath a point load on the surface of a semi-infinite elastic media. Figure 14.1 (after Deere et al., 1967) shows the variations of the RQD with depth beneath a jack plate and illustrates the weighing technique used. The weighted RQD for the buried gage (depth 2 to 18 ft) is 81 percent corresponding to a deformation modulus of  $6 \times 10^6$  psi. For the surface gage determination, the effect of fracturing around the opening reduces the RQD to 69 percent and a deformation modulus of  $1.4 \times 10^6$  psi.

In Figure 14.2, deformation moduli from the jack tests at Dworshak, Telachapi, Glen Canyon, and Yellowtail are plotted against the weighted RQD. Figure 14.3 shows the same relationship for modulus of elasticity. Although the relationships look promising as prediction charts, with correlation coefficients of 0.665 and 0.648, respectively, they have the same limitation as the graphs of  $E_d$  and  $E_e$  versus seismic modulus. The relationships can be used only at sites



DWORSHAK DAM  
PLATE JACK  
VC 912, ROOF

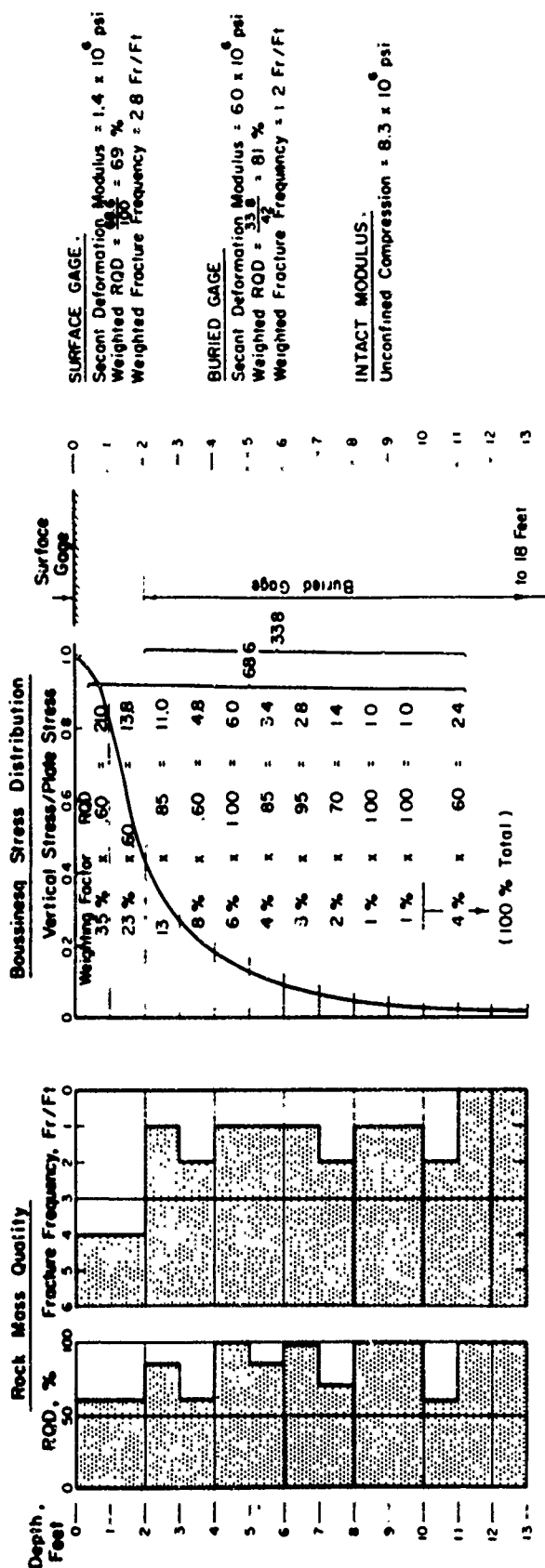


FIG 14.1 ILLUSTRATION OF A METHOD FOR OBTAINING A WEIGHTED ROCK QUALITY BENEATH A PLATE JACKING TEST (After Deere et al., 1967)  
Reproduced with the permission of A.I.M.E.

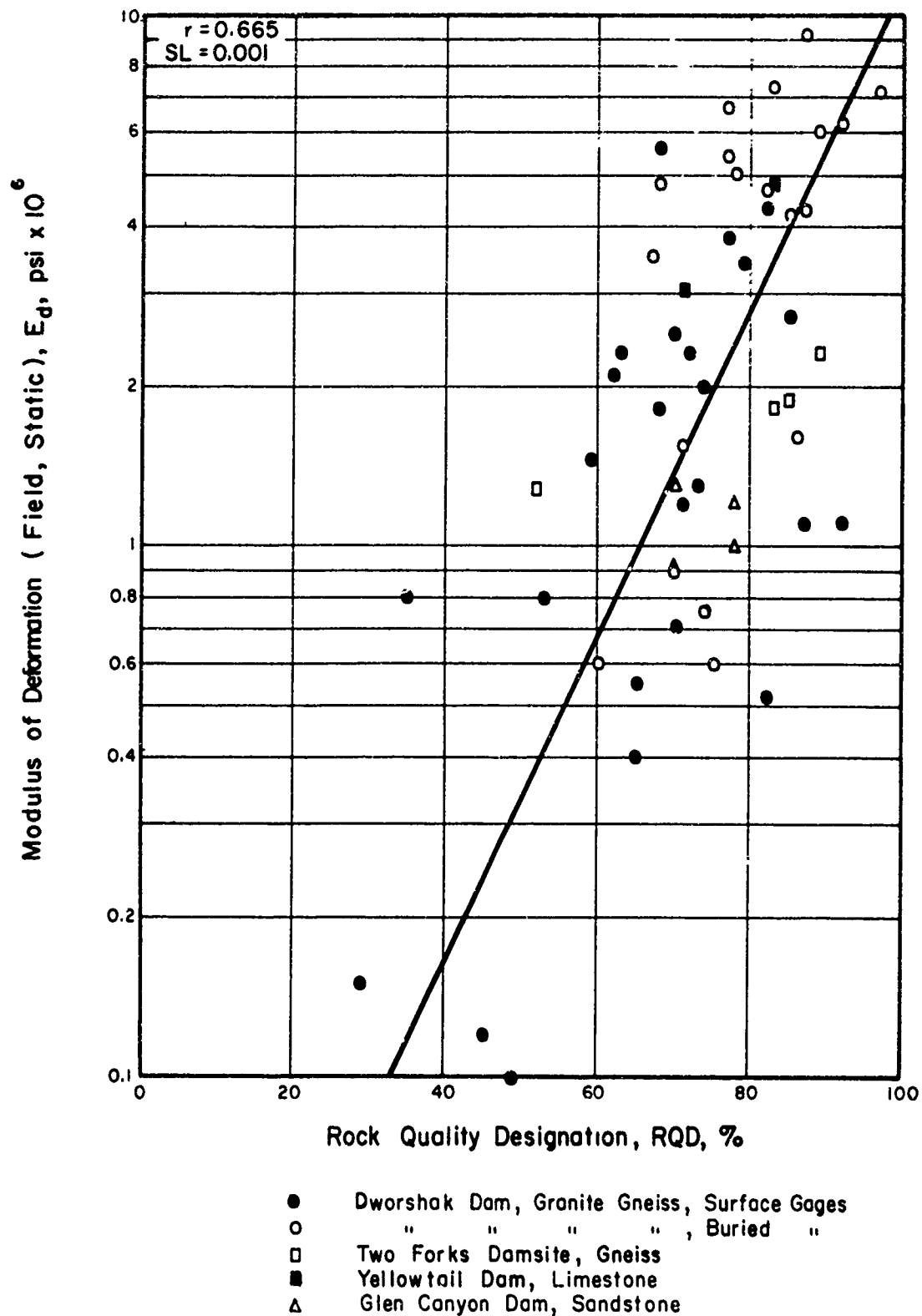


FIG. 14.2 COMPARISON OF IN-SITU STATIC MODULUS OF DEFORMATION AND ROCK QUALITY DESIGNATION

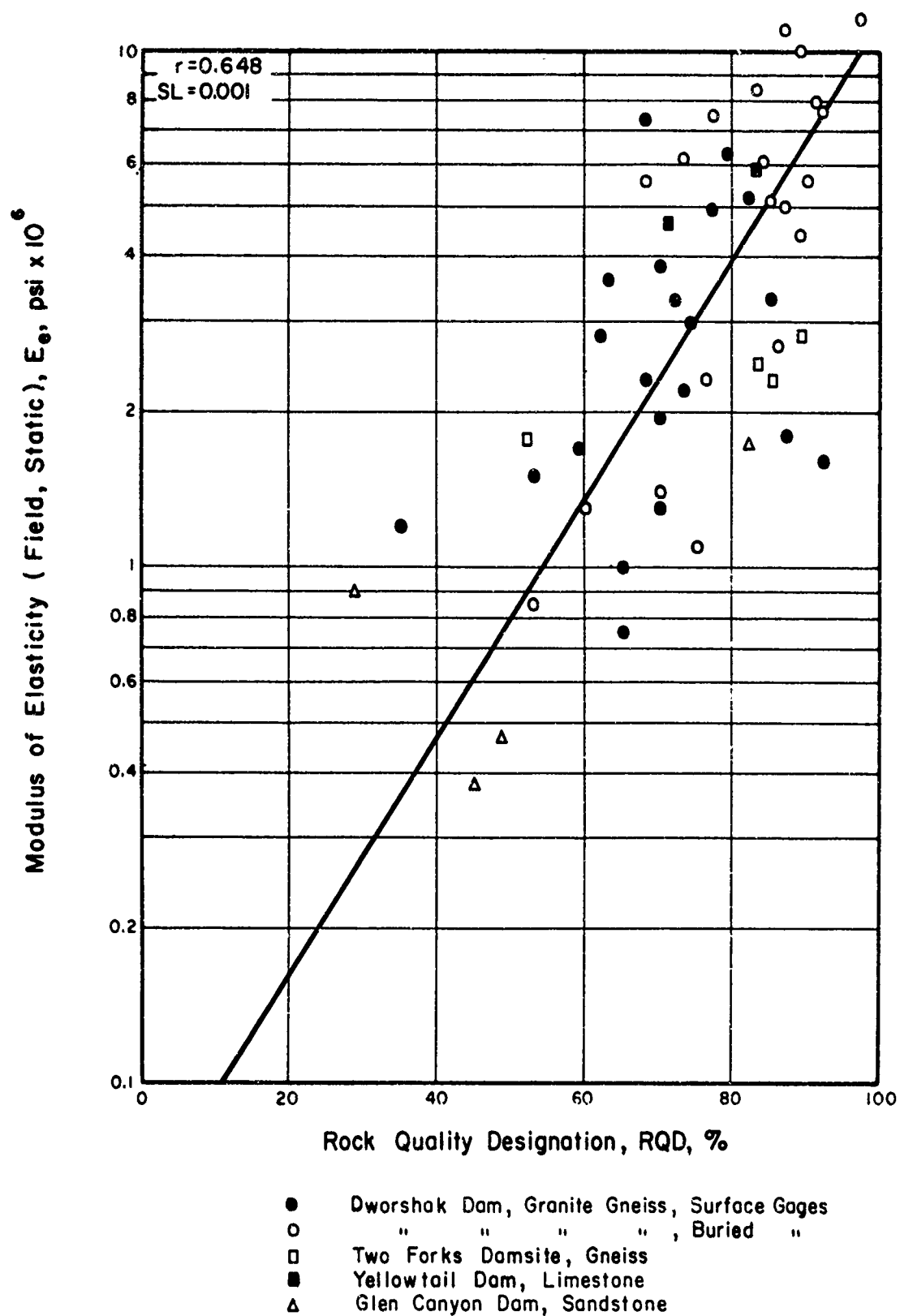


FIG. 14.3 COMPARISON OF IN-SITU STATIC MODULUS OF ELASTICITY AND ROCK QUALITY DESIGNATION

where the intact modulus of the rock is similar ( $3$  to  $10 \times 10^6$  psi). The limitation of this type of correlation is illustrated by the following example. Consider a sandstone with an intact modulus of  $1 \times 10^6$  psi. Suppose that an RQD of 80 percent is converted into a modulus estimate by using the relationships in Figures 14.2 and 14.3. The estimated modulus of deformation is  $2.8 \times 10^6$  psi. This value is obviously high by a factor of from 4 to perhaps 10.

### 3. Comparison of the Rock Quality Indices and Modulus Ratio

The limitations of Figures 14.2 and 14.3 can be avoided by normalizing the deformability of the in-situ rock by that of the intact rock specimen. The ratio of in-situ modulus and intact modulus is herein referred to as a Modulus Ratio. The intact modulus may be determined either by a static or dynamic test. Although a Modulus Ratio based on static field and laboratory tests is more acceptable from a theoretical point of view, it may be advantageous in some instances to define the intact modulus by using a dynamic test.

The dynamic modulus is determined from laboratory velocity measurements by the relationship:

$$E_{\text{dyn}} = \rho V_p^2 \frac{(1 + \nu)(1 - 2\nu)}{(1 - \nu)} \quad (14.1)$$

where  $\rho$  is the mass density,  $V_p$  the primary wave velocity, and  $\nu$  the value of Poisson's ratio. The appropriate Poisson's ratio may be estimated from laboratory static measurements or field dynamic tests which measure both the primary and shear wave velocity. Poisson's ratio is determined from velocity measurements by using the relationships:

$$a = V_p / V_s \quad (14.2)$$

and

$$\nu = \frac{a^2 - 2}{2(a^2 - 1)} \quad (14.3)$$

Figure 14.4 presents compressional and shear wave velocity measurements obtained by 3-D sonic and seismic testing. The graph shows that Poisson's ratio determined by dynamic tests is normally in the range 0.10 to 0.33. A value of 0.25 is assumed to be typical.

Figure 14.5 shows the relationship between dynamic moduli and static moduli for intact rock specimens from sites reported herein. The static moduli

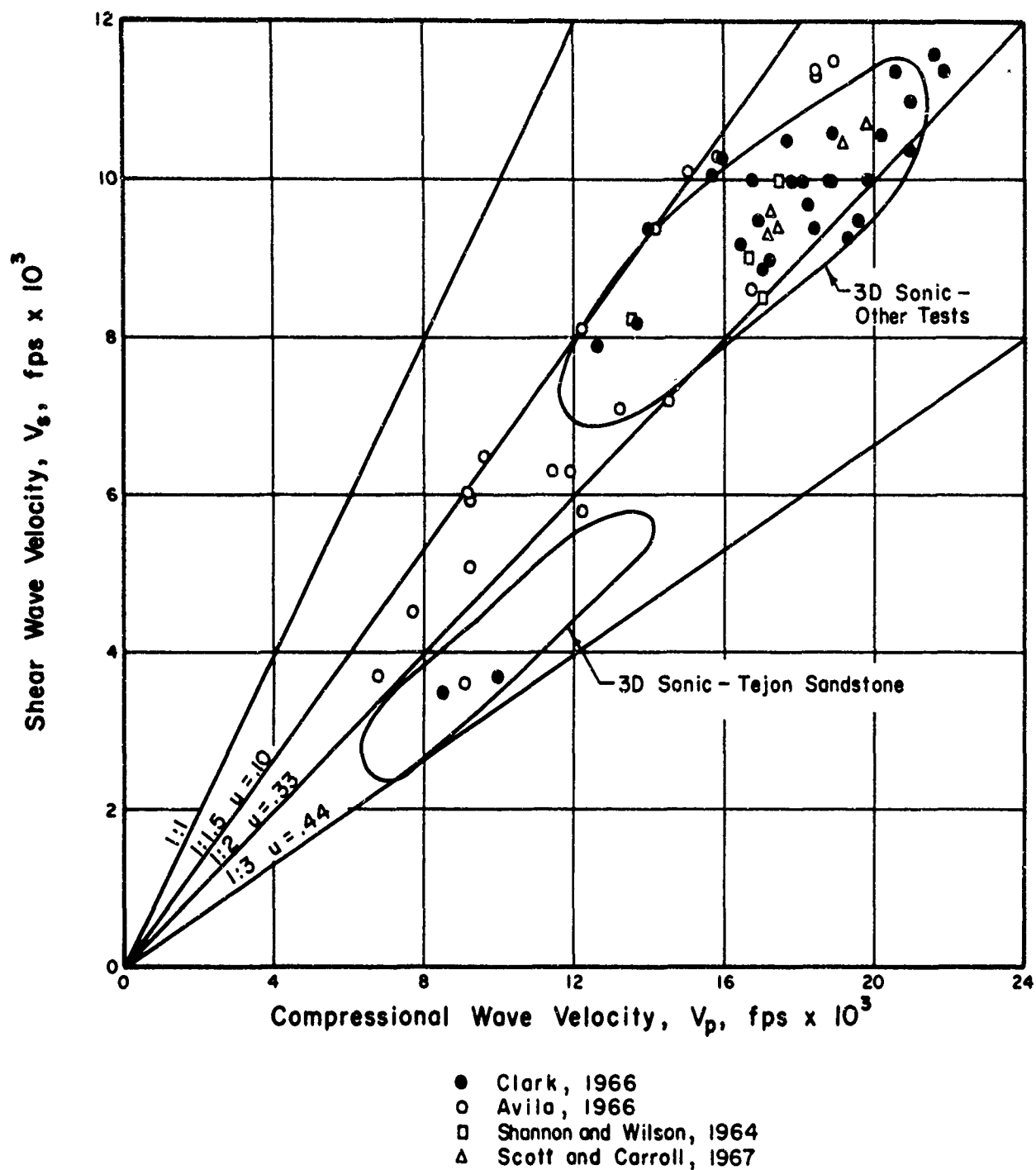


FIG. 14.4 COMPARISON OF IN-SITU PRIMARY WAVE AND SHEAR WAVE VELOCITY

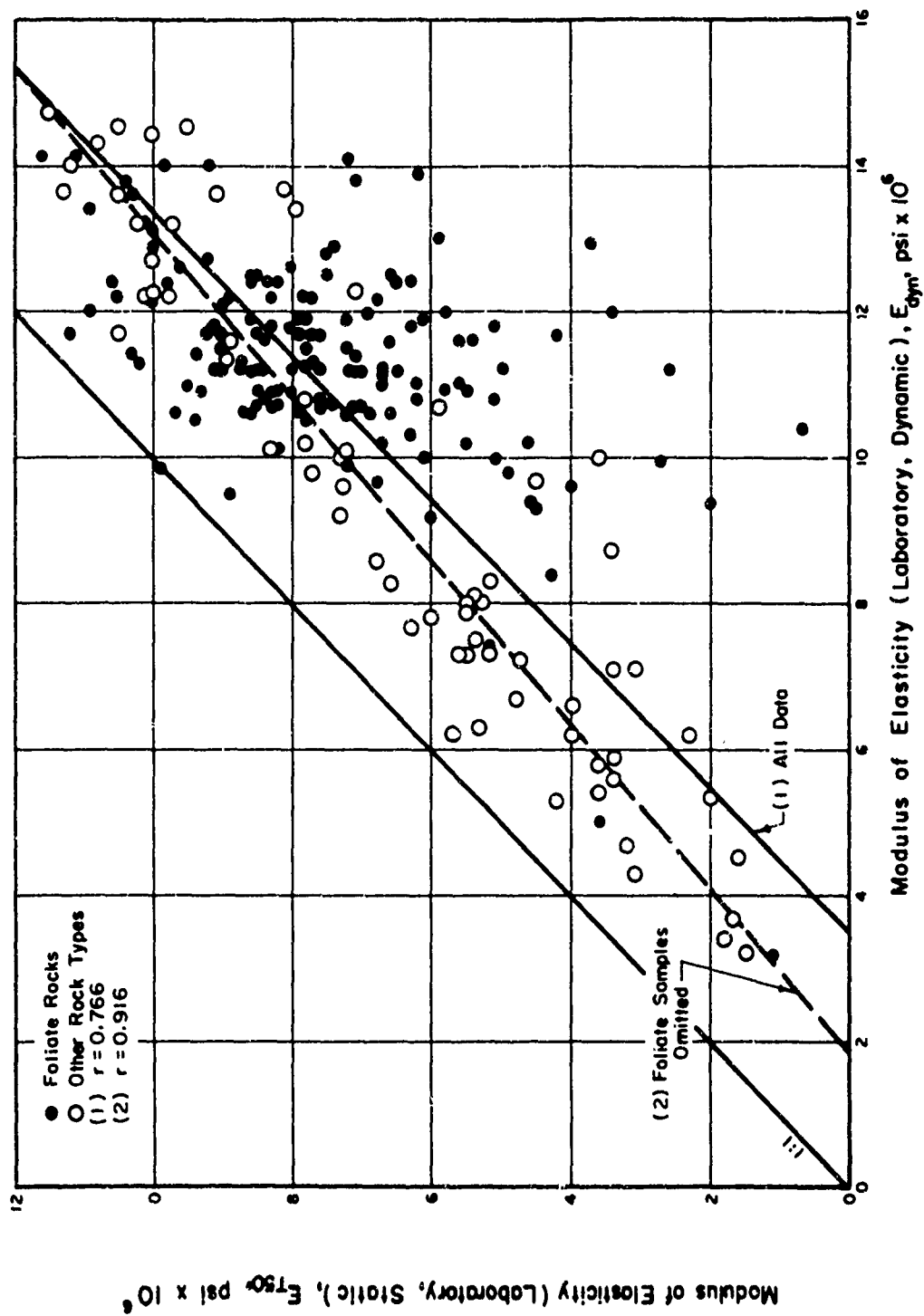


FIG. 14.5 COMPARISON OF LABORATORY STATIC AND DYNAMIC MODULI

was defined by the slope of the tangent to the stress-strain curve at 50 percent of the unconfined strength,  $E_{t50}$  (Deere and Miller, 1966). The coefficient of correlation for all data is  $r = 0.766$ . An examination of the data shows that the degree of correlation is lowered by the foliate rock samples which form a near vertical band with a dynamic modulus of from 10 to  $14 \times 10^6$  psi. The poor relationship is probably caused by variations in the foliation which have a significant effect on the static modulus but produce only minor changes in the dynamic modulus. The dynamic moduli are higher than the static moduli due to the difference in rate of loading and the load intensity. The dashed correlation line was determined by considering only the nonfoliate rock samples. The correlation coefficient for these samples is 0.916. Figure 14.5 shows that the laboratory dynamic moduli are generally 1 to  $6 \times 10^6$  psi higher than corresponding static moduli. Modulus Ratios calculated from dynamic laboratory tests will therefore be lower than those using static moduli. For this reason the two types of Modulus Ratios should not be plotted together to develop a correlation with rock quality. However, the relationship between the two laboratory moduli is sufficiently good to use the two Modulus Ratios to develop separate correlation graphs.

The preceding discussion suggests the possibility of constructing a number of graphs correlating rock quality and in-situ deformation. Two indices of rock quality, RQD and Velocity Index, can each be related to four Modulus Ratios,  $E_d/E_{t50}$ ,  $E_d/E_{dyn}$ ,  $E_e/E_{t50}$ , and  $E_e/E_{dyn}$ . The moduli  $E_d$  and  $E_e$  are respectively the modulus of deformation and modulus of elasticity of the in-situ static test. The  $E_{dyn}$  and  $E_{t50}$  are respectively the laboratory dynamic and static moduli. Each of the RQD methods discussed in Section 3 have been compared with the Modulus Ratios and it was concluded that the RQD with a base length of 0.35 ft has a slightly superior correlation. The relationships between RQD and the Velocity Index with the four modulus ratios are presented in Figures 14.6 to 14.13.

The graphs using RQD to define rock quality (Figures 14.6 to 14.9) have correlation coefficients ranging from 0.238 to 0.566, while the values for Velocity Index (Figures 14.10 to 14.13) range from 0.306 to 0.440. The superior correlation for the RQD method is probably the result of the weighing technique used in the RQD method and the fact that all seismic measurements represent the average dynamic modulus of a rock mass much larger than the rock affected by the static test. For this reason the graphs do not conclusively

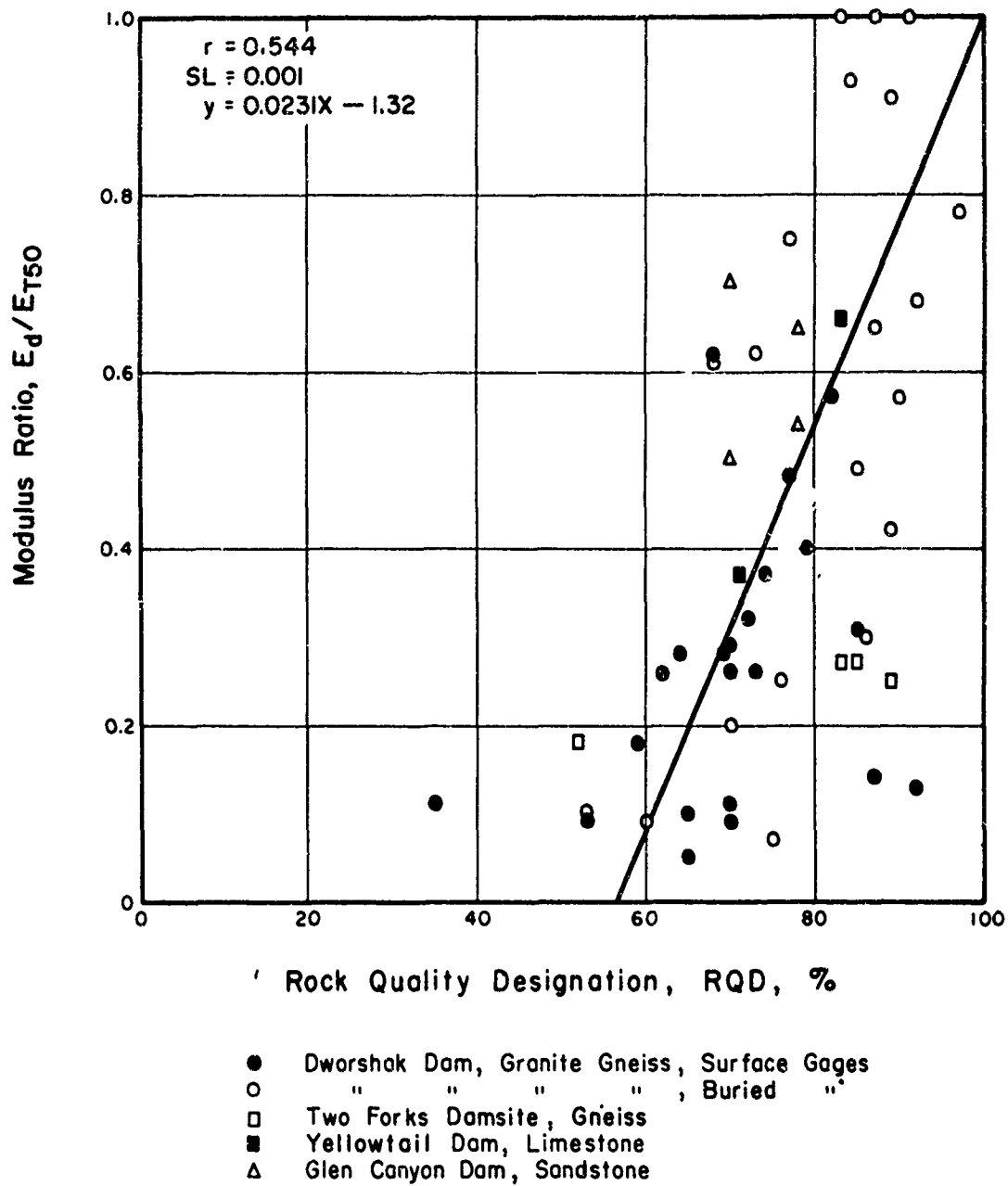


FIG. 14.6 VARIATION OF MODULUS RATIO,  $E_d/E_{T50}$ , WITH ROCK QUALITY DESIGNATION



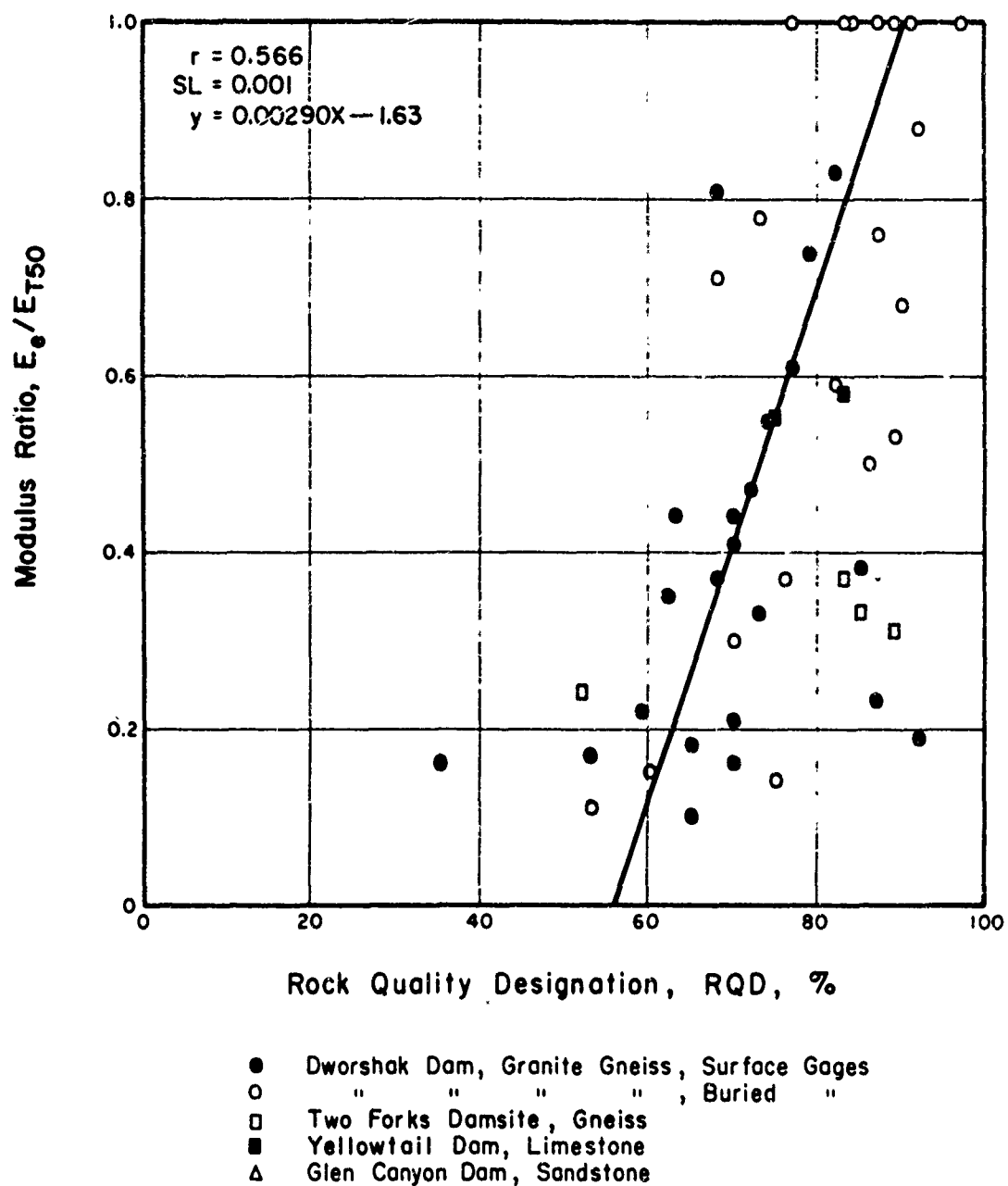


FIG. 14.7 VARIATION OF MODULUS RATIO,  $E_e/E_{T50}$ , WITH ROCK QUALITY DESIGNATION

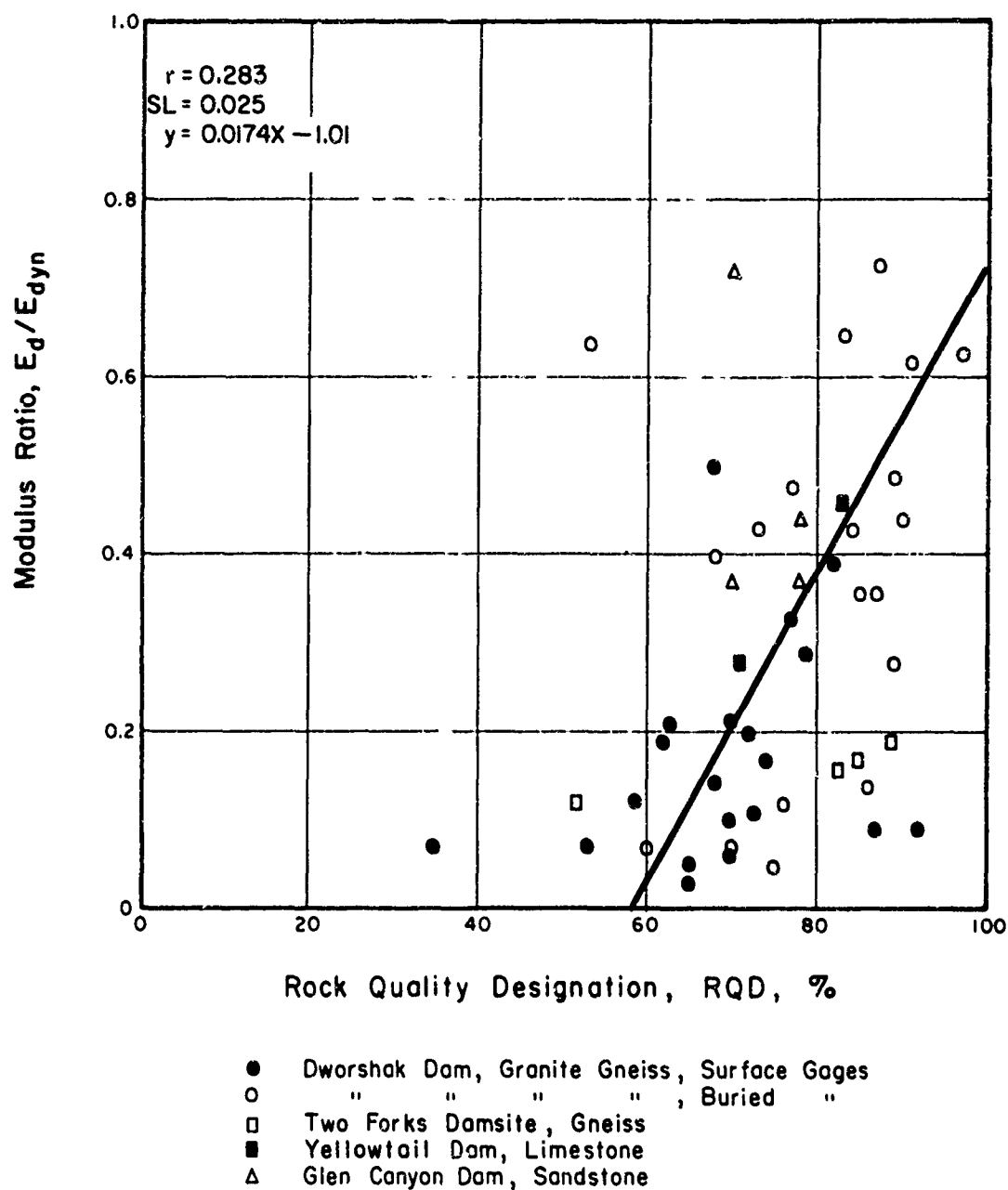


FIG. 14.8 VARIATION OF MODULUS RATIO,  $E_d/E_{dyn}$  WITH ROCK QUALITY DESIGNATION

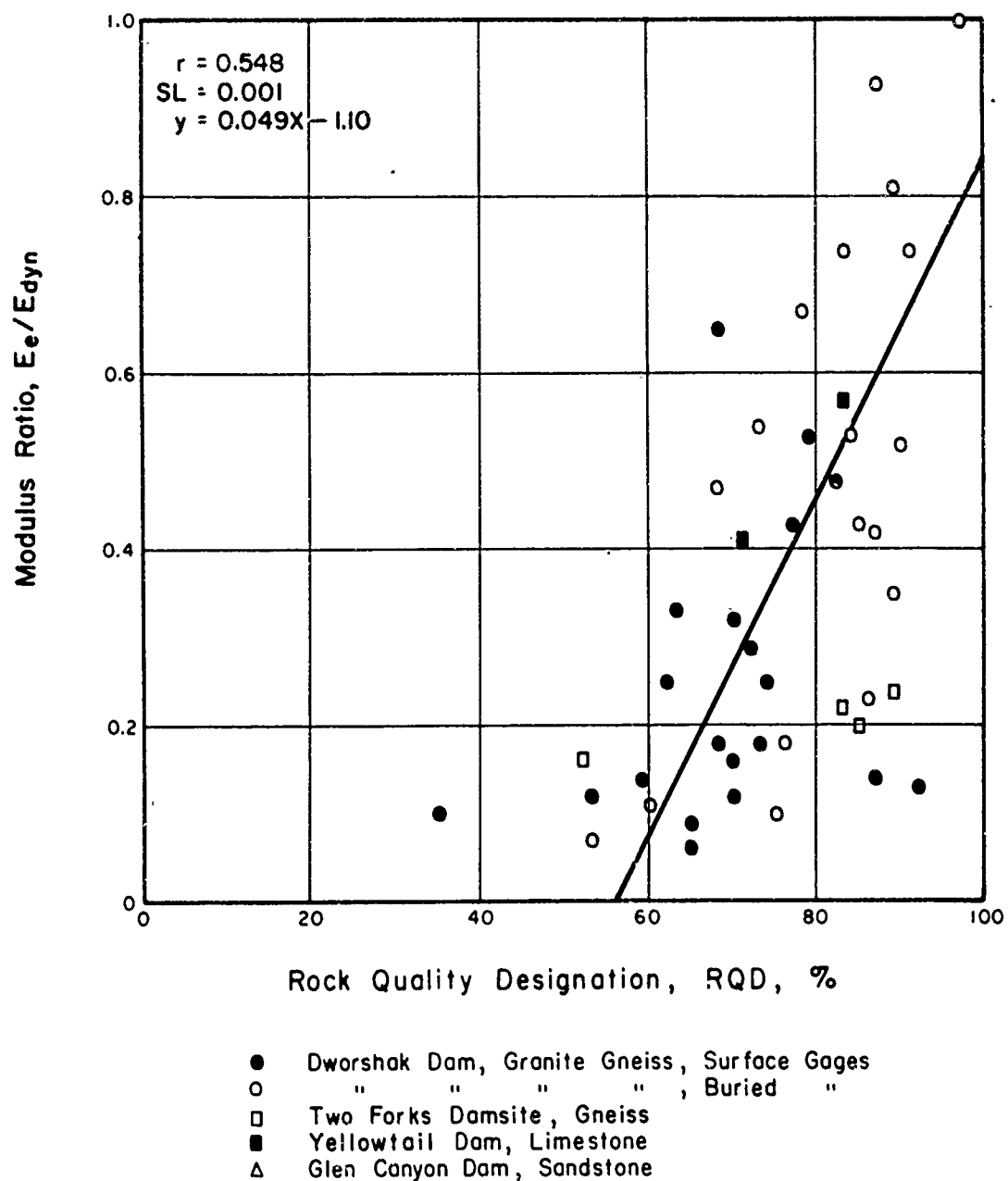


FIG.14.9 VARIATION OF MODULUS RATIO,  $E_e/E_{dyn}$  WITH ROCK QUALITY DESIGNATION

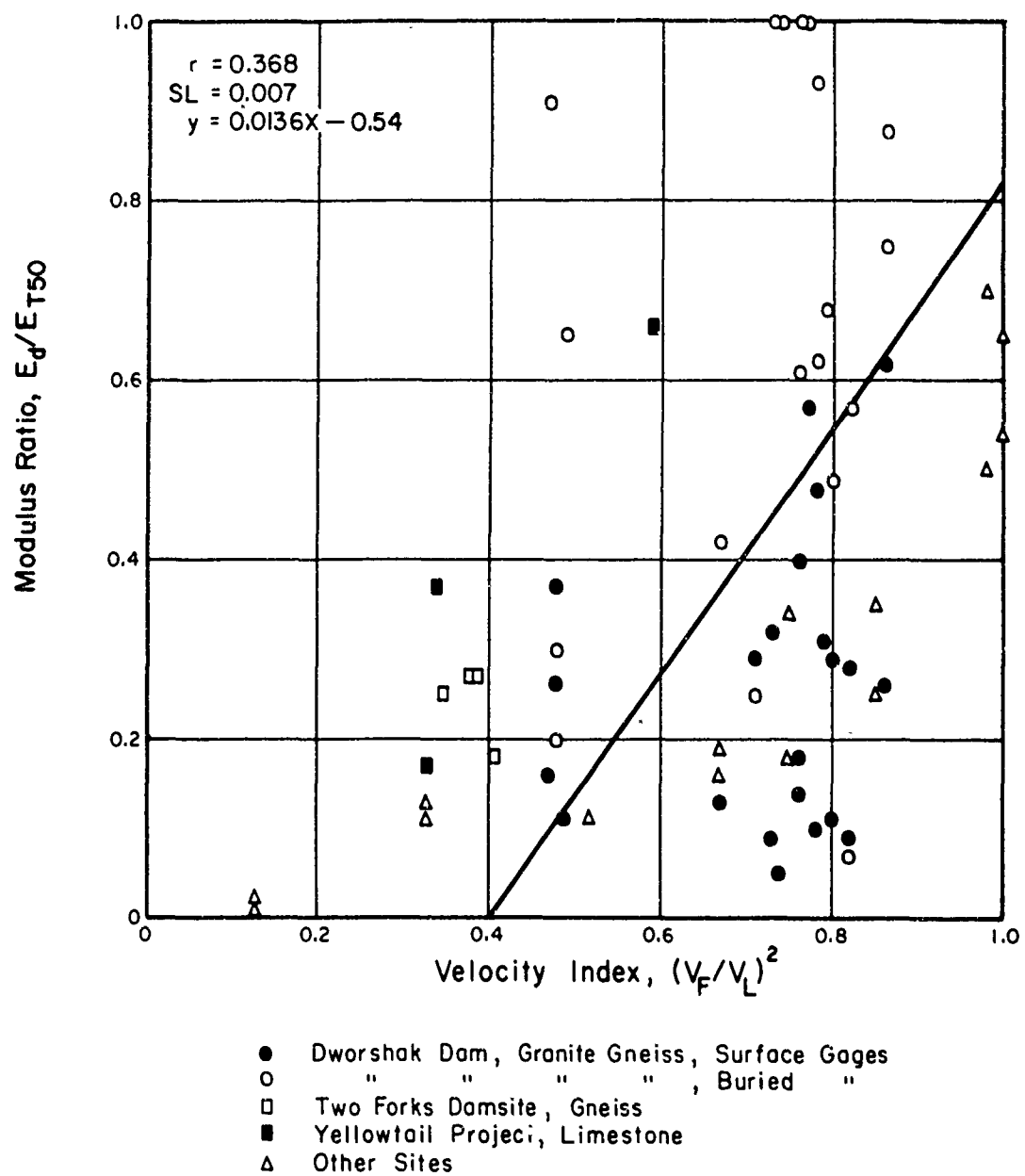


FIG. 14.10 VARIATION OF MODULUS RATIO,  $E_d/E_{T50}$ , WITH VELOCITY INDEX

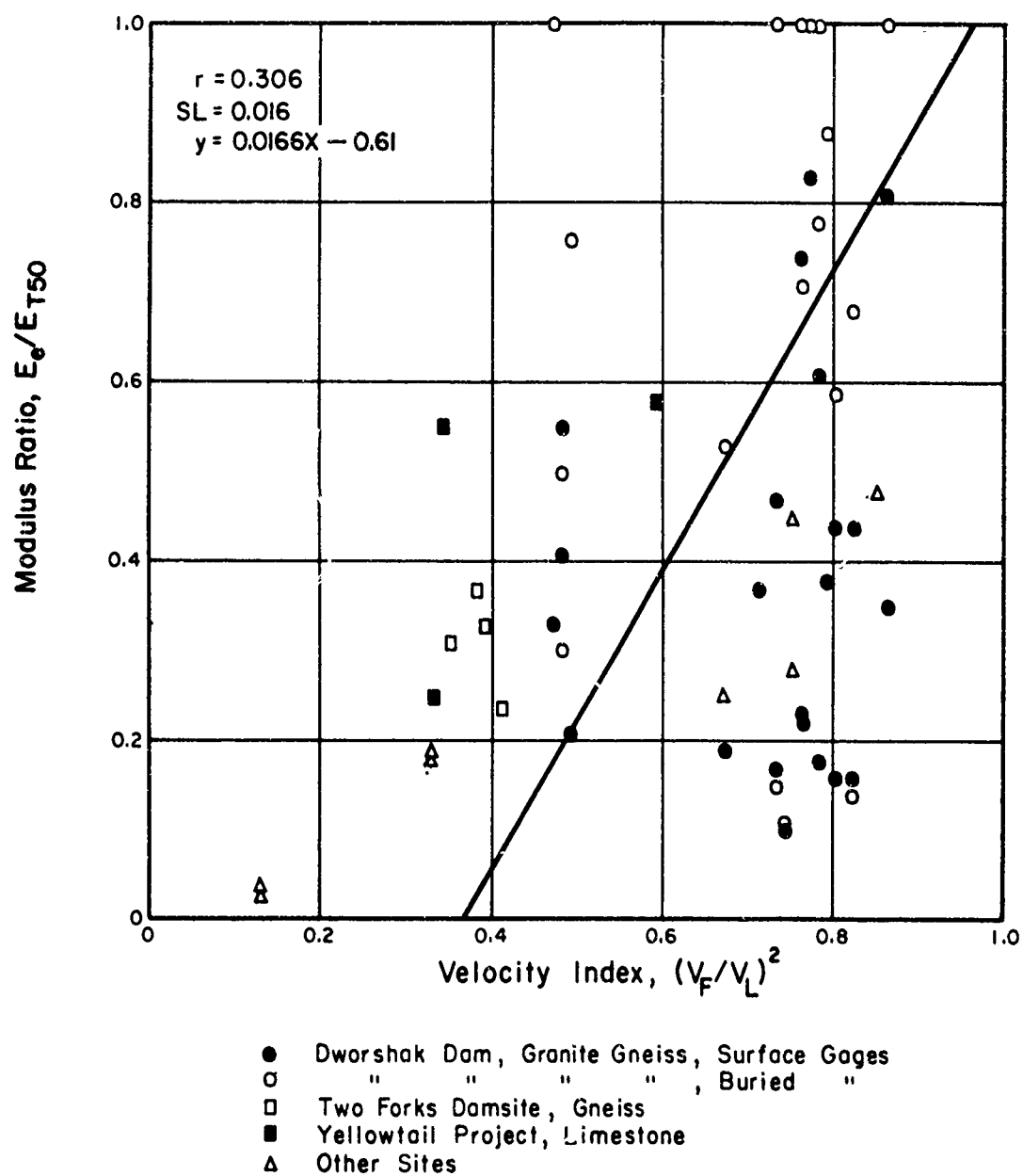


FIG. 14.11 VARIATION OF MODULUS RATIO,  $E_e/E_{T50}$ , WITH VELOCITY INDEX

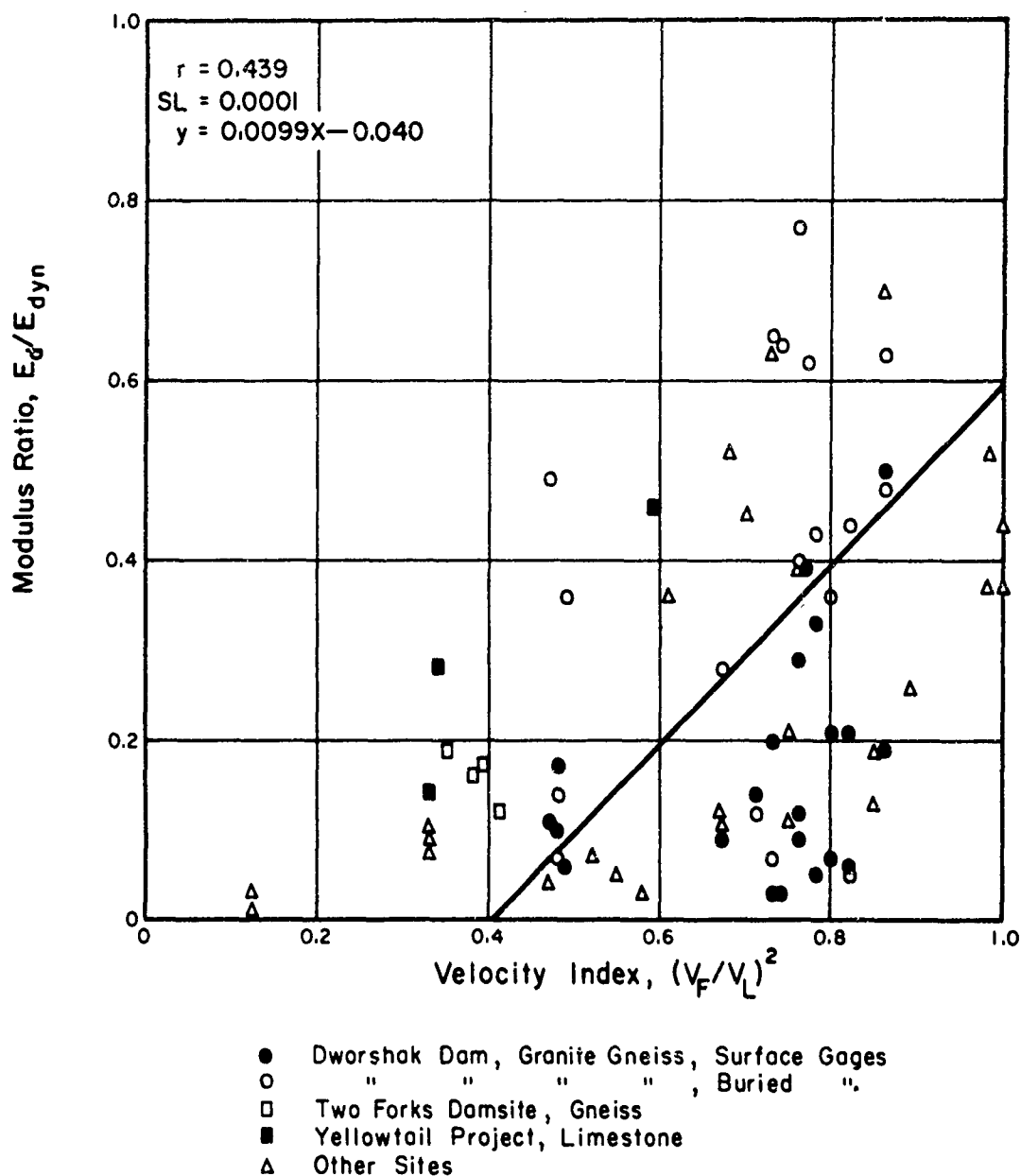


FIG. 14.12 VARIATION OF MODULUS RATIO,  $E_d/E_{dyn}$ , WITH VELOCITY INDEX

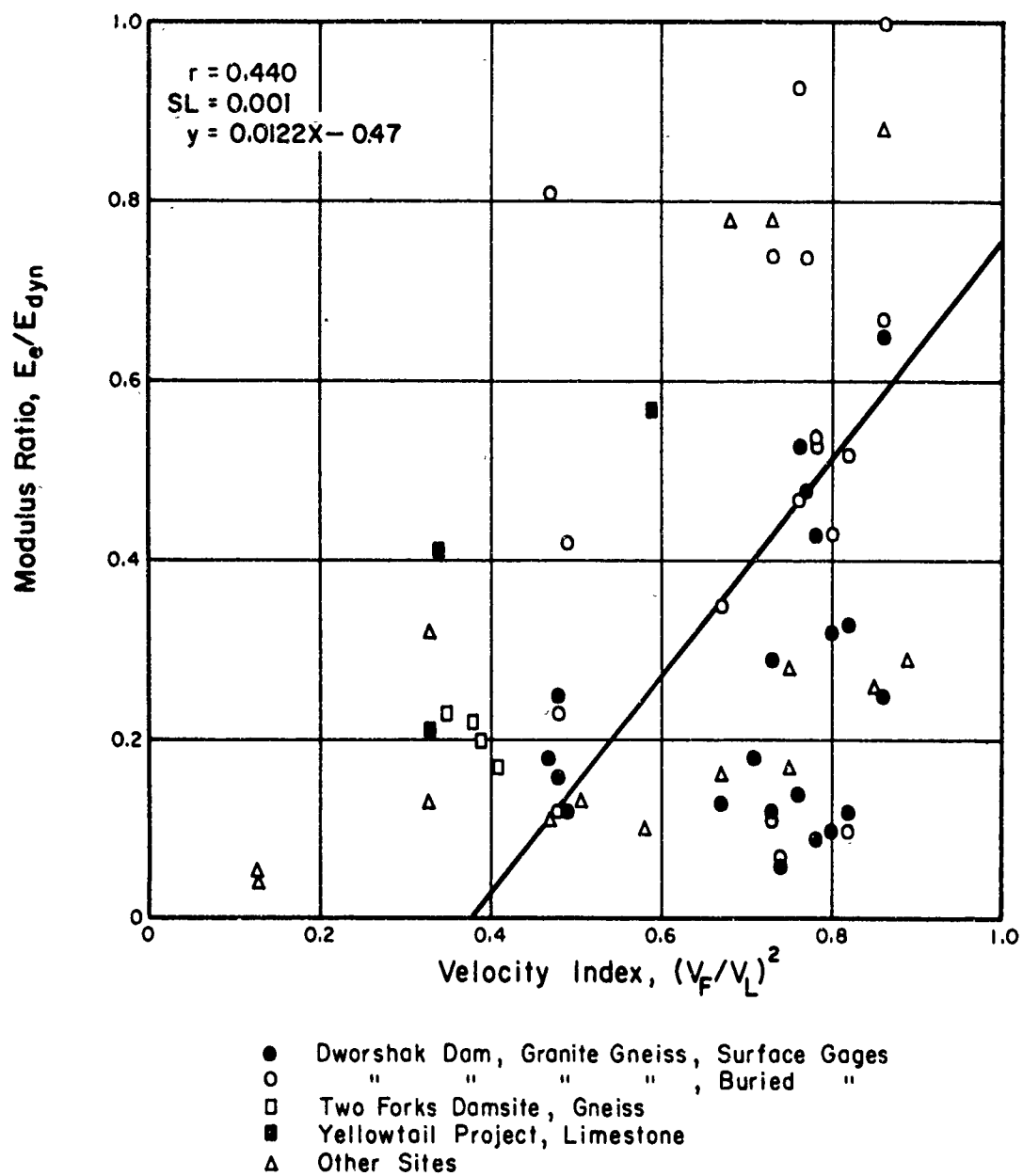


FIG. 14.13 VARIATION OF MODULUS RATIO,  $E_e/E_{dyn}$ , WITH VELOCITY INDEX

show that the RQD method is superior to the Velocity Index, but it is possible to state that the RQD method is superior to the Velocity Index determined by conventional seismic tests.

Three jack test borings at Dworshak were logged by the 3D sonic method in an attempt to obtain dynamic measurements on a scale representative of the rock loaded by the jack test. The results of this logging are not included in the Velocity Index graphs as the first useable measurements were obtained when the sonde was five feet from the surface. As the first five feet are the most critical, this sonic logger is not adequate for this type of testing. A sonic sonde with a shorter transmitter-receiver spacing (possibly a foot long) might provide the kind of detailed dynamic measurements required. Seismic uphole and cross-hole measurements using short test intervals and high-speed recording units might also provide the detailed dynamic measurements required.

Three of the graphs that compare RQD and various Modulus Ratios have similar correlation coefficients. The graphs of  $E_d/E_{t50}$ ,  $E_e/E_{t50}$ , and  $E_e/E_{dyn}$  (Figures 14.6, 14.7, and 14.9) have correlation coefficients of 0.544, 0.566, and 0.548, respectively. In each case the correlation line starts near a Modulus Ratio of 1.00 and an RQD of 100 percent and extends to a modulus ratio of zero and an RQD of approximately 60 percent. It appears that any one of the three Modulus Ratios can be used with RQD measurements.

#### 4. The Deformation Ratio

The ratio of elastic deformation to total deformation determined from the load-deformation curves of static test, herein termed the Deformation Ratio, is suggested by Deere et al. (1967) as an index property of the rock mass. This property cannot be used to predict in-situ moduli, but it can be useful in comparing in-situ test results. In Figure 14.14 the deformation modulus is plotted against the Deformation Ratio and in Figure 14.15 the modulus of elasticity versus the Deformation Ratio is given. Both graphs contain data from plate jack tests at Dworshak, Tehachapi, Two Forks, and Yellowtail. A good relationship is noted in each case, but correlation for the modulus of elasticity is superior. Figures 14.16 and 14.17 are plots of  $E_d$  versus Deformation Ratio and  $E_e$  versus Deformation Ratio, respectively, for additional testing reported in the literature. Considerable scatter is found in each of these graphs, but there is some indication of zoning by rock type. These relationships show that as the rock



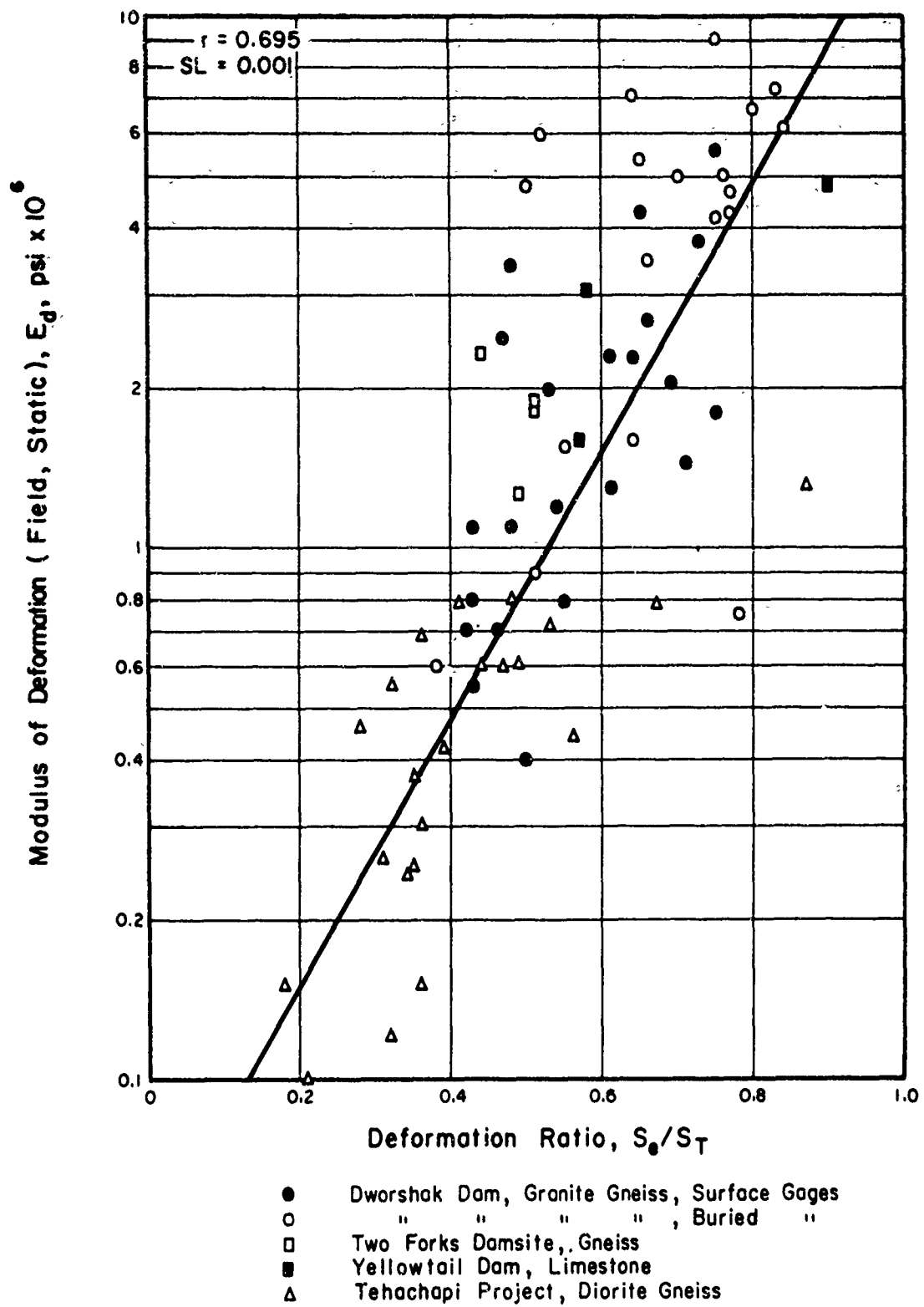


FIG. 14.14 COMPARISON OF IN-SITU STATIC MODULUS OF DEFORMATION AND DEFORMATION RATIO (PROJECT SITES)

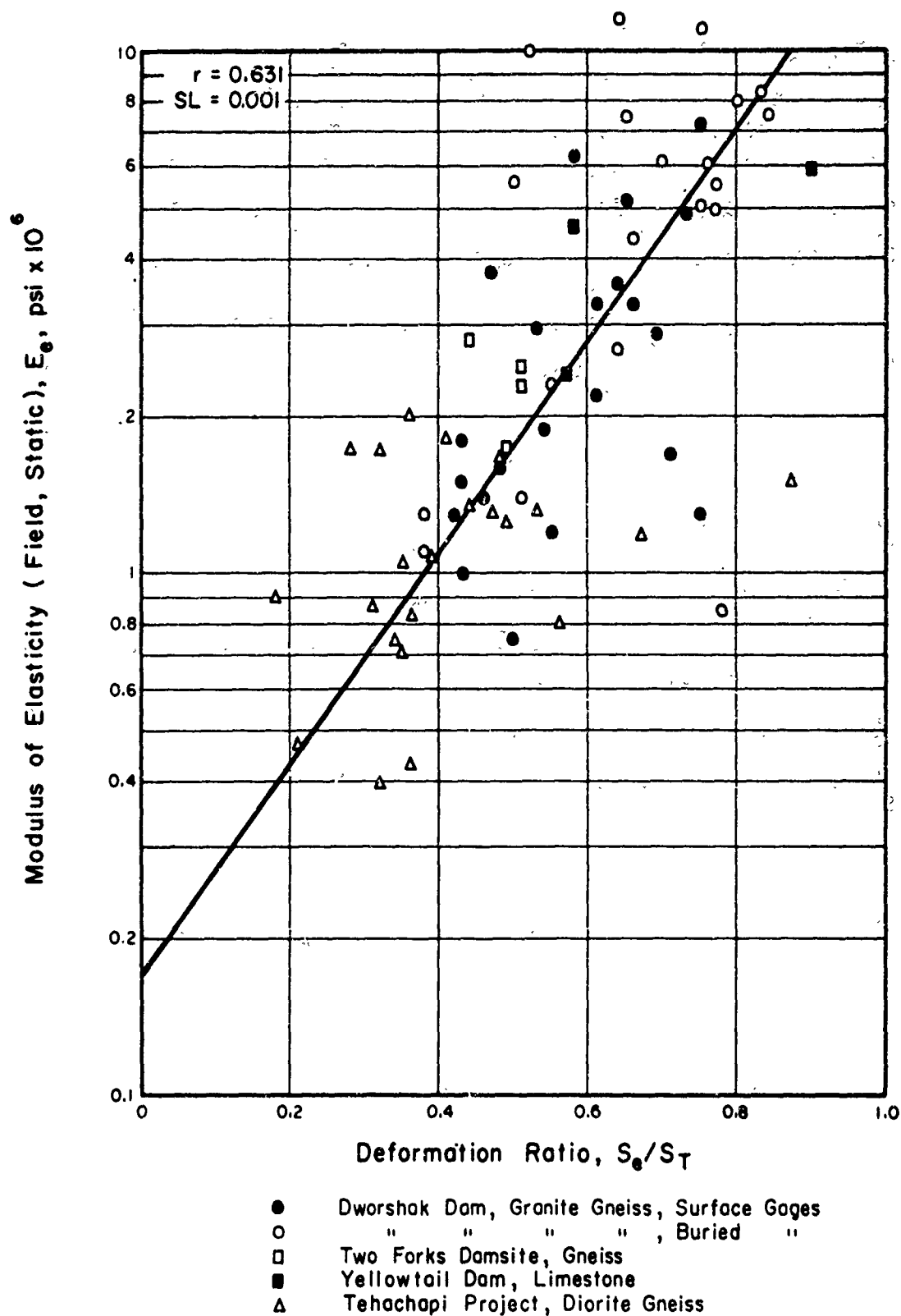


FIG. 14.15 COMPARISON OF IN-SITU STATIC MODULUS OF ELASTICITY AND DEFORMATION RATIO (PROJECT SITES)

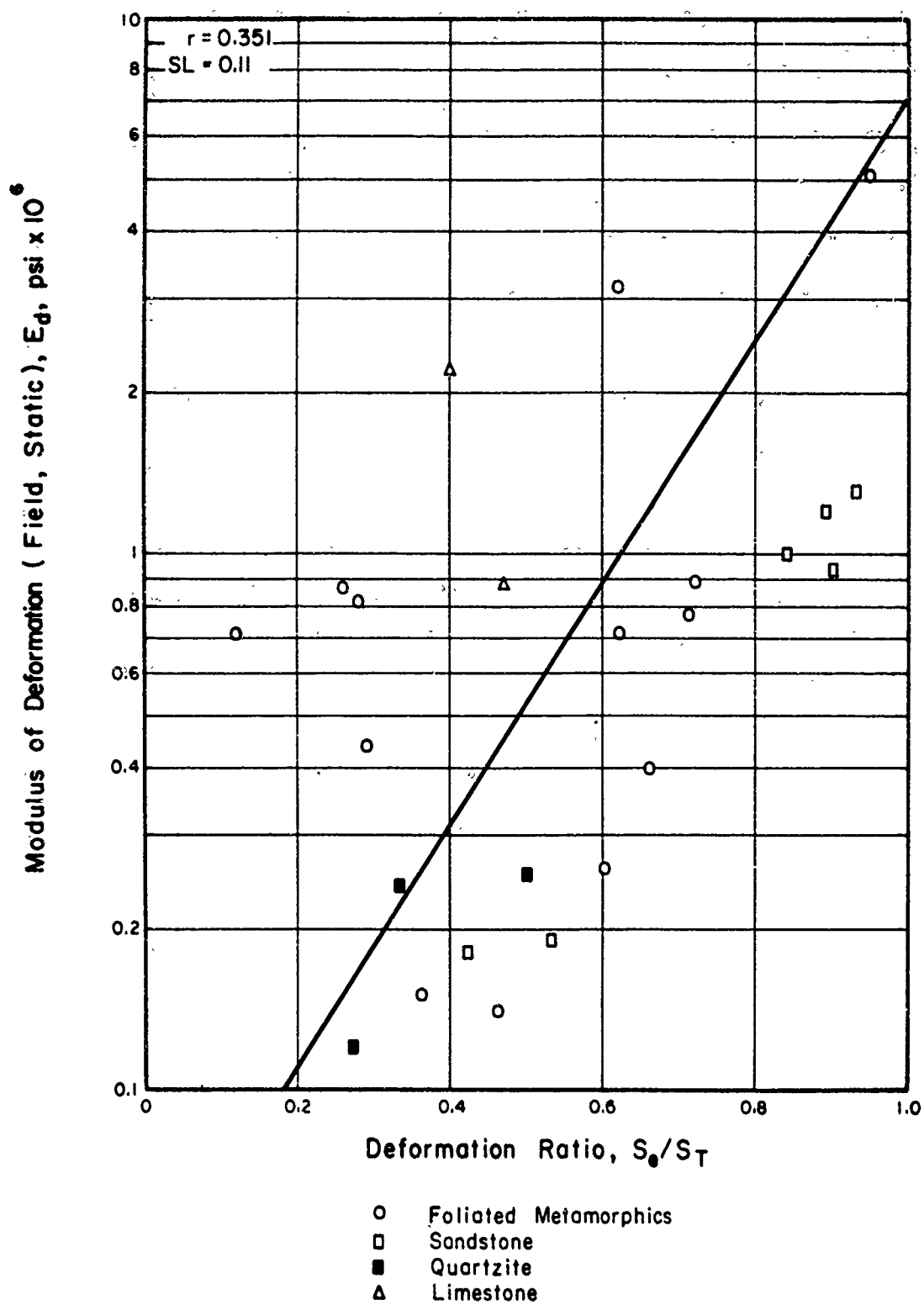


FIG. 14.16 COMPARISON OF IN-SITU STATIC MODULUS OF DEFORMATION AND DEFORMATION RATIO (OTHER SITES)

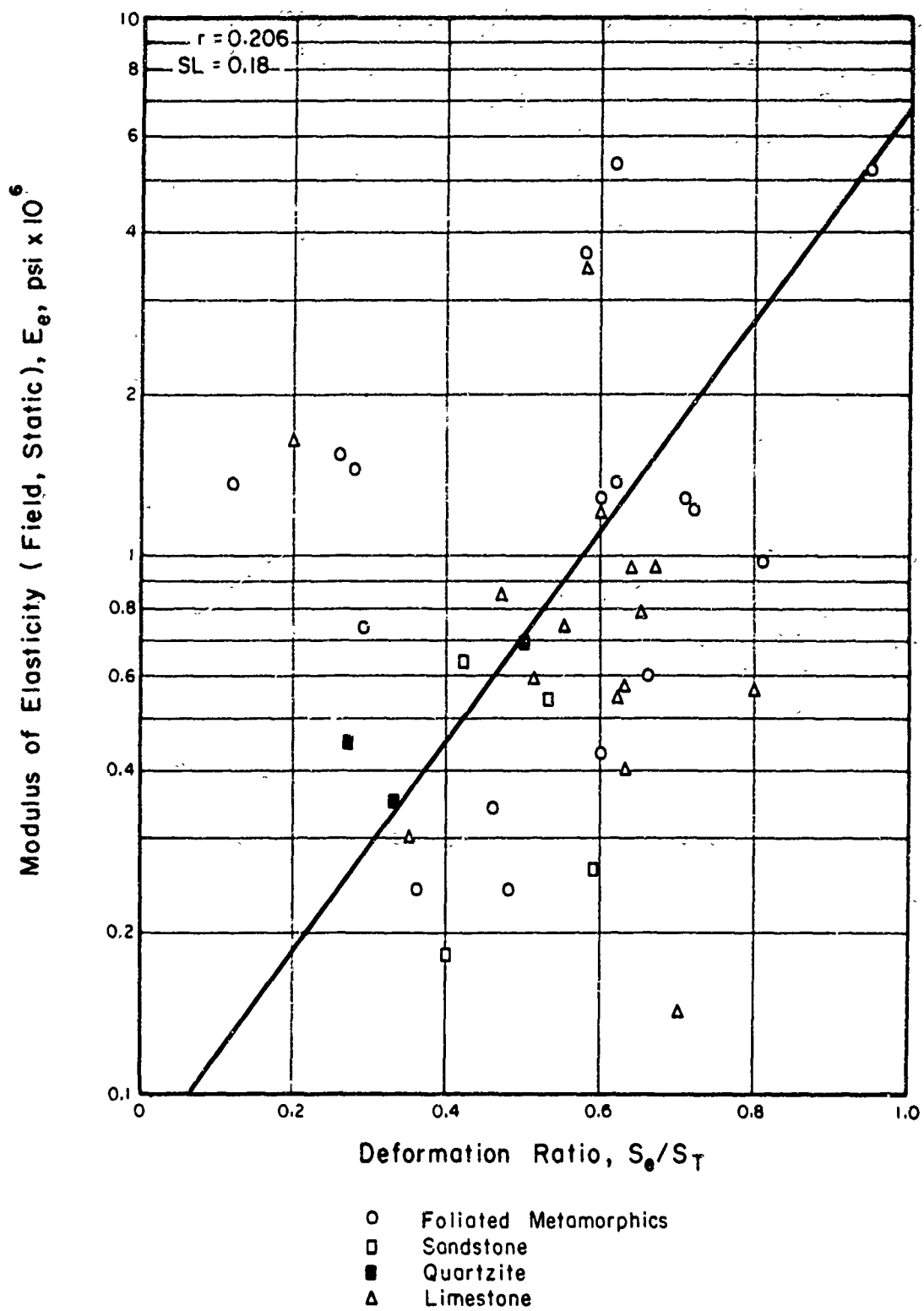


FIG. 14.17 COMPARISON OF IN-SITU STATIC MODULUS OF ELASTICITY AND DEFORMATION RATIO (OTHER SITES)

quality and in-situ modulus increase the elastic deformations form a greater portion of the total deformation measured in an in-situ test.

The deformation ratio may be useful in two ways. First, it can provide a means of comparing static tests. If the majority of tests show a consistent relationship between the calculated modulus and the deformation ratio, tests falling outside this trend might be checked for inadequate site preparation equipment malfunction, or incorrect data analysis. In addition, correlations between the other rock quality indices and the deformation ratio might be of assistance in estimating the long term deformation characteristics of the rock mass. Figure 14.18 is a graph of the Deformation Ratio versus RQD for Dworshak, Tehachapi, Two Forks, and Yellowtail. The fair correlation between the Deformation Ratio and the RQD indicates that the RQD could be used to estimate the plastic deformation caused by long-term loading and possibly the set caused by cyclic loading.



SECTION 15  
MEASUREMENT OF DEFORMATION CAUSED  
BY ENGINEERING STRUCTURES

1. Introduction

Deformation adjacent to engineering structures is measured to determine if foundation deformations are within design assumptions, and to gain advance warning of hazardous conditions indicated by large deformations or increases in the rate of deformation. Many large concrete dams have instruments within the dam or the foundation for measuring deformations and displacements. A few large buildings are now being instrumented for this purpose. Displacements are also measured in deep excavations such as spillways, dams, and the walls of large underground openings such as machine halls, power plants, and defense structures.

The deformations of in-situ rock caused by engineering structures provide the ultimate test of the validity of in-situ static test results. After examining methods of measuring deformation associated with structures, a summary of comparisons between the moduli calculated from observations in and beneath the structure and in-situ test moduli is presented.

2. Deformation Measurements Within the Structure

a. Absolute Displacement Measurements - Geodetic Method

The geodetic method is essentially the application of precise surveying techniques to determine movement of structures or rock surfaces. Horizontal movements are determined by precise triangulation, and vertical movements are measured by leveling. The position of fixed points is determined with precision from 0.5 to 1.0 mm, and the relative position of fixed points from 0.2 to 0.4 mm.

The major problem in using this technique at some sites is the difficulty of finding a fixed point from which the absolute movements can be measured. In the case of large dams, it has been found that the loads imposed by the reservoir can cause deformations which extend well beyond the site. At Sakuma dam, which created the largest reservoir in Japan, significant deformations caused by the dam and reservoir were measured two kilometers from the site by using a bench mark five kilometers away (Japanese National Committee on Large Dams, 1958). The measurement of absolute deformation within an underground

opening is often impractical because movements associated with the formation of the distressed zone make it difficult to establish fixed bench marks. Absolute displacements can be measured by establishing a bench mark outside the underground opening (Dodd, 1967) or by using fixed reference points in drill holes behind the distressed zone (Cording, 1967).

The geodetic method is very precise, but the time consuming calculations required somewhat limit its application. The use of automatic data processing promises to extend the usefulness of this technique.

#### b. Relative Displacements

The most commonly mentioned instruments for measuring relative displacement are strain meters, pendulums, and collimeters. Collimation uses a narrow beam of light aimed at a fixed or movable target to accurately measure relative movements up to several hundred feet. Pendulums in vertical tubes extending from the crest to the heel of a dam can be used to note lateral movements. Strain gages placed within the concrete or spanning joints in the concrete are used for the stress distribution within the structure.

### 3. Deformation Measurements Within the Rock Mass

The most useful measurements to the rock mechanics engineer are those made near the base of the dam by instruments buried in the foundation rock or spanning the concrete-rock contact. The Bureau of Reclamation has used three types of deformation gages in monitoring foundation deformations at Davis, Yellowtail, and Glen Canyon dams (Rauch et al., 1965).

At Davis Dam, mechanical deformation gages were installed in NX borings, from a gallery in the base of the dam to a depth of from 144 to 256 feet. The thickness of concrete and rock in these holes was not given. Each boring was cased to within a short distance of the bottom so that foundation grouting would not affect the measurements. The deformation gage consisted of the following: (1) an anchor in the form of a pipe reducer, (2) a three-fourth inch galvanized gage pipe, and (3) two gage heads. The gage pipe spanned the interval from the grouted anchor at the bottom of the hole and the floor of the gallery. One gage head was attached to the top of the gage pipe while the other was attached to the gallery floor. A precision dial gage was used to measure the gap between the gage heads.

This installation was simple, relatively inexpensive, and seemed to give consistent readings. Its major disadvantage was that concrete deformations



were included in all readings, and it was not possible to evaluate rock deformations accurately.

To overcome this disadvantage of the Davis Dam installation, the Yellowtail gages employed a Carlson jointmeter instead of a dial gage so that the entire gage could be installed in a foundation boring. The gages were mounted in uncased NX borings 20, 40, and 60 ft deep, with the jointmeter grouted in the boring just below the rock surface. The jointmeter cables pass through the concrete to measurement stations in the lower galleries of the dam. This type of installation also gave consistent readings except for one gage which showed exceptionally low deformation. It is likely that the gage hole was at least partly filled by the foundation grouting and the readings are not representative of deformations within the rock.

In the abutment tunnels at Glen Canyon Dam, the Bureau of Reclamation used specially mounted surveyor's tapes to measure the lateral deformation caused by the thrust of the dam. One end of the tape was fixed solidly to the wall of the tunnel. The other end was attached to a spring loaded yoke which was constructed so that a constant tension in the tape would be maintained despite changes in the distance between the two supports. Measurements from this type of installation were used to determine if grouting of the joints between monoliths was required.

Rock movements adjacent to underground openings can be measured by devices similar in principle to deformation gages. As the movements represent an increase in rock volume, i.e., the movements are positive, the devices are commonly called extensometers.

The simplest form of an extensometer consists of a gage rod anchored at the end of a boring and extending to the wall of the tunnel. At the wall, the rod passes into a gage head which is a short cylinder wedged or grouted in the end of the hole. Because the outer surface of the gage head is used as a reference for displacement measurements, it is normally machined. The gage rod is cut so that its outer end is within gage head and accurate measurements of its position can be made with a feeler gage.

This type of installation is inexpensive and rugged enough to be reliable even in a construction area. One limitation of this type of gage is that the displacements can be obtained from only one gage length. If the displacements at several depths are required, a group of extensometers of various lengths must be installed.

The multiple position borehole extensometer (MPBX) marketed by Terrametrics Inc., was developed to allow measurement of displacement on several gage lengths in the same boring (Hartman, 1965). The instrument consists of 8 flat wedge-spring type anchors connected to the surface by high modulus wires, and a measuring head containing 8 stainless steel cantilevers. The device is installed so each anchor is attached to one cantilever and the cantilevers are prestressed so that both positive and negative movements can be recorded. Movements of the cantilever are measured by linearly variable electrical transducers. The instrument is capable of measuring movements of plus or minus 0.4 inch with a sensitivity of 0.001 inch. The anchors may be set at any depth up to 200 ft.

A second type of multiple-position extensometer was developed by the Slope Indicator Co. of Seattle, Washington, and Professor D. U. Deere of the University of Illinois for measuring displacements in underground openings at the Nevada Test Site (Cording, 1966). The instrument uses 4 to 6 grouted anchors connected to the surface by steel wire. At the surface each wire is connected to a potentiometer pulley through a constant tension spring. The advantages of this instrument are constant cable tension and a measurement range of 2 inches.

#### 4. Comparison of Deformation Moduli from In-Situ Tests and Observations of Structures

While the literature provides an abundance of deformation records, very few articles present modulus values and compare them with in-situ test values. Possible reasons for this are explained in the following paragraphs.

While it is comparatively easy to obtain deformation measurements which show the vertical and horizontal movements of the monolith of a dam or the inward movements of the walls of an underground opening, it is difficult to obtain more than an estimate of the loads which caused the deformation. In the case of a monolith of a dam, a number of forces other than the weight of the concrete can be responsible for the movements. The thrust of the water behind the dam is an obvious factor which has to be considered. In most cases, this force is variable as the reservoir level fluctuates because of changes in run-off or water supply demands. In a structure as large as a dam, the thermal changes can also cause significant movements. Finally geologic factors such as

rock mass movements and earthquakes can produce movements of the structure which are difficult to evaluate.

A second complicating factor is that structures are generally rigid and the differential settlements observed do not fully represent the relative compressibility of zones in the foundation. As the more compressible areas begin to deform under a uniform loading, a part of the load is shifted to the less compressible zones. Unless this stress redistribution can be estimated, the modulus of the poor zones will be overestimated and that of the good zones will be underestimated.

Despite these problems some comparisons are presented in the literature. Figure 15.1 shows the computed modulus from displacement observations of structures versus modulus of deformation from field tests. (See Appendix A, Sites 85, 87, 88, 90, 91, 93, 94, 95, 97, 99). Over half of the field test moduli are within plus or minus 100 percent of the calculated moduli. In most instances, this accuracy is sufficient. Three of the four plate jack values underestimated the deformability of the foundation and design based on these tests would be conservative. The one pressure chamber value underestimates the foundation modulus by a factor of five. Borehole deformation tests are the most numerous test type on the graph and, also, the most consistent with the foundation moduli. However, several points show that the test may give values higher than the calculated foundation modulus. The two seismic tests overestimated the foundation modulus by a factor of three to four.

Although the data presented is very limited, the test moduli are zoned as was suggested earlier. In the order of increasing values of modulus, the pressure chamber value is one of the lowest, the plate jack modulus next, followed by borehole deformation values, and the seismic moduli are the highest. The foundation modulus is in the range between the borehole deformation and plate jack moduli although the data are too few to allow for meaningful comparisons.

Displacements measured in underground openings are summarized in Table 15.1. In general, the displacements are much greater than the movements predicated from elastic theory. Cording (1966) shows that the movements observed include an elastic portion which is approximately equal to displacements predicted by elastic theory, and both shallow and deepseated displacements along geologic discontinuities which are often an order of magnitude larger than the elastic movements. Static in-situ tests can predict only the elastic part of these deformations and would, therefore, predict the minimum displacements.

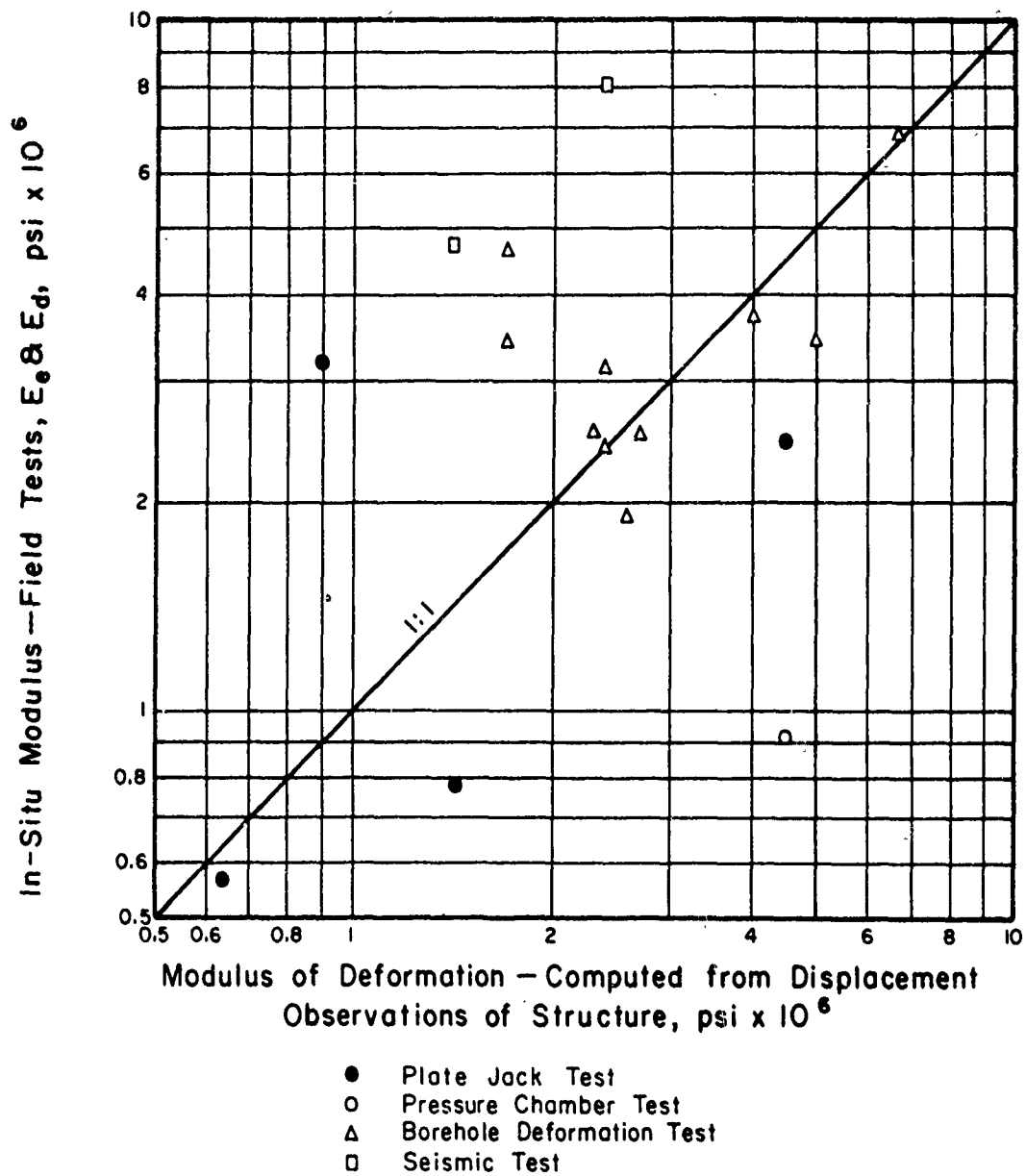


FIG.15.1 COMPARISON OF IN-SITU TEST MODULUS AND MODULUS COMPUTED FROM DISPLACEMENT OBSERVATIONS OF STRUCTURES

TABLE 15.1  
COMPARISON OF PREDICTED AND ACTUAL MOVEMENTS IN  
UNDERGROUND OPENINGS  
(Data from Cording, 1966)

Project	Rock	Length ft	Width ft	Height ft	Depth ft	Movements from Elastic Theory in.	Actual Movements	Type of Opening
Kariba Dam Rhodesia Myaswland	gneiss	468	75	132	200	0.15	generally greater than 0.5 in. (1.5 in. fault zone)	machine hall
Morrow Pt.	schist	206	57	134	400	0.05	0.02 - 0.35 in. (2 in. near fault)	machine hall
Picote	granite		53	115	260		Calculated modulus of deformation 30% to 100% of labora- tory static modulus	power plant
NTS Cavity 1	Tuff	100 diam.		140	1300	0.50	Approximately as predicted but locally larger	test chamber
2	Tuff	100 diam.		140	1300	0.50	Approximately as predicted but locally larger	test chamber
3	granite	60 diam.		80	350	0.02	Approximately as predicted but locally larger	test chamber

SECTION 16  
CORRELATION OF ROCK QUALITY AND RATE OF  
CONSTRUCTION OF TUNNELS

1. Introduction

The rate of construction of tunnels is important to both project designers and contractors. The designer must be able to estimate the rate of construction in order to plan completion dates for other portions of the project. Contractors must be able to estimate the rate of construction in order to plan equipment and personnel requirements. Both groups presently estimate the rate of progress on the basis of past experience, and a qualitative estimate of the rock conditions to be encountered. Conservative estimates are the rule because of the high degree of variation between projects, both in the quality of the rock encountered and the construction techniques used.

The projects considered in this section are tunnels driven by conventional drilling and blasting techniques. Tunnels driven by large diameter drills or moles and large underground openings excavated in stages are beyond the scope of the present study.

The conventional method of driving underground openings consists of five steps: (1) drilling, (2) loading, (3) blasting, (4) venting, and (5) mucking. The entire sequence is called a round. The drilling step is the most important as it determines to a great extent the success of the round. The number, depth, and spacing of holes drilled depends upon the size of the opening and the ability of the blast to loosen the rock efficiently. A drilling pattern may consist of from 20 to well over 100 holes with the holes ranging in depth from 5 to 12 ft. An efficient round will break the rock to within 1 ft of the back of the holes. Therefore, the advance per round should be just a little less than the length of the drill holes. In the loading step, explosives and primers are connected by lead wires to the detonator a safe distance down the tunnel. The charge is set off and the tunnel is vented (usually by forced air circulation) until the workers can return to the face area. The fifth and final step is the removal of the debris or muck created by the blast. Installation of supports is generally done during the drilling step of the next round.

The rate at which the face of an underground excavation can be advanced depends upon the time required to complete the five steps and the length of the round. Both the length of the round and the efficiency of the cycle depend on the quality of the rock mass. In higher quality rock, the support systems are less complex, and therefore, there is less interference in the cycle.

However, the rate of advance also depends upon other factors not related to the rock quality. The size of the tunnel limits the amount of working room at the face and, thus, determines the size of the crew and the type of drilling and mucking equipment which can be used. Tunnel size also determines the amount of drilling required. The time required for each round is also controlled by the capacity of the equipment used and the proficiency of the crews.

On sites where the rock quality changes rapidly, the ability of the contractor to change his blasting and support techniques can have a pronounced effect upon the average rate of advance. The contractor's response time to changing rock conditions is certainly influenced by his experience and the variety of equipment and supports he has on hand. The most important factor, however, is the accuracy of predictions of the rock quality ahead of the working face.

With such a variety of factors influencing the rate of advance, the job of estimating rates of construction requires considerable experience and judgment. If the quality of the rock mass could be expressed quantitatively, it would provide a frame of reference to aid in making these predictions, and would assist in evaluating the effectiveness of a construction technique at different sites. This section presents three case histories: (1) a shaft in metamorphic rock, (2) two tunnels in gneiss, and (3) a pilot tunnel in granite and metamorphics. In each case, the rock quality is compared with the rate of advance.

## 2. Case History No. 1: Shaft in Schist, East Coast

This site provides an excellent opportunity to compare rate of construction with RQD. The upper 475 ft of the 16 ft diameter shaft followed an NX exploration core boring. Construction records provided information on shaft progress and type of construction operation for each shift. The case history

is even more useful because the shaft was driven in a wide range of rock qualities (poor to excellent) using similar sinking techniques.

The shaft was sunk by conventional drilling and blasting in schist using rounds that ranged from 4 to 6 feet. Temporary supports were limited to occasional timbers and rock bolts in bad areas as a permanent concrete lining poured in 20-ft sections was maintained as close as possible to the working face.

The first 275 ft of the shaft was driven in essentially dry rock of fair to good quality. The rate of sinking was fairly high. Below this level, zones of poor rock were encountered and with these zones, considerable groundwater inflow. Flows up to 350 gpm are shown in the construction records. The poor zones were generally at the contacts of pegmatite intrusions where the rock was crushed and altered and the adjacent rock sheared. On four to five occasions during the shaft sinking, the groundwater inflows could not be controlled by pumping, and it was necessary to stop sinking operations in order to grout the rock below the working face. Holes up to 40 ft deep were drilled below the working face and grouted to consolidate the zone ahead and seal off lateral flow. A pad of concrete up to 4-feet thick was poured in the bottom of the shaft to provide a seal for the grouting.

A comparison of rate of construction and rock quality was made for 50-ft intervals of the shaft. Fifty-foot intervals were chosen to obtain a zone short enough to be described adequately by an average RQD but long enough to obtain significant values for rate of advance. Figure 16.1 is a plot of RQD and the average rate of advance in feet per shift using the total number of sinking and grouting shifts in each fifty-foot interval. A good correlation ( $r = 0.743$ ) between the rate of progress and rock quality is obtained with the rate decreasing from nearly 2 ft per shift at an RQD of 94 percent to about 0.5 ft per shift for an RQD of 44 percent. Figure 16.2 is a plot made from the same data with the exception that the rate is calculated by using only the shifts required for sinking operations. In this case, a significant increase in the correlation is noted ( $r = 0.888$ ) as only one type of construction operation is included in the calculated rate. Figure 16.3 is a plot of the same rock quality values versus the number of grouting shifts per 50-ft interval. A negative correlation,  $r = -0.726$ , is obtained showing that rock of higher quality requires less, if any, grouting. The scatter in this plot indicates



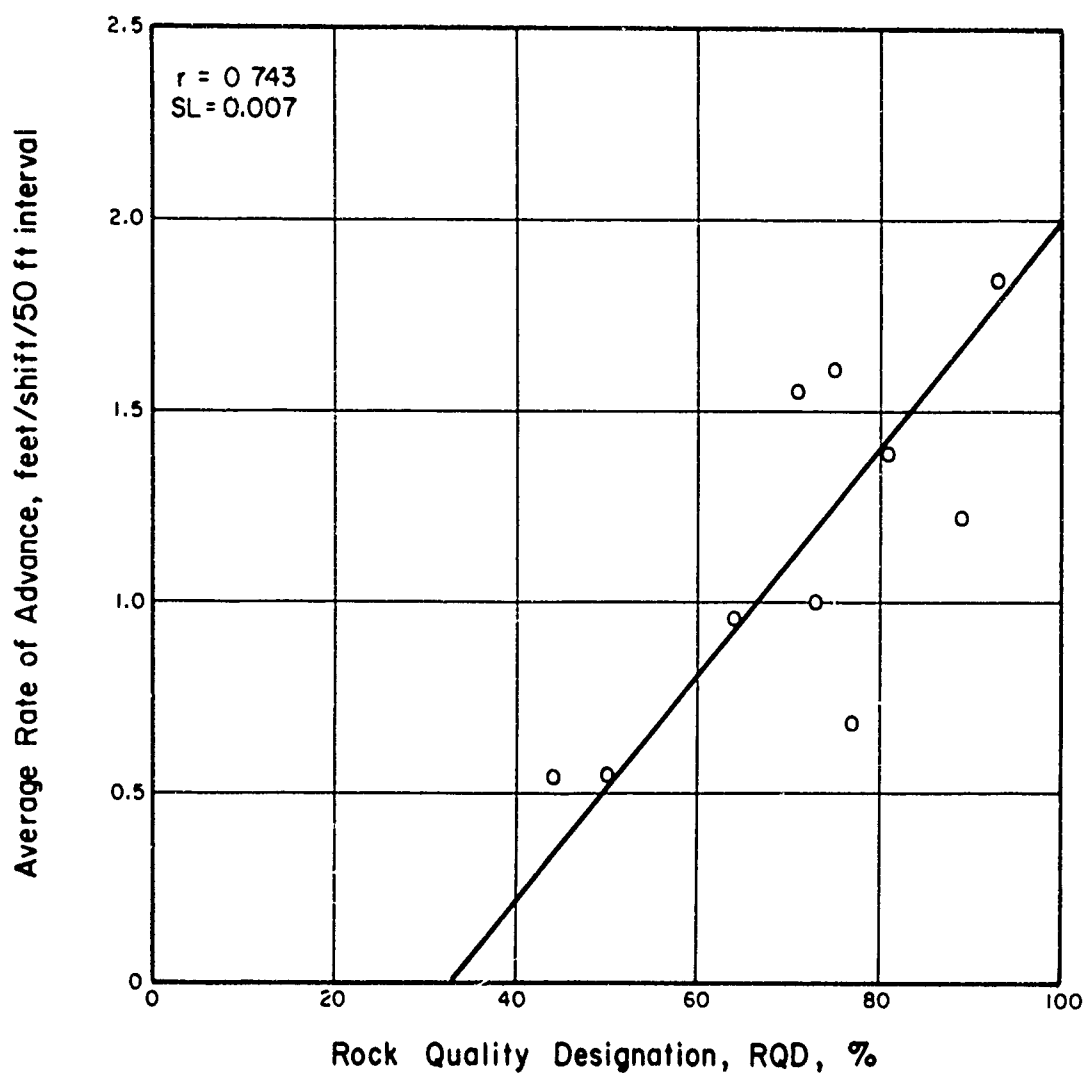


FIG. 16.1 COMPARISON OF AVERAGE RATE OF ADVANCE FOR SINKING AND GROUTING SHIFTS AND ROCK QUALITY DESIGNATION, SHAFT, EAST COAST.

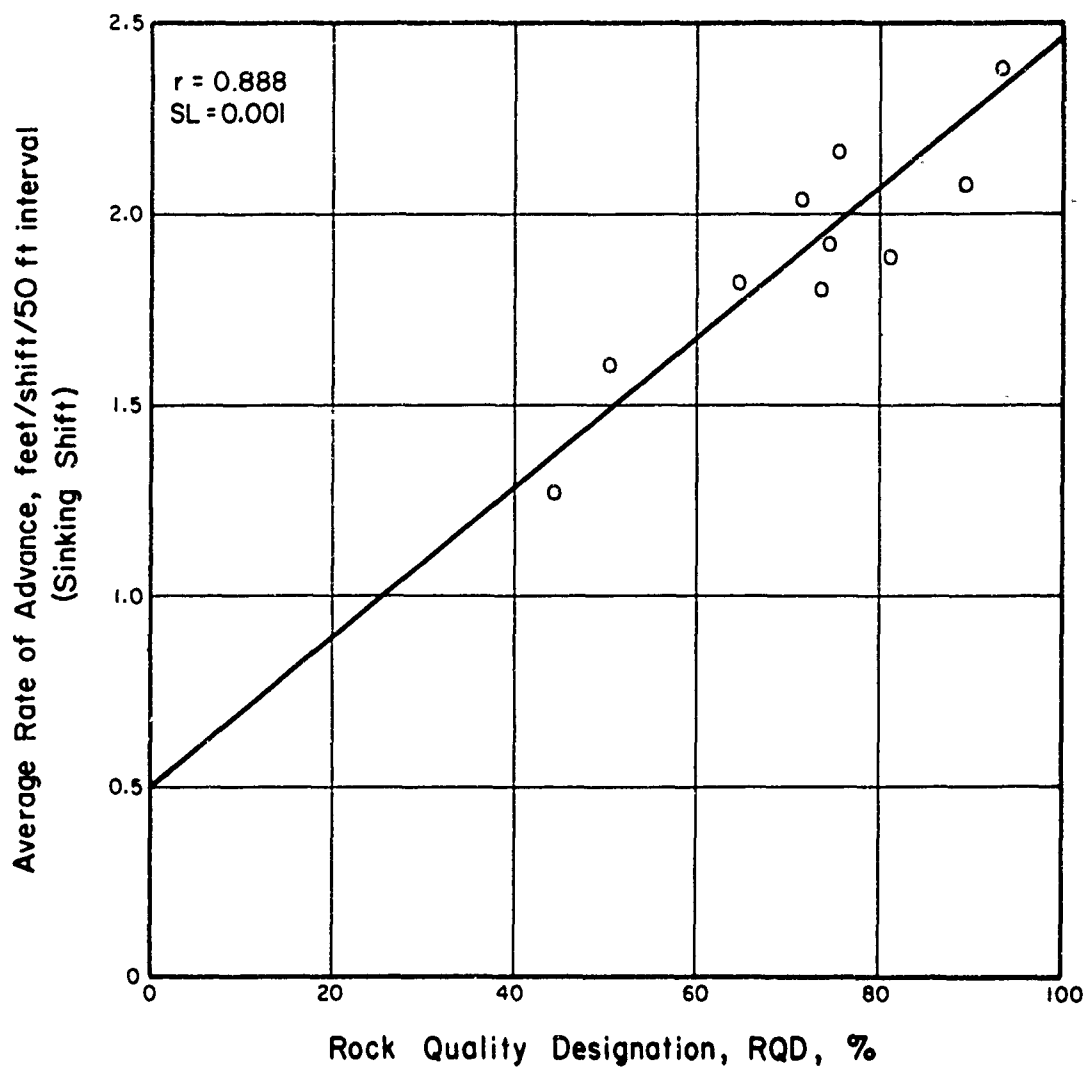


FIG. 16.2 COMPARISON OF AVERAGE RATE OF ADVANCE FOR SINKING SHIFTS AND ROCK QUALITY DESIGNATION, SHAFT, EAST COAST.

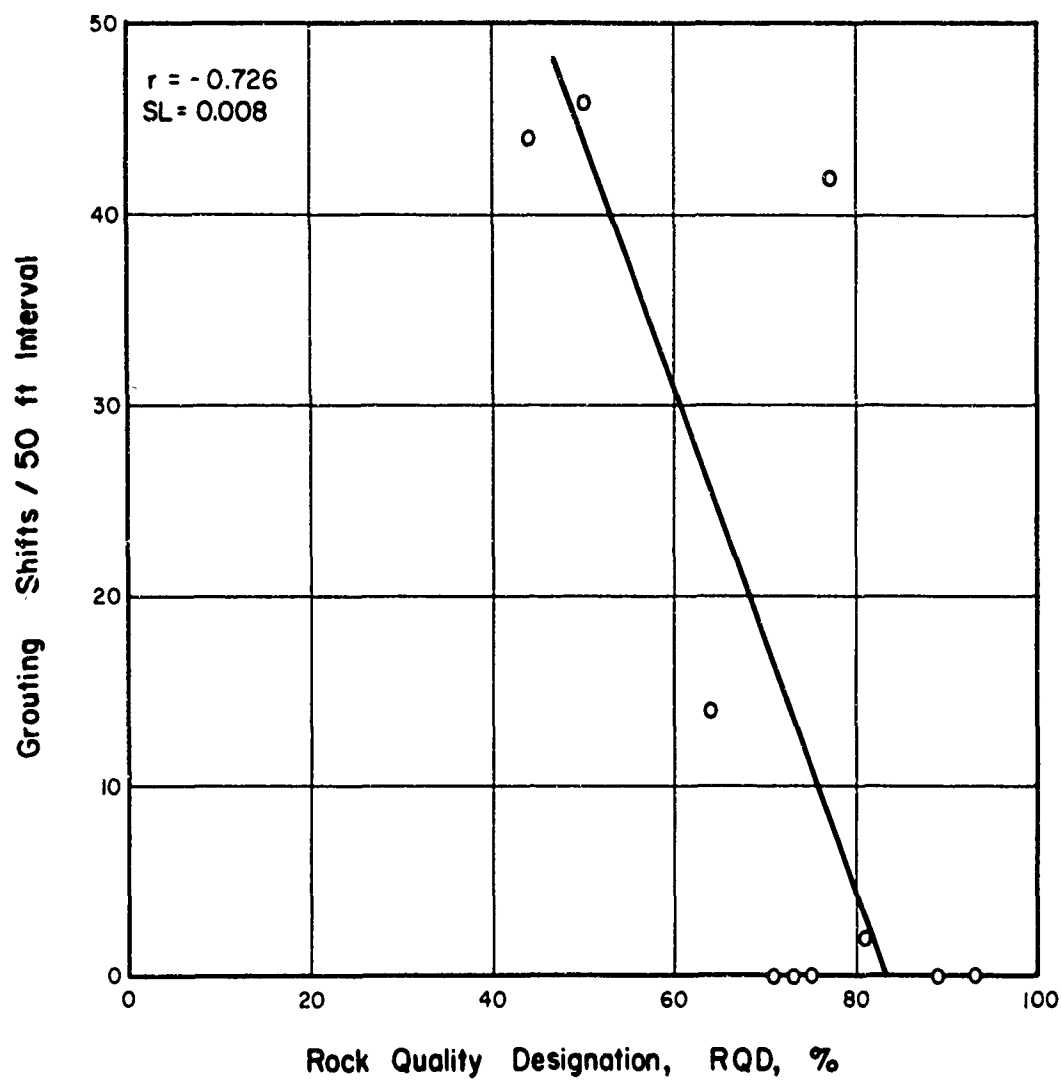


FIG. 16.3 COMPARISON OF GROUTING SHIFTS/50 FT. INTERVAL AND ROCK QUALITY DESIGNATION, SHAFT, EAST COAST.

that rock quality indices can only approximate the degree of openness in a rock mass, which, in this case, is measured by the time spent in grouting operations.

3. Case History No. 2: Tunnels No. 1 and No. 2, Tehachapi Project, California

These tunnels are part of a series of underground openings at the southern end of the California Aquaduct designed to carry the water from the San Joaquin Valley to the Los Angeles area. The geology of the two sites is similar, namely, a crystalline complex of diorite gneiss. The gneiss is variable ranging from a relatively sound rock with a wide joint spacing to intensely fractured and altered rock.

Each tunnel was driven full face by conventional drilling and blasting techniques. Tunnel No. 1, which is 21 ft high, was driven using rail-mounted equipment. The average round consisted of 73 drill holes which varied in depth from 4 to 10 ft.

Tunnel No. 2, which is 28 ft high, was driven full face using rubber-tired equipment. In zones where the rock was suitable for rock bolt support, the drilled depth was 10 to 11 ft and the average round consisted of 125 holes. In the sections supported by steel ribs, the number of holes was the same, but the length of the round was varied from 4 to 7 ft to accommodate steel sets on 3- to 6-foot centers.

The rock quality at the two sites was approximated from the number of joints observed in the tunnel wall because core borings were not available to measure the RQD. Figure 16.4 shows the relationship between the rock quality based on average joints per ten feet versus the average rate of advance expressed in feet per shift. Although there is considerable scatter in the data from both sites, the rate of tunneling generally increases as the joint frequency decreases. The average lines are approximately parallel with the line for tunnel No. 2, about eight feet per shift higher than the average line for tunnel No. 1. The higher average rates experienced in tunnel No. 2 are apparently due to the greater mobility of the rubber-tired equipment.

4. Case History No. 3: Straight Creek Tunnel Pilot Bore, Colorado

An extensive exploration program was conducted by the Colorado Department of Highways and the U.S. Geologic Survey at the Straight Creek Tunnel site approximately 55 miles west of Denver. The program included

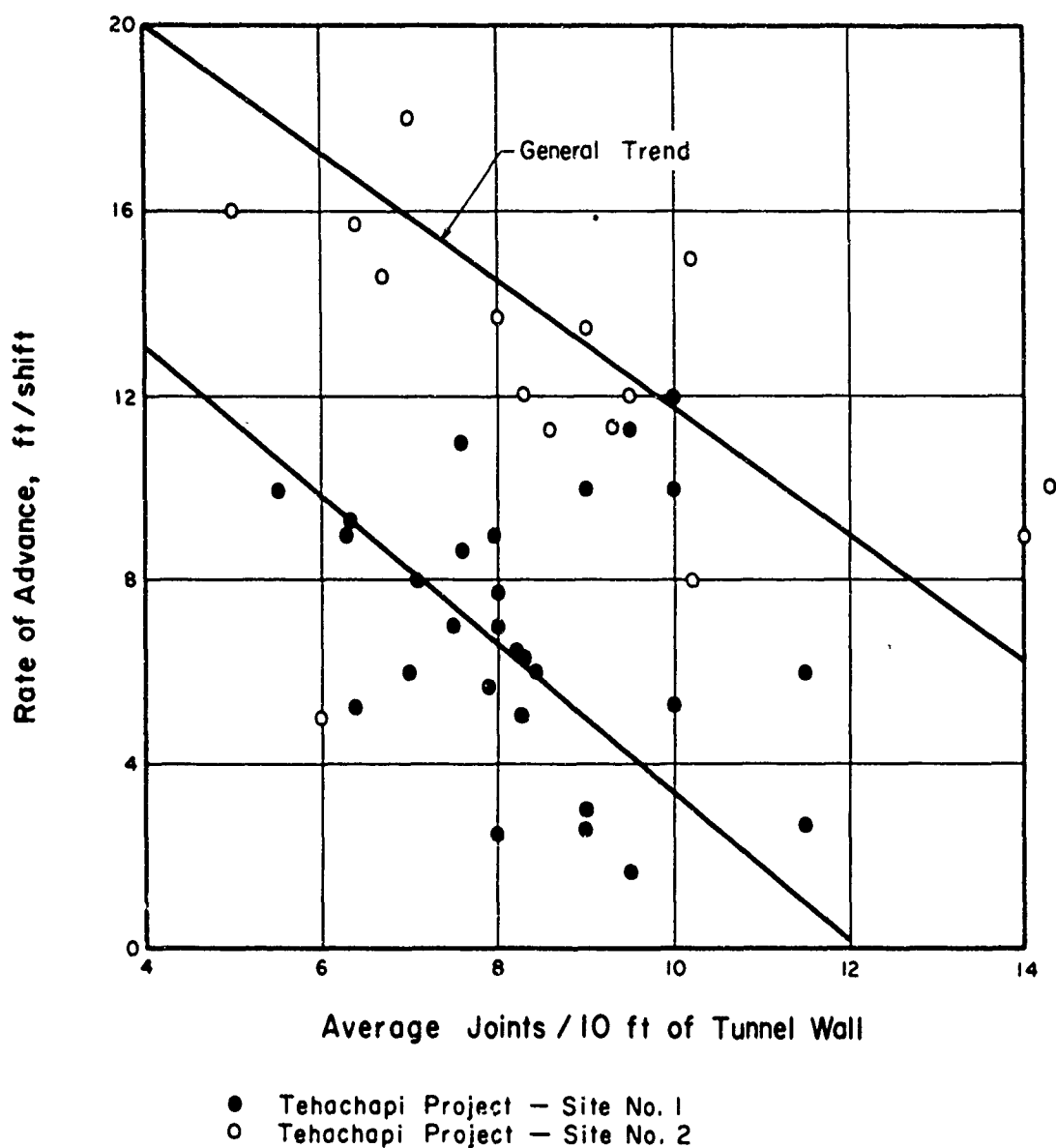


FIG. 16.4 COMPARISON OF RATE OF ADVANCE AND JOINTS/10FT, TUNNELS AT SITES NO. 1 AND 2, TEHACHAPI PROJECT, CALIFORNIA.

surface mapping, mapping of a pilot bore approximately 13 feet in diameter and 8,300 long, and geophysical measurements. The geophysical measurements consisted of seismic and resistivity measurements in the tunnel and in exploration borings along the tunnel right-of-way.

The geology of the site is quoted from Scott and Carroll (1967),

Results (of the surface geologic mapping program) indicated that the bedrock in this area consists chiefly of Precambrian granite (about 75%) with inclusions of Precambrian metasedimentary rock (about 25% composed of biotite rich gneiss, schist and migmatite), and a few small dioritic dikes of probably Tertiary age. The bedrock is extensively faulted and sheared and is locally altered.

Underground geophysical measurements were performed by the U.S. Geological Survey. Electrical resistivity and seismic refraction measurements were made at locations chosen to represent the full range of rock quality present in the pilot bore. The rock was given a quality designation 1 through 5 with 1, representing rock of highest quality nearly free of fractures and mineral alteration, and 5, the lowest quality characterized by intensive fracturing and severe mineral alteration. The criteria used for determining the exact classification are: (1) fracture spacing, (2) mineral alteration, percent of rock, (3) faulting, (4) foliation of schistosity, and (5) rock type. The criteria are listed in the descending order of importance. Criteria 1 and 2 are quantitative and 3 through 5 are qualitative.

Details of the seismic measurements are quoted from Scott and Carroll (1967).

Underground seismic measurements were made with high resolution, ten channel refraction seismic equipment capable of detecting energy in the frequency range of 10 to 4000 cycles per second. Accelerometers used to detect the seismic energy from explosive energy sources were placed along the tunnel walls about 4 feet above the floor in linear arrays that were about 200 feet long. Spacing between accelerometers ranged between 5 ft to 25 ft. Small explosive charges (0.1 pound dynamite) were detonated in one foot deep shot holes drilled into the rock at both ends and at the midpoint of each array of ten accelerometers. Seismic energy was recorded on photo sensitive paper by means of an accelograph having a speed of 250 inches per second.

Details of the resistivity measurement are quoted from the same source.

Underground electrical resistivity measurements were made with conventional Gish-Rooney equipment and special sponge-rubber electrodes impregnated with a mixture of brine and bentonite to provide good electrical contact with the rock exposed along the walls and the pilot bore. Measurements were made in the Wenner electrode configuration with electrode spacing expanded from 1 to 30 feet in a step-wise manner keeping the array

symmetrical about a center point and parallel with the tunnel axis. This procedure provided a means of interpreting resistivity layering from the surface to the depth of ten feet or more.

The seismic measurements show that the distressed zone around the tunnel has a velocity of 4,200 to 10,800 fps and a thickness of less than 1 to 17 ft. The velocity behind the distressed zone ranges from 13,750 to 20,150 fps. The resistivity measurements shows that the distressed zone has a relatively high resistivity ranging from 60 to 5,300 ohm-meters and a thickness of from less than 1 ft to about 10 ft. The very high resistivity is partly attributed to moisture losses by evaporation at the tunnel walls. The rock behind the distressed layer has a resistivity range of 36 to 2,200 ohm-meters.

The electrical resistivity and seismic velocity measurements have been related to the rate of construction and the cost per foot of tunnel. These correlations are shown in Figure 16.5. The cost per foot was calculated assuming a constant average cost per day. The authors comment that this assumption is not completely valid, but is sufficiently accurate for this analysis. Each graph contains the best fit lines, standard deviation lines, standard error, and correlation coefficient.

The seismic velocity and electrical resistivity used in these correlations are those deep layers behind the distressed zone. The authors state that the values were used in preference to those of the distressed zone to obtain more consistent correlations, and because geophysical tests to predict the engineering properties of the rock mass would be performed on relatively undisturbed rock ahead of the tunnel face.

The relationship between electrical resistivity and rate of construction is on the same order as the RQD versus rate of construction for case history No. 1. From the number of data points, it may be concluded that a fairly representative portion of the adit has been tested. The relationship for seismic velocity versus rate of construction ( $r = 0.995$ ) is exceptionally good; however, it should be noted that it contains only five points, a rather small sampling.

## 5. Summary

The three case histories show a fair to good correlation between rock quality expressed by RQD, fracture spacing, or geophysical measurements and the rate of construction. Case History No. 1 indicates that the rate of construction in Fair to Poor quality rock is approximately one-half that in Excellent rock. The average trend of data presented in Case History No. 2 show that the rate of

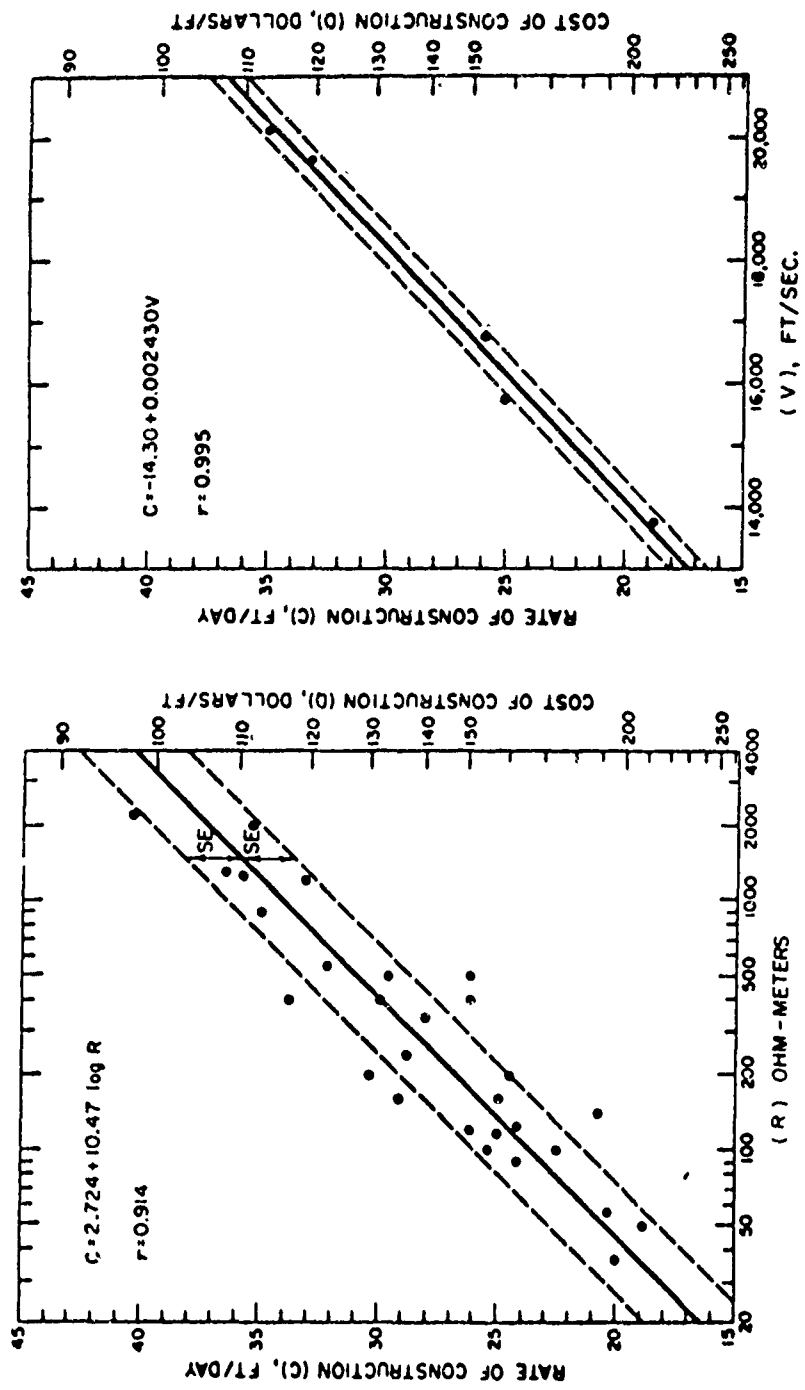


FIG. 16.5 RATE OF CONSTRUCTION AND COST PER LINEAR FOOT PLOTTED AGAINST ELECTRICAL RESISTIVITY AND SEISMIC VELOCITY (After Scott and Carroll, 1967)



advance may increase 50 to 200 percent as the jointing decreases from 10 joints per 10 ft to 6 joints per 10 ft. The data from Case History No. 3 indicate a doubling of the rate of construction when the electrical resistivity changes from about 50 to 2,000 ohm-meters and when the seismic velocity increases from 14,000 to 20,000 fps. The seismic velocities can be expressed as a Velocity Index by assuming the intact velocity is 20,000 fps. The rate of construction increases by 100 percent when the Velocity Index increases from 0.49 to 1.00. The data, therefore, indicate the same relative increase in construction rate using three methods of measuring rock quality. It should be noted that the data presented is limited to sites in metamorphic rock, and the actual rate of advance depends on the geologic conditions and method of construction.

SECTION 17  
CORRELATION OF ROCK QUALITY AND SUPPORT REQUIREMENTS  
FOR UNDERGROUND OPENINGS

1. Introduction

The supports installed during the excavation of an underground opening may provide only temporary support to avoid rock falls or they may be designed to become part of the permanent structure. On civil engineering projects, many of the temporary supports are integrated into the finished support system. Support systems used in underground works include one or more of the following types: (1) wooden framing, (2) steel ribs, and (3) rock bolts.

Until a few decades ago, wooden supports were the major type of support used in both mining and civil engineering. Today, steel supports have replaced wood except in support of small openings. Wooden supports have the advantage of high flexibility, that is, the beam can deform as the rock moves into the opening. Also, they are constructed on the site and, therefore, can be easily fitted to the contour of the rock. In addition, they give visible and audible evidence of high loads well before the supports fail. At many sites, timber supports have the advantage of low material cost.

Wooden support systems have, however, many important disadvantages that are largely responsible for the change to steel supports in recent years. Timbers have very low strength and low resistance to bending over long spans which necessitate the use of numerous joints in constructing ribs for large diameter tunnels. Because skilled workmen are required to construct large wooden supports, the high installation costs can make wooden supports uneconomical in spite of low material cost.

Proctor and White (1946) present an excellent summary of types of steel support and their application. The simplest form of steel support is a horseshoe-shaped support or set consisting of two curved pieces bolted at the crown of the opening. For wider spans, the set consists of four pieces bolted at the crown and each springline of the tunnel, i.e., the point where vertical tunnel walls meet the base of the tunnel arch. In zones where lateral loads must be resisted a steel beam, called an invert strut, is placed between the legs of the set at floor level to prevent inward movements. In cases of even more severe lateral forces, a circular tunnel cross-section is used and the

steel supports are ring beams consisting of four or more sections. Because the cross-section of tunnels driven by conventional blasting techniques is irregular and the steel ribs must be rolled to some predetermined shape off the site, it is necessary to place lagging and blocking between the steel and the rock to ensure that rock loads are carried by the steel before excessive rock movements occur. Wood or steel beams spanning two or more sets are commonly used to obtain this contact. If the tunnel is to be concrete lined, much of the wood lagging may be removed before the lining is poured to reduce the danger of a failure of the lining due to decay of the wood.

An even more recent innovation in underground support is the introduction of steel bolts to supplement or replace steel supports. The rock bolt support system works on a different principle than either wooden or steel supports which resist inward rock movements by their structural rigidity. Rock bolts utilize the fact that the rock behind the distressed zone has significant load carrying capacity. The bolts provide a structural link between loosened rock in the distressed zone and sound rock behind. The bolts, commonly 5 to 50 ft long, are anchored in borings commonly drilled perpendicular to the tunnel wall. The end away from the tunnel must be anchored securely in the sound rock while the end at the tunnel wall must have a bearing surface sufficiently large so that local failures will not allow the supported block to break loose. Bolting one block can support several adjacent blocks if the shape of the bolted block allows it to act as a keystone. Rock bolting stratified rock apparently creates a beam in much the same manner as nailing wooden planks together. In fractured rock the rock bolt appears to reduce the rock movements by increasing the normal load and hence the frictional resistance along the discontinuities.

The effectiveness of a rock bolt installation depends primarily on the strength of the anchor. The bolt may be anchored by a wedge flaring the slotted end of the bolt as the bolt is driven against the end of the hole or by means of an expanding sleeve. These techniques are effective in high strength rocks. In low strength or highly fractured rock, a grouted anchor is most effective as the load is distributed over a larger area.

The rock at the tunnel wall is held in place by means of a bearing plate about 6 to 8 inches square held in turn by a steel nut. The load developed in the bolt may be estimated by the torque applied to the nut. The load, however, can be measured directly by tensioning the bolt by means of a hydraulic jack. In this case the nut is merely snugged against the bearing plate and the jack removed.

A continuous support system is obtained by installing the bolts in a pattern with a vertical and horizontal spacing of from 3 to 10 feet, and by placing straps or wire mesh around the bearing plates. The purpose of the straps or mesh is to extend the retaining power of the bolt to adjacent rock blocks to prevent or limit rock movements that would lead to additional destressing of the rock wall.

Rock bolting has several advantages over steel or wooden rib supports. The first is that rock bolts can be installed closer to the face of the excavation than steel ribs because they are less susceptible to blast damage. This results in less destressing of the rock and, consequently, fewer stability problems. Rock bolts are placed in direct contact with the wall, therefore, the lagging is not required. Finally, unlike rib supports, they present no obstacle to construction activities.

Until recently, it was impossible to determine quantitatively the loads on support members. The magnitude of the load could only be estimated from the deformation of steel ribs or wooden beams and lagging. For this reason, the design of support members was quite conservative in order to minimize the number of failures. Recent measurements, reported by Hartman (1965) provide a more complete picture of the load history of tunnel supports. These measurements were obtained from load cells mounted in steel sets, rock bolts, and extensometer installations. They provide the following information about the behavior of rock in the tunnel walls: (1) Rock movement indicating redistribution of stresses normally begins well in front of the excavation face. (2) Stress redistribution within the rock mass does not take place suddenly, but extends over a period of time measured in hours to weeks, and during this redistribution time, high stresses are placed upon the support system. They are accompanied by rock mass movements of the order of one-half to one inch. (3) Once the distressed zone has formed, the pressures on the supports are much lower than during the redistribution process. (4) Lateral pressures existing in shear zones may be four or more times the vertical pressure. (5) In places where the joint spacing is less than one tenth foot, and where appreciable quantities of clay materials have formed due to alteration, a relatively long stabilization period is observed.

Hartman states that the rock loads measured in steel sets during the formation of the distressed zone are often cyclic. The loads generally increase until the support deflects and then it drops abruptly. In time the load increases again until the rib deflects a second time or the full development of

the distressed zone causes it to decrease. He comments that this behavior is probably the major cause of disagreement between contractors and owners over the amount of support used in an opening. The contractors' personnel are most interested in support requirements while the distressed zone is forming. The owners representatives, who are rarely at the tunnel face, often feel that the contractor has been overly conservative in placing the supports.

From the above, it can be concluded that the amount of support required depends on the extent of the distressed zone. The size of the distressed zone depends on the initial state of stress in the rock mass, the quality of the rock, and construction techniques. It has been found that the in-situ state of stress cannot be quantitatively determined without field testing, and can only be estimated from the geologic conditions (Deere et al., 1967).

Because support requirements cannot be accurately predicted, many extraneous factors influence the decision concerning the type and spacing of supports. The contractor, for instance, may be overly conservative in the number of supports used if he has a good price for supports. He may also use a conservative approach if the rock quality changes frequently, and prefer to continue all the way with the supports required for the poorest rock encountered. On the other hand, the designer may be overly conservative in the support system he requires if rock movements would endanger other structures.

This discussion shows that the prediction of support requirements is complicated by factors that are difficult to evaluate before construction and even in a well documented case history. It is evident that rock quality is only one of several factors which determine the amount of support used. However, a quantitative measure of rock quality should simplify the problem of comparing and predicting support requirements.

## 2. Case History No. 1: Tunnels 1 and 2, Pigeon River, North Carolina

In the early 1950's the North Carolina Highway Department began construction of a road between Ashville, N. C. and Knoxville, Tenn. The route followed, in part, the Pigeon River in Pisgah National Forest to the North Carolina state line. A major construction feature of this route is a tunnel, herein, to be called tunnel No. 1. The tunnel is a horseshoe-shaped opening with an overall height of 27 to 28 ft, a width of 30 ft, and a length of about 1,000 ft. It was driven through a 400-ft high ridge of quartzite which contains some thinner layers of siltstone and phyllite. The tunnel was driven without

difficulty and was entirely unsupported. After the tunnel was completed, the right-of-way was designated as part of future Interstate route No. 40, and the North Carolina Highway Department halted construction.

Several years ago, work on the Interstate route commenced. Tunnel No. 1 which had stood for ten years without maintenance and without support was found to be in excellent condition. The tunnel was largely dry except for some minor seeps from small shear zones near the south portal.

At this time, tunnel No. 2 was started four miles to the south of the first tunnel. It had a similar cross-section, and length, and the rock was apparently similar to that at the site of tunnel No. 1. As exploration borings at the site of tunnel No. 2 had an average core recovery of 90 percent it was concluded that only local support would be required.

During portal operations, a major slide caused a considerable delay in construction. When the tunnel had been driven a short distance from the portal area, it became apparent that heavy support would be required. Steel ribs 8 x 9 in. were used throughout the tunnel on spacing ranging from 4 to 6 ft.

In the design studies for a third tunnel a reassessment was made of the engineering geology at the two tunnels and the reasons for the construction problems. The geology of the two sites was mapped and RQD logs of the borings at tunnel No. 2 and recent borings at tunnel No. 1 were recorded. This investigation shows that the unsatisfactory behavior in tunnel No. 2 is caused by a combination of effects (Deere and Patton, 1965): (1) A prominent series of joints strikes subparallel to the entire length of tunnel No. 2 while joints at site No. 1 cross the tunnel alignment at a high angle. (2) The joints at tunnel No. 2 are much more persistent and more closely spaced than those at No. 1. (3) Clay seams, rock alteration and staining created by weathering are much more common along joints and shear zones at site No. 2. (4) There is considerably more water at the second site. (5) Although the lithologies are somewhat similar, the proportions are different. At site No. 1, quartzite is dominant with only thin zones of slate and phyllite. At site No. 2 the quartzite percent is reduced while the other rock types increase. (6) The average RQD for 6 borings at site No. 1, the unsupported tunnel, is 87 percent while the average RQD for an 89-ft interval from a boring at site No. 2 was 29 percent.

The RQD at each site expresses quantitatively the rock quality shown by qualitative geologic observations, and provides a comparison which corresponds to the engineering properties of the sites. In contrast the core recovery which

averages about 95 percent at tunnel No. 1 and about 90 percent at tunnel No. 2 is apparently insensitive to the geologic factors which determine the engineering properties of the two sites.

### 3. Case History No. 2: Tunnel No. 3, Tehachapi Project, California

Geology of this tunnel and construction procedures are similar to Tehachapi Site No. 1 described in Section 16. A portion of this tunnel is ideally suited for this investigation as a 180-ft section of the tunnel was explored by means of a horizontal NX core boring before construction. Additionally, the contractor tailored the supports to the quality of the rock. Figure 17.1 is a plan view of this section of the tunnel showing the rock quality expressed by RQD and joints per 10 ft and the supports used. Rock bolts are used where the RQD is greater than 50 to 60 percent while steel sets are required where the RQD is less than 50 to 60 percent. In contrast the joint frequency does not indicate a significant difference between bolt-supported and steel-supported zones. This observation suggests that the RQD is more sensitive than joint frequency to the geologic factors that determine support requirements.

### 4. Case History No. 3: Straight Creek Tunnel Pilot Bore, Colorado

The geology and testings at this site are described in Section 16. Although on-site investigations were not performed during this study, geologic and tunnel support maps obtained from the Colorado State Highway Department are used to compare rock quality and support used. In their report of the Straight Creek site, Scott and Carroll (1967) present a relationship between rock quality measured by electrical resistivity and seismic velocity of the deep layer shown in Figure 17.2. The resistivity measurements are more numerous than seismic measurements and the correlation coefficient  $r = 0.827$ , probably indicates the amount of scatter to be expected in this type of analysis. Although there is considerable overlap in the resistivity measurements for the 2-ft and 4-ft spacing, the trend of increasing set spacing with increasing electrical resistivity is apparent. The seismic velocity versus set spacing has a correlation coefficient,  $r = 0.985$ , but unfortunately there are not enough measurements to determine if seismic velocity is superior to electrical resistivity in predicting support requirements.

A geologic map and profile obtained from the Colorado State Highway Department shows the tunnel supports, the location of major joints and faults,

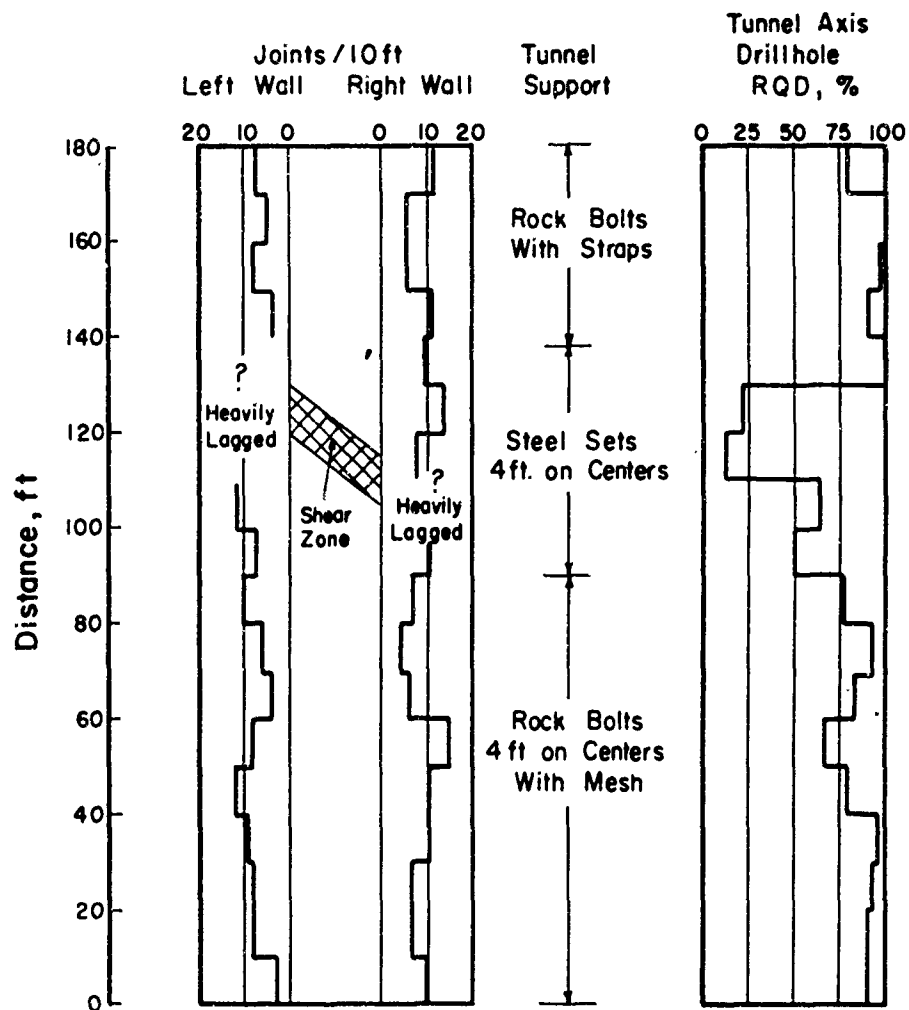
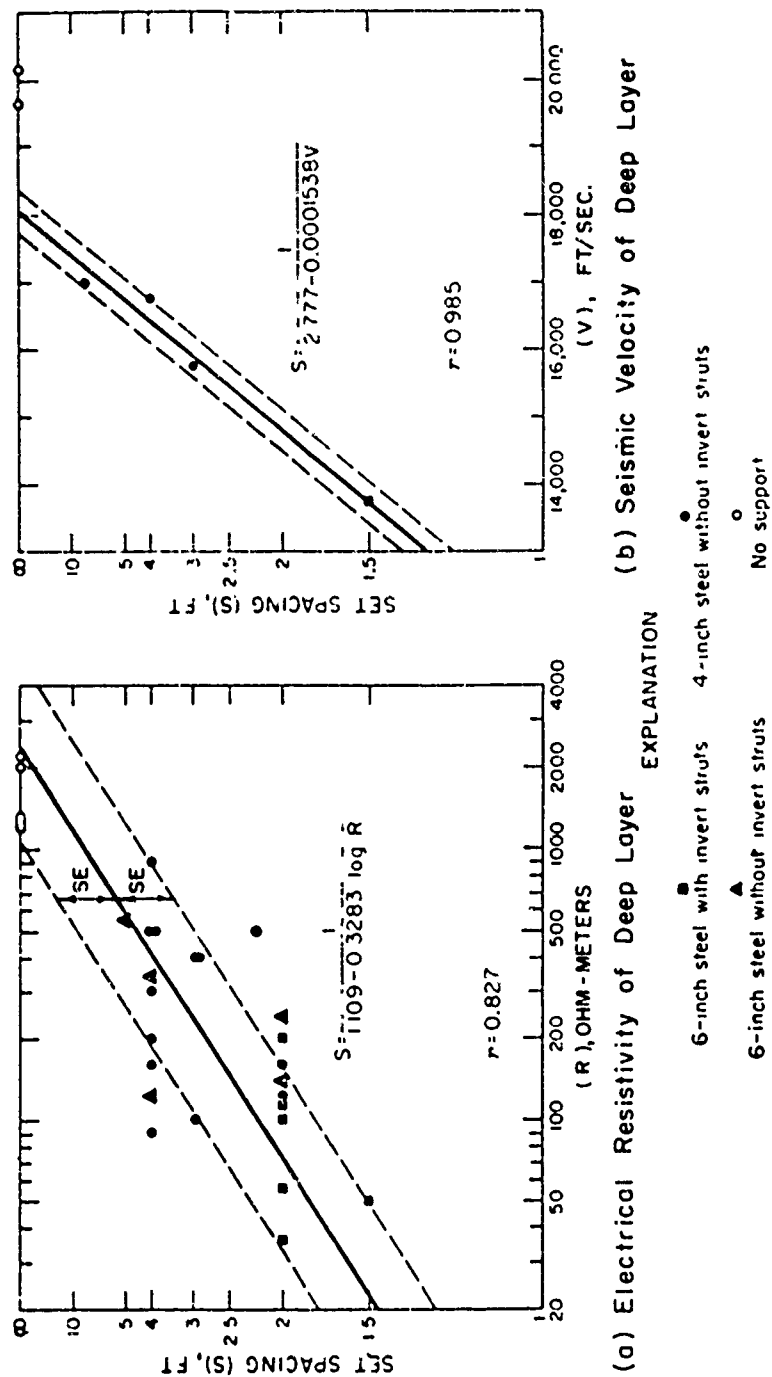


FIG. 17.1 COMPARISON OF ROCK QUALITY AND TUNNEL SUPPORT, SITE NO. 3, TEHACHAPI PROJECT, CALIFORNIA.





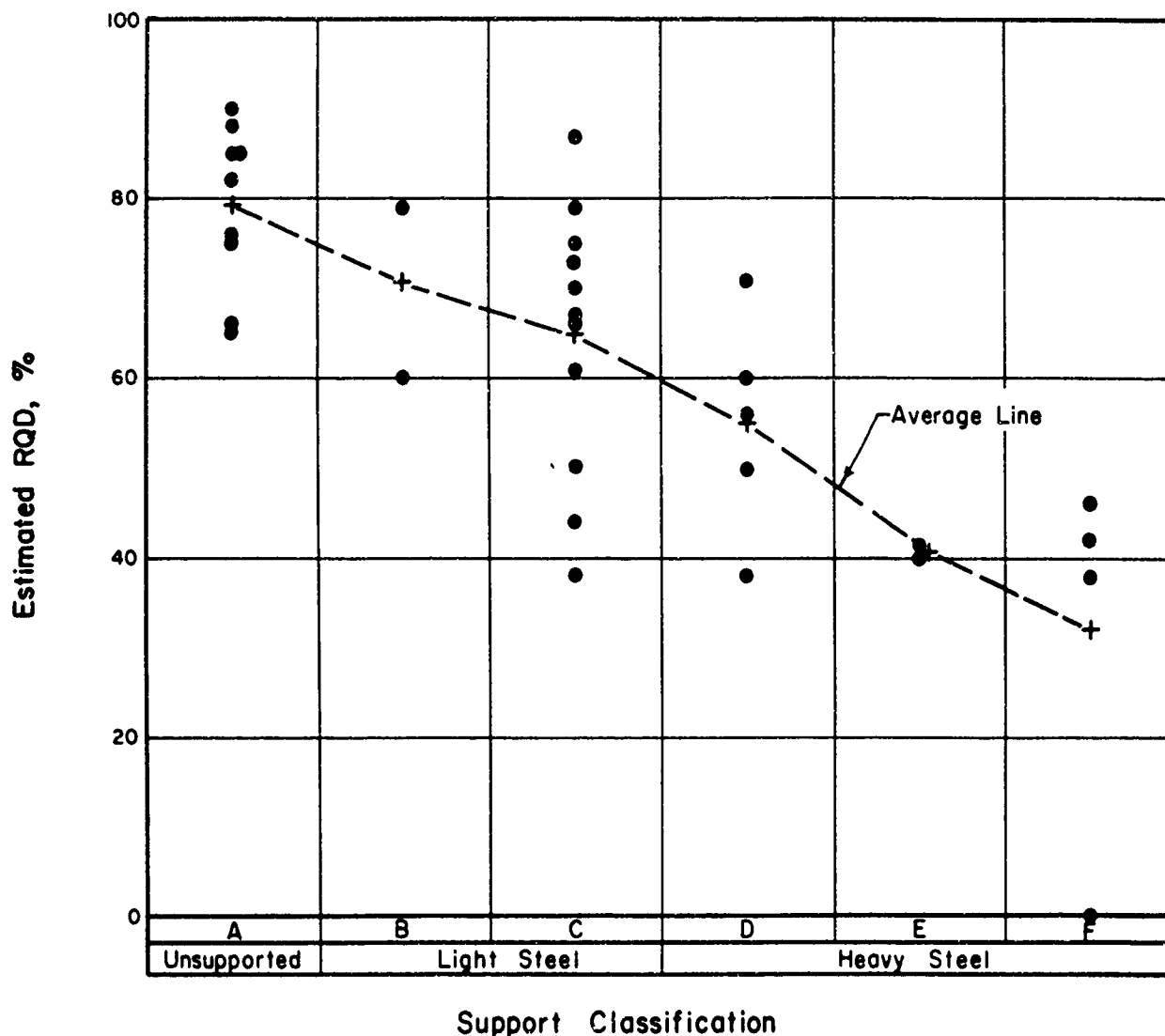
Note: In graph (b) data points representing no support (open circles) were omitted in calculating the correlation coefficient.

FIG. 17.2 SET SPACING PLOTTED AGAINST ELECTRICAL RESISTIVITY AND SEISMIC VELOCITY (After Scott and Carroll, 1967)

and a summary of the geologic observations expressed in terms of average joint spacing and average percentage of mineral alteration. A study of this map suggests that the tunnel can be divided into zones with uniform support ranging in length from 30 to 300 ft. The supports are subdivided into 6 classes: (a) unsupported, (b) 4-inch ribs on 4- to 5-ft spacing, (c) 4-inch ribs on 2- to 3-ft spacing, (d) 6-inch ribs on 4- to 5-ft spacing, (e) 6-inch ribs on 2- to 3-ft spacing, (f) 6-inch ribs with invert struts. For each of the support zones, an estimated RQD is calculated using the average joint spacing and percent alteration. An average joint spacing of greater than 1 ft is assigned an RQD of 90 percent. Average joint spacing of 1/2 to 1 ft and less than 1/2 ft are assigned average RQD's of 75 and 50 percent, respectively. The resulting RQD estimate is further modified by the percent alteration. The percent alteration, ranging from 0 to 100 percent in 5 to 10 percent increments, is subtracted from the RQD based on joint spacing to provide the final estimate.

Figure 17.3 shows the results of these calculations. The support classification is plotted against estimated RQD. This relationship, like those presented by Scott and Carroll, shows considerable overlap between support zones, but the average rock quality for each support classification decreases with increasing support requirements.

To support these RQD estimates, the seismic velocities for the deep layer reported by Scott and Carroll (1967) are used to estimate Velocity Indices. As laboratory velocities are not available, the highest seismic velocity, 20,000 fps, was used as the intact velocity. This value is a reasonable estimate for gneiss and schist based on laboratory tests on similar rock. The higher velocity is obtained in the best rock on the site that had an average fracture spacing greater than 1 ft and no mineral alteration. A Velocity Index of 1.00 was assigned to this rock. The lowest velocity reported was approximately 14,000 fps in a rock with fracture spacing less than one-half foot and a considerable amount of mineral alteration. The Velocity Index calculated for this rock is 0.49. Using the relationship presented in Section 6, these Velocity Index values are converted into RQD's. A Velocity Index of 1.00 corresponds to an RQD of approximately 100 percent while the Velocity Index in poor rock corresponds to an RQD of 56 percent. The support in these sections of the tunnel suggest average RQD's of 80 and 65 percent respectively which indicates that the estimated RQD's are reasonable.



RQD estimate based on reported average joint spacing and percent altered.

Assumed : Joint Spacing	RQD
> 1 ft	90
1 - 1/2	75
< 1/2	50

$$\text{RQD (est.)} = \text{RQD (jt. spacing)} - \% \text{ altered}$$

Support Classification:

- A - Unsupported
- B - 4 in. Ribs, 4-5' Spacing
- C - 4 in. Ribs, 2-3' Spacing
- D - 6 in. Ribs, 4-5' Spacing
- E - 6 in. Ribs, 2-3' Spacing
- F - 6 in. Ribs with Struts

FIG. 17.3 COMPARISON OF ESTIMATED ROCK QUALITY DESIGNATION AND SUPPORT CLASSIFICATION FOR THE STRAIGHT CREEK TUNNEL PILOT BORE

## 5. Summary of Support Data

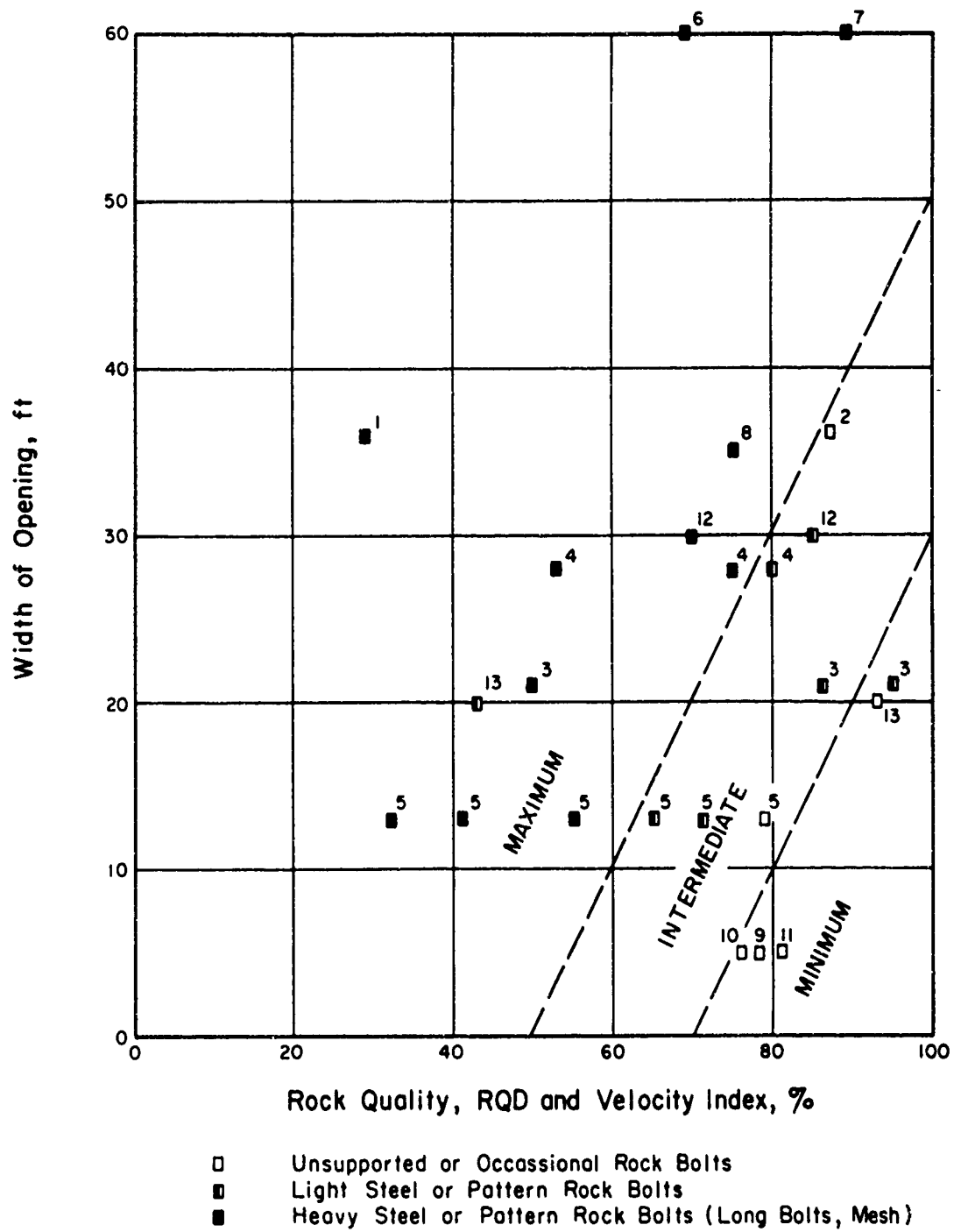
The three case histories presented above suggest that support requirements can be related to rock mass quality. The Pigeon River case history indicates that RQD values distinguish between a site requiring little or no support and one requiring heavy steel support. The Tehachapi data indicates that a change from rock bolt to steel support occurs when the RQD drops below the range of 50 to 60 percent. The Straight Creek data indicates that unsupported sections have an RQD of 70 to 100 percent, light steel support ranges from 65 to 80 percent, and the heavy steel support is required in an RQD of less than 60 percent.

The above case histories, others from the literature, and private consulting files are summarized in Table 17.1. Figure 17.4 is a plot of rock quality versus tunnel width or span using the data in Table 17.1. Each point shows the type of support and the calculated or estimated rock quality. Although the data are somewhat limited there is a suggestion that support requirements can be generalized into minimum, intermediate, and maximum zones as suggested by the dashed boundary lines. Although many factors influence the selection of supports, it is felt that the investigation method presented herein can be used to relate data from various sites.

TABLE 17.1

SUMMARY OF WIDTH OF TUNNEL OPENING, SUPPORT REQUIREMENTS, AND  
ROCK QUALITY INDICES

Project	Width of Opening, ft.	Support	RQD or Velocity Index
1 Pigeon River No. 1	36	Unsupported	87
2 Pigeon River No. 2	36	8 in. WF 10 to 4 ft	29
3 Tehachapi Site 3	21		See Fig. 17.1
4 Tehachapi Site 1	28	8 x 8 in. 6 ft o.c., and bolts 5 ft o.c.	54-80
5 Straight Creek	13	Heavy support to unsupported	See Fig. 17.3
6 Cavity I, NTS	Hemisphere with radius of 60 ft	Top 32 ft - bolts, 3 ft o.c. Mid 24 ft - bolts, 3 ft o.c. Bot 16 ft - bolts, 6 ft o.c.	72 90
7 Cavity II, NTS	Hemisphere with radius of 60 ft	Top 32 ft - bolts, 3 ft o.c. Mid 24 ft - bolts, 3 ft o.c. Bot 16 ft - bolts, 6 ft o.c.	69
8 Cavity III, NTS	Hemisphere with radius of 35 ft	Top 24 ft - bolts, 3 ft o.c. Mid 16 ft - bolts, 3 ft o.c. Bot 8-16 ft - bolts, 6 ft o.c.	75
9 Adit at Two Forks	5		78
10 Adit at Yellowtail Dam	8		
11 Adits at Dworshak Dam	5		81
12 Diversion Tunnel at Dworshak Dam granite gneiss 960 ft	30	47% ribs, 53% bolts	Estimated 85
Schistose gneiss 760 ft	11	77% ribs, 23% bolts, ribs 5 ft o.c.	Estimated 70
13 Shaft, East Coast	20	Temporary timber and bolts - concrete lining w/ i 20 ft of face	44-93
14 Tunnel, NTS	10	Unsupported	75



Numbers refer to Table 17.1

FIG. 17.4 COMPARISON OF SUPPORT REQUIREMENTS BY WIDTH OF OPENING AND ROCK QUALITY

SECTION 18  
CONCLUSIONS AND RECOMMENDATION FOR FUTURE RESEARCH

1. Engineering Classification of In-Situ Rock

The Engineering Classification of In-Situ Rock presented in Section 6 is based upon two indices of rock quality, the RQD and the Velocity Index. The RQD is a modified core recovery which includes only those pieces of sound core 4 inches (0.35 ft) or longer. The Velocity Index is the square of the ratio of field velocity to laboratory velocity. The field velocity is measured by either seismic or sonic tests. The laboratory velocity is measured by a sonic test on a saturated cylinder of core under a 3,000 psi axial load. According to the value of the RQD or Velocity Index, in-situ rock is described as Excellent, Good, Fair, Poor, or Very Poor.

Correlations of in-situ test data and the RQD and in-situ test data and the Velocity Index presented in Sections 12 to 17 suggest that the engineering classification can be used to estimate in-situ deformability, rate of tunneling, and underground support requirements. These results are summarized in Table 18.1 and in the following paragraphs.

2. Measurement of In-Situ Deformability

a. General

The deformation characteristics of in-situ rock can be measured by static or dynamic tests. The static tests include the plate jack, pressure chamber, radial jack, borehole deformation, and cable tests. Dynamic moduli of in-situ rock can be calculated from seismic tests and sonic logging in exploratory borings. Although the velocity measurements do reflect the presence of jointing and weathering of the rock mass, the dynamic moduli are consistently higher than the moduli measured by static tests at the same location. The discrepancy is apparently a result of the difference in the stress level and rate of loading involved in the two types of testing. Because the loading conditions in the static tests are closer to those of engineering structures, the static test moduli should be used for engineering design and the dynamic moduli should be used as an index of rock quality.

TABLE 18.1  
"CORRELATION OF ENGINEERING BEHAVIOR AND THE  
ENGINEERING CLASSIFICATION OF IN-SITU ROCK"

Rock Quality Classification	Rock Quality Indices		Engineering Properties of In-Situ Rock			Construction Factors		
	RQD	Velocity Index (Fig. 6.16)	Deformation Ratio, $\epsilon_e/\epsilon_c$ (Fig. 14.18)	Permeability $k_e/k_{t50}$ Fig. 14.6	Slope Stability * Number of Potential Failure Surfaces	Support Requirements		Rate of Construction Predicted Rate / Rate in Best Rock
						Width of Opening 10 ft	50 ft	
Excellent	90-100	80-100	0.8-1.0	0.8-1.0	Few	Minimum to Inter	Inter to Maximum	0.8 - 1.0
Good	75-90	60-80	0.6-0.8	0.5-0.8	Some	Minimum to Inter	Inter to Maximum	0.5 - 0.8
Fair	50-75	40-60	0.4-0.6	0.1-0.5	Many	Inter to Maximum	Maximum	0.2 - 0.6 *
Poor	25-50	20-40	0.1-0.4	<0.2	Many	Maximum	Maximum	0.1 - 0.3 *
Very Poor	0-25	0-20	<0.1	<0.2	Many	Maximum	Maximum	>0.1 *

\* Estimated



b. Pressure Chamber and Radial Jack Tests

The pressure chamber test is probably the most ideal static test as it loads the largest volume of rock and allows simultaneous measurement of deformation in several directions. The high installation cost, however, limits the use of this test to relatively large engineering projects. In fact, only one series of pressure chamber tests has been run in this country although they are fairly common at hydroelectric projects in other countries. The most important applications of this test are the design of pressure tunnels and to determine the foundation modulus for arch dams.

The radial jack test has been developed in recent years to overcome the high installation cost of the pressure chamber test while at the same time loading a large volume of rock. In contrast to the pressure chamber test which is a permanent installation, the radial jack test is a temporary installation which can be rapidly assembled for a test and then disassembled and moved to another test location.

c. Plate Jack Test

In rocks with medium to close joint spacing, plate jack tests using large diameter flexible plates should give moduli suitable for design purposes. The use of small diameter rigid-plate tests is not desirable because the test does not load a large enough volume of rock and the stresses under a rigid plate are difficult to evaluate. On sites where the joints are widely spaced, even large diameter flexible plate setups may give erroneous results. Some designers are trying to overcome this limitation by using flexible plates up to 1.6 meters in diameter in a typical plate-jack setup or large flat jacks in slots drilled or sawed into the rock mass.

d. Other Tests

Other in-situ tests use borehole deformation devices and methods for loading large areas by means of cable tendons. Borehole deformation devices offer an inexpensive and rapid method of measuring in-situ deformation characteristics in an exploratory boring. Most of the devices, however, are small diameter to reduce the cost of drilling the test hole and to increase the portability of the instrument. The use of a small diameter boring decreases the accuracy of the instrument because a smaller, and hence less representative, area is loaded during the test.

Several deformation test setups have been proposed using one or more reinforced concrete blocks loaded by means of cable tendons anchored in the

rock mass. By using a large concrete block and several cables, it is possible to develop relatively high contact pressures on a rock surface comparable in area to that loaded by a pressure chamber test. This test is less expensive than the pressure chamber test in foundation testing for large buildings, bridges, and even arch dams because it does not require a test adit and the test block can be incorporated into the foundation of the structure.

c. Conclusions

With the exception of the small diameter rigid plate jack test, each of the tests described has characteristics which favor its continued use in field testing. In theory, the pressure chamber, radial jack, and cable tests are the most desirable but economic considerations will probably continue to favor the plate jack test at many sites. Borehole deformation tests are the least desirable but they may provide approximate moduli where more expensive testing methods cannot be justified.

3. Relationship of Classification and In-Situ Deformability

Correlation of in-situ deformation moduli suggests that they depend on the type of deformation test used, the method of evaluating the load-deformation curves, and the characteristics of the rock. A limited number of comparisons indicate that pressure chamber tests yield lower deformation moduli than plate jack tests, and that the plate jack moduli are lower than borehole deformation moduli. This observation indicates that the modulus of in-situ rock decreases with an increase in the size of the loaded area. Examination of a large number of load deformation curves suggests that a uniform method of defining test moduli is essential for comparison of test results. It is suggested that the results of each deformation test include a modulus of deformation determined by the maximum pressure and the maximum deformation measured in the test, and a modulus of elasticity determined from the slope of the rebound curve from maximum pressure to zero pressure.

When a series of tests are performed with the same test equipment and using the same method to analyze the load-deformation curves, it is possible to compare the moduli with the characteristics of the rock mass. Correlation of in-situ moduli with the direction of loading (perpendicular and parallel to bedding) and the orientation of the test (vertical and horizontal) show that the parallel and horizontal tests yield higher moduli. Scatter in these

relationships indicate that the moduli are related to these and other characteristics which collectively determine the deformability of the rock mass.

A comparison of in-situ moduli and RQD is presented in Figures 14.2 and 14.3. Consistent trends in both graphs suggest that the RQD can be used to predict in-situ modulus. However, the data used in these graphs represent a relatively limited range of in-situ conditions. The graphs, for instance, do not include tests on highly deformable rocks such as weak sandstones or shales with in-situ moduli less than 1 million psi. If such data were included the RQD would probably not appear to have a unique correlation with modulus. This possibility, which appears to be a very real limitation of these graphs, can be eliminated by expressing the deformability as a ratio of the modulus of in-situ rock to the intact or laboratory modulus.

In Section 14 this ratio, referred to as the Modulus Ratio, is calculated using both the in-situ modulus of deformation and modulus of elasticity to define the field deformability and the laboratory static and dynamic moduli to define the intact deformability. By combining these moduli a total of four Modulus Ratios can be calculated. A comparison of the four Modulus Ratios with RQD and Velocity Index is presented in Figures 14.6 to 14.13. Each graph has about the same trend but the RQD versus Modulus Ratio graphs have a higher correlation. The RQD graphs all show a rapid decrease in the Modulus Ratio to about 0.2 as the RQD decreases from 100 to 60 percent. When the RQD is less than 60 percent, the Modulus Ratio is generally less than 0.2 but the data in this range is too limited to define the relationship.

The graphs of Velocity Index versus Modulus Ratio have a greater scatter than the RQD versus Modulus Ratio which is apparently due to a difference in the scale of the tests rather than a failure of the Velocity Index to measure rock quality correctly. For this reason it is suggested that the RQD versus Modulus Ratio graphs be used to develop the relationship between rock quality and deformability, and velocity measurements can be used in these relationships by first converting them to an equivalent RQD (Figure 6.1).

#### 4. Relationship of Classification and Rate of Construction of Tunnels and Shafts

In Section 16, the rock quality expressed by RQD, fracture frequency, and geophysical measurements is compared with the rate of construction. The comparisons indicate an almost linear relationship over the range of Fair to Excellent rock with construction rates increasing about 100 percent. The data

do not indicate a means of estimating absolute rate of construction, but rather relative rates when the method of construction and geology are similar. The data also does not provide information on Poor and Very Poor rock. Experience indicates that the rates are much lower in these rock quality categories and it is expected that the overall rock quality to rate of advance relationship will be curvilinear.

#### 5. Relationship of Classification and Support Requirements

Section 17 presents the relationship between rock quality and the support requirements of underground openings. A limited amount of data indicates that the support requirements can be predicted in a general manner from rock quality and the width of the opening (Figure 17.4). From these data zones of minimum, intermediate, and heavy support are suggested.

#### 6. Relationship of Classification and In-Situ Permeability and Slope Stability

A comparison of in-situ permeability measurements and rock quality indicates that they are independent properties of the rock mass. While this observation limits the application of the proposed classification, it suggests that these two properties may be used together to provide a more complete picture of in-situ conditions.

While this investigation did not include an evaluation of the relationship between slope stability and rock quality measurements, the nature of slope stability problems indicates that rock quality measurements can be used at least qualitatively in some problems. Slope stability problems are generally of two classes. The first deals with near surface ravelling caused by slippage along a large number of geological discontinuities. Rock quality measurements which express the average spacing of the geological discontinuities should assist in evaluating this kind of slope stability problem. The second class of slope stability problem involves deep-seated movement along one adversely oriented geological discontinuity. Rock quality measurements would probably be of little assistance in this problem because it involves a geologic detail rather than the general character of the rock mass.

#### 7. Recommendations for Future Research

a. Nearly all the data presented in this investigation are from rock classed as Fair to Excellent. Although zones of poor rock are commonly quite

limited on construction sites, their presence may require significant design changes. For this reason it is important to extend the relationships presented to include Poor and Very Poor rock.

b. The Modulus Ratio versus RQD or Velocity Index relationship represent a limited sampling of rock types. Six of the sites are in gneiss or schist, two are in sandstone, two are in limestone, and two are in flow rocks. Additional studies of other rock types should be made to complete the relationships.

c. The correlations between the Modulus Ratio and Velocity Index are inferior to those using RQD as the rock quality measurement. The correlation between the Velocity Index and RQD (Figure 6.1) shows that the indices are of about equal sensitivity. The scatter in the Modulus Ratio versus Velocity Index graphs is probably the result of a difference in scale between the static and dynamic tests. The use of small-scale seismic or sonic testing at the location of in-situ testing should provide a rock quality versus Modulus Ratio relationship as sensitive as those developed from RQD measurements.

d. While the RQD logging system offers an easily performable and reproducible measure of rock quality, it cannot determine the subtle characteristics of the discontinuities which significantly affect in-situ tests. Estimates of joint openness and filling made from core observation are often inadequate. These characteristics, which are especially critical in the first 5 to 10 ft of rock immediately beneath the loaded surface of an in-situ test, could be measured by borehole camera, television, or periscope observations. Such observations, when combined with the RQD or Velocity Index, might improve the relationships presented in Section 14.

e. The correlations between rock quality and rate of construction, and rock quality and support requirements represent a rapid means of comparing and predicting these important construction factors within broad limits. The reliability of these techniques should improve appreciably as additional experience is obtained and correlated with the rock quality measurements.

# APPENDIX A

## IN-SITU STATIC TESTS SUMMARY OF FIELD AND LABORATORY PROPERTIES

Site No.	Project	Bibliography	Rock Type	Test Details		Field Properties (before grouting)				Laboratory Properties		Field Properties (after grouting)			
				Static Test	P psi	Ed psi x10 <sup>6</sup>	Es psi x10 <sup>6</sup>	Ed psi x10 <sup>6</sup>	Es psi x10 <sup>6</sup>	Est psi x10 <sup>6</sup>	Edyn psi x10 <sup>6</sup>	Ed psi x10 <sup>6</sup>	Es psi x10 <sup>6</sup>	Ed psi x10 <sup>6</sup>	Es psi x10 <sup>6</sup>
1	Agri River, Italy	Lotti & Beomonte (1964)	conglomerate sandstone	Jack	4250		1.66		1.6					2.67	
2	Alpe Gera, Italy	Capozza et al (1966)	serpentine schist	Jack (rigid)	1420 1420		3.63 1.27								
3	Alvito Sussudenga, Portugal	Rocha (1964)	quartzite	Jack		0.92 1.06 0.21 1.06						0.68 0.78 0.99 1.85			
4	Ananaigawa, Japan	Kavabuchi (1964)		Jack		0.54			4.0	4.4					
5	Bemposta & Miranda, Portugal	Rocha (1964)	shale	Jack		0.47 0.64 2.55 2.98 4.26 3.98 2.56 2.42 1.85 1.70 1.06						1.56 2.27 6.39 4.97 5.82 4.54 2.84 2.56 1.85 1.70 1.21			

(table continued on next page)

APPENDIX A - (Continued)  
IN-SITU STATIC TESTS  
SUMMARY OF FIELD AND LABORATORY PROPERTIES

Site No.	Project	Bibliography	Rock Type	Test Details		Field Properties (before grouting)			Laboratory Properties		Field Properties (after grouting)		
				Static Test	P psi	Ed psi x10 <sup>6</sup>	Ee psi x10 <sup>6</sup>	Eseis psi x10 <sup>6</sup>	Est psi x10 <sup>6</sup>	Edyn psi x10 <sup>6</sup>	Ed psi x10 <sup>6</sup>	Ee psi x10 <sup>6</sup>	Eseis psi x10 <sup>6</sup>
6	Bhakra, India	Bhatnagar & Shah (1964)	sandstone & claystone	Jack		2.91					6.0		
						4.25					6.45		
						2.69					4.65		
						1.68					2.94		
						1.08					2.26		
7	Cambambe, Portugal	Sarmento & Vaz	arkosic, sandstone & shale	Jack		1.98					2.01		
							1.15	3.6	8.5			1.95	
							0.91	3.6	8.5			2.68	
							0.51	3.6	8.5				
							1.12	3.6	8.5				
							0.42	3.6	8.5				
							1.16	3.6	8.5				
							1.36	3.6	8.5				
							1.88	3.6	8.5				
							0.16	3.8	8.5			3.47	
8	Davis Dam, USA	USBR (1948)	rhyolite & gneiss	Jack	700	0.03							
						0.11							
						0.02							
						0.04							
							1.36	3.8	8.5			4.24	
							1.99	3.8	8.5			.78	
												6.50	

(table continued on next page)

APPENDIX A - (Continued)

IN-SITU STATIC TESTS  
SUMMARY OF FIELD AND LABORATORY PROPERTIES

Site No.	Project	Bibliography	Rock Type	Test Details		Field Properties (before grouting)			Laboratory Properties		Field Properties (after grouting)			
				Static Test	P psi	Ed psi x10 <sup>6</sup>	Ee psi x10 <sup>6</sup>	Eseis psi x10 <sup>6</sup>	Est psi x10 <sup>6</sup>	Edyn psi x10 <sup>6</sup>	Ed psi x10 <sup>6</sup>	Ee psi x10 <sup>6</sup>	Eseis psi x10 <sup>6</sup>	
9	D'Avenue, France	Mayer (1963)	quartzite & schist	Jack perpendicular		0.14	0.68							
				parallel		0.28	0.49							
				perpendicular		0.77	1.32							
				parallel		0.72	1.70							
				perpendicular		0.92	2.42							
10	Dworshak, USA	Group De Travail (1964)	quartzite & schist	parallel		1.02	2.70							
				Jack perpendicular			0.68							
				parallel			0.49							
				perpendicular			0.85							
				parallel			0.32							
		Shannon & Wilson (1964)	granite gneiss	Jack (surface gages)	1000	2.7	3.3	9.2	8.6					
				vertical		2.5	3.8	9.2	8.6	11.7				
				horizontal		2.1	2.8	9.2	8.1	11.2				
				horizontal		0.8	1.2	9.2	7.5	11.5				
				horizontal		5.6	7.3	9.2	7.2	11.2				
				horizontal		1.45	1.7	9.2	7.9	12.0				
				vertical		0.8	1.5	7.1	8.8	12.1				
				vertical		3.4	6.3	7.1	8.5	11.8				
		horizontal		1.1	1.8	7.1	8.0	12.5						
		horizontal		0.7	1.3	7.1	8.0	11.1						
		vertical		2.3	3.3	7.7	7.1	11.3						
		vertical		0.4	0.75	7.7	7.5	11.8						
		horizontal		1.8	2.3	7.7	6.2	13.0						

(table continued on next page)

(table continued on next page)



APPENDIX A - (Continued)  
IN-SITU STATIC TESTS  
SUMMARY OF FIELD AND LABORATORY PROPERTIES

Site No.	Project	Bibliography	Rock Type	Test Details		Field Properties (before grouting)				Laboratory Properties		Field Properties (after grouting)					
				Static Test	P psi	Ed psi x10 <sup>6</sup>	Ee psi x10 <sup>6</sup>	Eseis psi x10 <sup>6</sup>	Est psi x10 <sup>6</sup>	Edyn psi x10 <sup>6</sup>	Ed psi x10 <sup>6</sup>	Ee psi x10 <sup>6</sup>	Eseis psi x10 <sup>6</sup>				
10 Con't	Dworshak, USA	Shannon & Wilson (1964)	granite gneiss	horizontal		1.1	1.6	7.7	8.3	12.6							
				vertical		3.8	4.9	7.1	8.0	11.5							
				vertical		0.55	1.0	7.1	5.4	11.6							
				horizontal		2.3	3.6	7.1	8.2	10.8							
				horizontal		4.3	5.2	7.1	6.3	10.9							
				vertical		1.3	2.2	5.9	6.6	12.3							
				vertical		0.7	1.4	5.9	6.6	11.8							
				horizontal		2.0	2.95	5.9	5.4	11.6							
				horizontal		1.2	1.9	5.9	4.6	12.0							
			granite gneiss	Jack (buried gages)	1000												
				vertical		6.2	7.6	9.2	8.6	11.7							
				vertical		4.2	5.1	9.2	8.6	11.2							
				horizontal		5.4	7.5	9.2	7.2	12.0							
				horizontal		4.8	5.6	9.2	7.9	12.0							
				vertical		0.6	1.3	7.1	8.8	12.1							
				horizontal		0.6	1.1	7.1	8.0	11.1							
				vertical		7.3	8.4	7.7	7.1	11.3							
				vertical		0.75	0.85	7.7	7.5	11.8							
				horizontal		1.55	2.3	7.7	6.2	13.0							
				horizontal		3.5	4.4	7.7	8.3	12.6							
				vertical		5.0	6.2	7.1	8.0	11.5							
				vertical		5.0	6.1	7.1	5.4	11.6							
				horizontal		4.7	5.6	7.1	8.2	10.8							
				horizontal		6.7	8.0	7.1	6.3	10.9							
				vertical		6.0	10.0	5.9	6.6	12.3							
				vertical		4.3	5.0	5.9	6.6	11.8							

(table continued on next page)

APPENDIX A - (Continued)  
IN-SITU STATIC TESTS  
SUMMARY OF FIELD AND LABORATORY PROPERTIES

Site No.	Project	Bibliography	Rock Type	Test Details		Field Properties (before grouting)			Laboratory Properties		Field Properties (after grouting)		
				Static Test	P psi	Ed psi x10 <sup>6</sup>	Ee psi x10 <sup>6</sup>	Eseis psi x10 <sup>6</sup>	Est psi x10 <sup>6</sup>	Edyn psi x10 <sup>6</sup>	Ed psi x10 <sup>6</sup>	Ee psi x10 <sup>6</sup>	Eseis psi x10 <sup>6</sup>
10 Con't	Dworshak, USA	Shannon & Wilson (1964)	granite gneiss	horizontal horizontal		1.6 0.9	2.7 1.4	5.9 5.9	5.4 4.6	11.6 12.0			
11	Funil, Brazil	Serafim & Nunes (1966)	gneiss	Jack vertical horizontal vertical horizontal	355 330 285 285	1.06 4.40 4.40 3.47			4.97 9.65 4.97 9.65				
12	Glagno, Italy	Capozza et al (1966)	dolomite	Jack vertical vertical	1420 1420		1.02 1.56						
13	Glen Canyon, USA	Rice (1964)	sandstone	Jack (flex. 34 in $\phi$ ) vertical horizontal vertical horizontal		1.30 0.93 1.20 1.00		2.45 2.45 2.70 2.70	1.85 1.85 1.85 1.85	2.50 2.50 2.70 2.70			
14	Grado, Spain	Salas & Uriel (1964)	marl	Jack vertical horizontal vertical horizontal	1700 1700 1700 1700	1.44 2.09 1.96 1.08							

(table continued on next page)

APPENDIX A - (Continued)  
IN-SITU STATIC TESTS  
SUMMARY OF FIELD AND LABORATORY PROPERTIES

Site No.	Project	Bibliography	Rock Type	Test Details		Field Properties (before grouting)			Laboratory Properties		Field Properties (after grouting)		
				Static Test	P psi	Ed psi x10 <sup>6</sup>	Ee psi x10 <sup>6</sup>	Eseis psi x10 <sup>6</sup>	Est psi x10 <sup>6</sup>	Edyn psi x10 <sup>6</sup>	Ed psi x10 <sup>6</sup>	Ee psi x10 <sup>6</sup>	Eseis psi x10 <sup>6</sup>
15	Greoux, France	Group De Travail (1964)	limestone	Jack vertical horizontal vertical horizontal		0.81 3.79 1.02 1.73						1.63 1.32 1.30 2.18	
16	Grosio, Italy	Barioli (1966)	chloritic schist	Jack	370	3.28	5.35	7.6					
17	IM Font, Morocco	Mayer (1963)		Jack perpendicular parallel		0.14 0.18	0.82 0.62					1.42 2.84	
18	Iznajar, Spain	Salas & Uriel (1964)	marl	Jack vertical horizontal	850 850	0.33 0.73							
19	Karadj, Iran	Waldorf et al (1963)	diorite	Jack			2.22 1.82 1.88 1.82 2.48 1.08						
20	Kariba Dam, Rhodesia	Lane (1964)	quartzite quartzite gneiss gneiss	Jack	200 200 200 200	0.12 0.24 0.77 0.88	0.45 0.35 1.27 1.32	1.15 1.15 3.30 3.30	10.5 10.5 6.9 6.9	8.8 8.8 10.0 10.0			

(table continued on next page)

APPENDIX A - (Continued)  
IN-SITU STATIC TESTS  
SUMMARY OF FIELD AND LABORATORY PROPERTIES

Site No.	Project	Bibliography	Rock Type	Test Details		Field Properties (before grouting)			Laboratory Properties		Field Properties (after grouting)		
				Static Test	P psi	Ed psi x10 <sup>6</sup>	Ee psi x10 <sup>6</sup>	Eseis psi x10 <sup>6</sup>	Est psi x10 <sup>6</sup>	Edyn psi x10 <sup>6</sup>	Ed psi x10 <sup>6</sup>	Ee psi x10 <sup>6</sup>	Eseis psi x10 <sup>6</sup>
21	Koshibu, Japan	Multipurpose Dam Testing Group	amphibolite granodiorite	Jack	710 710 425	4.20 3.69 3.35		6.54 7.10 5.74					
22	Kurobegawa, Japan	Nose (1964)	gneiss	Jack		0.28 0.16 0.24 0.18 0.43 0.22 0.39	0.44 0.38 0.46 0.34 0.85 0.42 0.52		0.79 0.72 0.76 1.07 0.84 0.59 0.72				
23	Latiyan, Iran	Lane (1964)	quartzite sandstone	Jack	200 200 200	0.25 0.18 0.19	0.68 0.63 0.54	2.60 3.73 2.41		5.10 6.45 5.10			
		Knill & Jones (1965)	sandstone sandstone sandstone sandstone & shale	Jack Jack Jack Jack		0.85 0.64 0.21 0.25	2.13 1.42 0.57 0.28	3.50 2.90 1.75 1.05					
24	Limberg, Austria	Link (1964)	limestone	Jack	370	0.11	0.28	1.65					

(table continued on next page)

APPENDIX A - (Continued)  
IN-SITU STATIC TESTS  
SUMMARY OF FIELD AND LABORATORY PROPERTIES

Site No.	Project	Bibliography	Rock Type	Test Details		Field Properties (before grouting)			Laboratory Properties		Field Properties (after grouting)		
				Static Test	P psi	Ed psi x10 <sup>6</sup>	Ee psi x10 <sup>6</sup>	Eseis psi x10 <sup>6</sup>	Est psi x10 <sup>6</sup>	Edyn psi x10 <sup>6</sup>	Ed psi x10 <sup>6</sup>	Ee psi x10 <sup>6</sup>	Eseis psi x10 <sup>6</sup>
25	Mequinenza, Spain	Salas & Uriel (1964)	limestone limestone & lignite limestone & lignite	Jack vertical vertical horizontal	1700	3.32 0.30 0.39							
26	Mine near Antioch, Calif., USA	Ewoldsen & Goodman (1965)	sandstone	Jack		0.54		0.75	0.78	0.54			
27	Mis, Italy	Capozza et al (1966)	dolomite & limestone	Jack (rigid)		0.95							
28	Morrow Pt., USA	USBR (1965)	gneiss pegmatite	Jack (flex. 34 in $\phi$ ) vertical horizontal vertical horizontal	600 600 600 600 600	0.99 0.86 1.50 1.08 0.90	1.30 1.33 2.08 2.09 1.40	5.4 5.4 6.9 6.9 6.1	5.3 5.3 4.3 4.3 5.0	8.1 (UI) 8.1 8.1 8.1 8.1			
29	Mossyrock, USA	Harza Engr.	rhyolite	Jack		0.81 0.90 0.99		4.8 4.6	2.6 5.6 2.0		0.95 1.60		

(table continued on next page)

APPENDIX A - (Continued)  
IN-SITU STATIC TESTS  
SUMMARY OF FIELD AND LABORATORY PROPERTIES

Site No.	Project	Bibliography	Rock Type	Test Details		Field Properties (before grouting)				Laboratory Properties		Field Properties (after grouting)		
				Static Test	P psi	Ed psi x10 <sup>6</sup>	Ee psi x10 <sup>6</sup>	Eseis psi x10 <sup>6</sup>	Est psi x10 <sup>6</sup>	Edyn psi x10 <sup>6</sup>	Ed psi x10 <sup>6</sup>	Ee psi x10 <sup>6</sup>	Eseis psi x10 <sup>6</sup>	
29 Con't	Mossyrock, USA	Harza Engr.	rhyolite	Jack		2.00 1.40 2.60 1.60		7.4 5.4	3.2 2.8 4.4 2.6		1.90			
30	Naruko, Japan	Japanese Nat. Comm. on Ig. Dams (1964)	granite	Jack		0.57								
31	Prague Czechoslovakia	Zaruba & Bukovansky (1966)	shale	Jack		0.21 0.28	0.31 0.71							
32	Roujanel, France	Group de Travail (1964)	schist	Jack vertical horizontal vertical horizontal		0.30 0.56 0.40 0.65						0.39 0.78 0.82 0.80		
33	St. Cassein, France	Group de Travail (1964)	gneiss	Jack vertical horizontal vertical horizontal		4.64 1.04 0.70 1.06						3.47 1.55 0.78 1.31		

(table continued on next page)

APPENDIX A - (Continued)  
IN-SITU STATIC TESTS  
SUMMARY OF FIELD AND LABORATORY PROPERTIES

Site No.	Project	Bibliography	Rock Type	Test Details		Field Properties (before grouting)				Laboratory Properties		Field Properties (after grouting)																																																																																																																																																																																																																																																																																																																																																																																																																																																																																																																																																																																																																																																																																																																																																																																																																																																																																																																																																																		
				Static Test	P psi	Ed psi x10 <sup>6</sup>	Ee psi x10 <sup>6</sup>	Eseis psi x10 <sup>6</sup>	Est psi x10 <sup>6</sup>	Edyn psi x10 <sup>6</sup>	Ed psi x10 <sup>6</sup>	Ee psi x10 <sup>6</sup>	Eseis psi x10 <sup>6</sup>																																																																																																																																																																																																																																																																																																																																																																																																																																																																																																																																																																																																																																																																																																																																																																																																																																																																																																																																																																	
34	St. Jean du Gard, France	Mayer (1963)	gneiss (altered)	Jack vertical vertical horizontal		0.14	0.34																																																																																																																																																																																																																																																																																																																																																																																																																																																																																																																																																																																																																																																																																																																																																																																																																																																																																																																																																																							
						0.40	0.60	4.12																																																																																																																																																																																																																																																																																																																																																																																																																																																																																																																																																																																																																																																																																																																																																																																																																																																																																																																																																																						
						0.26	0.43	3.90																																																																																																																																																																																																																																																																																																																																																																																																																																																																																																																																																																																																																																																																																																																																																																																																																																																																																																																																																																						
35	Speccheri, Italy	Link (1964)	gneiss (sound)	Jack		0.71	1.36	8.80																																																																																																																																																																																																																																																																																																																																																																																																																																																																																																																																																																																																																																																																																																																																																																																																																																																																																																																																																																						
							8.53	7.82																																																																																																																																																																																																																																																																																																																																																																																																																																																																																																																																																																																																																																																																																																																																																																																																																																																																																																																																																																						
36	Tana Termini, Italy	Ferratini (1966)	limestone	Jack (flex 19 in ϕ)		5.70	6.68	6.10																																																																																																																																																																																																																																																																																																																																																																																																																																																																																																																																																																																																																																																																																																																																																																																																																																																																																																																																																																						
						6.03	7.60	7.18																																																																																																																																																																																																																																																																																																																																																																																																																																																																																																																																																																																																																																																																																																																																																																																																																																																																																																																																																																						
						4.45	6.68	5.92																																																																																																																																																																																																																																																																																																																																																																																																																																																																																																																																																																																																																																																																																																																																																																																																																																																																																																																																																																						
						2.27	2.52	6.83																																																																																																																																																																																																																																																																																																																																																																																																																																																																																																																																																																																																																																																																																																																																																																																																																																																																																																																																																																						
						0.87	1.46	2.71																																																																																																																																																																																																																																																																																																																																																																																																																																																																																																																																																																																																																																																																																																																																																																																																																																																																																																																																																																						
37	Tehachapi, USA	Calif. Dept. Resources (1967)	diorite gneiss	Jack	1000	0.12	0.38																																																																																																																																																																																																																																																																																																																																																																																																																																																																																																																																																																																																																																																																																																																																																																																																																																																																																																																																																																							
						0.46	1.72																																																																																																																																																																																																																																																																																																																																																																																																																																																																																																																																																																																																																																																																																																																																																																																																																																																																																																																																																																							
						0.15	0.90																																																																																																																																																																																																																																																																																																																																																																																																																																																																																																																																																																																																																																																																																																																																																																																																																																																																																																																																																																							
						0.10	0.47																																																																																																																																																																																																																																																																																																																																																																																																																																																																																																																																																																																																																																																																																																																																																																																																																																																																																																																																																																							
						0.78	1.83																																																																																																																																																																																																																																																																																																																																																																																																																																																																																																																																																																																																																																																																																																																																																																																																																																																																																																																																																																							
						0.68	1.98																																																																																																																																																																																																																																																																																																																																																																																																																																																																																																																																																																																																																																																																																																																																																																																																																																																																																																																																																																							
						1.30	1.50																																																																																																																																																																																																																																																																																																																																																																																																																																																																																																																																																																																																																																																																																																																																																																																																																																																																																																																																																																							
						0.55	1.72																																																																																																																																																																																																																																																																																																																																																																																																																																																																																																																																																																																																																																																																																																																																																																																																																																																																																																																																																																							
						0.42	1.07																																																																																																																																																																																																																																																																																																																																																																																																																																																																																																																																																																																																																																																																																																																																																																																																																																																																																																																																																																							
						0.71	1.32																																																																																																																																																																																																																																																																																																																																																																																																																																																																																																																																																																																																																																																																																																																																																																																																																																																																																																																																																																							
						0.44	0.81																																																																																																																																																																																																																																																																																																																																																																																																																																																																																																																																																																																																																																																																																																																																																																																																																																																																																																																																																																							
						0.60	1.29																																																																																																																																																																																																																																																																																																																																																																																																																																																																																																																																																																																																																																																																																																																																																																																																																																																																																																																																																																							

(table continued on next page)

APPENDIX A - (Continued)

IN-SITU STATIC TESTS  
SUMMARY OF FIELD AND LABORATORY PROPERTIES

Site No.	Project	Bibliography	Rock Type	Test Details		Field Properties (before grouting)			Laboratory Properties		Field Properties (after grouting)		
				Static Test	P psi	Ed psi x10 <sup>6</sup>	Ee psi x10 <sup>6</sup>	Eseis psi x10 <sup>6</sup>	Est psi x10 <sup>6</sup>	Edyn psi x10 <sup>6</sup>	Ed psi x10 <sup>6</sup>	Ee psi x10 <sup>6</sup>	Eseis psi x10 <sup>6</sup>
37 Tehachapi, USA Con't		Calif. Dept. Resources (1967)	diorite gneiss	Jack		0.15	0.43						
						0.60	1.34						
						0.24	0.74						
						0.30	0.83						
						0.60	1.26						
						0.80	1.65						
						0.25	0.70						
38 Tsuruga, Japan		Kitsunezaki (1965)	granite	Jack horizontal vertical vertical		0.26	0.86						
						0.37	1.06						
						0.78	1.18						
								4.80					
39 Two Forks, USA		USBR (1966)	gneiss	Jack (flex)	1000	0.69	1.04	4.80					
						0.38	0.38	4.80					
						1.26	1.75	4.3	7.2	10.4			
						1.88	2.27	4.3	6.9	11.1			
40 Valdecana, Portugal		Rocha (1964)	granite	Jack	1000	1.81	2.48	4.3	6.7	11.3			
						2.31	2.78	4.3	9.1	12.2			
						0.21					0.21		
						0.22					0.26		
						0.23					0.23		
						0.23					0.24		
						0.24					0.20		
						0.21					0.36		
						0.26					0.36		
						0.37					0.34		

(table continued on next page)



APPENDIX A - (Continued)  
IN-SITU STATIC TESTS  
SUMMARY OF FIELD AND LABORATORY PROPERTIES

Site No.	Project	Bibliography	Rock Type	Test Details		Field Properties (before grouting)				Laboratory Properties			Field Properties (after grouting)		
						Static Test	P psi	Ed psi x10 <sup>6</sup>	Ee psi x10 <sup>6</sup>	Eseis psi x10 <sup>6</sup>	Est psi x10 <sup>6</sup>	Edyn psi x10 <sup>6</sup>	Ed psi x10 <sup>6</sup>	Ee psi x10 <sup>6</sup>	Eseis psi x10 <sup>6</sup>
40 Con't	Valdecana, Portugal	Rocha, (1964)	granite	Jack				0.38 0.78 0.47 0.71 0.74 0.75 1.45					0.36 0.26 0.78 0.74 0.85 1.06 2.27		
41	Val Vestino, Italy	Capozza, et al (1966)	dolomite	Jack (rigid) horizontal vertical horizontal vertical	140 140 1400 1400				0.95 0.56 0.55 0.54	5.56 5.56 5.42 5.42					
42	Vouglans, France	Duffaut & Comes (1966)	limestone dolomite	Jack				1.42 0.46 2.62	2.27 1.01 3.75						
43	Yellowtail Montana, USA	Rice (1964)	limestone	Jack (flex 34 in $\phi$ )	600 600 600			1.60 3.10 4.80	2.40 4.6 5.9	3.80 3.80 6.15	9.5 (UT) 8.3 7.3	11.5 11.2 10.4			
44	Dams in Czechoslovakia	Drozdz & Louma (1966)	biotite gneiss & amphibolite	Jack (flex 28 in $\phi$ )				2.20 0.69 1.04 0.36 0.76	5.21 2.40 3.61 1.95 3.55	7.23 2.92 3.75 2.50 4.45					

(table continued on next page)

APPENDIX A - (Continued)  
IN-SITU STATIC TESTS  
SUMMARY OF FIELD AND LABORATORY PROPERTIES

Site No.	Project	Bibliography	Rock Type	Test Details		Field Properties (before grouting)			Laboratory Properties		Field Properties (after grouting)		
				Static Test	P psi	Ed psi x10 <sup>6</sup>	Ee psi x10 <sup>6</sup>	Eseis psi x10 <sup>6</sup>	Est psi x10 <sup>6</sup>	Edyn psi x10 <sup>6</sup>	Ed psi x10 <sup>6</sup>	Ee psi x10 <sup>6</sup>	Eseis psi x10 <sup>6</sup>
45	Hydroplants, Yugoslavia	Kujundzic & Grujic (1966)	limestone	Flat Jack			0.42	1.85					
							0.64	2.48					
							0.71	3.55					
							0.99	3.76					
							1.78	4.26					
							1.70	4.40					
							0.99	5.54					
							1.14	5.96					
							2.13	5.96					
							3.26	6.82					
							1.71	8.23					
							2.84	9.22					
							5.40	8.23					
							6.03	8.23					
							1.42	3.48					
							1.06	3.34					
							1.28	4.83					
							2.06	5.18					
							1.28	5.40					
							1.63	6.39					
							2.84	7.31					
							2.98	9.15					
46	Hydro Projects, USSR	Sapegin & Shiryeau (1966)	limestone bituminous limestone fractured gneiss	Jack (flex)	475	2.20						3.68	
					475	0.87						1.65	
					475	0.07						0.23	

(table continued on next page)

APPENDIX A - (continued)

IN-SITU STATIC TESTS

SUMMARY OF FIELD AND LABORATORY PROPERTIES

Site No.	Project	Bibliography	Rock Type	Test Details		Field Properties (before grouting)				Laboratory Properties		Field Properties (after grouting)			
				Static Test	P psi	Ed psi x10 <sup>6</sup>	Ee psi x10 <sup>6</sup>	Eseis psi x10 <sup>6</sup>	Est psi x10 <sup>6</sup>	Edyn psi x10 <sup>6</sup>	Ed psi x10 <sup>6</sup>	Ee psi x10 <sup>6</sup>	Eseis psi x10 <sup>6</sup>		
47	Hydro Project, Japan	Onodera (1963)	arkosic sandstone	Jack (rigid 2 sq ft)			0.18	0.88							
							0.32	1.18							
							0.19	0.88							
							0.46	0.74							
							0.18	0.74							
							0.21	0.74							
48		Dvorak (1957)	sandstone & slate	(2 sq ft)			0.22	1.32							
							0.29	1.47							
							0.77	3.68							
							0.22	1.17							
							1.25	1.91							
							0.60	3.38							
							0.15	0.29							
							0.28	0.29							
							0.47	2.90							
							0.41	3.68							
			granodiorite	(.7 sq ft)			1.47	4.70							
				(5 sq ft)			0.71	4.40							
				(.7 sq ft)			1.05	5.15							
				(2 sq ft)			0.89	3.68							
			tuff	(2 sq ft)			1.05	4.70							
			andesite	(2 sq ft)											
			shale w/ quartzite shale weathered shale sound	Jack			0.14	0.35							
							0.15	0.84							
							1.09	3.10							

(table continued on next page)

APPENDIX A - (Continued)  
IN-SITU STATIC TESTS  
SUMMARY OF FIELD AND LABORATORY PROPERTIES

Site No.	Project	Bibliography	Rock Type	Test Details		Field Properties (before grouting)			Laboratory Properties		Field Properties (after grouting)		
				Static Test	P psi	Ed psi x10 <sup>6</sup>	Ee psi x10 <sup>6</sup>	Eseis psi x10 <sup>6</sup>	Est psi x10 <sup>6</sup>	Edyn psi x10 <sup>6</sup>	Ed psi x10 <sup>6</sup>	Ee psi x10 <sup>6</sup>	Eseis psi x10 <sup>6</sup>
49	Not Reported	Bernard (1953)	achist quartzite	Jack (flex 16 in $\phi$ ) perpendicular parallel perpendicular parallel			1.03 2.70 2.98 5.40						
50	Agri River, Italy	Lotti & Beamonte (1964)	conglomerate sandstone	P.C.			0.18 0.26						
51	Alpe Geva, Italy	Capozza et al (1966)	serpentine schist	P.C.	255		0.98						
52	Ambiesta, Italy	Link (1964)	limestone	P.C.	170		1.77	4.08					
53	Beauregard, Italy	Capozza et al (1966)	schist gneiss	P.C. vertical horizontal	425 100 160		3.41 0.14 0.85	5.69 2.42 2.42				0.78 1.78	5.94
54	Caprile, Italy	Capozza et al (1966)	sandstone	P.C.	370		1.46	5.30					

(table continued on next page)

APPENDIX A - (Continued)  
IN-SITU STATIC TESTS  
SUMMARY OF FIELD AND LABORATORY PROPERTIES

Site No.	Project	Bibliography	Rock Type	Test Details		Field Properties (before grouting)			Laboratory Properties		Field Properties (after grouting)		
				Static Test	P psi	Ed psi x10 <sup>6</sup>	Ee psi x10 <sup>6</sup>	Eseis psi x10 <sup>6</sup>	Est psi x10 <sup>6</sup>	Edyn psi x10 <sup>6</sup>	Ed psi x10 <sup>6</sup>	Ee psi x10 <sup>6</sup>	Eseis psi x10 <sup>6</sup>
55	Dworshak, USA	Shannon & Wilson (1964)	granitic	P.C.	60 180	2.00 3.20		7.2 9.2			0.28 0.35		
56	Fedaia, Italy	Link (1964)	limestone	P.C.			1.06	5.55					
57	Pfestiniog, Wales	Chapman (1961)	siltstone	P.C.		0.94 1.64 9.32							
58	Porto Buso, Italy	Link (1964)	quartz porphyry	P.C.	425	3.95	0.85	4.54					
59	Giouaretto, Italy	Link (1964)	gneiss	P.C.	425								
60	Glagno, Italy	Capozza et al (1966)	dolomite	P.C.	340 340		0.74 0.54					0.79 0.53	
61	IM Font, Morocco	Mayer (1963)		P.C.			0.36					1.38	
62	Kaunertal, Austria	Lauffer & Seeber (1966)	calcareous schist sericite	R.J. R.J.	810 135	0.82 0.15	1.46 0.24	2.7			1.39 0.12	1.60 0.10	

(table continued on next page)

APPENDIX A - (Continued)  
IN-SITU STATIC TESTS  
SUMMARY OF FIELD AND LABORATORY PROPERTIES

Site No.	Project	Bibliography	Rock Type	Test Details		Field Properties (before grouting)			Laboratory Properties		Field Properties (after grouting)		
				Static Test	P psi	Ed psi x10 <sup>6</sup>	Ee psi x10 <sup>6</sup>	Eseis psi x10 <sup>6</sup>	Est psi x10 <sup>6</sup>	E <sub>dyn</sub> psi x10 <sup>6</sup>	Ed psi x10 <sup>6</sup>	Ee psi x10 <sup>6</sup>	Eseis psi x10 <sup>6</sup>
62 Kamertal, Austria		Lauffer & Sceber (1966)	schist calcareous phyllite schistose gneiss augen gneiss calcareous schist	R.J.	270	0.44	0.74				0.21	0.38	
				R.J.	540	0.71	1.38				0.72	1.62	
				R.J.	570	5.10	5.25				5.40	5.70	
				R.J.	810	0.87	1.55	2.7			1.15	2.44	
63	Koshibu, Japan	Multipurpose Dam Testing Group (1964)	amphibolite granodiorite	P.C.	425	3.35		5.74		9.4			
64	Mae, Italy	Capozza et al (1966)	dolomite limestone	P.C.	325 325		1.21 0.95	4.40 3.69				1.42 8.2	
65	Mis, Italy	Capozza et al (1966)	dolomite	P.C.	255		0.57					0.78	
66	Mulargia, Sardinia	Link (1964)	porphyrite slate	P.C.	170								
67	Nevada Test Site USA	Judd (1965)	vesicular dacite	P.C.	1500	0.38		2.8	3.6	5.35			

(table continued on next page)

APPENDIX A - (Continued)  
IN-SITU STATIC TESTS  
SUMMARY OF FIELD AND LABORATORY PROPERTIES

				Test Details		Field Properties (before grouting)				Laboratory Properties		Field Properties (after grouting)			
Site No.	Project	Bibliography	Rock Type	Static Test	P psi	Ed psi x10 <sup>6</sup>	Ee psi x10 <sup>6</sup>	Eseis psi x10 <sup>6</sup>	Est psi x10 <sup>6</sup>	Edyn psi x10 <sup>6</sup>	Ed psi x10 <sup>6</sup>	Ee psi x10 <sup>6</sup>	Eseis psi x10 <sup>6</sup>		
68	Pietra Del Pertusillo, Italy	Link (1964)	sandstone & conglomerate	P.C.	210		0.28	3.55							
69	Pieve Di Cadore, Italy	Capozza et al (1966)	limestone	P.C.	230		0.43					0.60			
70	Vajont, Italy	Link (1964)	limestone	P.C.	170		0.53	2.98				0.57			
71	Val Gallina, Italy	Capozza et al (1966)	limestone	P.C.	340 570		0.64 1.70	4.83 4.45							
72	Not Reported	Bernard (1953)	schist	P.C. perpendicular parallel perpendicular parallel perpendicular parallel	170 340		0.59 0.40								
			quartzite				2.84 5.12 6.43 9.55 6.95 4.63 1.56 4.26								

(table continued on next page)

APPENDIX A - (Continued)  
IN-SITU STATIC TESTS  
SUMMARY OF FIELD AND LABORATORY PROPERTIES

Site No.	Project	Bibliography	Rock Type	Test Details		Field Properties (before grouting)			Laboratory Properties		Field Properties (after grouting)		
				Static Test	P psi	Ed psi x10 <sup>6</sup>	Ee psi x10 <sup>6</sup>	Eseis psi x10 <sup>6</sup>	Est psi x10 <sup>6</sup>	Edyn psi x10 <sup>6</sup>	Ed psi x10 <sup>6</sup>	Ee psi x10 <sup>6</sup>	Eseis psi x10 <sup>6</sup>
72 Con't	Not Reported	Bernard (1953)	gypsum	perpendicular parallel perpendicular parallel			0.64 0.64 0.71 3.41						
73	Bajina Basta, Yugoslavia	Kujundzic & Stojakovic (1964)	clay shale	B.D.	240								
74	Barbellino, Italy	Capozza et al (1966)	schist, sandstone	B.D.			6.8						
75	Caresev, Italy	Capozza et al (1966)	quartz, phyllite gneiss	B.D.			3.4						
76	Dubrovnik, Yugoslavia	Kujundzic & Stojakovic (1964)	limestone & dolomite	B.D.	710	0.624	0.895						
77	La Bathie, France	Group de Travail (1964)	gneiss	B.D.		5.04			5.9				
78	Malga Bissana, Italy	Capozza et al (1966)	quartz diorite	B.D.			3.1						

(table continued on next page)



APPENDIX A - (Continued)  
IN-SITU STATIC TESTS  
SUMMARY OF FIELD AND LABORATORY PROPERTIES

Site No.	Project	Bibliography	Rock Type	Test Details		Field Properties (before grouting)			Laboratory Properties		Field Properties (after grouting)		
				Static Test	P psi	Ed psi x10 <sup>6</sup>	Ee psi x10 <sup>6</sup>	Eseis psi x10 <sup>6</sup>	Est psi x10 <sup>6</sup>	Edyn psi x10 <sup>6</sup>	Ed psi x10 <sup>6</sup>	Ee psi x10 <sup>6</sup>	Eseis psi x10 <sup>6</sup>
79	Morasco, Italy	Capozza et al (1966)	mica schist	B.D.			2.5						
80	Pantano D'Avio, Italy	Capozza et al (1966)	granodiorite	B.D.			3.4						
81	Sabbione, Italy	Capozza et al (1966)	calcareous schist	B.D.			3.7						
82	Trona, Italy	Capozza et al (1966)	sandstone & conglomerate	B.D.			1.9						
83	Vouglans, France	Duffaut & Comes (1966)	limestone & dolomite	B.D.		2.70 0.92 4.84	3.70 1.89 5.44						
84	Not Reported	Dvorak (1967)	shale w/ quartzite	B.D.		0.23	0.51						
85	Alpe Gera, Italy	Capozza, et al (1966)	serpentine schist	S.D.			4.5						
86	Barbellino, Italy	Capozza, et al (1966)	sandstone	S.D.		6.7							

(table continued on next page)

APPENDIX A - (Continued)  
IN-SITU STATIC TESTS  
SUMMARY OF FIELD AND LABORATORY PROPERTIES

Site No.	Project	Bibliography	Rock Type	Test Details		Field Properties (before grouting)			Laboratory Properties		Field Properties (after grouting)		
				Static Test	P psi	Ed psi x10 <sup>6</sup>	Ee psi x10 <sup>6</sup>	Eseis psi x10 <sup>6</sup>	Est psi x10 <sup>6</sup>	Edyn psi x10 <sup>6</sup>	Ed psi x10 <sup>6</sup>	Ee psi x10 <sup>6</sup>	Eseis psi x10 <sup>6</sup>
87	Gareser, Italy	Capozza, et al (1966)	gneiss	S.D.		5.0							
88	Davis, USA	USBR (1948)		S.D.		0.35-1.20							
89	Inferno, Italy	Capozza, et al (1966)	sandstone et conglomerate	S.D.		2.0							
90	Malga Bissana, Italy	Capozza, et al (1966)	quartz diorite	S.D.		2.4							
91	Morasco, Italy	Capozza, et al (1966)	mica schist	S.D.		2.7 3.0							
92	Nagase, Japan	Japanese Nat. Comm. or Large Dams (1964)	sandstone shale conglomerate	S.D.		1.42							
93	Haruko, Japan	Japanese Nat. Comm. on Large Dams (1964)	granite	S.D.		0.64							

(table continued on next page)

APPENDIX A - (Concluded)

IN-SITU STATIC TESTS  
SUMMARY OF FIELD AND LABORATORY PROPERTIES

Site No.	Project	Bibliography	Rock Type	Test Details		Field Properties (before grouting)			Laboratory Properties		Field Properties (after grouting)		
				Static Test	P psi	Ed psi x10 <sup>6</sup>	Ee psi x10 <sup>6</sup>	Eseis psi x10 <sup>6</sup>	Est psi x10 <sup>6</sup>	Edyn psi x10 <sup>6</sup>	Ed psi x10 <sup>6</sup>	Ee psi x10 <sup>6</sup>	Eseis psi x10 <sup>6</sup>
94	Pantano D'Auio, Italy	Capozza, et al (1966)	granodiorite	S.D.		1.7 2.4 1.7							
95	Sabbione, Italy	Capozza, et al (1966)	calcareous schist	S.D.		5.0							
96	Sufes, Switzerland	Schnitter (1964)	gneiss	S.D.		1.42	2.84	4.7	3.89	2.34			
97	Trona, Italy	Capozza et al (1966)	sandstone conglomerate	S.D.		2.6							
98	Yellowtail Montana, USA	Rice (1964)	limestone	S.D.		0.4- 1.4							

Note: Ed = Modulus of Deformation (field, static)  
Ee = Modulus of Elasticity (field, static)  
Eseis = Modulus of Elasticity (field, dynamic)

Est = Modulus of Elasticity (laboratory, static)  
Edyn = Modulus of Elasticity (laboratory, dynamic)

# APPENDIX B

## IN-SITU STATIC TESTS SUMMARY OF MODULUS RATIOS AND ROCK QUALITY INDICES

Site No.	Project	Static Test	In-Situ Test Moduli			Modulus Ratios				Rock Quality Indices		
			Ed psi x10 <sup>6</sup>	Ee psi x10 <sup>6</sup>		$\frac{Ed}{Est}$	$\frac{Ed}{Edyn}$	$\frac{Ee}{Est}$		Rock Quality Designation RQD %	Velocity Index ( $V_F/V_L$ ) <sup>2</sup>	Deformation Ratio, Elastic/ Total
1	Agri River, Italy	Jack		1.66 0.34								0.20 0.35
2	Alpe Gera, Italy	Jack		3.63 1.27								0.58 0.60
4	Ananaigawa, Japan	Jack	0.54			0.12						
7	Cambambe	Jack		1.15 0.91 0.51 1.12 0.42 1.16 1.36 1.88 0.16 2.36 1.85 4.50 1.36 1.99				0.14 0.11 0.06 0.13 0.05 0.14 0.16 0.14 0.02 0.28 0.22 0.53 0.16 0.23				

(table continued on next page)

APPENDIX B - (Continued)

IN-SITU STATIC TESTS  
SUMMARY OF MODULUS RATIOS AND ROCK QUALITY INDICES

Site No.	Project	Static Test	In-Situ Test Moduli			Modulus Ratios			$\frac{E_e}{E_{dyn}}$	Rock Quality Indices		
			Ed psi x10 <sup>6</sup>	Ee psi x10 <sup>6</sup>		$\frac{E_d}{E_{est}}$	$\frac{E_d}{E_{dyn}}$	$\frac{E_e}{E_{est}}$		Rock Quality Designation RQD %	Velocity Index ( $V_F/V_L$ ) <sup>2</sup>	Deformation Ratio, Elastic/ Total
10	Dworshak, USA	Jack	2.7	3.3		0.31		0.38		85	0.79	0.66
			2.5	3.8		0.29	0.21	0.44	0.32	70	0.80	0.47
			2.1	2.8		0.26	0.19	0.35	0.25	62	0.86	0.69
			0.8	1.2		0.11	0.07	0.16	0.10	35	0.80	0.55
			5.6	7.3		0.62	0.50	0.81	0.65	68	0.86	0.75
			1.45	1.7		0.18	0.12	0.22	0.14	59	0.76	0.71
			0.8	1.5		0.09	0.07	0.17	0.12	53	0.73	0.43
			3.4	6.3		0.40	0.29	0.74	0.53	79	0.76	0.48
			1.1	1.8		0.14	0.09	0.23	0.14	87	0.76	0.43
			0.7	1.3		0.09	0.06	0.16	0.12	70	0.82	0.42
			2.3	3.3		0.32	0.20	0.47	0.29	72	0.73	0.61
			0.4	0.75		0.05	0.03	0.10	0.06	65	0.74	0.50
			1.8	2.3		0.29	0.14	0.37	0.18	68	0.71	0.75
			1.1	1.6		0.13	0.09	0.19	0.13	92	0.67	0.48
			3.8	4.9		0.48	0.33	0.61	0.43	77	0.78	0.73
			0.55	1.0		0.10	0.05	0.18	0.09	65	0.78	0.43
			2.3	3.6		0.28	0.21	0.44	0.33	63	0.82	0.54
			4.3	5.2		0.57	0.39	0.83	0.48	82	0.77	0.65
			1.3	2.2		0.16	0.11	0.33	0.18	73	0.47	0.61
			0.7	1.4		0.11	0.06	0.21	0.12	70	0.49	0.46
			2.0	2.95		0.37	0.17	0.55	0.25	74	0.48	0.53
			1.2	1.9		0.26	0.10	0.41	0.16	70	0.48	0.64
			6.2	7.6		0.68	0.36	0.88		92	0.79	0.84
			4.2	5.1		0.49	0.36	0.59	0.43	85	0.80	0.75
			5.4	7.5		0.75	0.48	1.04	0.67	77	0.86	0.65
			4.8	5.6		0.61	0.40	0.71	0.47	68	0.76	0.50

(table continued on next page)

APPENDIX B - (Continued)

IN-SITU STATIC TESTS  
SUMMARY OF MODULUS RATIOS AND ROCK QUALITY INDICES

Site No.	Project	Static Test	In-Situ Test Moduli		Modulus Ratios			Rock Quality Indices			
			Ed psi x10 <sup>6</sup>	Ee psi x10 <sup>6</sup>	Ed Est	Ed Edyn	Ee Est	Ee Edyn	Rock Quality Designation RQD %	Velocity Index (V <sub>F</sub> /V <sub>L</sub> ) <sup>2</sup>	Deformation Ratio, Elastic/ Total
10 Con't	Dworshak, USA	Jack	0.6	1.3	0.09	0.07	0.15	0.11	60	0.73	0.38
			0.6	1.1	0.07	0.05	0.14	0.10	75	0.82	0.38
			7.3	8.4	1.03	0.65	1.18	74	83	0.73	0.83
			0.75	0.85	0.10	0.64	0.11	0.07	53	0.74	0.78
			1.55	2.3	0.25	0.12	0.37	0.18	76	0.71	0.55
			3.5	4.4	0.42	0.28	0.53	0.35	89	0.67	0.66
			5.0	6.2	0.62	0.43	0.78	0.54	73	0.78	0.70
			5.0	6.1	0.93	0.43	1.13	0.53	84	0.78	0.76
			4.7	5.6	0.57	0.44	0.68	0.52	90	0.82	0.77
			6.7	8.0	1.06	0.62	1.27	0.74	91	0.77	0.80
			6.0	10.0	0.91	0.49	1.51	0.81	89	0.47	0.52
			4.3	5.0	0.65	0.36	0.76	0.42	87	0.49	0.77
			1.6	2.7	0.30	0.14	0.50	0.23	86	0.48	0.64
			0.9	1.4	0.20	0.07	0.30	0.12	70	0.48	0.51
11	Funil, Italy	Jack	1.06		0.22						
			4.40		0.46						
			4.40		0.88						
			3.47		0.36						
12	Glagno, Italy	Jack		1.02							0.29

(table continued on next page)

APPENDIX B - (Continued)

IN-SITU STATIC TESTS  
SUMMARY OF MODULUS RATIOS AND ROCK QUALITY INDICES

Site No.	Project	Static Test	In-Situ Test Moduli		Modulus Ratios			$\frac{E_e}{E_{dyn}}$	Rock Quality Indices		
			Ed psi $\times 10^6$	Ee psi $\times 10^6$	$\frac{Ed}{Est}$	$\frac{Ed}{E_{dyn}}$	$\frac{E_e}{Est}$		Rock Quality Designation RQD %	Velocity Index $(V_p/V_L)^2$	Deformation Ratio, Elastic/ Total
13	Glen Canyon, USA	Jack	1.30 0.93 1.20 1.00			0.70 0.50 0.65 0.54	0.52 0.37 0.44 0.37		70 70 78 78	0.98 0.98 0.100 0.100	0.93 0.90 0.89 0.84
16	Grosio, Italy	Jack	3.28	5.35							0.62
20	Kariba Dam, Rhodesia	Jack	0.12 0.24 0.77 0.88	0.45 0.35 1.27 1.32	0.01 0.02 0.11 0.13	0.01 0.03 0.08 0.09	0.04 0.03 0.18 0.19	0.05 0.04 0.13 0.13		0.13 0.13 0.33 0.33	0.27 0.33 0.71 0.72
21	Koshiu, Japan	Jack	4.20 3.69 3.35			0.45 0.39 0.36				0.70 0.76 0.61	
22	Kurobegawa, Japan	Jack	0.28 0.16 0.24 0.18 0.43 0.22 0.39	0.44 0.38 0.46 0.34 0.85 0.42 0.52	0.35 0.22 0.32 0.17 0.51 0.37 0.54		0.56 0.53 0.61 0.32 1.01 0.71 0.72				

(table continued on next page)

APPENDIX B - (Continued)

IN-SITU STATIC TESTS  
SUMMARY OF MODULUS RATIOS AND ROCK QUALITY INDICES

Site No.	Project	Static Test	In-Situ Test Moduli		Modulus Ratios			Rock Quality Indices			
			Ed psi x10 <sup>6</sup>	Ee psi x10 <sup>6</sup>	Ed Est	Ed Edyn	Ee Est	Ee Edyn	Rock Quality Designation RQD %	Velocity Index ( $V_F/V_L$ ) <sup>2</sup>	Deformation Ratio, Elastic/ Total
23	Latiyan, Iran	Jack	0.25 0.18 0.19	0.68 0.63 0.54		0.05 0.03 0.04		0.13 0.10 0.11		0.51 0.58 0.47	0.50 0.42 0.53
26	Mine near Antioch, USA	Jack		0.54			0.69	1.00		1.39	
27	Mis., Italy	Jack		0.78							0.65
28	Morrow Pt., USA	Jack	0.99 0.86 1.50 1.08 0.90 1.70	1.30 1.33 2.08 2.09 1.40 2.28	0.19 0.16 0.35 0.25 0.18 0.34	0.12 0.11 0.19 0.13 0.11 0.21	0.25 0.25 0.48 0.48 0.28 0.45	0.16 0.16 0.26 0.26 0.17 0.28		0.67 0.67 0.85 0.85 0.75 0.75	
29	Mossyrock, USA	Jack	0.81 0.90 0.99 2.00 1.40 2.60 1.60		0.31 0.16 0.50 0.62 0.50 0.59 0.62						

(table continued on next page)



APPENDIX B - (Continued)

IN-SITU STATIC TESTS  
SUMMARY OF MODULUS RATIOS AND ROCK QUALITY INDICES

Site No.	Project	Static Test	In-Situ Test Moduli		Modulus Ratios			Ee Edyn	Rock Quality Indices		
			Ed psi x10 <sup>6</sup>	Ee psi x10 <sup>6</sup>	Ed Est	Ed Edyn	Ee Est		Rock Quality Designation RQD %	Velocity Index (V <sub>F</sub> /V <sub>L</sub> ) <sup>2</sup>	Deformation Ratio, Elastic/ Total
34	St. Jean du Gard, France	Jack	0.14	0.34							0.46
			0.40	0.60							0.66
			0.26	0.43							0.60
			0.09	0.24							0.48
			0.71	1.36							0.62
36	Tana Termini, Italy	Jack	5.70	6.68		0.66		0.78		0.73	
			6.03	7.60		0.70		0.88		0.86	
			4.45	6.68		0.52		0.78		0.68	
			2.27	2.52		0.26		0.29		0.89	
			0.87	1.46		0.10		0.32		0.33	
37	Tehachapi, USA	Jack	0.12	0.38					45		0.32
			0.46	1.72					82		0.28
			0.15	0.90					29		0.18
			0.10	0.47					49		0.21
			0.78	1.83							0.41
			0.68	1.98							0.36
			1.30	1.50							0.87
			0.55	1.72							0.32
			0.42	1.07							0.39
			0.71	1.32							0.53
			0.44	0.81							0.56
			0.60	1.29							0.47
			0.15	0.43							0.36

(table continued on next page)

APPENDIX B - (Continued)

IN-SITU STATIC TESTS  
SUMMARY OF MODULUS RATIOS AND ROCK QUALITY INDICES

Site No.	Project	Static Test	In-Situ Test Moduli		Modulus Ratios			$\frac{E_e}{E_{dyn}}$	Rock Quality Indices		
			Ed psi x10 <sup>6</sup>	Ee psi x10 <sup>6</sup>	$\frac{Ed}{Est}$	$\frac{Ed}{E_{dyn}}$	$\frac{Ee}{Est}$		Rock Quality Designation RQD %	Velocity Index ( $V_F/V_L$ ) <sup>2</sup>	Deformation Ratio, Elastic/ Total
37 Con't	Tehachapi, USA	Jack	0.60	1.34							0.44
			0.24	0.74							0.34
			0.30	0.83							0.36
			0.60	1.26							0.49
			0.80	1.65							0.48
			0.25	0.70							0.35
39	Two Forks, USA	Jack	0.26	0.86							0.31
			0.37	1.06							0.35
			0.73	1.18							0.67
			1.26	1.75	0.18	0.12	0.24	0.17	52	0.41	0.49
			1.88	2.27	0.27	0.17	0.33	0.20	85	0.39	0.51
			1.81	2.48	0.27	0.16	0.37	0.22	83	0.38	0.51
41	Val Vestino, Italy	Jack	2.31	2.78	0.25	0.19	0.31	0.23	89	0.35	0.44
43	Yellowtail	Jack									0.67
											0.80
46	Not Reported- Hydroprojects USSR	Jack	1.60	2.40	0.17	0.14	0.25	0.21	71	0.33	0.57
			3.10	4.60	0.37	0.28	0.55	0.41	83	0.34	0.58
			4.80	5.90	0.66	0.46	0.58	0.57		0.59	0.90
			2.20								0.40
			0.87								0.47
			0.07								

(table continued on next page)

APPENDIX B - (Continued)

IN-SITU STATIC TESTS  
SUMMARY OF MODULUS RATIOS AND ROCK QUALITY INDICES

Site No.	Project	Static Test	In-Situ Test Moduli		Modulus Ratios			Rock Quality Indices			
			Ed psi x10 <sup>6</sup>	Ee psi x10 <sup>6</sup>	Ed Est	Ed Edyn	Ee Est	Ee Edyn	Rock Quality Designation RQD %	Velocity Index (V <sub>F</sub> /V <sub>L</sub> ) <sup>2</sup>	Deformation Ratio, Elastic/ Total
50	Agri River, Italy	P.C.		0.18 0.26							0.40 0.59
51	Alpe Gera, Italy	P.C.		0.98							0.81
53	Beauregard, Italy	P.C.		3.41 0.14 0.85							0.58 0.70 0.47
60	Glagno, Italy	P.C.		0.74 0.54							0.55 0.62
62	Kaunertal, Austria	R.J.	0.82 0.87 0.15 0.44 0.19 0.71 5.10	1.46 1.55 0.24 0.74 0.41 1.38 5.25							0.28 0.26 0.36 0.29
64	Mae, Italy	P.C.		1.21 0.95							0.12 0.95 0.60 0.64

(table continued on next page)

APPENDIX B - (Concluded)

IN-SITU STATIC TESTS  
SUMMARY OF MODULUS RATIOS AND ROCK QUALITY INDICES

Site No.	Project	Static Test	In-Situ Test Moduli		Modulus Ratios			Ee Edyn	Rock Quality Indices		
			Ed psi x10 <sup>6</sup>	Ee psi x10 <sup>6</sup>	Ed Est	Ed Edyn	Ee Est		Rock Quality Designation RQD %	Velocity Index (V <sub>F</sub> /V <sub>L</sub> ) <sup>2</sup>	Deformation Ratio, Elastic/ Total
65	Mis, Italy	P.C.		0.57							0.63
67	Nevada Test Site, USA	P.C.	0.38		0.11	0.07				0.52	
71	Val Gallina, Italy	P.C.		0.59 0.40							0.51 0.63
94	Pantano D'Avio, Italy	S.D.	2.4 1.7					0.270 0.183			
96	Surfes, Switzerland	S.D.	1.42	2.84	0.36	0.61	0.73	1.22			

Note: Ed = Modulus of Deformation (field static)      Est = Modulus of Elasticity (laboratory, static)  
Ee = Modulus of Elasticity (field, static)      Edyn = Modulus of Elasticity (laboratory, dynamic)

# BIBLIOGRAPHY

- Alger, R. P., W. R. Raymer, W. R. Hoyle and M. P. Tixer, 1963, "Formation Density Log Applications in Liquid-Filled Holes," Journal Petroleum Technology, p. 321-332.
- Avila, F. P., 1966, "Som Applications of Seismic Field Tests in Rock Media," Proceedings of the First Congress of the International Society of Rock Mechanics, Lisbon, Vol. 1, p. 3-6.
- Barioli, I. E., 1966, "Physical Properties of Rock Mass and Research of a Correlation Between Static and Dynamic Modulus of Elasticity," Proceedings of the First Congress of the International Society of Rock Mechanics, Lisbon, Vol. 1, p. 237-242.
- Benard, P., 1953, "Mesure des Modules Elastiques et Application au Calcul des Galeries en Charge," Proc. Third Int. Conf. on Soil Mech. and Fdn. Eng., Vol. 2, p. 145-156.
- Berned, J., and E. Absi, 1966, "Determination of Modulus of Subgrade Reaction Around Underground Excavations," Proceedings of the First Congress of the International Society of Rock Mechanics, Lisbon, Vol. 1, p. 411-444.
- Bhatnagar, P. S., 1964, "Experiments on Bhakra Dam Foundations," Eighth Int. Cong. on Large Dams, Edinburgh, Vol. 1, R.58, Q.28, p. 1081-1108.
- Birch, F., 1960, "The Velocity of Compressional Waves in Rocks to 10 Kilobars," Part I, Journal of Geophysical Research, Vol. 65, p. 1083-1102.
- Birch, F., and D. Bancroft, 1938, "Elasticity and Internal Friction in a Long Column of Granite," Bull. Seism. Soc. of America, Vol. 28, p. 234-254.
- Bjerrum, L., and F. Jorstad, 1963, "Discussion of the Paper by K. W. John, An Approach to Rock Mechanics," Proc. ASCE, Vol. 89, SMI, p. 300-302, p. 1-30.
- Bleifuss, D. J., 1955, "Theory for the Design of Underground Pressure Conduits," Proc. ASCE, Vol. 81, Paper No. 741, p. 10.
- Bollo, M. F., 1964, "The Findings on Geotechnical Research on a Series of Dam Sites," Eighth Int. Cong. on Large Dams, Edinburgh, Vol. 1, R.21, Q.28, p. 405-423.
- Borowicka, H., 1936, "Influence of Rigidity of a Circular Foundation Slab on the Distribution of Pressures Over the Contact Surface," Proc. First Int. Cong. Soil Mech. and Fdn. Eng., Vol. 2, p. 144.
- Building Research Station, 1967, "Site Tests for Giant Accelerator," Building Research Station News, Vol. 2, Garston, Hertfordshire, England, Autumn.

- Burwell, E. B., and R. H. Nesbitt, 1954, "The NX Borehole Camera," Transactions AIME, Vol. 199, p. 805-808.
- Bussey, W. H., 1963, "Some Rock Grouting Experiences," Grouts and Drilling Muds in Engineering Practice, Butterworths, London, p. 65-70.
- Capozza, P., and A. Marazio, 1966, "Deformability of the Foundation Rocks at Some Italian Dams," Proceedings of the First Congress of the International Society of Rock Mechanics, Lisbon, Vol. 2, p. 603, 616.
- Carroll, R., and J. Scott, 1966, "Uphole Seismic Measurements as an Indication of Stress Relief in Granitic Rock Tunnels," USGS Prof. Paper 500-D.
- Chapman, E. J., 1961, "Pressure Tests on Rock Galleries for the Ffestiniog Pumped Storage Plant," Seventh Int. Cong. on Large Dams, Rome, Vol. 2, R.22-Q.25, p. 237-260.
- Christensen, D. M., 1963, The 3-D Sonic Velocity Log, Birdwell Co., Tulsa, Oklahoma.
- Christensen, D. M., 1964, "A Theoretical Analysis of Wave Propagation in Fluid Filled Drill Holes for the Interpretation of the 3 Dimensional Velocity Log," Society of Professional Well Log Analysts, (Fifth Annual Symposium), Tulsa, Oklahoma, p. K1-K29.
- Clark, S. P., 1966, Handbook of Physical Constants, Geol. Soc. of Amer., Memoir 97.
- Coates, D. F., 1964, "Classification of Rocks for Rock Mechanics," International Journal of Rock Mechanics and Mining Sciences, Vol. 1, p. 421-431.
- Coates, D. F., 1965, Rock Mechanics Principles, Department of Mines and Technical Surveys Branch, Monograph 874, Ottawa, Canada.
- Cording, E. J., 1966, The Stability During Construction of Three Large Underground Openings, Ph.D. Thesis, University of Illinois.
- Deere, D. U., 1963, Private Communication.
- Deere, D. U., 1964, Personal Files.
- Deere, D. U., 1965, "Rock Mechanics Considerations, World Trade Center," Consulting Report.
- Deere, D. U., and F. Patton, 1965, From the Report, Engineering of Proposed Tunnels Adjacent to Tunnel No. 1, Interstate No. 40, Haywood County, North Carolina.
- Deere, D. U., and R. P. Miller, 1966, Classification and Index Properties for Intact Rock, AFWL-TR-65-116, AF Special Weapons Center, Kirtland AFB, New Mexico.

- Deere, D. U., A. J. Hendron, F. D. Patton, and E. J. Cording, 1967, "Design of Surface and Near-Surface Construction in Rock," Failure and Breakage of Rock, (Proceedings of the Eighth Symposium on Rock Mechanics), Minneapolis, AIME, p. 237-303.
- Denissov, N., G. Paushkin and A. Zayszev, 1966, "Applying the Information Received in the Process of Drilling for the Estimation of the State of Rocks," Proceedings of the First Congress of the International Society of Rock Mechanics, Lisbon, Vol. 1, p. 199-203.
- Dobrin, M. B., 1960, Introduction to Geophysical Prospecting, Second Edition, McGraw-Hill Co., New York.
- Dodd, J. S., 1967, "Morrow Point Underground Powerplant: Rock Mechanics Investigations," Bureau of Reclamation Technical Publication, Denver, Colorado.
- Drozdz, K. B. L., 1966, "The Correlation of Moduli of Elasticity Determined by Microseismic Measurement and Static Loading Test," Proceedings of the First Congress of the International Society of Rock Mechanics, Lisbon, Vol. 1, p. 291-293.
- Duffaut, P., and G. Comes, 1966, "Stress-Strain Comparative Measuring on a Foundation Material Measured in Place on the Face of an Excavation and on a Borehole Wall," Proceedings of the First Congress of the International Society of Rock Mechanics, Lisbon, Vol. 1, p. 399-403.
- Duncan, N., 1965, "Geology and Rock Mechanics in Civil Engineering Practice," Water Power, London, England, Jan.
- Dvorak, A., 1957, "Field Tests of Rocks on Dam Sites," Proc. Fourth Int. Conf. on Soil Mech. and Fdn. Eng., London, Vol. 1, p. 221-224.
- Dvorak, A., 1967, "Determination of Deformation Properties of Rocks in Drill-holes by Sounding Deformeter and Comparison with Plate Loading Tests," Rock Mechanics and Engineering Geology, Supplement III, p. 1-10.
- Ege, J. R., 1967, Private Communication.
- Fairhurst, C., and N. Cook, 1966, "The Phenomenon of Rock Splitting Parallel to the Direction of Maximum Compression in the Neighborhood of a Surface," Proceedings of the First Congress of the International Society of Rock Mechanics, Lisbon, Vol. 1, p. 687-692.
- Fergusson, F., and P. Lancaster-Jones, 1964, "Testing the Efficiency of Grouting Operations at Dam Sites," Eighth Int. Cong. on Large Dams, Edinburgh, Vol. 1, R.7, Q.28, p. 121-139.
- Ferratini, I., 1966, "Seismic Tests and Hydraulic Jack Tests to Determine the Modulus of Elasticity of the Foundation Rock of Tana Termini Dam," Proceedings of the First Congress of the International Society of Rock Mechanics, Lisbon, Vol. 1, p. 549-557.

- Fisher, R., 1963, "Statistical Methods for Research Workers," Hafner Publishing Co., New York.
- Gaskell, R. F., and P. Threadgold, 1960, "Borehole Surveying," Methods and Techniques in Geophysics, Vol. 1, S. Runeson ed., Interscience Publishers Inc., New York, p. 62-104.
- Gicot, H., 1948, "Mesures de la Deformabilite du sol de Fondation du Barrage de Rossens," Third Int. Cong. on Large Dams, Stockholm, Vol. 2, R-56, Q.9.
- Goodman, R., and H. Ewoldsen, 1965, The Relationship Between Field and Laboratory Measurements of the Mechanical Properties of Sandstone, University of California.
- Griffiths, D. H., and R. F. King, 1965, Applied Geophysics for Engineers and Geologists, Pergamon Press, London.
- Grimm, W., E. Richter, and G. Rosetz, 1966, "A Study of the Deformation and Strength Properties of Rocks by Block Tests In-Situ in Iron Ore Mines," Proceedings of the First Congress of the International Society of Rock Mechanics, Lisbon, Vol. 1, p. 457-463.
- Group de Travail de Comite National Francais, 1964, "Measurement of the Moduli of Deformation in Rock Masses and in Drillholes," Eighth Int. Cong. on Large Dams, Edinburgh, Vol. 1, R.16, Q.28, p. 313-327.
- Group de Travail de Comite National Francais, 1964, "Les Effets Physico-Chimiques De L'Eau Dans Les Appuis De Barrage," Eighth Int. Cong. on Large Dams, Edinburgh, Vol. 1, R.17, Q.28, p. 329-349.
- Group de Travail de Comite National Francais, 1964, "Measurement of Rock Mechanics Properties Before and After Grouting," Eighth Int. Cong. on Large Dams, Edinburgh, Vol. 1, R.18, Q.28, p. 351-376.
- Hagerman, T., 1966, "Rock Bodies and Particular Zones in Rock, The Geological Structure as a Factor in Rock Stability," Proceedings of the First Congress of the International Society of Rock Mechanics, Lisbon, Vol. 1, p. 159-161.
- Hartman, B., 1965, Rock Mechanics Instrumentation for Tunnel Construction, Riley's Reproductions, Inc., Denver, p. 153.
- Harza Engineering Corp., 1965, Private Communications, D. Roberts.
- Hasselstrom, B., L. Rahm, and K. Scherman, 1964, "Methods for the Determination of the Physical and Mechanical Properties of Rock," Eighth Int. Cong. on Large Dams, Vol. 1, R.33, Q.28, p. 611-626.
- Hughes, D. S., and J. L. Kelley, 1952, "Variation of Elastic Wave Velocity with Saturation in Sandstone," Geophysics, Vol. 17, p. 739-752.



- Illiev, I. G., 1966, "An Attempt to Estimate the Degree of Weathering of Intrusive Rocks from their Physico-Mechanical Properties," Proceedings of the First Congress of the International Society of Rock Mechanics, Lisbon, Vol. 1, p. 109-114.
- Jaeger, C., 1961, "Recent British Experience on Underground Work and Rock Mechanics," Seventh Int. Cong. on Large Dams, Rome, Vol. 2, R.6, Q.25, p. 167-289.
- Japanese National Committee on Large Dams, 1958, "Present Status of Measurement of Structural Behavior of Dams in Japan," Sixth Int. Cong. on Large Dams, New York, Vol. 2, R.25, Q.21, p. 301-357.
- John, K. W., 1962, "An Approach to Rock Mechanics," Journal of the Soil Mechanics and Foundation Engineering Division, Proceedings of the American Society of Civil Engineers, Vol. 88, Part 1, p. 1-30.
- Judd, W. R., 1965, "Some Rock Mechanics Problems in Correlating Laboratory Results with Prototype Reactions," Int. Jour. Rock Mech., and Mining Sciences, Vol. 2, No. 2, p. 197-218.
- Kawabuchi, K., 1964, "A Study of Strain Characteristics of a Rock Foundation," Eighth Int. Cong. on Large Dams, Edinburgh, Vol. 1, R.11, Q.28, p. 209-218.
- Kawamoto, T., 1966, "On the Calculation of the Orthotropic Elastic Properties from States of Deformation Around a Circular Hole Subjected to Internal Pressure in Orthotropic Elastic Medium," Proceedings of the First Congress of the International Society of Rock Mechanics, Lisbon, Vol. 1, p. 269-272.
- King, M. S., 1966, "Wave Velocities in Rocks as a Function of Changes in Overburden Pressure and Pore Fluid Saturants," Geophysics, Vol. 31, No. 1, p. 50-73.
- Kitsunezaki, C., 1965, "In-Situ Determination of Variation of Poisson's Ratio in Granite Accompanied by Weathering Effect and its Significance in Engineering Projects," Bulletin of the Disaster Prevention Research Institute, Vol. 15, Part 2, No. 92, Nov.
- Knill, J. L., and K. S. Jones, 1965, "The Recording and Interpretation of Geological Conditions in the Foundations of the Roseires, Kariba, and Latiyan Dams," Geotechnique, Vol. 15, p. 95-124.
- Kudo, S., 1963, "Geophysical Investigation on Dam Foundation Rocks," from Onadera, 5th Symposium on Rock Mechanics, Pergamon Press, New York, p. 517-535.
- Kujundzic, B., 1964, "A Contribution to the Experimental Investigation of Changes of Mechanical Characteristics of Rock Massives as a Function of Depth," Eighth Int. Cong. on Large Dams, Edinburgh, Vol. 1, R.56, Q.28, p. 1051-1067

- Kujundzic, B., 1966, "Correlation Between Static and Dynamic Investigations of Rock Mass In-Situ," Proceedings of the First Congress of the International Society of Rock Mechanics, Lisbon, Vol. 1, p. 565-570.
- Kujundzic, B., 1966, "A Contribution to the Investigation of the Pressure Grouting Effect on Consolidation of Rock Masses," Proceedings of the First Congress of the International Society of Rock Mechanics, Lisbon, Vol. 2, p. 633-638.
- Kujundzic, B., and B. Corlic, 1957, "Determination of the Elasticity Modulus of Rocks and of the Depth of the Disaggregated Zones in Hydraulic Pressure Tunnels by Means of the Seismic Refraction Method," Hidrotehnicki Institut, Transactions, No. 8, Beograd, 1957.
- Lakshmanan, J., 1966, "New Trends in Seismic Investigation of Rock Masses," Proceedings of the First Congress of the International Society of Rock Mechanics, Lisbon, Vol. 1, p. 63-66.
- Lane, R. G. T. L., 1964, "Rock Foundations, Diagnosis of Mechanical Properties and Treatment," Proceedings of Eighth Congress of Large Dams, Edinburgh, Vol. 1, p. 141-166.
- Lane, R., 1966, "The Interpretation of Rock Test Results for the Design of Structures," Proceedings of the First Congress of the International Society of Rock Mechanics, Lisbon, Vol. 2, p. 563-566.
- Lauffer, H., and G. Seeber, 1966, "Measurement of the Rock Deformability with the Aid of the Radial Jack of the TIWAG and Verification of the Measuring Results Through the Pressure Shaft Lining of the Kaunertal Power Plant," Proceedings of the First Congress of the International Society of Rock Mechanics, Lisbon, Vol. 2, p. 347-356.
- Lawrence, H. W., 1964, "In-Situ Measurement of the Elastic Properties of Rocks," Proceedings Sixth Symposium on Rock Mechanics, Rolla, Missouri.
- Le May, Y., and G. Comes, 1966, "Dam Foundation-Rock Investigation with an Acoustic Extensometer Including Expanding Heads," Proceedings of the First Congress of the International Society of Rock Mechanics, Lisbon, Vol. 2, p. 543-547.
- Link, H., 1964, "Evaluation of Elasticity Moduli of Dam Foundation Rock Determined Seismically in Comparison of Those Arrived at Statically," Eighth Int. Cong. on Large Dams, Edinburgh, Vol. 1, R.45, Q.28, p. 833-858.
- Little, A. L., J. C. Stewart and P. J. Fookes, 1963, "Bedrock Grouting Tests of Mangla Dam, West Pakistan," Grouts and Drilling Muds in Engineering Practice, Butterworths, London, p. 91-98.
- Lotti, C., and M. Beamonte, 1964, "Execution and Controls of Consolidation Works Carried out in the Foundation Rock of an Arch Gravity Dam," Eighth Int. Cong. on Large Dams, Edinburgh, Vol. 1, R.37, Q.28, p. 671-695.

- Mann, R. L., and I. Fatt, 1960, "Effects of Pore Fluids on the Elastic Properties of Sandstones," Geophysics, Vol. 25, p. 433-444.
- Masuda, H., 1964, "Utilization of Elastic Longitudinal Wave Velocity for Determining the Elastic Property of Dam Foundation Rocks," Eighth Int. Cong. on Large Dams, Edinburgh, Vol. 1, R.13, Q.28, p. 253-331.
- Mayer, A., 1963, "Recent Work in Rock Mechanics," Geotechnique, Vol. 13, June, p. 108-121.
- Menard, L., 1966, "Use of the Pressuremeter to Study Rock Masses," Rock Mechanics and Engineering Geology Journal of Int. Society of Rock Mechanics, Vol. 4, No. 2, p. 160-171.
- Miller, R., and J. Kahn, 1962, "Statistical Analysis in the Geological Sciences," John Wiley and Sons, New York, p. 204-210.
- Monahan, C. J., and E. A. Sibley, 1965, "Rock Mechanics for Dworshak Dam," Geological Society of America, 65th Annual Meeting.
- Morgenstern, N. R., and P. R. Vaughn, 1963, "Some Observations on Allowable Grouting Pressures," Grouts and Drilling Muds in Engineering Practice, Butterworth, London, p. 36-43.
- Multipurpose Dam Rock Testing Group, 1964, "Rock Tests in Multipurpose Dams in Japan," Eighth Int. Cong. on Large Dams, Edinburgh, Vol. 4, p. 715-752.
- Nose, M., 1964, "Rock Test In-Situ, Conventional Tests on Rock Properties and Design of Kurobegawa No. 4 Dam Based Thereon," Eighth Int. Cong. on Large Dams, Edinburgh, Vol. 1, p. 219-252.
- Nugent, R. C. and D. C. Banks, 1965, Project Sulky, Preshot Geologic Investigations, Corps of Engineers, Vicksburg, Mississippi.
- Obert, L., and W. I. Duvall, 1967, Rock Mechanics and the Design of Structures in Rock, J. Wiley, New York.
- Onodera, T. F., 1963, "Dynamic Investigation of Foundation Rocks In-Situ," Proceedings of 5th Symposium on Rock Mechanics, Pergamon Press, New York, p. 517-535.
- Pickell, J. J., and J. G. Heacock, 1960, "Density Logging," Geophysics, Vol. 25, p. 891-904.
- Pirson, S. J., 1963, Handbook of Well Log Analysis for Oil and Gas Formation Evaluation, Prentice-Hall Inc., New Jersey.
- Proctor, R., and R. White, 1946, Rock Tunneling with Steel Supports, Commercial Shearing and Stamping, Youngstown, Ohio.
- Rauch, G., J. Richardson, and D. Mistered, 1965, "Measurement of Rock Deformations in Foundations of Massed Concrete Dams," Paper for Meeting for ASTM, Symposium on Instrumentation in Apparatus for Soils and Rock, Purdue University, June.

- Rice, L. O., 1964, "In-Situ Testing of Foundation and Abutment Rock for Dams," Eighth Int. Cong. on Large Dams, Edinburgh, Vol. 1, R.5, Q.28, p. 87-101.
- Rocha, M., 1955, "Deformability of Foundation Rocks," Fifth Int. Cong. on Large Dams, Paris, Vol. 3, R.75, Q.18, p. 531-559.
- Rocha, M., 1964, "Mechanical Behavior of Rock Foundations in Concrete Dams," Eighth Int. Cong. on Large Dams, Edinburgh, Vol. 1, p. 785-831.
- Rocha, M., J. Lopez, J. DaSilva, 1966, "A New Technique for Applying the Method of Flat Jack in the Determination of Stresses Inside Rock Masses," Proceedings of the First Congress of the International Society of Rock Mechanics, Lisbon, Vol. 2, p. 57-65.
- Ruiz, M., 1966, "Anisotropy of Rock Masses in Various Underground Projects in Brazil," Proceedings of the First Congress of the International Society of Rock Mechanics, Lisbon, Vol. 1, p. 263-267.
- Ruiz, M., 1966, "Some Technological Characteristics of Twenty-Six Brazilian Rock Types," Proceedings of the First Congress of the International Society of Rock Mechanics, Lisbon, Vol. 1, p. 115-119.
- Rusch, H., 1960, "Research Toward a General Flexural Theory for Structural Concrete," Proc. Amer. Concrete Institute, Vol. 57, p. 1-28.
- Salas, J. A., and S. Uriel, 1964, "Some Recent Rock Mechanics Testing in Spain," Eighth Int. Cong. on Large Dams, Edinburgh, Vol. 1, R.5, Q.28, p. 998-1002.
- Sapegin, D. D., and R. A. Shiryayev, 1964, "Deformability Characteristics of Rock Foundations Before and After Grouting," Proceedings of the First Congress of the International Society of Rock Mechanics, Lisbon, Vol. 1, p. 755-760.
- Sarment, G., 1964, "Cambambe Dam Problems Posed by the Foundation Ground and Their Solution," Eighth Int. Cong. on Large Dams, Edinburgh, Vol. 1, R.23, Q.28, p. 443-464.
- Scalabrini, M., 1964, "Determination In-Situ of the State of the Frera Dam Foundation Rock by the Sonic Method, Its Improvement by Consolidation Grouting and Verification of the Result by Again Using the Sonic Method," Eighth Int. Cong. on Large Dams, Edinburgh, Vol. 1, R.31, Q.28, p. 585-600.
- Schnitter, N., 1964, "Properties and Behaviour of the Foundation Rock at Suffers Arch Dam," Eighth Int. Cong. on Large Dams, Edinburgh, Vol. 1, R.39, Q.28, p. 717-729.
- Scott, J. H., and R. D. Carroll, 1967, "Surface and Underground Geophysical Studies at the Straight Creek Tunnel Site, Colorado," Highway Research Board Meeting, January, In Press.

- Serafim, J., 1961, "Discussion to Q.25," Seventh Int. Cong. on Large Dams, Rome, Vol. 2, p. 45-51.
- Serafim, J., 1964, "Rock Mechanics Considerations in a Design of Concrete Dams," International Conference State of Stress in the Earth's Crust, Santa Monica, California, Elsevier Publ. Co., N. Y., p. 611-650.
- Serafim, J., 1966, "Importance of Studies with Elastic Waves in the Geotechnical Exploration on the Foundations of Concrete Dams," Proceedings of the First International Society of Rock Mechanics, Lisbon, Vol. 2, p. 655-660.
- Serafim, J., 1967, Private Communication.
- Serafim, J., J. Laginha, and M. Guerreiro, 1966, "In-Situ Tests for the Study of Rock Foundations of Concrete Dams," Proceedings of the First Congress of the International Society of Rock Mechanics, Lisbon, Vol. 2, p. 549-556.
- Serafim, J., and A. Nunes, 1966, "Studies of Dam Foundations Under a Residual Cover," Proceedings of the First Congress of the International Society of Rock Mechanics, Lisbon, Vol. 2, p. 639-644.
- Serdengecti, S., and G. D. Boozer, 1961, "The Effects of Strain Rate and Temperature on the Behavior of Rocks Subjected to Triaxial Compression," Proc. Fourth Symposium on Rock Mechanics, Bull. Mineral Indus. Exper. Sta., Penn. St. Univ., No. 76.
- Shannon and Wilson, Inc., 1964, Report on In-Situ Rock Tests, Dworshak Dam Site, for U.S. Army Engineer District, Walla Walla, Corps of Engineers, Seattle, Washington, 1964.
- Stucky, A., 1953, "Foundation Problems for Large Dams and Storage Reservoirs, Mauvoisin and Granddixence Dams," Proceedings of the Third International Conference on Soil Mechanics and Foundation Engineering, Switzerland, Vol. 3, p. 326-341.
- Talobre, J., 1961, "La Determination Experimentale de la Resistance des Roches D'Appui des Barrages et des Parois de Soutterrains," Seventh Int. Cong. on Large Dams, Rome, Vol. 2, 12-37, p.
- Terrassa, M., P. Duffaut, J. Garnier, and M. Bollo, 1966, "Auscultation Seismic Investigation of Foundation Rock at the Roujanel Dam," Proceedings of the First Congress of the International Society of Rock Mechanics, Lisbon, Vol. 2, p. 597-602.
- Terzaghi, K., 1946, "Rock Defects and Loads on Tunnel Supports," Section I, Rock Tunneling with Steel Supports, The Commercial Shearing and Stamping Co., Youngstown, Ohio.
- Terzaghi, R., 1965, "Sources of Error in Joint Surveys," Geotechnique, Vol. XV, No. 3, p. 287.

- Underwood, L. B., 1964, "Chalk Foundations at Four Major Dams in the Missouri River Basin," Eighth Int. Cong. on Large Dams, Edinburgh, Vol. 1, R.2, Q.28, p. 23-47.
- Underwood, L. B., 1966, Classification and Identification of Shales, ASCE Water Resources Engineering Conference, Denver.
- Underwood, L. B., and C. J. Distefano, 1964, "Development of a Rock Bolt System for Permanent Support at NORAD," Proc. Sixth Symposium on Rock Mechanics, Rolla, Missouri, p. 43-86.
- U.S. Bureau of Reclamation, 1948 and 1951, "Foundation Bearing Tests at Davis Dam," St. Res. Lab. Rep., SP18 and SP18A, Denver, Colorado.
- U.S. Bureau of Reclamation, 1963, Earth Manual, U.S. Government Printing Office, Washington, D.C.
- U.S. Bureau of Reclamation, 1965, "Morrow Point Dam and Power Plant Foundation Investigation," A Water Resources Technical Publication, Denver.
- U.S. Bureau of Reclamation, 1966, Private Communication, G. Wallace.
- Waldorf, W. A., J. A. Veltrop, and J. J. Curtis, 1963, "Foundation Modulus Tests for Karadj Arch Dam," Proc. ASCE, Vol. 89, SM4, pp. 91-126.
- Walker, T., 1964, "The Interpretation of the Fracture Finder Micro-Seismogram Log," Transactions Fifth Symposium, Society of Professional Well Log Analysts, Tulsa, Oklahoma, p. 11.
- Walsh, J. B., 1965, "The Effect of Cracks on the Uniaxial Elastic Compression of Rocks," Journal of Geophysical Research, Vol. 70, p. 399.
- Wantland, D., 1963, "Geophysical Measurements of Rock Properties In-Situ," Proceedings of the International Conference on State of Stress in the Earth's Crust, Santa Monica, Elsevier Publ. Co., N. Y., p. 409-448.
- Weyermann, W., 1966, "Deformations of Dam Foundations on Rock," Proceedings of the First Congress of the International Society of Rock Mechanics, Lisbon, Vol. 2, p. 557-562.
- Wyllie, M. R. J., A. R. Gregory, and L. W. Gardner, 1965, "Elastic Wave Velocities in Heterogeneous and Porous Media," Geophysics, Vol. 21, p. 41-70.
- Wyllie, M. R. J., A. R. Gregory, and L. W. Gardner, 1958, "An Experimental Investigation of Factors Affecting Elastic Wave Velocities in Porous Media," Geophysics, Vol. 23, p. 459-493.
- Wyllie, M. R. J., 1963, The Fundamentals of Well Log Interpretation, Third Edition, Academic Press, New York, p. 73.

- Yague, A. G., 1966, "Geophysical Exploration and Surveying of Rock Masses. Related Contributions and Problems," Proceedings of the First Congress of the International Society of Rock Mechanics, Lisbon, Vol. 1, p. 7-10.
- Zangar, C. H., 1953, "Theory and Problems of Water Percolation," U.S. Bureau of Reclamation, Eng. Monograph No. 8.
- Zaruba, R., 1966, "Mechanical Properties of Ordovician Shales of Central Bohemia," Proceedings of the First Congress of the International Society of Rock Mechanics, Lisbon, Vol. 1, p. 421-424.
- Zerneke, K., 1966, "Final Geologic Report on the Construction of Adit to Discharge Line Tunnels, Tehachapi Pumping Plant," The Project Geologic Report, C-18, California Dept. of Water Resources, December.
- Zienkiewicz, O., and K. Stagg, 1966, "The Cable Method of In-Situ Testing," Proceedings of the First Congress of the International Society of Rock Mechanics, Lisbon, Vol. 1, p. 667-672.
- Zienkiewicz, O., and K. Stagg, 1967, "Cable Method of In-Situ Rock Testing," Int. Journal Rock Mechanics and Min. Sci., Vol. 4, p. 273-300.

UNCLASSIFIED

Security Classification

DOCUMENT CONTROL DATA - R & D		
<i>(Security classification of title, body, of abstract and indexing annotation must be entered when the overall report is classified)</i>		
1. ORIGINATING ACTIVITY (Corporate author)		2a. REPORT SECURITY CLASSIFICATION
University of Illinois, Department of Civil Engineering Urbana, Illinois 61801		UNCLASSIFIED
3. REPORT TITLE		2b. GROUP
ENGINEERING CLASSIFICATION OF IN-SITU ROCK		
4. DESCRIPTIVE NOTES (Type of report and inclusive dates)		
15 June 1965-1 November 1967		
5. AUTHOR(S) (First name, middle initial, last name)		
Don U. Deere; Richard F. Coon; Andrew H. Merritt		
6. REPORT DATE	7a. TOTAL NO. OF PAGES	7b. NO. OF REFS
January 1969	296	142
8a. CONTRACT OR GRANT NO.	9a. ORIGINATOR'S REPORT NUMBER(S)	
AF 29(601)-6850	AFWL-TR-67-144	
b. PROJECT NO.	9b. OTHER REPORT NO(S) (Any other numbers that may be assigned this report)	
5710		
c. Task Area:		
RSS2144		
d.		
10. DISTRIBUTION STATEMENT This document is subject to special export controls and each transmittal to foreign governments or foreign nationals may be made only with prior approval of AFWL (WLDC), Kirtland AFB, NM, 87117. Distribution is limited because of the technology discussed in the report.		
11. SUPPLEMENTARY NOTES		12. SPONSORING MILITARY ACTIVITY
		AFWL (WLDC) Kirtland AFB, NM 87117
13. ABSTRACT (Distribution Limitation Statement No. 2)		
<p>An engineering classification for in-situ rock is proposed which is based upon the results of field exploration and laboratory testing. The field program included a study of more than fifteen construction projects from which data were obtained from geophysical testing, borehole photography, water pressure testing, and geologic mapping. Laboratory analyses of 530 samples taken from these projects included physical and mineralogical descriptions, unit weights, absorption, strength, modulus of elasticity, and sonic velocities (saturated and dry). The rock types investigated included granite, basalt, gneiss, schist, sandstone, limestone, and siltstone. Geologic discontinuities such as joints, faults, and weathered rock are of major importance in an engineering evaluation of in-situ rock because of their effect upon the deformability, shear strength, and permeability of the mass. A quantitative description of these features can be made using two methods of indexing rock quality; the RQD and the Velocity Index. The RQD (Rock Quality Designation) is a function of the length of core pieces bounded by joint surfaces and is calculated for each coring run. The Velocity Index is the square of the ratio of in-situ to laboratory sonic velocities. The relationship between these two indices suggests that each is influenced to about the same degree by the amount of jointing in the rock. Therefore, either method can be used in classifying in-situ rock. The application of the proposed classification to the prediction of in-situ rock properties is shown by comparing rock quality measurements with other engineering data. Comparisons are presented between rock quality and the modulus of deformation determined by plate jack and pressure chamber tests, in-situ permeability determined by water pressure tests, and the overall character of the rock indicated by the rate of construction and support requirements for underground openings.</p>		

DD FORM 1 NOV 65 1473

UNCLASSIFIED

Security Classification



UNCLASSIFIED  
Security Classification

14. KEY WORDS	LINK A		LINK B		LINK C	
	ROLE	WT	ROLE	WT	ROLE	WT
In-situ rock Rock Rock Classification Rock Engineering Rock Construction Rock Mechanics Classification of Rock Geophysical Exploration Borehole Photography Water Pressure Testing Geologic Mapping Tunnels						

AFSC-HOLLOMAN AFB, NMEX

UNCLASSIFIED  
Security Classification